Predicting the *in vivo* performance of bio-enabling formulations by combining biorelevant *in vitro* tools with Physiologically Based Absorption Modelling

Publikationsbasierte Dissertation
zur Erlangung des Doktorgrades
der Naturwissenschaften

Vorgelegt beim Fachbereich 14
(Biochemie, Chemie und Pharmazie)
der Johann Wolfgang Goethe -Universität
in Frankfurt am Main

von
Charalampia Litou
aus Athen, Griechenland

Frankfurt am Main, 2020

Vom Fachbereich für Biochemie, Chemie und Pharmazie der Johann Wolfgang Goethe -

Universität als Dissertation angenommen.

Dekan: Prof. Dr. Clemens Glaubitz

1. Gutachter: Prof. Dr. Jennifer B. Dressman
2. Gutachter: Prof. Dr. Martin Kuentz

Datum der Disputation: 11.12.2020

Στον Ξενοφώντα και το γιο μου, Άρη.

Στους γονείς μου, Μαργαρίτα και Γιώργο, και την αδερφή μου, Ειρήνη.

.

Contents

1   Preface

PEARRL (Pharmaceutical Education and Research with Regulatory Links) is a European Research and Innovation Programme which aims to deliver innovative drug development strategies as a means to facilitate earlier access of patients to "breakthrough therapy" drugs (www.pearrl.eu). It is an international Programme which brings together five European academic partners, with Pharmaceutical Industry and Regulatory Agency partners and it is divided into three work packages (Figure 1.1).
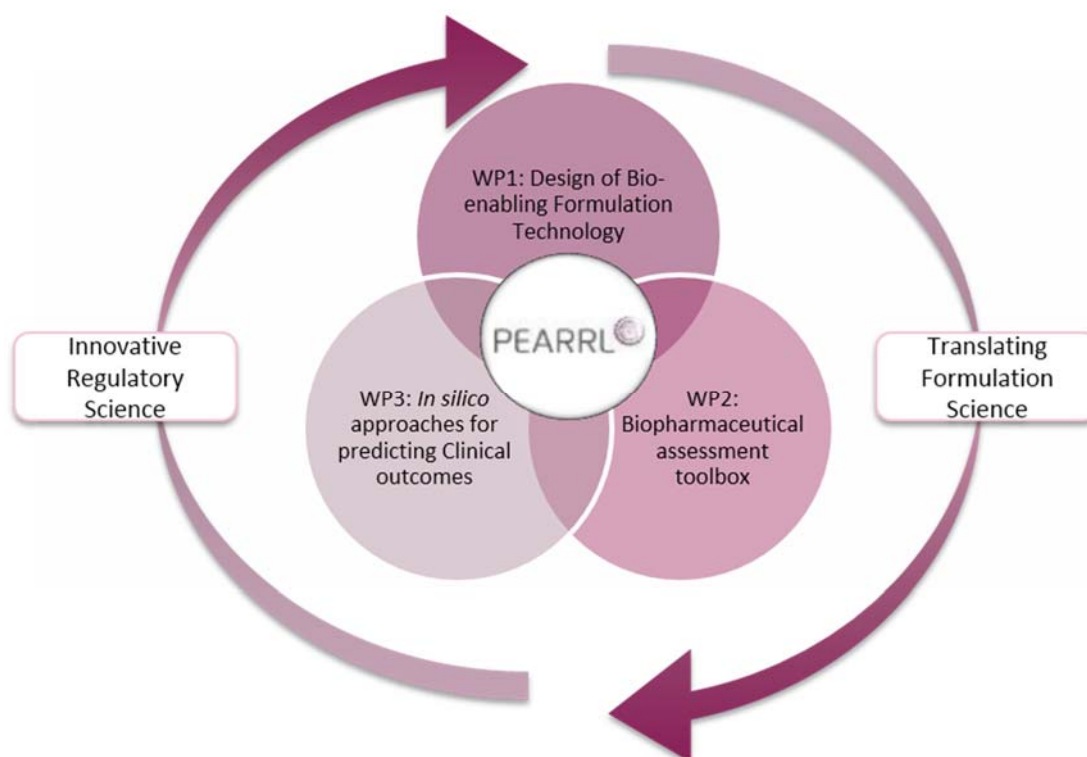
Figure 1.1: PEARRL work packages

The objective of work package 1 (WP1) is to provide innovative formulations for poorly soluble drugs to enhance oral drug bioavailability. The objective of work package 2 (WP2) is to develop *in vitro* biopharmaceutics tools, as well as *in vivo* (preclinical and clinical) models to evaluate the effect of various parameters, such as formulation factors, on the *in vivo* drug product performance. The objective of work package 3 (WP3) is to develop predictive *in silico* approaches for the *in vivo* drug product performance in healthy as well as special populations, e.g. patients with gastrointestinal diseases, and devise ways of integrating data generated with the novel

biopharmaceutics tools of WP2 into Physiologically Based Pharmacokinetic (PBPK) models. The three work packages are well-defined, however, a collaborative effort between all partners of the different work packages is important in order to achieve optimum results.

For this dissertation, which is part of WP 3, the gastrointestinal parameters and processes which can affect drug absorption, as well as the importance of their appropriate *in vitro* simulation, were first reviewed and evaluated. The *in vitro* characterization of the complex drug formulations used in this work was performed by using biorelevant *in vitro* tools and suggestions were made in order to address challenges that can rise when handling such formulations *in vitro*. In the next steps, the *in vitro* results obtained with the various biopharmaceutics tools were coupled with *in silico* PBPK modelling and simulation techniques in order to predict the *in vivo* performance of the drug formulations investigated. In the context of these efforts, approaches were proposed to address challenges that rise when modelling the *in vivo* behavior of complex formulations.

Last but not least, secondments at a Regulatory Agency and at a Pharmaceutical Industry partner were mandatory in the PEARRL Programme. The regulatory secondment took place at the Regulatory Agency of Germany (Bundesinstitut für Arzneimittel und Medizinprodukte, BfArM, Bonn, Germany), while the industrial secondment took place at Janssen Pharmaceutica (Beerse, Belgium). The hands-on experience gained through these secondments was a valuable asset and addition to the thesis work

2 Introduction

Despite the various routes of drug administration, the oral route constitutes the most frequent route of administration due to its simplicity and convenience, both of which encourage patient compliance. In fact, according to the Food and Drug Administration (FDA) data more than half of the novel drugs which were granted Marketing Authorization Approval each year up until 2019 (including dyes in surgery and diagnostic agents in imaging techniques) are administered orally.[1]

However, the bioavailability (the fraction of the administered dose of unchanged drug that reaches the systemic circulation) of drugs which are orally administered varies greatly. This is because oral drug absorption is a complex process that can be affected by a range of parameters related to the drug, the formulation and the underlying physiology of the gastrointestinal (GI) tract. Parameters affecting drug release and absorption can ultimately have a great impact on drug bioavailability and consequently on the clinical efficacy of the drug. Therefore, predicting the *in vivo* performance of orally administered drug formulations has become a major goal of scientists working in the pharmaceutical industry.

In order to be able to predict the *in vivo* performance of an orally administered compound it is necessary to define the critical physicochemical, formulation and physiological factors that determine the product performance. It is also important to investigate and understand the interplay of physiological parameters and drug formulation in the GI tract. Developing both *in vitro* and *in silico* models which can be used to robustly predict the *in vivo* performance of formulated drug products provides the way forward to selecting the optimal formulation of a compound in an efficient manner in terms of both time and resources, and thus to facilitating the access of patients to innovative medicines. Indeed, this approach is a cornerstone of the Quality by Design concept.[2]

The next chapters present a detailed overview of the GI physiology and the physiological factors most relevant to drug release and absorption, the formulation strategies currently followed to address the challenge of poor bioavailability of orally administered compounds and the tools currently used to simulate the *in vivo* drug performance in the laboratory. These tools can then be used to 'link the lab to the patient'.[2]

2.1   Physiological processes and parameters affecting drug absorption in the upper gastrointestinal tract

Various physiological factors, such as the composition of GI fluids and the contraction patterns which drive gastric emptying, may affect *in vivo* drug release and absorption. Additionally, many of these physiological factors are affected by food intake and therefore, the prandial state may play a key role in *in vivo* drug release and absorption.[3] In particular it should be noted that, when evaluating food/meal effects, the composition and time of administration of the meal in relation to the intake of the drug product can significantly affect drug release and absorption.[4]

2.1.1   pH and Buffer Capacity in the upper gastrointestinal tract

Fasted State

The intragastric pH in fasted, healthy adults is mainly regulated by the concentration of hydrochloric acid. Using perfusion techniques, hydrogen ion concentrations have been measured in the range 56 to 160 mM.[5–8] According to *ex vivo* measurements performed in human aspirates collected from the stomach of fasted, healthy volunteers, median pH values are typically below 3. Lindahl et al. reported a median (range) pH value of 1.8 (1.4-7.5), measured immediately upon sample aspiration in gastric aspirates of twenty-four healthy volunteers, without prior administration of water.[9] Similarly, a median (range) pH value of 1.94 (1.16–5.96) was reported by Pedersen et al., having been measured in pooled gastric aspirates collected from nineteen healthy volunteers without prior administration of water.[10] Values measured in gastric aspirates of healthy volunteers after administration of 250 mL water fall in the same range. For example, median pH values of 2.4 and 1.7 at 20 min and 40-60 min after water administration were reported by Kalantzi et al.,[11] while median (range) values of 2.7 (1.9-3.9) at 10 min, 1.7 (1.3-2.0) at 20 min and 1.6 (1.1-2.4) at 35 min after water administration were reported by Litou et al. [12] By contrast, Hens et al.[13] reported a mean (range of mean values) of 2.6 (1.8-3.7) throughout the 7 h of aspirations.

On the other hand, the intestinal pH (at least in the fasted state) is considered to be mainly controlled by bicarbonates, which are secreted by the pancreas and the enterocytes and are also present in the bile.[14–17] The bicarbonate concentration in the upper intestine (duodenum and jejunum) of fasted adults has been measured to range between 2 and 20 mM using the pCO_2/pH method, and the influx of hydrochloric acid into the upper small intestine has been shown to result in a significant increase in bicarbonate secretion rates.[6,18–21] Dressman et al.[22] reported a median pH value of 6.1 measured in the duodenum of healthy adults by using a Heidelberg capsule. Kalantzi et al.[11] and Litou et al.[12] reported median (range) duodenal pH values of 6.2 at 30 min after water administration and 6.8 (6.4-7.2) at 5 min, 6.2 (2.3-7.1) at 15 min, 6.3 (3.0-7.0) at 30 min and 6.5 (2.7-7.7) at 50 min after water administration, respectively. Fadda et al. reported a mean (SD) pH value of 7.1 (0.5) measured in pooled aspirates collected from the jejunum of healthy volunteers.[23] It should be noted that the pH in the upper small fasted intestine is also affected by the pH of the gastric contents which are emptied into the intestine during the interdigestive migrating motor complex (IMMC).[24]

The buffer capacity of GI fluids, i.e. their resistance to change in pH, is determined by the physiological pH-regulating agents that are present in the region of interest as well as any food and drink that is ingested by the patient. Furthermore, the transfer of gastric contents and the various protein-based pancreatic secretions can both have an additional effect on the buffer capacity of the fluids in the upper intestine.

The buffer capacity of the GI contents can be estimated by aspirating the luminal contents from the region of interest and titrating the sample with a strong acid or base. The average buffer capacity of the fasted gastric fluids, measured immediately upon fluid aspiration in pooled healthy gastric aspirates was reported by Kalantzi et al.[11] to be 18 mmol/L/ΔpH. Litou et al. reported average (SD) buffer capacity values, measured immediately upon aspiration in healthy, fasted gastric aspirates, of 4.7 (4.6) mmol/L/ΔpH at 10 min, 21.3 (11.4) mmol/L/ΔpH at 20 min and 27.6 (15.7) mmol/L/ΔpH at 35 min after administration of 250 mL of water, respectively.[12]

The mean buffer capacity of upper intestinal fluid in the fasted state has been reported to range between 4 and 19 mmol/L/ΔpH.[11,12,23,25,26] However it should be noted that the various handling

procedures of aspirates and any storage prior to the measurements can have an important effect on the buffer capacity measurements, especially in the case of intestinal aspirates which contain the volatile bicarbonate buffer system. For the same reason, one should keep in mind that the buffer capacity measurements are performed *ex vivo* and therefore, the reported values could be an underestimation of the "true" *in vivo* buffer capacity of the intestinal fluids.[27]

Fed State

With regard to the physicochemical properties of the GI fluids in the fed state, the type and content of the meal are highly relevant. Various characterization studies of the fed state GI fluids have been performed after the administration of a liquid (i.e. a nutritional drink) or a solid meal.[4] The "reference meal", as described by the European Medicines Agency (EMA) and the US-FDA, is a high-calorie (800–1000 calories), high fat (approximately 50% of total caloric content of the meal) meal, which consists of two eggs fried in butter, two strips of bacon, two slices of toast with butter, four ounces of hash brown potatoes and a glass of whole milk.[28,29]

The median gastric pH values reported from Malagelada et al.,[30] Dressman et al.[22] and Koziolek et al.[31] 30 min after consumption of a solid–liquid meal, range between 3.6 and 4.1. Furthermore, it was reported that more than three hours are needed to return to baseline pH. After administration of the reference meal similar median gastric pH values were reported, however, higher inter-subject variability was observed.[31] The median pH values of the upper small intestine approximately 30 min after administration of a liquid meal, were reported to range between 6.2 and 6.6,[11,32,33] with the values decreasing through the course of digestion.[4,11,33]

The buffer capacity of the fed state gastric fluid is reported to range between 25 and 30 mmol/L/ΔpH, as measured in the first three hours after meal administration (i.e. slightly higher than the values reported for the fasted state gastric fluids), but it is to a large extent determined by the contents of the meal.[4,11] The buffer capacity values of the fed state upper intestinal fluids (12-28 mmol/L/ΔpH) are similar to those of the gastric fluids in the fed state.[11,33] The values are clearly higher than those in fasted state and are most likely dependent on the buffering effect of

food components and their digestion products.[24] It should be noted that till now, buffer capacity values in the fed GI fluids have been measured only after administration of a liquid meal and not after the administration of the reference meal.

2.1.2   Osmolality and Surface Tension

Fasted State

In the fasted stomach, all existing ions (e.g. chloride, sodium, potassium)[9,12] contribute to the osmolality of the gastric fluids. The osmolality of the fasted gastric fluids is greatly dependent on the amount of water given prior to the measurement in the study. Kalantzi et al. reported mean osmolality values of 98, 132 and 141 mOsm/kg at 20 min, 40 min and 60 min after administration of 250 mL of water, respectively.[11] Similarly, Litou et al. reported mean (SD) values of 4.9 (22.6), 103.6 (41.5) and 144.0 (44.0) mOsmol/kg at 10 min, 20 min and 35 min after administration of 250 mL of water.[12] Therefore, despite the fact that gastric secretions seem to increase the osmolality of the fasted gastric fluids, the fasted gastric contents are always hypo-osmotic. In agreement are the data published by Pedersen et al. and Lindahl et al., who reported values of 220 ± 58 mOsm/kg and 191 ± 36 mOsm/kg, respectively, without prior water administration.[9,10]

The osmolality of the contents of the upper small intestine can have an effect on the absorption of water and nutrients. Litou et al. reported mean (SD) osmolality values of samples aspirated from the fasted, healthy duodenum at 5, 15, 30 and 50 min after administration of 250 mL of water of 92.5 (17.9), 126.9 (49.2), 207.4 (31.6), and 217.4 (44.5) mOsmol/kg, respectively.[12] In general, in the fasted upper small intestine, osmolality ranges between 136 and 301 mOsm/kg, with an overall mean value of 197 mOsm/kg.[27]

With regard to surface tension, mean (±SD) values of the surface tension of fasted gastric contents after administration of 250 mL of water, were reported to be 43.22 (0.74), 41.9-45.7, and 34.8 (5.2) mN/m, by Litou et al., Kalantzi et al. and Pedersen et al., respectively.[10–12] It should be noted that the surface tension of pure water is 72 mN/m. This value, in comparison to the surface tension values of the fasted gastric fluid, clearly indicates the presence of surface active

components in the fasted gastric fluids e.g. bile salts present in the stomach due to gastroduodenal reflux, saliva enzymes etc.[24]

Till now, the osmolality of the contents of the fed stomach has been measured only after administration of a liquid meal and it was reported to be 531 mOsm/kg 30 min after the administration of the meal, with the value decreasing to 321 mOsm/kg at 3 h after meal administration.[11]

The duodenal contents are in most cases hyperosmotic after intake of a liquid-meal.[4] During the first 30 min after administration of a liquid meal, osmolality of the upper small intestinal contents ranges between 291 and 391 mOsm/kg.[11,33] Clarysse et al. reported that osmolality ranges between 122 and 516 mOsm/kg and 174 and 619 mOsm/ kg in fed and fat-enriched fed states, respectively.[34]

With regard to surface tension, the value is lowered to approximately 30 mN/m in both the fed gastric and upper intestinal contents.[4] This is expected to have a positive impact on the wetting of solid dosage forms.

2.1.3 Bile Acids and Lipids

Fasted State

Bile acids are normally present in the small intestine, where they emulsify lipids in order to facilitate their absorption. The intestinal fluid contains a mixture of mixed micelles and liposomes, which are usually formed by bile acids and lipid-hydrolysis products (e.g. glycerol, free fatty acids and cholesterol).[35] These colloidal aggregates facilitate the solubilization of lipophilic drugs but may also interact directly with the dosage form or the formulation excipients.[24]

Bile acids/salts may exist in very small concentrations in the fasted gastric contents, but their presence is only possible due to GI reflux. For example, Pedersen et al.[10] and Lindahl et al.[9] reported mean (SD) bile salt concentration in the fasted gastric contents of 0.3 (0.3) and 0.2 (0.5)

mM, while Litou et al. reported median(range) values for total bile salt content at 10 min, 20 min and 35min, after administration of 250 mL of water, of 0 (0-145), 0 (0-114) and 54.0 (0-620) µM, respectively.[12]

Regarding the bile salt concentration in the fasted duodenum, a range of 0.3 to 9.6 mM has been reported. Based on the study of Fuchs and Dressman in 2014, the overall mean of the published aspiration studies in fasted duodenal aspirates is 3.3 mM.[27] These data are in line with the later study of Litou et al., who reported mean (median) values for total bile salt content in samples aspirated from the fasted duodenum at 5 min, 15 min, 30 min and 50 min after administration of 250 mL of water, of 1.1 (1.1), 4.8 (2.3), 7.7 (5.0), and 3.3 (1.9) mM, respectively.[12]

With regard to lipids, fasted state intestinal fluid contains generally low concentrations of neutral lipids (including approximately 0.1 mM fatty acids) and phospholipids (approximately 0.2 mM).[12,24]

Fed State

Generally, bile salts are not detected in fed gastric aspirated samples.
On the other hand, bile salt concentrations in the fed upper intestinal contents are very variable and are reported to range between 4 and 37 mM.[24]
In the fed stomach, phospholipid and cholesterol levels decrease over time after meal administration, from 2.9 to 0.9 mM and 1.2 to 0.7 mM, respectively.[36] Concentrations of free fatty acids are not significantly changed during the first 3 h after meal administration and are reported to range between 7 and 15 mM.[4,36]
It should be noted that the bile salt/phospholipid ratio in the fed upper intestinal contents remains fairly constant at approximately 3.36[32], whereas the respective ratio in the fasted state can be quite variable (overall bile salts mean in fasted state duodenal fluids is reported to be 3.3 mM, whereas overall mean phospholipid concentration in the fasted human duodenal fluids is calculated to be 0.53 ± 0.64 mM).[27]

2.1.4   Gastric emptying / Gastrointestinal Transfer

The Interdigestive Migrating Motor Complex (IMMC) is a cyclic motility pattern which regulates contractions in the fasted stomach. It consists of three phases: Phase 1, with a duration of 45 to 60 min, in which there is no substantial movement of the gastric fluid; Phase 2, which is characterized by 30 to 45 min of irregular contractile activity, and Phase 3, which is characterized by 2 to 10 minutes of intense contractions and during which the entire stomach contents are transferred into the small intestine.[37]

With regard to oral drug absorption, the physiological process of transferring the gastric contents into the upper small intestine in both the fasted and fed states can play a key role in drug bioavailability, and thus the clinical effect, by affecting the proportion of the drug which is available over time for absorption and/ or the onset of action. The gastric residence time of a solid dosage form depends on the size of the dosage form and the prandial state.[38,39] In the fasted state, small solids (< 2 mm) may empty from the stomach during all IMMC phases, whereas the gastric emptying of larger solids (>2 mm) is dependent on the IMMC Phase 3. During the fed state, small solid particles empty more slowly than in the fasted state. In fact, their gastric residence time becomes more variable and may increase to more than two hours, depending on the meal composition.[24] For larger, non-disintegrating solid particles there is a more pronounced effect of food on gastric residence e.g. it has been reported that after a very heavy meal, non-disintegrating tablets can be retained in the stomach for over 14 hours.[40]

Regarding gastrointestinal transfer in the fasted state, drug absorption may be affected by several phenomena. These are associated not only with the rate of transfer from the stomach to the upper small intestine, but also due to the differences in the characteristics between the gastric and intestinal fluids. Under fasting conditions, weakly basic drugs usually have higher solubility values in the acidic environment of the stomach compared to the respective solubility values in the intestinal fluids. Therefore, weakly basic drugs may reach concentrations in the small intestine after transfer from the stomach that are higher than the drug's solubility in the intestinal fluids. However, since this supersaturated state is thermodynamically unstable, precipitation may result. It has been shown that the degree of supersaturation is a major driving

force for precipitation.[41] Precipitation of the drug results in reduced availability for absorption and incomplete bioavailability. Therefore, the therapeutic efficacy of the drug can be at risk. As precipitation may vary highly among individuals according to the composition of their intestinal fluids and the rate of gastric emptying, this phenomenon can also induce large intra- and inter-individual variability in drug exposure.[42]

During the fed state the interdigestive motility pattern is interrupted and the gastric emptying rate of the meal depends on its caloric content.[38] In particular, gastric emptying rate in fed state has been reported to be approximately 120–240 kcal/h.[4,43,44] However, with regard to the emptying of water it has been reported that emptying from the fed stomach can be as fast as in the fasted state.[4] During digestion, various contractions allow for the transfer of liquids and small particles (< ~2 mm) from the stomach into the duodenum, whereas larger particles remain in the stomach for further grinding.[45] Larger, indigestible solids remain in the stomach until the recurrence of the Phase 3 of IMMC.[46]

2.1.5   Simulating the composition of gastrointestinal fluids

When evaluating the factors that will most likely affect the *in vivo* absorption of a drug product, one major target is to estimate the *in vivo* dissolution behavior of the formulation from appropriately designed *in vitro* laboratory experiments. To this end, more than twenty years ago the concept of "biorelevant media", i.e. aqueous media which simulate the composition of GI fluids based on the data acquired from the aspiration studies, emerged. Biorelevant media attempt to reflect the physiological composition of the GI fluids in terms of pH, buffer capacity, osmolality and bile salts/lipid concentrations. Markopoulos and Andreas et al. have recently proposed four different levels of simulation of the GI contents in both fasted and fed states.[47] Simulated gastric and intestinal fluids at Level 0 are simple aqueous solutions, the pH of which is usually adjusted with a buffer system to represent the pH in the respective part of the GI tract. At simulation Level I, both pH and buffer capacity are adjusted to reflect the mean observed values. Bile salts, lipids and main digestive products are added to the simulated gastric and intestinal fluids at Level II in order to account for the possible *in vivo* solubilization by native surfactants, as well as to reflect the prandial states. Finally, Level III simulated gastric and

intestinal fluids attempt to simulate the presence of proteins and enzymes which are normally present in the aqueous phase of GI contents and are thus the most complex in terms of composition. Level III media may also account for the intraluminal hydrodynamic conditions. A graphical representation of the Levels of simulation of biorelevant media can be found in Figure 2.1.

The biorelevant media which are routinely used today to simulate the contents of the healthy upper GI tract in the fasted and fed state are presented in detail below (Table 1 and Table 2). For a detailed review of the various biorelevant media which simulate the healthy GI environment and which have been proposed in the literature to date, the reader is referred to the article of Markopoulos and Andreas et al.[47]

Fasted state gastric fluids

Various attempts have been made to simulate the healthy, fasted gastric fluids.

Simulated Gastric Fluid (SGF), which is recommended by various pharmacopoeias, e.g. the US Pharmacopoeia, is an aqueous medium with pH 1.2 and it can be used without (SGFsp) or with addition of pepsin (SGF). However, it should be mentioned that the concentrations of pepsin used in SGF are higher than those reported for the healthy fasted stomach (i.e. 0.11-0.22 mg/mL)[11]. Furthermore, as previously mentioned, small amounts of bile salts might be present in the fasted gastric stomach due to reflux. The bile salts in combination with the pepsin result in a decreased surface tension of the gastric fluids to approximately 40 mN/m (as opposed to a surface tension value of approximately 70 mN/m in SGF).[11,12] Taking these into consideration Vertzoni et al. proposed the Level III Fasted State Simulating Gastric Fluid (FaSSGF).[48] The composition of Level III FaSSGF can be found in

Table 1.

**Levels of simulation of
luminal composition**

+ dietary proteins, enzymes (not
digestion products), viscosity effects

Level III

+ bile components, dietary lipids,
lipid digestion products, osmolality

Level II

+ buffer capacity

Level I

pH
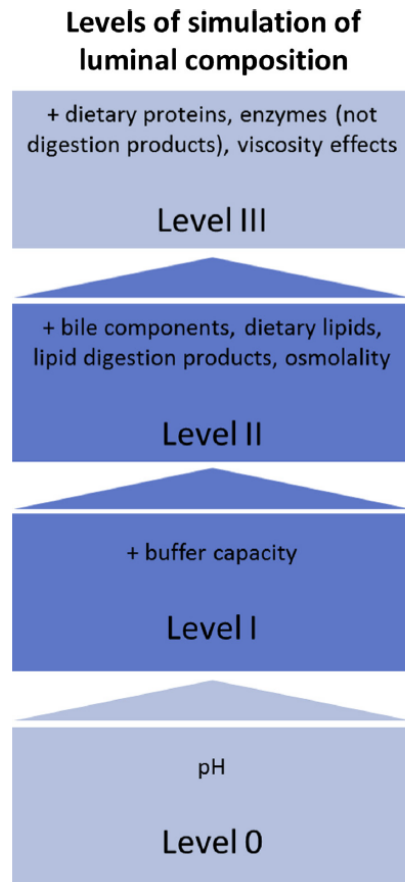
Level 0

Figure 2.1: Levels of simulation of media simulating the composition of gastrointestinal fluids as proposed by Markopoulos and Andreas et al.[47]

Fasted state intestinal fluids

The US Pharmacopeia first proposed an aqueous medium with pH 7.5 to simulate the fasted small intestinal contents, i.e. the Simulated Intestinal Fluid (SIF). However, after the suggestions of Gray and Dressman in 1996, the pH value of SIF was changed to 6.8 in order to match the pH values observed in the upper small intestine more closely.[49] Nonetheless, SIF does not take into account either the presence of native surfactants, nor the physiological buffer capacity and osmolality values. In an attempt to better reflect the composition of the fasted upper small intestine Dressman et al. proposed Level II Fasted State Simulating Intestinal Fluid (FaSSIF V1), which has pH and buffer capacity values more representative of the values measured from the mid-duodenum to the proximal ileum and also contains bile salts (sodium taurocholate) and phospholipids (lecithin) in a 4 to 1 ratio.[50]

Based on the aspiration study data available at the time, Jantratid et al. proposed changes in the FaSSIF V1 composition and introduced FaSSIF V2. In this medium, which contains maleates as buffer system, the osmolality is set at 180 mOsm/kg (as opposed to 270 mOsm/kg in FaSSIF V1) and the phosphatidylocholine concentration is decreased to 0.2 mM (instead of 0.75 mM as in FaSSIF V1) (bile salts to lecithin ratio 15 to 1).[51] In 2015 Fuchs and Dressman conducted an extensive review of all data available from aspiration studies and introduced a new version of FaSSIF, i.e. FaSSIF V3, which also contains cholesterol (bile salts to phospholipids ratio 9 to 1).[27,52] The detailed composition of the different versions of Level II FaSSIF is presented in Table 1.

Table 1: Composition and physicochemical characteristics of biorelevant media simulating the fasted stomach and upper small intestine.

	Level III FaSSGF	Level II FaSSIF V1	Level II FaSSIF V2	Level II FaSSIF V3
Pepsin (mg/mL)	0.1	-	-	-
Sodium taurocholate (mM)	0.08	3	3	1.4
Glycocholate (mM)	-	-	-	1.4
Sodium Oleate (mM)	-	-	-	0.315
Cholesterol (mM)	-	-	-	0.2
Lecithin (mM)	0.02	0.75	0.2	0.035
Lysolecithin (mM)	-	-	-	0.315
HCl (mM)	qs pH 1.6	-	-	-
NaOH (mM)	-	13.8	34.8	3.19
Sodium dihydrogen phosphate (mM)	-	28.7	-	13.51
Maleic acid (mM) -	-	-	19.1	-
Sodium chloride (mM)	34.2	105.85	68.6	91.62
pH	1.6	6.5	6.5	6.7
Osmolality (mOsm/kg)	120.7±2.5	270	180	215±10
Buffer Capacity (mmol/L/ΔpH)	-	12	10	5.6

Fed state gastric fluids

As previously mentioned, the luminal composition in the fed stomach is dependent on the composition of the meal ingested. Ideally, the biorelevant medium used to simulate the fed gastric environment should have similar properties to the recommended US FDA standard breakfast, which is used to investigate food effects in bioavailability/ bioequivalence studies,[28] as well as to reflect the changing gastric environment through the course of digestion.

Various attempts have been made over the last years to simulate the fed stomach, including media which consist of milk or Ensure® Plus.[51,53,54]

The attempt of Jantratid et al. was the first to account for the changing composition of the gastric environment through the course of digestion. In particular, Jantratid et al. proposed three biorelevant media ("snapshot media") simulating the fed stomach at 0-75 min, 75-160 min and > 160 min after the administration of 500 mL Ensure® Plus in healthy adults, i.e. $FeSSGF_{early}$, $FeSSGF_{middle}$, $FeSSGF_{late}$, respectively. These media are based on UHT homogenized full-fat milk.[51] It is considered that $FeSSGF_{middle}$ reflects the general changes in the gastric fed state best and therefore, in the literature it is usually referred to simply as FeSSGF.[47]

In order to overcome the difficulties associated with handling samples which contain milk proteins, the use of Lipofundin® MCT 20 has been proposed as an alternative. Lipofundin® MCT 20 does not contain proteins but it has similar physicochemical characteristics and lipid content as full-fat milk and therefore media based on Lipofundin® MCT 20 can be used easier without the need to handle the proteins in the sample.[47,55] The composition of FeSSGF based on Lipofundin® MCT 20 is presented in Table 2.

Fed state intestinal fluids

As in the stomach, the contents of the intestine in the fed state are highly dependent on the ingested type of meal. In order to reflect the main physicochemical parameters, such as pH, osmolality, buffer capacity etc., of the upper small intestine after meal ingestions, a Fed State Simulating Intestinal Fluid (FeSSIF V1) was developed in 1998 by Galia et al.[56]

Following the concept of the "snapshot media" and based on the available data from aspiration studies, a new medium representing the conditions in the upper small intestine after meal ingestion was designed, i.e. FeSSIF-V2. In this medium, the physicochemical characteristics with

respect to pH, buffer capacity and osmolality are kept similar, while lipolysis products that reflect aqueous phase values in the aspirates have been added. In particular, FeSSIF-V2 contains lower concentrations of bile salts than FeSSIF V1 but this is compensated for by the addition of digestion products (e.g. monoglycerides and free fatty acids).[57]

The detailed compositions of Level II FeSSIF V1 and Level II FeSSIF V2 are given in Table 2.

Table 2: Composition and physicochemical characteristics of biorelevant media simulating the fed stomach and upper small intestine.

	Level II FeSSGF	Level II FeSSIF V1	Level II FeSSIF V2
Acetic acid (mM)	18.31	144	-
Sodium acetate (mM)	32.98	-	-
Maleic acid (mM)	-	-	55.02
Sodium taurocholate (mM)	-	15	10
Glyceryl monooleate (mM)	-	-	5
Sodium oleate (mM)	-	-	0.8
Lecithin (mM)	-	3.75	2
NaOH (mM)	-	101	81.65
HCL/NaOH	qs pH 5.0	-	-
Lipofundin®/Buffer	8.75/91.25	-	-
Sodium chloride (mM)	181.7	-	125.5
Potassium chloride (mM)	-	204	-
pH	5	5	5.8
Osmolality (mOsm/kg)	400	635	390
Buffer Capacity (mmol/L/ΔpH)	25	76	25

2.1.6 Physiologically-Based Pharmacokinetic Modelling

In the last years, in *silico* simulation approaches have become an integral part of drug discovery and development. Physiologically-Based Pharmacokinetic (PBPK) Modelling is an example of such

approaches. PBPK models attempt to mechanistically capture the absorption, distribution, metabolism and excretion processes of a substance in humans and several animal species, by mapping drug movement in the body onto a compartmental structure, using sets of differential equations.[58] The PBPK model parameters are divided into three categories, i.e. the system parameters (e.g. age, weight, height), the drug parameters (e.g. physicochemical and metabolic characteristics) and the study design parameters (e.g. dose, route and frequency of administration, the effect of concomitant drugs and food).[59] One of the advantages of PBPK models is the direct input of parameters derived from *in vitro* experiments. Thus, they can be used even at early stages in pharmaceutical development, when no clinical data are available. After PBPK models are developed with the relevant parameters, they can be used to simulate various "what-if" scenarios, and when clinical data become available, their ability to predict real-world cases can be assessed.[58]

PBPK modelling has gained acceptance at various regulatory agencies as part of the submission package. In 2016 the Committee for Medicinal Products for Human Use (CHMP) of EMA and FDA published a draft guidance, regarding the use of PBPK modelling to support marketing authorization.[60,61]

2.2 Drug physicochemical and formulation properties affecting drug absorption in the gastrointestinal tract

2.2.1 The formulation challenge

Over the last decade, the number of new therapeutic targets as well as the investments in Research and Development (R&D) in the pharmaceutical industry have risen.[62] According to the European Federation of Pharmaceutical Industries (EFPIA), the global Research and Development (R&D) expenses in 2010 climbed to more than $120 billion from under $70 billion in 2002.[62,63] However, the efficiency of developing new drugs and getting them approved by the regulatory authorities is consistently on the decline. For example, the number of new medicines approved per $1 billion invested in R&D has been decreasing by 50% every nine years since the 1950s, reflecting the high attrition rates encountered in transforming drug molecules to formulations.[64]

One of the major challenges to which the high attrition rates can be attributed is the "developability" of the new chemical entities/ drug candidates into successful drug formulations. Despite vastly increased understanding of the main factors that can affect drug absorption, it is estimated that 40-70% of current drug candidates display poor bioavailability due to their "hostile" physicochemical properties with respect to solubility and/ or lipophilicity.[65] Most new candidate drugs in todays' pipelines are characterized by solubility and/or dissolution rate limited bioavailability, i.e. complete dissolution of the drug would require larger GI fluid volumes than are present in the GI tract, and/ or greater GI transit times.[66] Furthermore, increased lipophilicity (which is usually associated with poor solubility in GI fluids) can lead to increased susceptibility to food effects.[67]

Most new drug candidates therefore require special formulation approaches (the so-called "bio-enabling" formulations) to achieve acceptable bioavailability, but at the same time, patient access to them should be facilitated as quickly as possible. Bio-enabling formulations are increasingly being sought in drug development pipelines, however, there are still gaps in understanding of how these formulations perform *in vivo*. Understanding the key biopharmaceutical processes and the interplay of the formulation properties with the

physiological factors which affect drug absorption, can provide a way forward to efficient and successful design of bio-enabling formulations within the framework of Quality by Design.[2] Application of suitable biopharmaceutical tools, combining their results with PBPK models and validating of the resulting models is key to successful prediction of the *in vivo* performance of bio-enabling formulations. Using these models to identify the right formulation, attrition of drugs in the pipeline during clinical development can be minimized.[68]

In the next chapters, the classification systems which are mainly used in current regulatory, industrial and scientific frameworks to assist recognition of key challenges in developing optimal oral formulations for drug candidates are presented in detail. Last but not least, bio-enabling formulation approaches are discussed.

2.2.2   The Biopharmaceutics Classification System (BCS)

The Biopharmaceutics Classification System (BCS), developed in the early 1990s by Amidon et al., classifies drug molecules into four groups according to their solubility and intestinal permeability.[69] The BCS has been developed with the aim of providing a scientific classification tool that can be used as a "regulatory standard" when assessing bioequivalence of two drug products. However, today it is being used extensively not only in the regulatory environment, but also in drug discovery and development.

According to the BCS, there are four potential drug classes into which an Active Pharmaceutical Ingredient (API) can fall. BCS Class I molecules are characterized by high solubility and high permeability, BCS Class II molecules by low solubility and high permeability, BCS Class III molecules by high solubility and low permeability and BCS Class IV molecules by low solubility and low permeability (Figure 2.2).
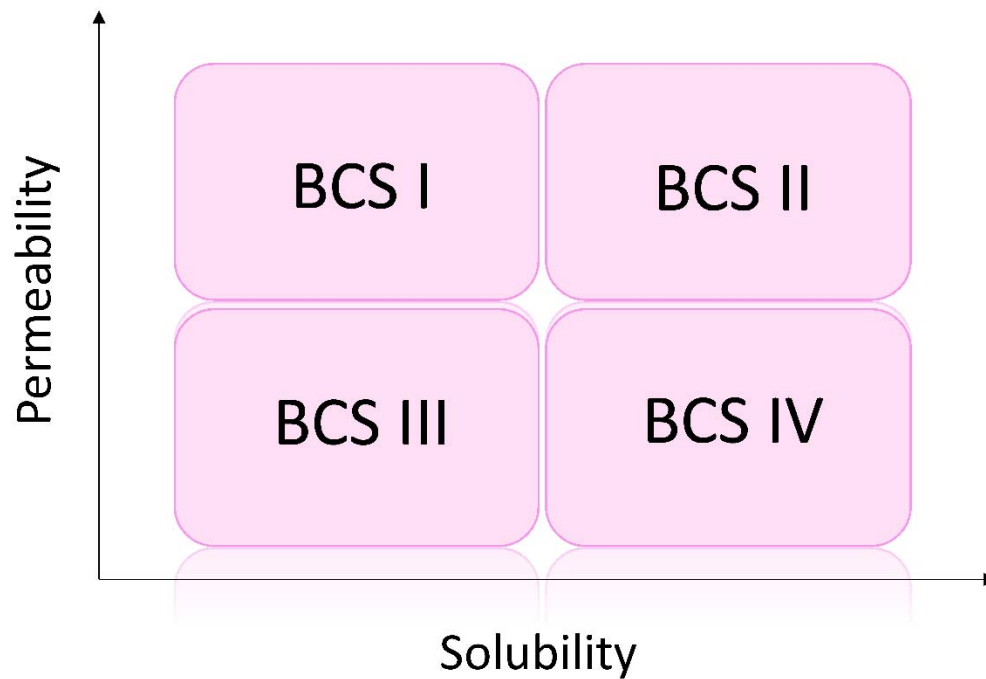
Figure 2.2: The Biopharmaceutics Classification System

According to the BCS the criteria for high solubility of the drug substance is met when the highest single dose recommended in the Summary of Product Characteristics (SmPC) can be dissolved in 250 mL (since solid dosage forms are typically administered with a glass of water) of aqueous media or less over the pH range 1 to 6.8 at $37 \pm 1^{\circ}C$, as currently defined by the FDA and EMA.[29,70] A drug substance is considered to be highly permeable when the systemic bioavailability or the extent of absorption in humans is determined to be 85 % or more of an administered dose based on a mass balance determination (along with evidence showing stability of the drug in the GI tract) or in comparison to an intravenous reference dose.[29,70]

The absorption of BCS Class I drugs is likely to be limited by physiological parameters/processes, e.g. gastric emptying time (given that dissolution is rapid), while intestinal permeability is the rate controlling step in case of BCS Class III drugs. In the case of BCS Class II drug substances, the absorption is expected to be dissolution and/or solubility limited, whereas for BCS Class IV both low solubility and low permeability can hinder the extent of absorption. It should be noted that BCS Class II is a complex group that contains compounds with various physicochemical properties.

For example, in the case of BCS Class II weak acids the intestinal dissolution may be rapid even though the low solubility at gastric pH precludes classification as BCS Class I. In this case, the acidic drug will be completely absorbed. [71] Poorly soluble weak bases, on the other hand, may dissolve well in the stomach, only to then precipitate upon entry into the small intestine, where the pH is higher and thus the solubility lower. The precipitation of the drug may preclude complete drug absorption. However, there are also weak acids that are also poorly soluble at intestinal pH as well as weak bases that do not readily precipitate after transfer into the small intestine.

The BCS can be applied at every stage of drug discovery and development, as well as in the marketing authorization applications. At early stages, in combination with compound potency and target specificity, the BCS classification of the drug candidate can be used to assess its "developability" and if this looks promising, to guide the early formulation approach for administration to animals. Even later on, in clinical development, the BCS classification can provide a framework for rational formulation design.

On a regulatory level, the US FDA and EMA allow BCS-based biowaiver submissions for immediate release dosage forms containing BCS Classes I and III drugs.[29,70] It should be noted that the possibility of extending the BCS-based biowaiver to other BCS classes has attracted extensive interest.[72]

2.2.3 The Developability Classification System (DCS)

Despite the wide application and acceptance of the BCS over the last decades, there are some important limitations of this classification system, especially when considering the GI environment and the actual behavior of a drug substance *in vivo*. In particular, as previously reported, the BCS criteria for the solubility classification depends on the *in vitro* solubility value of the drug substance in aqueous buffers over a range of pH which aims to simulate the actual pH range in the upper GI tract. Although this is reasonable for compounds which have a pH-dependent solubility, pH thus being the main factor affecting their *in vivo* solubility and dissolution, it can definitely lead to underestimations for compounds for which not only the pH but also (and sometimes more importantly) the solubilization by native surfactants affects their

in vivo solubility and dissolution. Furthermore, the assumption that a fixed volume of 250 mL is available for drug dissolution might also be an oversimplification, especially when considering the variable GI environment in both fasted and fed states. Further, the fact that drug dissolution-drug absorption is a dynamic process should be taken into account.

Taking all of the above into consideration, in 2010 Butler and Dressman proposed the Developability Classification System (DCS), which focuses on drug developability and formulation development.[66] The DCS rests on two major pillars:

a) Solubility measurements in biorelevant media should be used as the criterion for predicting the *in vivo* solubility of a drug substance.

b) The "solubility limited absorbable dose" criterion, allows for the fact that drug solubility and permeability in the small intestine are dynamic and compensatory processes. Also, a fluid volume of about 500 mL is used as an approximation of the total volume of fluid available for drug dissolution in the GI tract in the fasted state.

Based on the above, the authors divided the highly permeable and poorly soluble compounds into two subclasses, i.e. DCS Class IIa (for which absorption is dissolution rate-limited) and DCS Class IIb (for which absorption is solubility-limited). A schematic representation of the DCS can be seen in Figure 2.3.

Recently, the refined Developability Classification System (rDCS) was proposed by Rosenberger et al.[73] to allow for better application of the DCS in the pharmaceutical industry. The main refinements proposed are the introduction of a "dose diversity risk assessment" to account for the uncertainty of the exact dose at early stages of drug development, as well as the further classification of weakly basic drugs based on their solubility and possible supersaturation/precipitation kinetics during transfer from the stomach to the upper small intestine.[73]
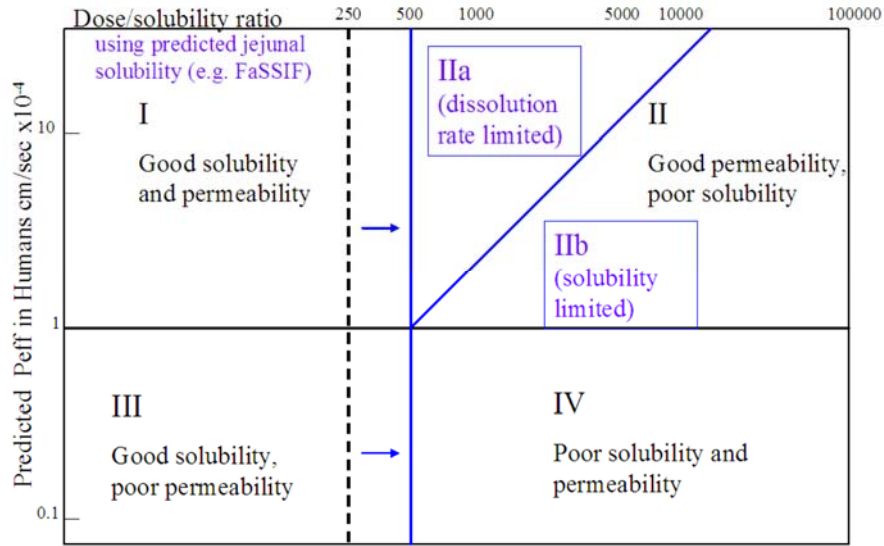
Figure 2.3: The Developability Classification System[66]

2.2.4 Bio-enabling formulations

As previously mentioned, the successful delivery of poorly soluble, highly lipophilic drug candidates often relies today on the use of novel bio-enabling formulation approaches, with primary focus on developing formulations which enhance the solubility and/or dissolution of the respective poorly soluble drug candidates. One of the approaches to meeting this goal is to generate and maintain a metastable state in which the drug concentration exceeds the equilibrium solubility in the respective dissolution medium, in other words to generate a supersaturated state. This state has been described in the literature as a "spring", since it enhances oral drug bioavailability.[74] However, a supersaturated state is a thermodynamically unstable state and therefore, there is a high risk that drug precipitation will follow. In order to hinder the possible precipitation, bio-enabling formulations often include a "parachute", e.g. a precipitation inhibitor.[74,75] According to Williams et al. the approaches designed to improve drug solubility and/ or dissolution are salt formation, formation of co-crystals, addition of co-solvents, complexation with cyclodextrins, nanosization, lipid-based formulations and amorphous solid dispersions.[76] In the following, the approaches of nanosizing and amorphous solid dispersions are presented in detail.

Particle size reduction / Nanosizing

Particle size reduction is routinely used to improve the oral bioavailability of poorly soluble compounds, since it leads to an increase in the surface area available for solvation and therefore, an increase in the rate of dissolution of solid drug particles.[77]

In the first published attempt (1897) to describe the rate of dissolution of solid particles, Noyes and Whitney proposed Equation 2.1, according to which the rate of change in concentration of the dissolved material is directly proportional to the concentration difference between the saturation solubility Cs and the bulk concentration Cx at time t.[78]

$$\frac{dC}{dt} = k\,(Cs - Cx) \tag{2.1}$$

Nernst and Brunner improved upon this theory by introducing the concept of an unstirred diffusion layer across which the solute diffuses from the solid surface to bulk solution.[79] In this theory the rate constant k is defined as shown in Eq. 2.2, where A is the solid surface area, D is the diffusion coefficient, and h the thickness of the diffusion layer.

$$k = A\frac{D}{h} \tag{2.2}$$

As can be seen from Eq. 2.1 and 2.2 particle size reduction leads to an increase in the surface area of drug particles which in turn leads to a direct and proportional increase in the dissolution rate. Thereby, for drugs with dissolution rate limited exposure, the bioavailability can be increased.

Furthermore, it has been postulated that nanosizing can lead to an increase in the solubility of drug molecules due to changes in particle curvature and the introduction of defects into the crystal lattice.[80,81] In particular, the Ostwald-Freundlich Equation suggests that solubility increases when particle size is reduced, with the effect becoming significant below a particle radius of 0.5 µm:

$$\log\frac{Cs}{C\infty} = \frac{2\sigma Vm}{2.303RT\rho r} \tag{2.3}$$

where Cs is the saturation solubility, $C\infty$ is the solubility of the solid consisting of large paticles, σ is the interfacial tension of the solid substance, Vm is the molar volume of the particles, R the gas constant, T is the absolute temperature, ρ the density of the solid and r the particle radius. [81] However, the quantitative effect of nanosizing on saturation solubility remains unclear.[82–84]

In general, changes in dissolution rather than solubility remain the dominant advantage of nanosizing.

Nanosized drugs can be used for oral and parenteral delivery both preclinically as a suspension and clinically as tablet or capsule formulations.[76] An example of currently marketed products which contain nanosized drugs and are orally administered can be found in Table 3.

Table 3: Marketed products which contain nanosized drug (adapted from Williams et al.)[76].

Marketed Product	API	Pharmaceutical Form
Rapamune®	Rapamycin	Tablet
Emend®	Aprepitant	Capsule
Tricor 145®	Fenofibrate	Tablet
MegaceES®	Megestrol	Solution
Triglide®	Fenofibrate	Tablet

Amorphous solid dispersions

The term "solid dispersion" covers a range of different formulations in which a drug is dispersed within a carrier matrix. The drug can be suspended in the carrier as crystalline or amorphous particles, or may exist as a solid solution i.e. molecularly dispersed within the carrier.[76,85] It has been reported that solid dispersions in which the drug is in the amorphous form usually show faster dissolution rates than formulations which contain the crystalline drug and are thus often preferred.[86] Amorphous drugs can display an increase in apparent solubility up to several orders of magnitude in comparison to the solubility of the corresponding crystalline form. This leads to the generation of supersaturation upon dissolution, which acts as the driving force to enhance uptake across the intestinal epithelium and thus improve oral bioavailability.[74] However, due to the higher free energy of the system via the metastable state of drugs in supersaturated solutions, the supersaturation generated after dissolution can be transient and lead to precipitation of drug in a crystalline form, which is the free system favorable state. Furthermore, it should be noted that there is a high risk of reversion of the amorphous drug to its crystalline form during storage. Therefore, stabilizers are needed (usually polymer or mesoporous silica carriers) to mitigate or avoid these effects.[87]

Kaletra® (Abbott Laboratories) and Sporanox® (Janssen Pharmaceutica) comprise two excellent examples of commercially available amorphous solid dispersions. Kaletra® consists of a combination of two anti-HIV drugs (ritonavir and lopinavir) in a polyvinylpyrrolidone / vinylacetate copolymer (PVPVA) solid dispersion prepared by hot-melt extrusion.[88] This formulation exhibited greater stability and no food-effect in comparison to the respective liquid-

filled gelatin capsule formulation.[89] Sporanox® contains an antifungal agent (itraconazole) molecularly dispersed in the carrier HPMC (hydroxypropyl methylcellulose) and sprayed onto inert sugar beads.[76] Sporanox® exhibited greater oral bioavailability when compared to a formulation containing the crystalline drug.[90]

Further examples of marketed amorphous solid dispersions can be found in Table 4.

Table 4: Marketed products formulated as solid dispersions.

Marketed Product	API	Pharmaceutical Form
Sporanox®	Itraconazole	Capsule
Intelence®	Etravirine	Tablet
Prograf®	Tacrolimus	Capsule
Nivadil®	Nilvadipine	Capsule
Certican®	Everolimus	Tablet
Isoptin SR®	Verapamil	Tablet
Zelboraf®	Vemurafenib	Tablet
Incivek®	Telaprevir	Tablet
Gris-Peg®	Griseofulvin	Tablet
Cesamet®	Nabilone	Capsule
Kaletra®	Lopinavir/Ritonavir	Tablet
Norvir®	Ritonavir	Tablet

3   *Aims of Thesis and issues addressed in this work*

Currently, Physiologically Based Pharmacokinetic (PBPK) modelling is being used mostly in applications for Marketing Authorization in the areas of drug-drug interaction (DDI) studies, first-in-human dosing and pharmacokinetic extrapolations into other disease states or populations.[91] To date, there has been limited application of PBPK/ absorption models in predicting the *in vivo* performance of bio-enabling formulations in regulatory applications.[92–94]

The main goals of this work were:

    a. to investigate whether combining *in vitro* biorelevant tools with *in silico* modelling can be successfully used to mechanistically explain and better understand the *in vivo* solubility /dissolution of bio-enabling formulations and predict their *in vivo* performance

    b. to identify the challenges when developing PBPK models for bio-enabling formulations and propose potential solutions to these challenges.

In this context, the following issues were also addressed:

    a. To broaden our understanding of the physiological parameters that can play a key role in the pharmacokinetics of an orally administered formulation, the effects of drugs used to treat GI diseases on the GI physiology and on the pharmacokinetics of co-administered drugs were reviewed.

    b. Aspiration studies comprise the most valuable source of information for the design of biorelevant dissolution media. However, the values that have been reported for some physiological parameters differ substantially among studies reported in the literature. Therefore, it was necessary to analyze and critique the methodologies used to collect and process the samples and propose a "best practices" way forward.

    c. Various *in vitro* set-ups have been proposed in the literature to assess drug supersaturation and/or precipitation in the upper GI tract. Their usefulness and current application was reviewed, and "best practices" for evaluating bio-enabling formulations were proposed.

Two case example formulations were selected for this study, one containing the drug in a nanosized form (aprepitant) and one containing the drug in an amorphous solid dispersion formulation (etravarine).

4   *Key Results and Discussion*

4.1   Effects of medicines used to treat gastrointestinal diseases on the gastrointestinal physiology and on the pharmacokinetics of co-administered drugs (Publication 1).

As mentioned in the introduction, various physiological parameters can have an effect on the absorption and bioavailability of orally administered compounds. Medications used for the treatment of GI diseases often alter the GI physiology and thus affect the absorption of concomitantly administered drug products. During this work, literature concerning the effects on GI physiology and mechanisms of action of various GI medicines was reviewed, with emphasis on the effects of agents affecting the GI motility (e.g. laxatives, prokinetic agents), dietary fibers, antiemetics, gastric acid reducing agents, antibiotics used for GI conditions, probiotics, anti-inflammatory and immunosuppressive drugs for inflammatory bowel diseases and bile-acid sequestrants.

From the literature, pH was identified as a key physiological parameter which can greatly affect the pharmacokinetics of orally administered compounds. In fact, the most prevalent pharmacokinetic Drug-Drug Interactions (DDIs) related to GI physiology occur due to concomitant administration of gastric acid reducing agents (ARA). It is worth noting that studies to evaluate the effect of increased GI pH on drug absorption are now required for the marketing authorization of orally administered medicines in the European Union and the United States.[95,96]

Reduced gastric acid secretion and consequently increased gastric pH due to co-administration of ARA, i.e. proton pump inhibitors (PPI), H_2-receptor antagonists (H_2RA) and antacids,[97] or GI disease (i.e. achlorhydria)[12], has been shown to significantly reduce the absorption of many weakly basic compounds. Understanding the underlying mechanism of the interaction between GI pH and the absorption of a drug product is key to rational formulation design and a predictable *in vivo* outcome.[97] For example, Jaruratanasirikul et al. investigated the effect of 40 mg of the oral proton pump inhibitor omeprazole on the pharmacokinetics of a single 20 mg oral dose of itraconazole. It was shown that concomitant use of omeprazole resulted in reduction of the mean AUC and C_{max} of itraconazole by 64% and 66% respectively, whereby inhibition of CYP3A4 by

omeprazole could be ruled out as a factor.[98] In another study, Johnson et al. investigated the effect of concomitant administration of 40 mg oral omeprazole with a 40 mg dose of itraconazole given as an oral solution. It was reported that there was no statistically significant difference on the AUC, T_{max} and C_{max} with the co-administration of omeprazole.[99] The results of these two studies suggest that the elevation of gastric pH affects the dissolution of itraconazole capsules, leading to reduced oral bioavailability.

By contrast, it has been reported that elevated gastric pH does not affect the bioavailability of fluconazole tablets.[100] Lim et al. investigated the effect of the H_2 receptor antagonist famotidine on the absorption of fluconazole and itraconazole. Co-administration of famotidine resulted in a 52.9% decrease in C_{max} and a 51.1% decrease in the AUC of itraconazole, but no difference was observed in the pharmacokinetics of fluconazole.[101] This contrasting behavior in response to co-administration of acid reducing agents is due to the differences in the physicochemical properties of itraconazole and fluconazole: the solubility of fluconazole is high over the entire pH range of the GI tract, whereas the solubility of itraconazole is poor above its pKa. Thus, stomach acidity does not influence the dissolution rate of fluconazole or its absorption but has a profound effect on itraconazole absorption.[102,103]

Budha et al. attempted to correlate the physicochemical properties and pH-solubility profiles of various weakly basic anticancer drugs with the observed effect on the absorption caused by the elevation of gastric pH after the administration of acid reducing agents.[104] It was concluded that the impact of increased gastric pH is more prominent for those anticancer drugs which exhibit an exponentially decreasing solubility over the pH range 1-4 and for which the maximum dose strength is not soluble in 250 mL of water.[97,104]

It is therefore evident that understanding the interplay of pH and the solubility/dissolution behavior of an orally administered drug product is key to identifying a robust drug formulation and appropriate dosing conditions. Once the mechanisms of interaction are identified, biorelevant *in vitro* tools, e.g. dissolution in biorelevant media, and PBPK/ absorption modelling can be combined to investigate any bioavailability risks. This approach has already been used to explore whether bioequivalence decisions based on the outcome of clinical trials in healthy adults can be extrapolated to special populations, such as the hypochlorhydric or achlorhydric

population, using virtual clinical trials in PBPK.[97,105–107] Furthermore, this approach can facilitate the development of bio-enabling formulation approaches, such as amorphous solid dispersions, which mitigate the effects of increased gastric pH on oral bioavailability.

4.2   *In vitro* simulation of the upper gastrointestinal environment

4.2.1   Effects of sample handling and storage conditions on the measurement of physiological parameters in healthy gastrointestinal aspirates (Publication 2)

As indicated in the Introduction, biorelevant dissolution media should be representative of the human GI fluids. In practice, a balance has to be struck between feasibility in terms of preparation, costs and analytics on the one hand, and accurate representation of the GI fluids on the other hand.[47] Therefore, in addition to a thorough understanding of the GI physiology, appropriate analysis of the human aspirated samples is important in order to achieve a successful representation of the GI contents.

During this work it was observed that, among the various aspiration studies published in literature, reported values for two key physiological parameters, the pH and buffer capacity, vary widely from study to study. Up till now there is no globally accepted protocol for human aspiration studies in order to assure that comparable results/measurements are reported. It was therefore hypothesized that the results may be influenced by the methodology used to collect and process the samples.[108] It should be noted that most of the time, pH and buffer capacity are measured immediately upon sample aspiration in order to have a measurement as close to the real *in* vivo value as possible, by mitigating artificial effects such as the escape of the volatile bicarbonate buffer system, which is present in the GI contents. Indeed, it has been reported that the pH of samples aspirated from the upper intestine drift to higher values when the samples remain on the bench at room temperature.[11] The authors attributed the drift to the transformation of bicarbonates to carbon dioxide and its subsequent loss to the atmosphere.[11] Moreover, in previous work it had demonstrated that subjecting the samples to a freeze-thaw cycle significantly reduces the measured buffer capacity values in aspirates collected from the fasted stomach and upper intestine.[12]

To investigate the hypothesis that sample handling methodology affects results, all available pH and buffer capacity data reported in literature were gathered and analyzed statistically. Pairwise statistical comparisons were performed in all cases using parametric or distribution-free tests, depending on the results of the normality and equal variance tests. For this analysis SigmaPlot 11.0 (Systat Software Inc. Chicago, IL, USA) was used. The Type I error was set at 0.05.

4.2.1.1 Impact of sample handling on pH and buffer capacity of gastric aspirates of healthy adult volunteers in the fasted state

For aspirates collected from the fasted healthy adult stomach,[10–12] measurements of pH made immediately upon sample aspiration, or after one freeze-thaw cycle proved to be not significantly different (pH 1.73, n=60 [11,12] vs. pH 1.92, n=16 [10,12], Mann-Whitney, p=0.078).[108] This result was somewhat anticipated since the intragastric pH in fasted, healthy adults is mainly regulated by the concentration of hydrochloric acid.

Interestingly, however, it was observed that the median buffer capacity of gastric fluids measured immediately upon aspiration (17.4 mmol/L/ΔpH, n=60)[11,12] was far higher than after a freeze-thaw cycle (6.6 mmol/L/ΔpH, n=16 [10,12]; Mann-Whitney, p=0.007).[108]

4.2.1.2 Impact of sample handling on pH and buffer capacity of upper intestinal aspirates of healthy adult volunteers in the fasted state

As for gastric samples, the pH of samples aspirated from the fasted upper small intestine is not significantly affected by a single freeze-thaw cycle (6.35, n=47 vs 6.86, n=18, Mann-Whitney, p=0.168)[11,12,25].[108] On the other hand, also similar to the gastric samples, the median buffer capacity measured immediately upon aspiration (7.0 mmol/L/ΔpH, n=45[11,12]) was significantly higher (Mann-Whitney, p=0.019) than after one freeze-thaw cycle (4.8 mmol/L/ΔpH, n=17[12,25]).[108]

For samples aspirated from the upper small intestine, the effect of centrifugation on the pH of the sample was also investigated. It was observed that vials containing aspirates from the upper small intestine must be sealed prior to centrifugation, otherwise the median (range) pH values

increased from 6.11 (2.67-6.74) to 6.70 (2.67-7.29) [109] (p=0.008) during centrifugation at 37 °C and 12560 g for 10 min.[108]

Overall, it is evident that the accuracy of the buffer capacity measurements of fluids aspirated from the upper GI tract is compromised when these are not performed immediately upon aspiration. It is therefore recommended that reporting of the physiological pH and buffer capacity values of fluids in the fasted upper GI lumen should rely exclusively on data collected immediately upon aspiration without any additional sample handling and/or storage to ensure accuracy of measurements and comparability of results across aspiration studies.[108]. Further, only values derived in this way should be taken into consideration in the design of the biorelevant dissolution media.
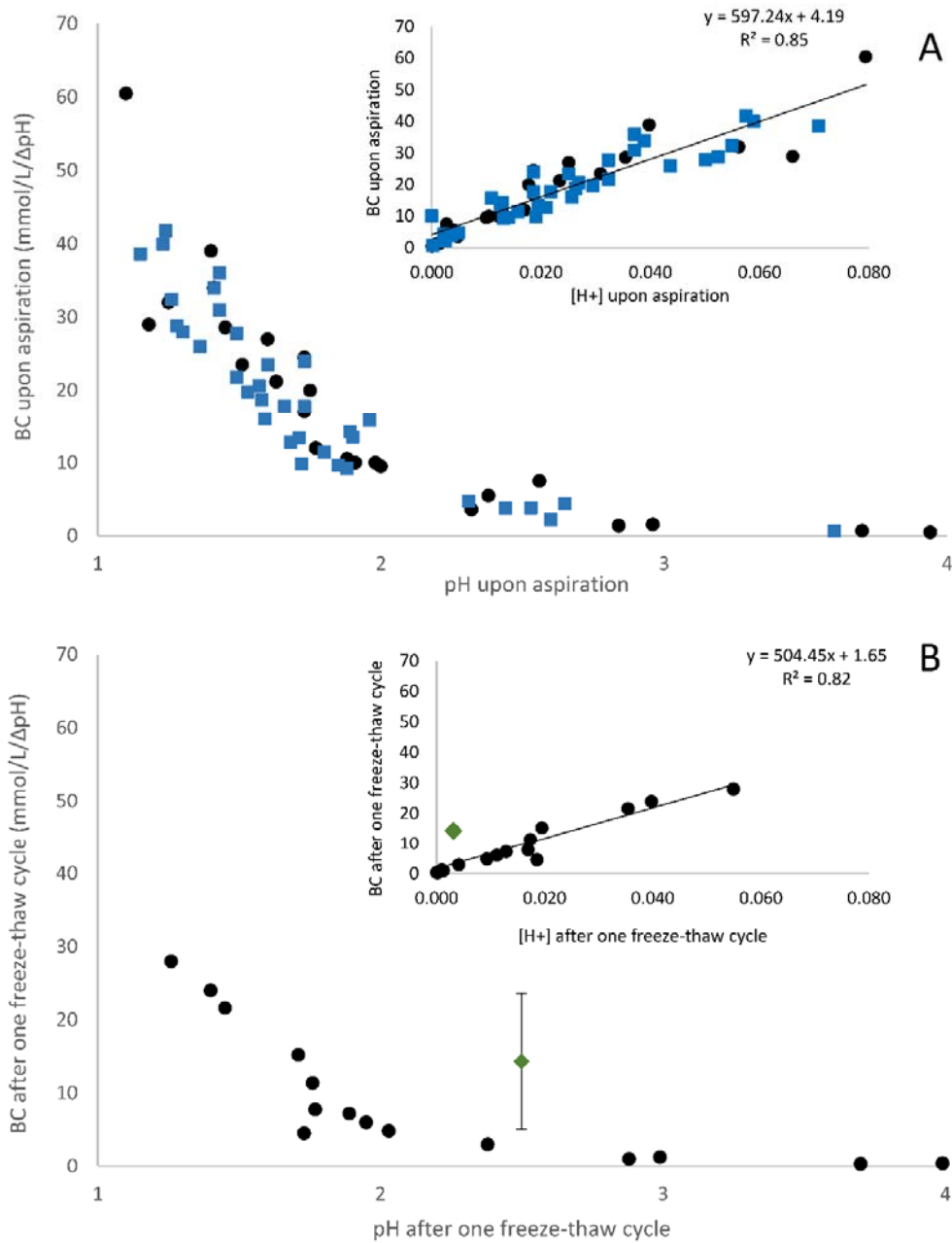
Figure 0.1: Data on the buffer capacity of gastric contents in fasted healthy adults vs. the corresponding pH values previously published by Litou et al.[12] (•, individual data), by Kalantzi et al.[11] (■, individual data), and by Pedersen et al.[10] (◆, mean ± SD data). (A) Data measured immediately upon aspiration; (B) data measured after one freeze-thaw cycle. The inserts in the figure represent the linear relationship between the buffer capacity, measured immediately upon aspiration or after one freeze-thaw cycle, with the concentration of hydrogen ions.[108]

4.2.2   *In vitro* setups to assess drug supersaturation and/ or precipitation in the upper small intestine (Publication 3)

As discussed in Chapter 1, the assessment of potential supersaturation and/ or precipitation in the GI tract is critical if the drug is a weak base with low aqueous solubility, or if a bio-enabling formulation is developed. On the one hand, for weakly basic compounds, supersaturation can occur after transfer from the stomach to the small intestine, due to the pH difference. On the other hand, in the case of bio-enabling formulations it is intended to create supersaturation for a prolonged period in the upper GI tract. However, despite the increasing interest in producing these formulations, there is still a lack of mechanistic understanding about how a supersaturated state intralumenally can be maintained.[110] In both cases, precipitation of drug results in less drug being available for absorption, which in turn often leads to reduced bioavailability, jeopardizing the therapeutic efficacy of the drug. Therefore, it is of great importance to establish reliable *in vitro* methods to simulate the transfer of the drug through the upper GI tract to predict *in vivo* supersaturation/precipitation characteristics/kinetics.[110]

Currently, there are various small and full scale *in vitro* setups to predict supersaturation and/ or precipitation in the upper small intestine. The small scale *in vitro* setups are used in the early stages of drug development, since they enable use of a small quantity of the drug candidate and reduce the quantity of biorelevant media required, which helps to reduce expenses, especially when large numbers of candidates are to be screened.[110] Full scale setups are used in later stages of formulation development, since larger amounts of the drug are available. Furthermore, at later stages, it is imperative to accurately characterize and predict the behaviour of the formulation after administration of clinically relevant doses and to understand the effect of different excipients on the precipitation kinetics of the formulated drug. The taxonomy classification of the various setups, as described during this work, is depicted in Figure 0.2.[110]
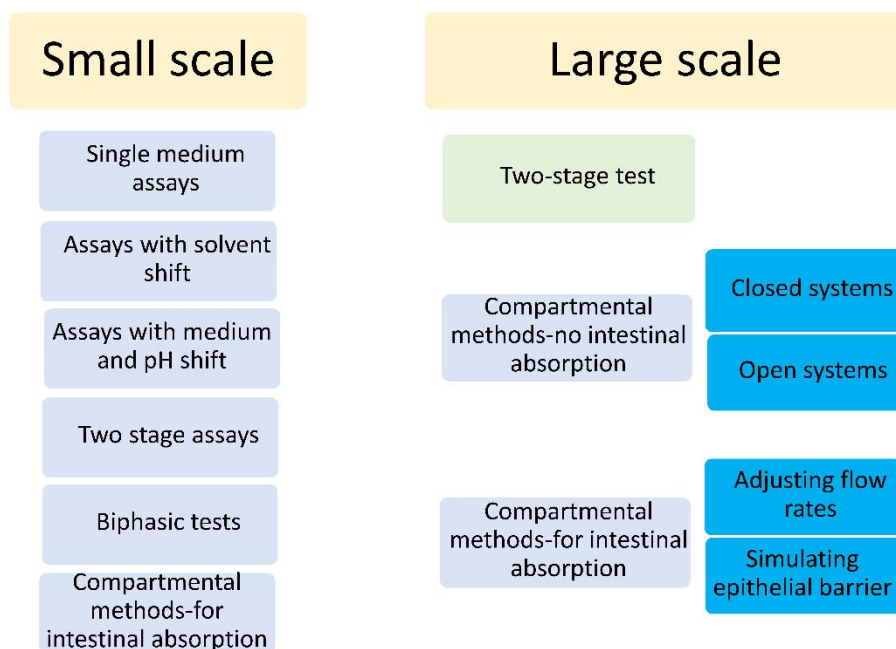
Figure 0.2: Classification of in vitro setups to assess drug supersaturation and/ or precipitation in the upper small intestine.[110]

In the present work, a full scale biorelevant *in vitro* setup, i.e. the "Kostewicz transfer model", was used to assess the supersaturation/precipitation kinetics of bio-enabling formulations. It is a two compartment compendial dissolution method, in which the contents of the "donor" vessel, in which dosage form's performance under simulated gastric conditions is evaluated, are continuously transferred with a pump into the "acceptor" vessel, in which the conditions in the small intestine are simulated.[111] It is referred to as a "closed system", since there is no attempt to simulate the absorption from the acceptor, i.e. "intestinal", vessel. Ruff *et al.*,[112] attempted to optimize the experimental conditions of the originally proposed transfer model, using ketoconazole as the model compound. In that study, the "average" physiological GI conditions were also taken into consideration. In the present work, a slightly updated version of the transfer model was used, as described previously by Berlin et al.[113] The results of the transfer model experiments are summarized for each formulation in the following sections.

Last but not least, as it has been shown for many cases that a combination of the *in silico* and *in vitro* methods can successfully simulate supersaturation and precipitation *in vivo*.[110,112,114–

118] Thus, for the drugs studied in this work, the *in vitro* data were coupled with *in silico* PBPK models.

4.3   Predicting the *in vivo* performance of bio-enabling formulations

4.3.1   Rationale for selecting the drugs and dosage forms

In order to meet the main goals of this dissertation, drugs with appropriate physicochemical characteristics and which are marketed as bio-enabling formulations were selected. In particular, the drug should belong to BCS Class II or BCS Class IV and have weakly basic properties, since this group is most prone to supersaturation/ precipitation issues after oral administration. With respect to the formulation, it should be available on the market in at least two dose strengths so that the effect of dose on the precipitation kinetics can be investigated and the developed PBPK model can be scaled from the lower to the higher dose (or *vice versa*). Last but not least, there should be enough clinical data on the formulations available in literature to be able to validate and assess the prediction success of the developed PBPK models.

Keeping all these criteria in mind, two drugs and their respective dosage forms were selected. These were EMEND® capsules, in which the drug, aprepitant, is nanosized, and INTELENCE® tablets, in which the drug, etravarine, is formulated as an amorphous solid dispersion.

4.3.1.1 Aprepitant/ EMEND®

Aprepitant is a selective substance P neurokinin (NK1) receptor antagonist which, in combination with other antiemetic agents, is indicated for the prevention of both acute and delayed nausea and vomiting associated with emetogenic cancer chemotherapy.[119,120] It is available as oral capsules (40, 80 and 125 mg), under the brand name EMEND® (reference listed product) and as a water soluble prodrug form, fosaprepitant dimeglumine, for intravenous administration (EMEND® for injection).[119] For ambulant therapy, EMEND® is administered for three days with a recommended dosing regimen of 125 mg given once orally on Day 1 and 80 mg given orally once daily on Days 2 and 3.[119]

Aprepitant has both very weak acidic and very weak basic properties and possesses a logD of 4.8 at pH 7.0.[81,82,116,121,122] According to Wu et al.,[121] it exhibits very low aqueous solubility (3-7

µg/mL over the pH range 2-10), although solubilities of just 0.37 µg/mL and 0.8 µg/mL in phosphate buffers at pH 6.5 were reported by Söderlind et al. and Takano et al., respectively.[123,124] A wide range of permeability values from Caco-2 assays have been reported for aprepitant in the open literature including a P_{app} of 7.8 x 10^{-6} cm/s (no reference substance value provided),[81,121] a P_{app} of 170 x 10^{-6} cm/s (no reference substance value provided),[116] or a P_{app} of 21 x 10^{-6} cm/s with metoprolol as a reference compound (P_{app} = 5 x 10^{-6} cm/s)[124]. Due to its permeability and solubility properties, aprepitant has been classified as a borderline BCS II/IV compound.[81,82]

The aprepitant tablet formulations used in the early clinical phases exhibited high variability and a large positive food effect on absorption. Considering the target patient group addressed by aprepitant (cancer patients suffering from nausea and vomiting), administration with food was deemed unacceptable and, therefore the next formulation efforts were focused on attenuating the food effect and improving dissolution characteristics. This was accomplished by decreasing the particle size to the nanoscale range (approx. 200 nm).[119,125] After administration of the EMEND® 80 mg and 125 mg capsules, which contain the nanosized drug, the absolute bioavailability under fasting conditions is 67% (62-73%) and 59% (53-65%), respectively. The mild increase in bioavailability after the administration of a standard breakfast (the geometric means AUC_{fed}/ AUC_{fasted} for the 125 mg and 80 mg dose are reported to be 1.20 and 1.09, respectively) is not considered clinically relevant.[119,125,126] Thus, the nanosized formulation allows full dosing flexibility with respect to food intake.

4.3.1.2 Etravirine/ INTELENCE®

Etravirine is a second generation non-nucleoside reverse transcriptase inhibitor used for the treatment of HIV-1 infection in treatment-experienced adult patients and pediatric patients two years of age and older, usually in combination with other anti-retroviral agents.[127–129] It has been classified as a BCS Class IV compound as it has very low aqueous solubility, irrespective of the pH (solubility in water is reported to be lower than 1 µg/mL)[130], and low to intermediate permeability.[131] It is a weakly basic compound (reported pKa values are 4.5, 3.75 and <3)[132–134] with a high logP value (reported values are 5.2 and 5.54)[132,135].

To overcome the poor physicochemical properties of crystalline etravirine and to improve its bioavailability, the manufacturer attempted a variety of different enabling technologies. However, most of them did not result in advantageous outcomes (for example, an orally dosed nano-suspension resulted in negligible plasma concentrations in dogs)[130]. Among the various formulations developed and administered in different phases of the clinical trials, the amorphous solid dispersion of etravirine was the most promising formulation, and is nowadays the commercial formulation (INTELENCE®).[130,131] The recommended dose of INTELENCE® for adults is 100 mg or 200 mg, taken orally twice daily following a meal.[128,129] The bioavailability of INTELENCE® in the fed state is increased by up to 50% in comparison to the bioavailability in the fasted state.[129,131,134] Moreover, the pharmacokinetics of INTELENCE® seem to be more than dose proportional. However, the absolute bioavailability has not been determined since no intravenous formulation is available.

4.3.2   Case example 1: Predicting the *in vivo* performance of EMEND® (Publication 4)

Studies during this work aimed to:

1) investigate the advantages of using biorelevant media vs. simple buffers in simulating the *in vivo* performance of aprepitant,
2) build a PBPK model by combining experimental data and information available in literature with the commercially available *in silico* software Simcyp Simulator V16.1 (Certara UK Ltd.) and
3) mechanistically understand the *in vivo* behavior of aprepitant in both the fasted and fed states.[136]

4.3.2.1 In vitro characterization of pure aprepitant and EMEND® capsules

At first, the pure unformulated API, namely aprepitant, and the EMEND® 80 mg and 125 mg capsules were fully characterized *in vitro* by utilizing biorelevant tools. For this purpose solubility, dissolution and transfer model experiments were conducted by using various versions of biorelevant media simulating both fasted and fed states.

Solubility

The solubility of pure aprepitant powder was investigated using the method of Andreas et al.[137] in Level I and Level II biorelevant media,[47] utilizing the Uniprep™ system (Whatman®, Piscataway, NJ, USA).

The solubility values obtained in Level II compared with Level I biorelevant media indicate a major impact of the amount and type of native surfactants on the solubility of aprepitant. Similar observations have been reported by Zhou et al. and Niederquell and Kuentz.[138,139]

Mean solubility values of pure aprepitant at 24 h in the various versions of biorelevant media are presented in Table 5.

Dissolution

In USP II dissolution experiments the dissolution of the pure drug was fast, incomplete and reached a plateau value at around 4 % dissolved within approximately the first 10 min. Interestingly, the concentrations of dissolved drug in the dissolution vessels exceeded the thermodynamic solubility observed for the pure drug in the respective media suggesting a transient supersaturation.

Decreasing the particle size of aprepitant to the nanoscale (in the formulation) results in a much higher dissolution rate, which can be attributed to the large increase in surface area and surface energy. The mean maximum concentrations of dissolved aprepitant achieved in the dissolution vessel in the various versions of biorelevant media, as well as the ratio of these concentrations to the thermodynamic solubility are presented in Table 5. The mean (±SD) % and concentrations of aprepitant dissolved from 80 mg and 125 mg EMEND® capsules in various biorelevant media can be found in Figure 0.3 and Figure 0.4, respectively.

The *in vitro* dissolution experiments suggest that, also during dissolution of EMEND® capsules, aprepitant achieves supersaturation. Moreover, it seems that the solubilization of aprepitant by native surfactants present in the intestine is likely one of the major factors affecting the *in vivo* dissolution of aprepitant from the marketed formulation. The experiments conducted in biorelevant media simulating the fed state also highlight the importance of surfactants on the apparent solubility of the nanosized aprepitant. For example, the maximum concentration

achieved in FeSSIF V1 (fed state) is more than 4-fold greater than that achieved in FaSSIF V1 (fasted state), which is similar to the ratio of NaTc in FeSSIF V1 to FaSSIF V1 (15:3).

Table 5: Aprepitant mean maximum dissolved concentrations achieved in the dissolution vessel resulting after dissolution experiments of 80 mg and 125 mg EMEND® capsules (formulated drug) in various biorelevant media, 24 h solubility value of the crystalline API and ratio of these values

Biorelevant Medium	Solubility crystalline drug (µg/mL)	Maximum concentration of dissolved drug (µg/mL)	Ratio
Fasted state			
Level III FaSSGF	5.8	15.5	2.7
Level II FaSSIF V1	9.9	26.8	2.7
Level II FaSSIF V3	3.0	27.6	9.2
Fed state			
Level II FeSSIF V1	53.9	120	2.2
Level II FeSSIF V2	68.6	149	2.2
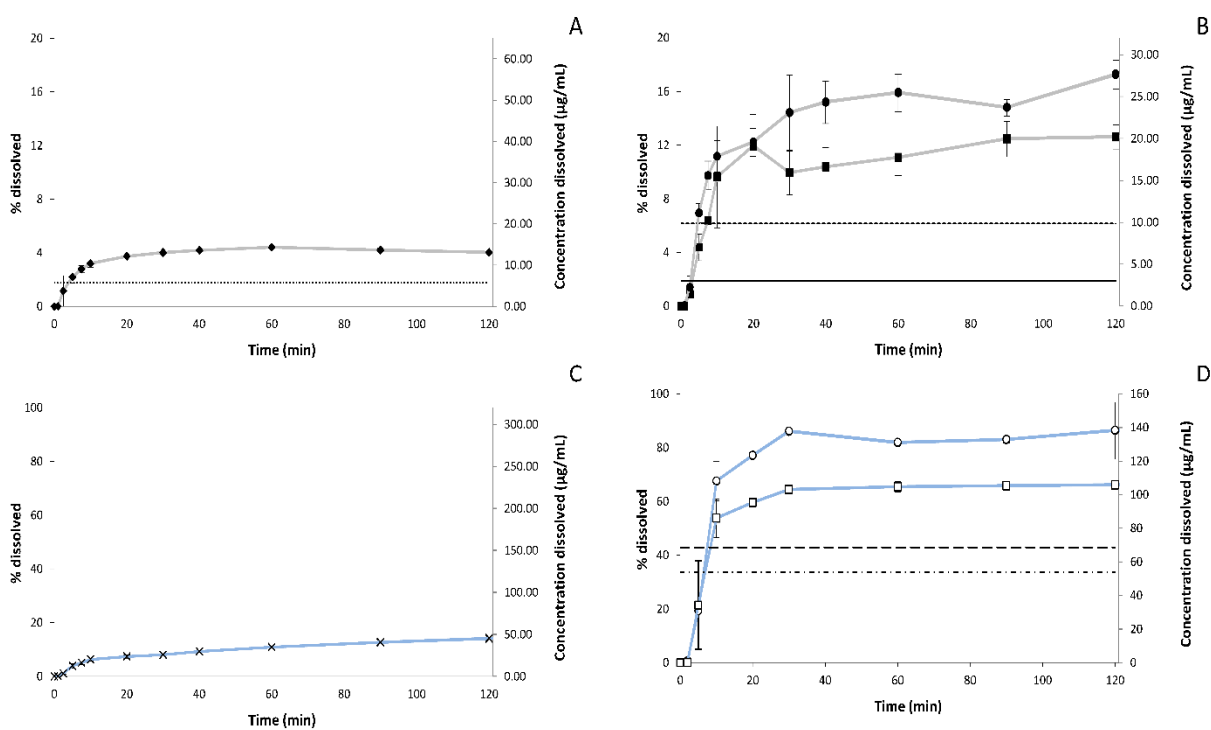
Figure 0.3: Mean (±SD) % and concentrations of aprepitant dissolved from 80 mg EMEND® capsules in: A) Level III FaSSGF (◆) B), Level II FaSSIF V1(■), Level II FaSSIF V3 (•), C) Level II FeSSGFmiddle (x) and D) Level II FeSSIF V1 (□) and Level II FeSSIF V2 (◯). With the round dotted line, square dotted line, solid line, dashed-dotted line and dashed line the solubility of the crystalline aprepitant in Level III FaSSGF, Level II FaSSIF V1, Level II FaSSIF V3, Level II FeSSIF V1 and Level II FeSSIF V2 is presented, respectively.[136]
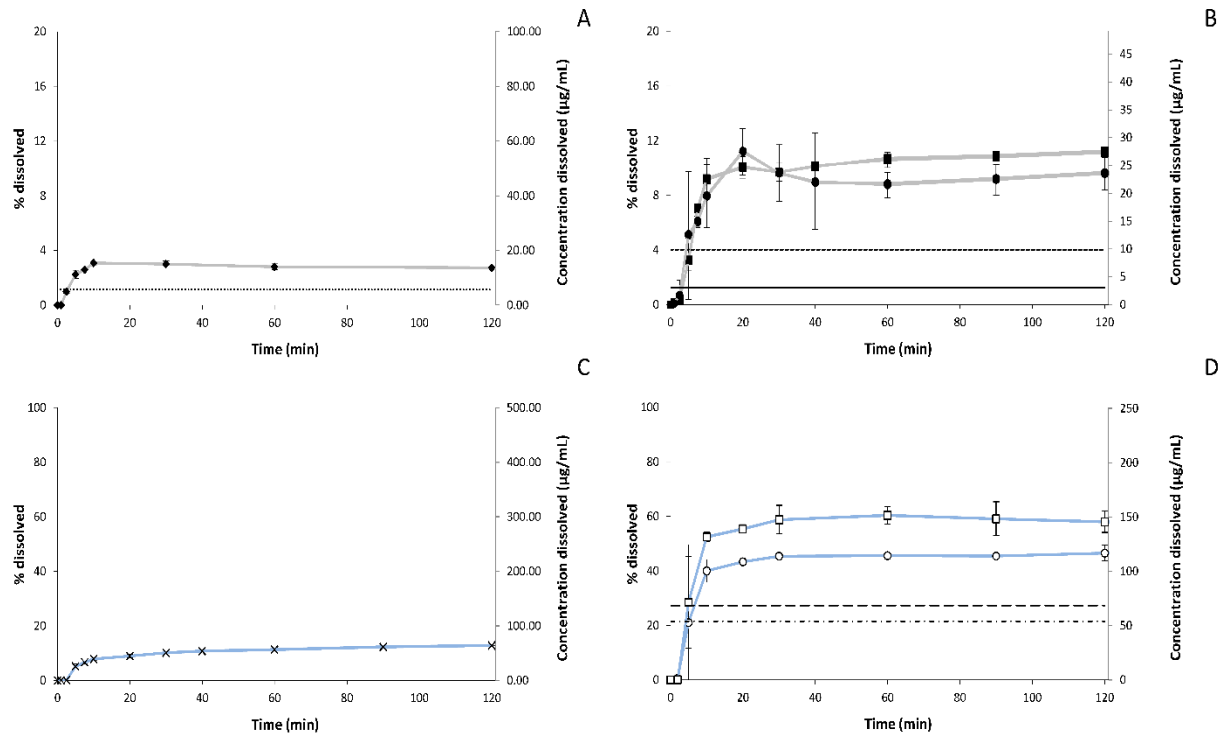
Figure 0.4: Mean (±SD) % and concentrations of aprepitant dissolved from 125 mg EMEND® capsules in: A) Level III FaSSGF (◆) B), Level II FaSSIF V1(■), Level II FaSSIF V3 (•), C) Level II FeSSGFmiddle (x) and D) Level II FeSSIF V1 (□) and Level II FeSSIF V2 (○). With the round dotted line, square dotted line, solid line, dashed-dotted line and dashed line the solubility of the crystalline aprepitant in Level III FaSSGF, Level II FaSSIF V1, Level II FaSSIF V3, Level II FeSSIF V1 and Level II FeSSIF V2 is presented, respectively.[136]

Transfer model

Transfer experiments were performed for both the 80 mg and 125 mg EMEND® capsules in USP II apparatus, as described previously by Berlin et al.[113] Briefly, 250 mL of Level III FaSSGF pH 2.0 and 350 mL of Level II FaSSIF V1 or FaSSIF V3 were used as the dissolution media in the gastric and intestinal compartment, respectively. The rotating speed of the paddles was set at 75 rpm. The temperature in the vessels was maintained at 37±0.5 °C throughout the experiment. A peristaltic pump set to first order kinetics ($t_{1/2}$ = 9 min) was used to transfer the medium from the gastric to the duodenal compartment, from which samples were withdrawn.[136]

During the four hours of the experiment, no precipitation of aprepitant was observed. The maximum dissolved concentration was achieved more slowly than in the dissolution

experiments, since the appearance of the drug in the intestinal compartment is limited by the rate of transfer from the compartment representing the stomach to the one representing the small intestine. Additionally, the maximum dissolved concentration and plateau values achieved in the transfer experiments were somewhat lower than those of the dissolution experiments in media simulating the fasted upper small intestine. This was attributed to the dilution of the intestinal compartment by fluid transferred from the gastric compartment.[136]

The mean (±SD) % aprepitant dissolved from 80 mg EMEND® and 125 mg capsules resulting from the transfer experiments is presented in Figure 0.5.
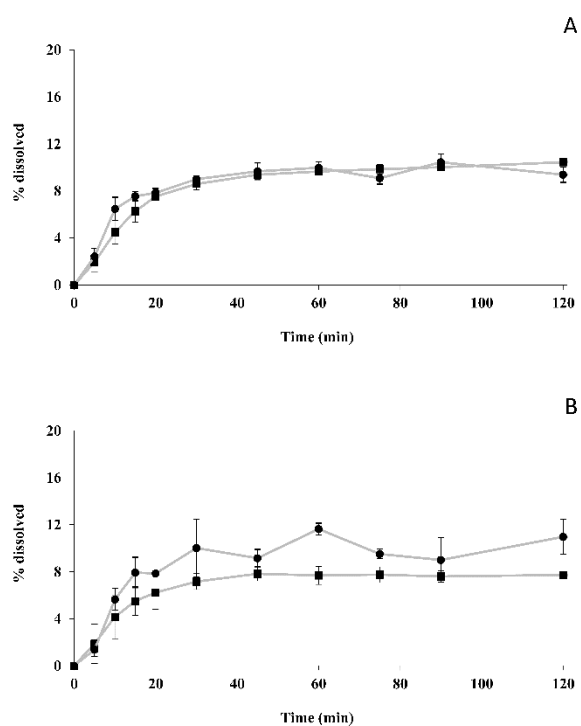
Figure 0.5: The mean (±SD) % aprepitant dissolved from: A) 80 mg EMEND® capsules and B) 125 mg EMEND® capsules, sampled from the intestinal compartment during transfer experiments from Level III FaSSGF (pH =2) to Level II FaSSIF V1 (■) and to Level II FaSSIF V3 (●).

4.3.2.2 Building a PBPK model for the EMEND® capsules

At first, disposition parameters were estimated from literature i.v. data.[126] The distribution of aprepitant was described using a minimal PBPK model with a Single Adjusting Compartment

(SAC) in the Simcyp Simulator® (V17.1, Certara UK Ltd.). SAC is a non-physiological compartment that represents a cluster of tissues (excluding the liver and portal vein).

To model the clearance, the "Enzyme Kinetics" option in Simcyp was chosen since aprepitant exhibits saturable metabolism and non-linear pharmacokinetics. The V_{max} (*in vitro* maximum velocity for metabolism of the compound by the given isoform of enzyme) and K_m (*in vitro* Michaelis-Menten constant for metabolism of the compound by the given isoform of enzyme) for CYP3A4 were derived by Sanchez et al.[140] The renal clearance for aprepitant was set at a minimum value corresponding to the product of plasma f_u (fraction unbound) and urine flow, as also indicated in the EMA scientific discussion document for the approval of EMEND® capsules.[141–143]

In order to continue building the PBPK model after oral administration of the aprepitant capsules, the so called "middle-out" approach was followed. The middle-out approach is a way of informing the modelling process with known clinical data, rather than relying only on the structure, permeability and physicochemical properties of the drug. This entailed the implementation of (i) the calculated post-absorptive parameters from the i.v. data together with (ii) the results from the *in vitro* dissolution and transfer model experiments.

In particular, to model the absorption process, the Advanced Dissolution, Absorption and Metabolism (ADAM) model was utilized.[144] This model divides the GI tract to 9 anatomically distinct segments starting from stomach through small intestine to the colon, and has been described in detail by Jamei et al. and Darwich et al.[144,145] There was no need to invoke precipitation in the PBPK simulations, based on the transfer model experiments. Moreover, since the experimental results demonstrated that the final concentration of aprepitant in the dissolution experiments is well above the equilibrium solubility, the maximum concentration measured in the dissolution experiments in each biorelevant medium was used to reflect the *in vivo* solubility of the formulated (nanosized) aprepitant. This approach led to an accurate simulation of the plasma profiles. Permeability was estimated by using the Parameter Estimation Tool by fitting the *in vivo* PK data following oral administration in the fasted state (simultaneous fit of PK profiles after administration of 80 mg and 125 mg) and was in line with the P_{app} values reported in literature by Shono et al.,[82] Wu et al.[121] and Takano et al.[124]

The simulated plasma profiles after i.v. administration of radio-labeled aprepitant, as well as after oral administration of capsules at both dose strengths in fasted and fed states vs. the observed plasma concentrations, are presented in Figure 0.6, Figure 0.7 and Figure 0.8, respectively.
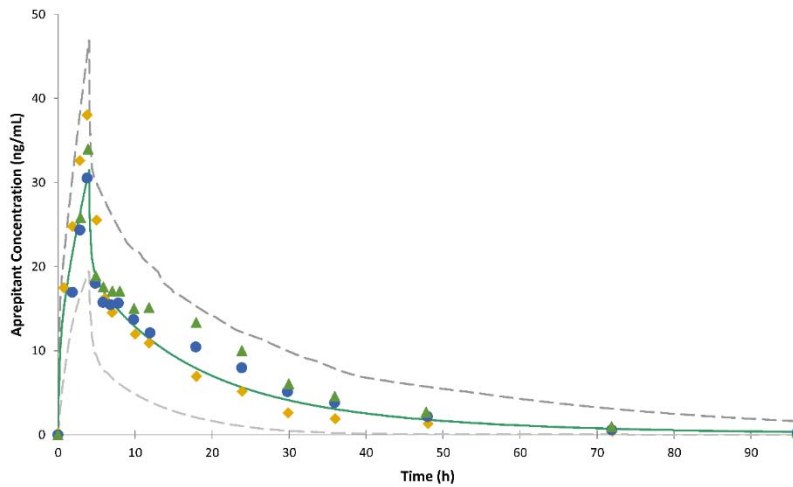
Figure 0.6: Simulated (thick green line, population mean; dash grey lines, 5th and 95th percentile of population) and clinically reported plasma concentration-time profiles after i.v. administration of 2 mg radio-labelled aprepitant (diamonds), 2 mg radio-labelled aprepitant i.v. concurrently with one 80 mg EMEND® capsule (circles) and 2 mg radio-labelled aprepitant i.v. concurrently with one 125 mg EMEND® capsule (triangles).[126,136]
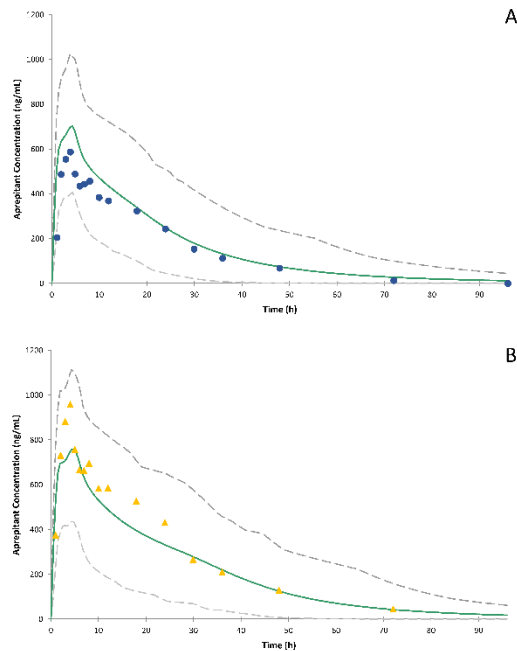
Figure 0.7: Simulated (thick green line, population mean; dash grey lines, 5th and 95th percentile of population) and clinically reported (circles) plasma concentration-time profiles after administration of an: A) 80 mg EMEND® capsule and B) 125 mg EMEND® capsule. [126,136]
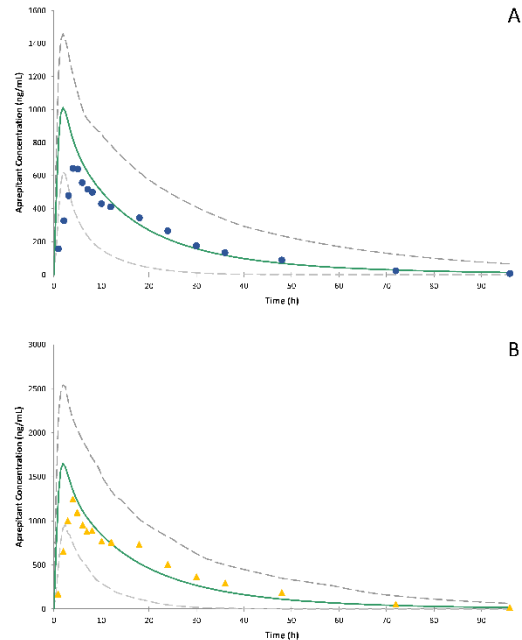
Figure 0.8: Simulated (thick green line, population mean; dash grey lines, 5th and 95th percentile of population) and clinically reported (circles) plasma concentration-time profiles after administration of an: A) 80 mg EMEND® capsule and B) 125 mg EMEND® capsule.[126,136]

4.3.2.3 Key results from case example 1 - EMEND®

The main observations resulting from the investigations with the bio-enabling formulation of aprepitant, i.e. the nano-sized EMEND® capsules, can be summarized as follows:

a. As indicated by the *in vitro* experiments, solubilization and wetting by native surfactants are the most important influence on the *in vivo* dissolution of aprepitant from the marketed formulation.[136]

b. Variation in the concentration of native surfactants has a greater impact than intestinal pH on the EMEND® *in vivo* profiles, as demonstrated by Parameter Sensitivity Analysis (PSA). According to the PSA, variations in the observed C_{max} can be explained by differences in bile component concentrations among subjects.[136] Furthermore, the PSA results suggested that variations in intestinal bile concentration among individuals would mainly affect C_{max} rather than AUC values.

c. Dissolution experiments with the formulated drug were crucial in identifying the apparent *in vivo* solubility of aprepitant in the commercial product. The use of Level II biorelevant media, which simulate the existence of native surfactants in the GI fluids, was imperative in order to identify this value.[136]

d. Taking all of the above points into consideration, along with the relatively high permeability of the compound, it seems that aprepitant should be classified as a DCS IIb compound,[66] i.e. a drug whose oral absorption is primarily limited by solubility.

4.3.3   Case example 2: Predicting the *in vivo* performance of INTELENCE® (Publication 5)

The *in vivo* performance of the amorphous solid dispersion of etravirine, i.e. INTELENCE® tablets was then investigated according to the approach that had been established for nano-sized aprepitant.

Studies during this work aimed to:

1) investigate and discuss the advantages of using biorelevant *in vitro* setups in simulating the *in vivo* performance of INTELENCE® 100 mg and 200 mg tablets, in the fed state
2) build a PBPK model by combining experimental data and literature information with the commercially available *in silico* software Simcyp® Simulator V17.1,
3) discuss the challenges when predicting the *in vivo* performance of an amorphous solid dispersion and identify the parameters which influence the pharmacokinetics of etravirine most, when administered orally in the fed state.[146]

4.3.3.1 In vitro characterization of pure etravirine and INTELENCE® tablets

First, pure etravirine as well as INTELENCE® 100 mg and 200 mg capsules were fully characterized *in vitro* by utilizing biorelevant tools. Solubility, dissolution and transfer model experiments were conducted using various versions of biorelevant media simulating both the fasted and fed states.

<u>*Solubility*</u>

The solubility of pure crystalline etravirine was investigated in various versions of Level II biorelevant media. Mean solubility values of pure etravirine at 24 h in the various versions of biorelevant media are presented in Table 6.

It should be noted that for simple aqueous buffers (i.e. Level I media, without the addition of native surfactants) the solubility of crystalline etravirine was always below the limit of quantification (0.05 μg/mL). It is interesting to note that the same observation was also made in Level III FaSSGF, despite the fact that etravirine is a weak base and thus higher solubility values are expected in media with acidic pH. These data are in line with those of Bevernage et al., who reported extremely low solubility values in Level II FaSSGF (approximately 0.009 μg/mL).[132]

By contrast, the solubility values of crystalline etravirine in Level II biorelevant media simulating the gastric and intestinal fluids in fasted and fed states were measurable and were dependent on the amount and type of surfactants used in the respective medium.[146] In particular, comparison of solubility between Level I and II media reveals the role of naturally occurring surfactants in the solubility of etravirine. These data are in line with those of Bevernage et al., who reported similar values in Level II FaSSIF V1 and Level II FeSSIF V1 (approximately 1 µg/mL and 6.2 µg/mL, respectively).[132,147] As for aprepitant, it seems that the amount and type of native surfactant rather than pH play a key role in the solubility of etravirine.

Dissolution

Dissolution experiments were performed on INTELENCE® tablets at both dose strengths in various biorelevant media simulating both the fasted and fed states. The mean concentration of dissolved etravirine with time during the first 4 h of the dissolution experiments is presented in Figure 0.9, Figure 0.10 and Figure 0.11.

As observed in these figures, dissolution at both doses is fast, incomplete and reaches a maximum value of dissolved etravirine concentration within 15-30 minutes. The dissolution results in biorelevant media simulating the fed vs. fasted state are clearly in agreement with the large food effect (approximately 50%) observed *in vivo* for INTELENCE® tablets.

Once the maximum value is reached, the concentration of dissolved drug decreases to a 24 h value, which is similar for the 100 mg and 200 mg tablets. The time to reach this 24 h value is dependent on the type of biorelevant medium used for the dissolution experiment and the dose / maximum dissolved concentration of etravirine achieved. The 24 h concentrations resulting from the dissolution experiments of the formulated drug, as well as their ratios to the 24 h solubility value of crystalline etravirine in the respective media, are presented in Table 6. Comparison of the 24 h value from the dissolution experiment with the formulated drug and the crystalline pure drug shows that the concentration of etravirine in the tablet dissolution experiment remains supersaturated over the entire duration of the experiment. Differential Scanning Calorimetry (DSC) experiments conducted with the solid collected at the end of the dissolution experiments revealed the absence of any crystalline drug. Taken together with the

concentrations achieved in dissolution of the INTELENCE® tablets, this result suggests that the solubility of the amorphous form is substantially higher than that of the crystalline form.[146] When comparing the ratios of the maximum concentrations reached after dissolution of the 200 mg and 100 mg INTELENCE® tablets in the various versions of biorelevant media, it is interesting to note that higher ratios (> 2:1) are observed in the media which also contain other components (e.g. glyceryl monooleate in Level II FeSSIF V2) rather than just sodium taurocholate (NaTC) and lecithin (e.g. Level II FaSSIF V1 and FeSSIF V1). This observation suggests that etravirine interacts differently with the various biorelevant components, such that addition of additional lipid components like glycerylmonooleate not only increases the amount of etravirine dissolved, but also leads to a longer duration of drug in solution.[146] This observation is similar as those made by Elkhabaz et al., who observed different interactions between the biorelevant components and the amorphous form of ezetimibe.[148]

Table 6: Etravirine mean dissolved concentrations resulting after 24 h dissolution experiments of 100 mg and 200 mg INTELENCE® tablets (formulated drug) in various biorelevant media, 24 h solubility value of the crystalline API and ratio of these values.

Biorelevant Medium	Solubility crystalline drug (µg/mL)	Mean concentration of drug dissolved after 24 h of dissolution (µg/mL)	Ratio
Fasted state			
Level III FaSSIF V1	0.7	6.1	8.7
Level II FaSSIF V2	0.2	1.7	7.0
Level II FaSSIF V3	0.1	0.7	6.2
Fed state			
Level II FeSSGF	3.7	29.4	8.0
Level II FeSSIF V1	3.2	23.9	7.3
Level II FeSSIF V2	3.5	13.4	3.7
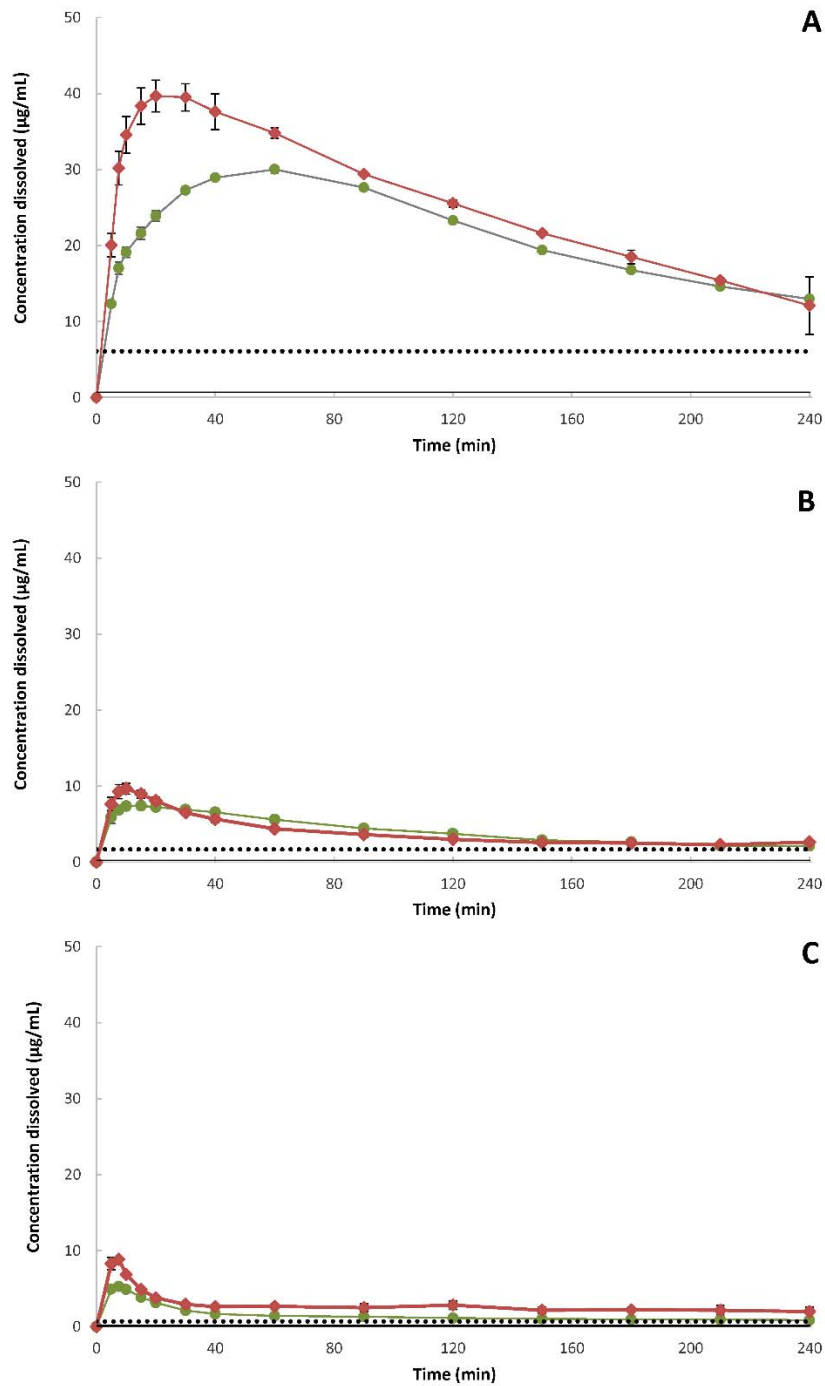
Figure 0.9: Mean (±SD) concentration of dissolved etravirine from 100 mg (●) and 200 mg (◆) INTELENCE® tablets in various media simulating the fasted upper small intestine: A) Level II FaSSIF V1, B) Level II FaSSIF V2 and C) Level II FaSSIF V3. The solid and dotted lines represent the 24 h solubility value of crystalline etravirine and the 24 h value resulting from the dissolution experiments of the formulated drug, respectively.[146]

Figure 0.10: Mean (±SD) concentration of dissolved etravirine from 100 mg ( ) and 200 mg ( ) INTELENCE® tablets in Level II FeSSGF. The solid and dotted lines represent the 24 h solubility value of crystalline etravirine and the 24 h value resulting from the dissolution experiments of the formulated drug, respectively.[146]
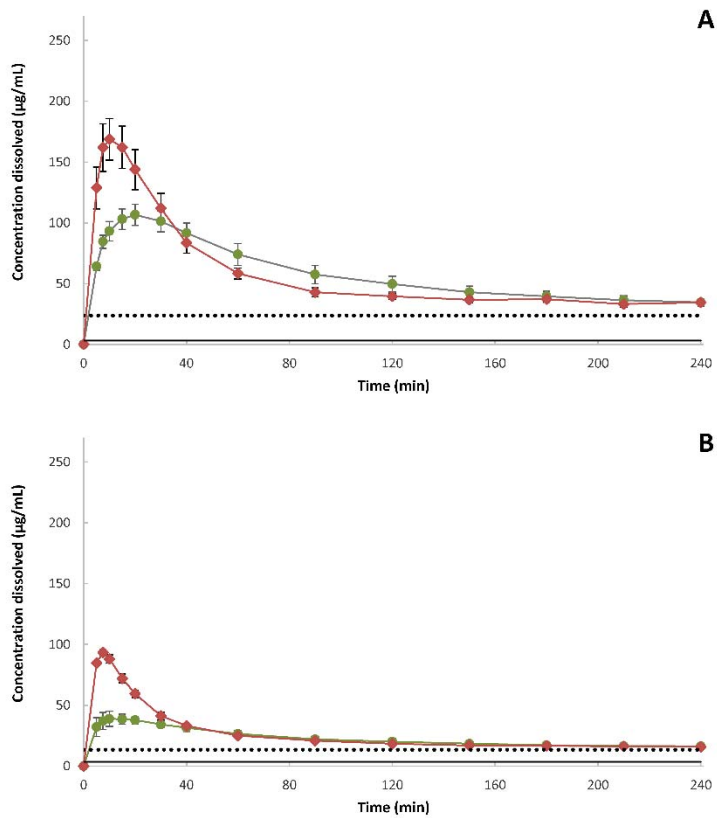
Figure 0.11: Mean (±SD) concentration of dissolved etravirine from 100 mg ( ) and 200 mg ( ) INTELENCE® tablets in various media simulating the fed upper small intestine: a) Level II FeSSIF V1 and b) Level II FeSSIF V2. The solid and

dotted lines represent the 24 h solubility value of crystalline etravirine and the 24 h value resulting from the dissolution experiments of the formulated drug, respectively. [146]

Transfer model

Transfer experiments were performed to further investigate the potential for supersaturation and precipitation of etravirine. The method followed was as described in 4.3.2.1 for aprepitant. In this case, for the intestinal compartment, in addition to Level II FaSSIF V1 and Level II FaSSIF V3, another medium, Level II FaSSIF V1$_{concentrated,}$ was utilized. Level II FaSSIF V1$_{concentrated}$ has the same composition as Level II FaSSIF V1, however, the concentration of NaTC is adjusted to 5.14 Mm (as opposed to 3 mM), in order to account for the dilution occurring during transfer.

The mean concentration (SD) of dissolved etravirine with time during the four hour transfer experiments from Level III FaSSGF to Level II FaSSIF V1, Level II FaSSIF V3 or Level II FaSSIF V1$_{concentrated}$ for the 100 mg and 200 mg INTELENCE® tablets are presented in Figure 0.12.

In accordance with the monophasic dissolution and solubility experiments, a pronounced effect of the amount and type of surfactants of the biorelevant medium on the concentration of etravirine generated in the transfer studies was observed. In particular, the maximum concentration dissolved during the transfer experiments were highest when the drug was transferred to a medium with an initially higher surfactant concentration, i.e. Level II FaSSIF V1$_{concentrated}$ (5.14 mM NaTC) vs. Level II FaSSIF V1 (3 mM NaTC). Furthermore, as previously mentioned, the type of surfactant seems to play a role in the dissolution of the amorphous etravirine. When etravirine is transferred from the amorphous solid dispersion into Level II FaSSIF V3, which also contains glycocholate and cholesterol, there is a greater ratio between the maximum concentration dissolved from 200 mg tablets vs. 100 mg tablets in comparison to the ratios achieved when the same formulation is transferred to media containing only sodium taurocholate and lecithin. [146]

Comparing the transfer with the dissolution experiments in media simulating the fasted state, the etravirine concentration starts to decrease later in the transfer experiments (after approximately 90-120 min) than in the dissolution experiments (after 30 min), and at a slower rate than observed in the single medium dissolution experiments. Although it would be interesting to know whether similar differences are observed under fed state conditions, there is

currently no validated transfer setup for simulating drug transfer from the fed stomach to the fed small intestine (noting that some early attempts have been made).[4] Nonetheless, the similar maximum concentrations of dissolved etravirine achieved in Level II FeSSGF and Level II FeSSIF V1, together with the moderate permeability of etravirine, suggest that precipitation is unlikely to happen in the fed state *in vivo*.[146]
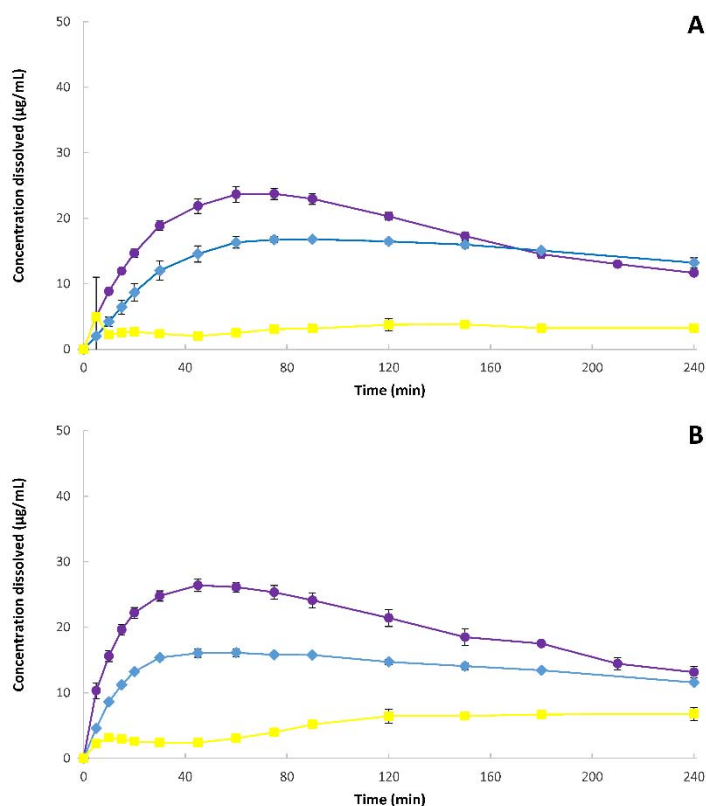
Figure 0.12: Mean (±SD) concentration of dissolved etravirine from A) 100 mg and B) 200 mg INTELENCE® tablets in Level II FaSSIF V1 (◆), Level II FaSSIF V3 (■) and Level II FaSSIF V1$_{concentrated}$ (●) after transfer from Level III FaSSGF.[146]

4.3.3.2 Building a PBPK model for the INTELENCE® tablets

Based on the properties of the compound as well as the apparent volumes of distribution (420-1370 L)[135,149–152] reported in the literature, a full PBPK model was set up for etravirine.

The apparent volume of distribution and clearance were estimated using the Parameter Estimation (PE) Tool, by simultaneously fitting these parameters to all individual PK profiles available for the 100 mg and 200 mg dose strength. For the enzyme kinetics the values reported

in the study of Yanakakis and Bumpus[153] were used, as previously described in population PK studies in the literature [150,154], whereas the clearance due to other pathways was estimated from the available individual *in vivo* profiles for the 100 mg and 200 mg doses under the assumption of a constant apparent volume of distribution at both doses. Since etravirine pharmacokinetics are not dose-proportional, the clearance estimated for the additional pathways was different for each dose, such that for the 200 mg dose the value was approximately half of the value estimated for the 100 mg dose.

To model the absorption process, the Advanced Dissolution, Absorption and Metabolism (ADAM) model was utilized. The apparent permeability of etravirine was set at 6.5×10^{-6} cm/s, as reported in a Caco-2 assay (Janssen data on file).

Based on the *in vitro* results obtained in the current study two approaches were followed to model the *in vivo* dissolution behavior of etravirine. In the first approach, the maximum concentration of dissolved etravirine observed in the medium was used as the "solubility" of the amorphous/formulated drug. This approach assumes that etravirine does not precipitate *in vivo*, due to rapid absorption of the drug and/or its dilution in the intestinal fluids, and will subsequently be referred to as the "no-precipitation approach". In the second approach, the concentration achieved in the dissolution vessel after 24 h was used to represent the "solubility" of the amorphous/formulated drug. Additionally, the observed supersaturation ratio and calculated precipitation rate constant parameter were implemented. The critical supersaturation ratio was calculated from the maximum observed concentration dissolved in the individual dissolution vessel divided by the 24 hour concentration in the same vessel. The precipitation rate constant was calculated according to the time-frame over which the concentration reverted from the maximum concentration to the 24 hour concentration. This approach will subsequently be referred to as the "implementation of precipitation" approach. [146]

The simulated plasma profiles after oral administration of a 100 mg or 200 mg INTELENCE® tablet in the fed state vs. the individual observed plasma concentrations (Janssen data on file), as well as the observed mean pharmacokinetic profiles reported in the literature[134,155,156], following both approaches are presented in Figure 0.13 and Figure 0.14.

After statistical analysis of the resulting fits it appears that the first approach, i.e. "no precipitation", is more representative of the behavior of etravirine *in vivo*. In particular, the "no precipitation" approach resulted in a good representation of the individual pharmacokinetic data (Figure 0.13A) after the administration of a 100 mg INTELENCE® tablet in the fed state as well as leading to overall good predictions of the mean observed pharmacokinetic profiles reported in the literature[134,155,156] (Figure 0.13C). By contrast, the second approach ("implementation of precipitation") led to substantial underprediction of the pharmacokinetics of etravirine (Figure 0.13B and Figure 0.13D). For the 200 mg INTELENCE® tablets an overall trend to underprediction of the pharmacokinetics of etravirine is observed, however, this trend is far greater when the "implementation of precipitation" approach is used (Figure 0.14). Comparing these simulations, it appears that etravirine does not precipitate to a significant extent when administered in the fed state *in vivo*.[146] This observation, along with the high permeability of etravirine (a P_{app} value of 6.5 x10^{-6} cm/sec which is translated to a P_{eff} of approx. 1.1 x10^{-4} cm/sec with Simcyp® Simulator internal calculation), suggests that it is more informative to consider etravirine as a DCS IIb drug [66] rather than as a BCS Class IV compound.
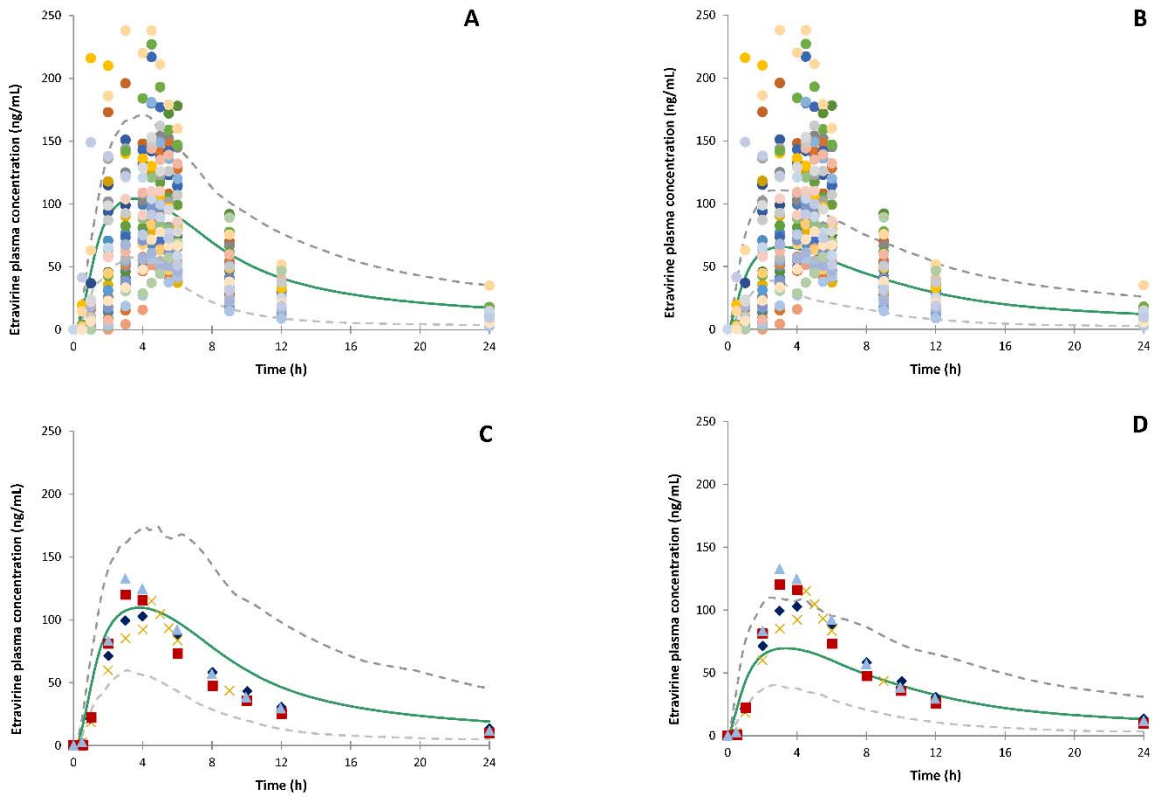
Figure 0.13: Simulated (thick solid line, population mean; thin dashed lines, 5th and 95th percentile of population) and clinically reported plasma concentrations after administration of a 100 mg INTELENCE® tablet following: A)/C) the first ("no-precipitation") and B)/D) the second ("implementation of precipitation") approach, in fed state. With circles (•) the individual pharmacokinetic data (Janssen data on file), whereas with x's (×) and diamonds (♦), squares (■) and triangles (▲) the mean pharmacokinetic profiles reported by Kakuda et al.[155] and Schöller-Gyüre et al.[134,156] are presented, respectively.[146]
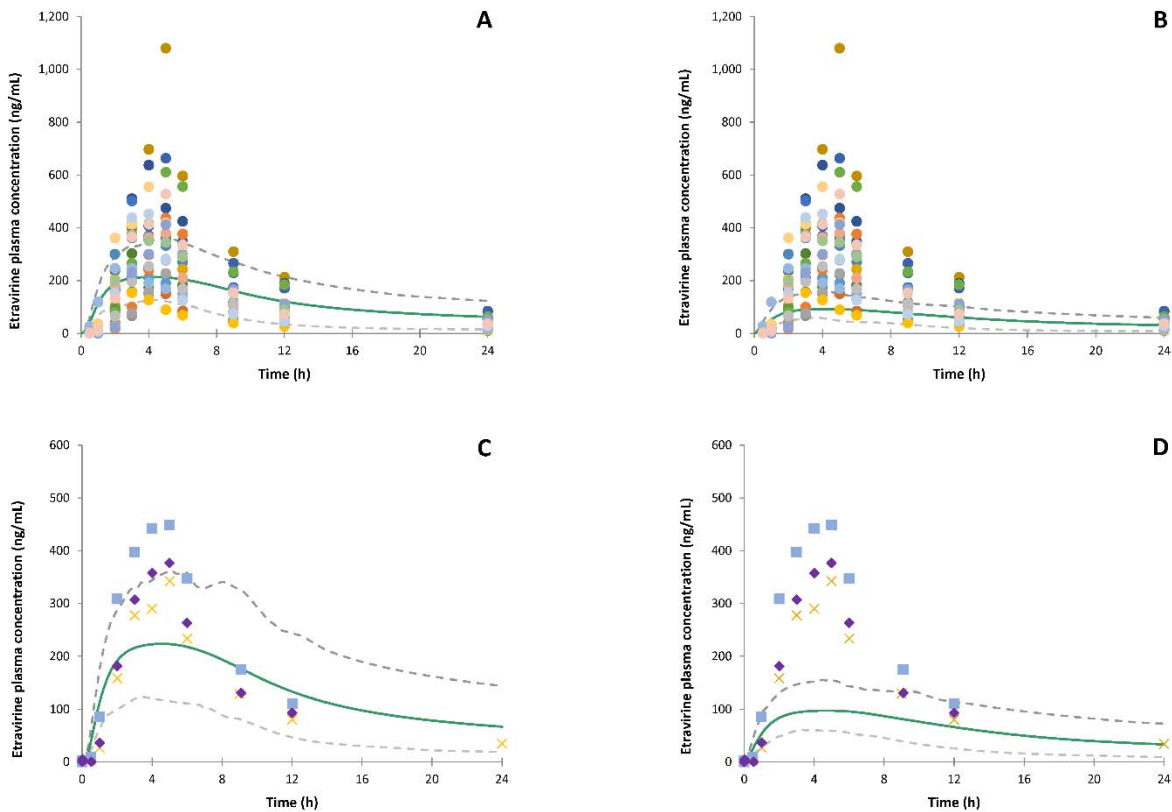
Figure 0.14: Simulated (thick solid line, population mean; thin dashed lines, 5th and 95th percentile of population) and clinically reported plasma concentrations after administration of a 200 mg INTELENCE® tablet following: A)/C) the first ("no-precipitation") and B)/D) the second ("implementation of precipitation") approach, in fed state. With circles (•) the individual pharmacokinetic data (Janssen data on file), whereas with x's (×) and diamonds (♦), squares (■) and triangles (▲) the mean pharmacokinetic profiles reported by Kakuda et al.[155] and Schöller-Gyüre et al.[157] are presented, respectively.[146]

4.3.3.3 Key points of case example 2 - INTELENCE®

The main observations resulting from investigations with the bio-enabling formulation of etravirine, i.e. the amorphous solid dispersion INTELENCE® tablets, can be summarized as follows:

a. As for aprepitant, native surfactants appear to have a greater effect than pH on the *in vivo* dissolution of etravirine from the marketed, bio-enabling formulation.[146]

b. The use of Level II biorelevant media, which simulate the existence of native surfactants in the GI fluids, was imperative in order to reach *in vivo*-relevant conclusions. [146] In fact,

solubility and dissolution experiments conducted in biorelevant media confirmed the large food effect observed clinically for etravirine. [146]

c. As for the aprepitant case example, an accurate simulation of the plasma profiles was achieved only by utilizing the dissolved drug concentration values resulting from the dissolution experiments as the *in vivo* solubility values. Implementation of the crystalline drug solubility lead to significant under-prediction.[146]

d. Comparison of results using alternate simulation approaches, i.e. "no precipitation" and "implementation of precipitation", led to the conclusion that etravirine does not precipitate *in vivo* when administered in the fed state. [146] In particular, it was reasoned that if no precipitation was observed in a transfer experiment conducted under fasted state conditions, it would be even less likely to precipitate in the fed state, where the solubility differential for a weak base is lower than in the fasted state. This hypothesis is supported by the similar maximum concentration of dissolved etravirine achieved in the media simulating the fed stomach and fed upper small intestine. [146]

4.3.4   Final Discussion and Outlook

In order to overcome bioavailability challenges associated with many drugs in current development pipelines, bio-enabling formulations have been proven to be a viable solution. However, there is still considerable lack of understanding regarding the *in vitro* characterization and *in vivo* behavior of these formulations, as well as the mechanisms and extent to which they can improve bioavailability. For example, the *in vitro* characterization of an amorphous solid dispersion can be quite complex because of their supersaturation and precipitation behavior, which may be dependent on interactions between the amorphous drug and various components of the biorelevant media used to characterize them.[148,158,159] Therefore, in the cases where solubilization by native surfactants rather than pH plays a key role in determining the *in vivo* performance of a formulated drug, the different kinds of surfactants used in the various versions of biorelevant media may lead to different solubilization behaviors.

As observed in the present research, one of the challenges that must often be faced when attempting to characterize a bio-enabling formulation *in vitro* and build a detailed solubility/dissolution model is the expectation that the properties of the pure unformulated drug will be very different than the properties of the formulated drug.

With particular regard to modelling the *in vivo* dissolution process and building a PBPK model for these formulations, it is of great importance to identify and input an appropriate "solubility" value for the formulated drug, especially in the following situations:

a) when a "solubilization ratio" to account for the *in vivo* solubilization by the native surfactants in fasted and/ or fed state (e.g. as required by most commercially available *in silico* softwares) needs to be estimated and

b) when a simulation of the dissolution experiments (and eventually the *in vivo* performance of the drug formulation) is to be attempted, given that dissolution rate is proportional to Cs-Ct, where Cs is the solubility at the particle surface in the respective medium and Ct the concentration of drug in the bulk solution at time t.

Through the work presented in this dissertation, two possible solutions were identified to address the aforementioned challenges:

a) in cases where no precipitation of the compound in the GI tract is expected (based on the drug properties and/ or the results of the *in vitro* dissolution and transfer experiments), the maximum drug concentration achieved in the dissolution vessel during the dissolution experiment of the formulated drug in Level II biorelevant media can be used as a more appropriate ("effective") solubility of the formulated drug in the respective part of the GI tract.

b) in cases where precipitation is expected / hypothesized, the drug concentration achieved in the dissolution vessel after 24 h can be used to represent the "effective" solubility of the formulated drug. Additionally, the supersaturation ratio can be calculated from the maximum observed concentration dissolved in the individual dissolution vessel divided by the 24 hour concentration in the same vessel. The precipitation rate constant can be calculated according to the time-frame over which the concentration reverts from the maximum concentration to the 24 hour concentration.

The application of these approaches enabled a better understanding and prediction of the *in vivo* performance of the investigated nanosized and amorphous solid dispersion bio-enabling formulations. To date, there has been limited application of PBPK / absorption models in predicting the *in vivo* performance of bio-enabling formulations due to their complex *in vitro* and *in vivo* dissolution processes.[92–94] However, some early attempts have already been published.[92–94] Further research of this nature will advance our understanding and help conquer the challenges of the bio-enabling formulations, thus facilitating access to innovative medicines. Currently, this methodology applies to healthy adult volunteers. Nonetheless, by using *in vitro* and *in silico* tools tailored to reflect the physiology changes occurring in special or diseased populations the same approach could be applied / extrapolated to these populations too.

5 *Summary and Outlook*

5.1 Summary

The work described in this thesis was part of the European Research and Innovation Programme – PEARRL, funded by the European Union's Horizon 2020 Marie Sklodowska-Curie actions, under grant agreement No 674909. This is an international Programme bringing together partners from academia, regulatory sector and pharmaceutical industry and aims to develop and provide tools for the characterization of innovative drug formulations, namely bio-enabling formulations, as a means to facilitate earlier access of patients to "breakthrough therapy" drugs.

In the last years, high attrition rates have been observed in the pharmaceutical Research and Development sector due to the difficulties encountered in transforming drug molecules to formulations.[64] Most new drug candidates in todays' pipelines have less than optimal properties with regard to solubility and dissolution [66] and display poor bioavailability when administered orally. Therefore, most new drug candidates require special formulation approaches to achieve acceptable oral bioavailability. These novel formulations are usually referred to as "bio-enabling" formulations and are increasingly being used in drug development pipelines. Nonetheless, there are still gaps in understanding the *in vivo* performance of these formulations.

The main goals of this thesis were to investigate whether by combining biorelevant *in vitro* tools with *in silico* modelling and simulation techniques, the *in vivo* solubility /dissolution of bio-enabling formulations can be mechanistically explained and better understood, and a successful simulation of their *in vivo* performance can be achieved.

This entailed, at first, a thorough understanding of the physiological factors and processes that will most likely affect the *in vivo* absorption process of such formulations. Furthermore, in order to characterize and assess the *in vivo* performance of bio-enabling formulations *in vitro* biorelevant tools i.e. setups and methods which simulate the GI environment as closely as possible were needed. The closer to a successful representation of the GI physiology an *in vitro* tool is, the better the chances to simulate *in vitro* the *in vivo* dissolution process of a bio-enabling formulation. The results attained with the biorelevant *in vitro* tools, along with information

obtained from literature, can be directly inputted in *in silico* modelling and simulation softwares. This way, Physiologically Based Pharmacokinetic (PBPK) models can be built for each respective Active Pharmaceutical Ingredients (API) and the *in vivo* performance of a drug product can be simulated.

As a first step, the physiological parameters which can mainly affect the pharmacokinetics of an orally administered formulation were identified by evaluating the effects of drugs used to treat GI diseases on the GI physiology and on the pharmacokinetics of co-administered drugs. Among others, pH was identified as a key physiological parameter which can greatly affect the pharmacokinetics of orally administered compounds. In fact, most of the absorption related pharmacokinetic Drug-Drug Interactions were found to occur after the concomitant administration of gastric acid reducing agents.

As a second step and with particular regard to the use of biorelevant *in vitro* tools to investigate the *in vivo* dissolution process of the bio-enabling formulations, focus has been given to biorelevant media, i.e. aqueous dissolution media which simulate the composition of the GI fluids, and to the *in vitro* setups which have been proposed in literature to assess the possible precipitation kinetics.

Till now, aspiration studies comprise the most valuable source of information for the design of biorelevant dissolution media. During this work it was observed that the reported values of some physiological parameters differ substantially among the aspiration studies published in literature. Therefore, it was investigated whether the results may be influenced by the methodology used to collect and process the samples, with a specific focus on pH and buffer capacity. It was shown that various sample handling processes e.g. centrifugation and prior storage of the sample can have a significant effect on the measured values. For example, one freeze-thaw cycle leads to significantly decreased measured values of pH and buffer capacity in aspirates collected from the stomach and/ or the upper small intestine of healthy volunteers. It was therefore concluded that the physiological pH and buffer capacity values of fluids in the fasted upper GI lumen should be measured immediately upon sample aspiration, without any additional sample handling and/or prior storage.

Bio-enabling formulations contain poorly soluble APIs which are usually formulated in a thermodynamically unstable state and therefore have high propensity to precipitate. Assessment of potential supersaturation and/ or precipitation in the GI tract is critical for the prediction of the *in vivo* performance of such formulations. However, there is still a lack of mechanistic understanding in maintaining a supersaturated state intralumenally.[110]Therefore, it is of great importance to utilize reliable *in vitro* methods to simulate the transfer of the drug from the stomach to the upper small intestine and accurately predict the *in vivo* precipitation characteristics/kinetics.[110] During this work, the *in vitro* setups, which until now have been proposed in literature to assess drug supersaturation and/ or precipitation in the upper GI tract were reviewed, and their usefulness and current applications were evaluated.

After addressing the aforementioned issues, two case example formulations were selected in order to investigate the main hypothesis/goal, i.e. to predict the *in vivo* performance of bio-enabling formulations by combining biorelevant *in vitro* testing with *in silico* PBPK modelling. The first formulation comes in the market under the brand name EMEND® and contains the API in a nanosized form. The second formulation is marketed as INTELENCE® and it is an amorphous solid dispersion of the API etravirine. By choosing two different formulation approaches, different case scenarios could be explored, thus allowing for broader suggestions when tackling the *in vitro* and *in silico* challenges of bio-enabling formulations.

In the case of the first case example, i.e. the EMEND® capsules, the *in vitro* experiments conducted with biorelevant tools revealed that during the dissolution of aprepitant from the EMEND® capsules results in a prolonged supersaturation. Furthermore, the *in vitro* experiments indicated a large effect of native surfactants on the solubility of aprepitant. Coupling the *in vitro* results with the PBPK model led to an appropriate simulation of aprepitant plasma concentrations after administration of EMEND® capsules in both the fasted and fed states. It is interesting to note that successful simulation of the plasma profiles after administration of the EMEND® capsules was achieved only by using the values of the dissolved drug resulting from the dissolution experiments, whilst implementation of the crystalline drug solubility led to significant under-predictions.

For the second case example, i.e. INTELENCE® tablets, similar observations were made. In particular, the *in vitro* experiments indicated a large effect of naturally occurring solubilizing agents on the solubility of etravirine. Interestingly, prolonged supersaturated concentrations of etravirine were also observed during its dissolution from INTELENCE® tablets. Coupling the *in vitro* results with the PBPK model provided the opportunity to investigate two possible absorption scenarios, i.e. with or without implementation of precipitation. The results from the simulations suggested that a scenario in which etravirine does not precipitate is more representative of the *in vivo* data. Also in this case, implementation of the crystalline drug solubility led to significant under-predictions.

Despite intensive recent research around bio-enabling formulations, there is still a lack of fundamental understanding with regard to their *in vivo* performance, the changes that may occur in the physicochemical properties of the API (for example, formation of amorphous or nano-crystalline drug, interactions with polymers which act as precipitation inhibitors, etc.) and how this information can be implemented into *in silico* PBPK models. To date, there has been limited application of PBPK / absorption models in predicting the *in vivo* performance of bio-enabling formulations due to the complex *in vitro* and *in vivo* dissolution process.[92–94] However, some early attempts have already been published and more studies of this nature are needed to advance our understanding in this field.[92–94] Following the approach described in this research work, a mechanistic understanding of the *in vivo* absorption process and a successful simulation of the plasma profiles resulting after administration of a nanosized and an amorphous solid dispersion bio-enabling formulation was achieved. Furthermore, possible ways to address some challenges with regard to the development of PBPK models for bio-enabling formulations were proposed. This work demonstrates the potential application and importance of absorption modelling in rational formulation design and in strengthening biopharmaceutics knowledge around bio-enabling formulations. By applying this approach, the main parameters which affect the pharmacokinetic behavior of poorly soluble APIs formulated as bio-enabling formulations can be identified and in turn enable robust prediction of clinical outcomes.

5.2   Outlook

In the present study it was demonstrated that the prediction of the *in vivo* performance of poorly soluble drugs can be achieved by combining PBPK modelling and simulation techniques with *in vivo* representative *in vitro* tools. However, it was also shown that it is crucial to have accurate predictive tools which simulate the *in vivo* GI environment as closely as possible. Setting up these predictive tools requires a thorough understanding of the physiological processes and the GI environment, as well as appropriate refinement and validation of both the *in vitro* methods and of the input parameters in PBPK models.

Regarding GI physiology, more information derived from aspiration studies according to a "best practices" protocol are needed in order to improve and/or refine the currently used biorelevant media and biorelevant *in vitro* tools. Only measurements of physiological parameters attained in this way can lead to *in vivo* representative results when integrated in PBPK models.

With particular regard to formulation characteristics and drug properties, the techniques presented in this thesis need to be applied to further compounds and/ or bio-enabling formulations in order to expand our knowledge in the effects of formulation on drug absorption and overall pharmacokinetic exposure and to trigger new "learn-confirm" cycles. Therefore, the developed PBPK models need to incorporate drug characteristics and mechanistic elements of drug release/dissolution relevant to interactions of the formulation with the GI environment, in such a way that these can be parameterized to describe the key formulation characteristics affecting the *in vivo* performance. This idea is linked to the "biopharmaceutics risk assessment roadmap (BioRAM)", which was proposed in 2014.[2] According to BioRAM, quality can be built into a product from early stages (following the concept of Quality by Design) when there is a thorough understanding of the drug product performance and of the manufacturing process, thus allowing for identification of the critical quality attributes. To this end, the concept of BioRAM can be put into practice for bio-enabling formulations by applying the approach presented in this thesis. In particular, mechanistically developed PBPK models can be used to predict e.g. the impact of variations in critical formulation variables, or critical process

parameters, thus creating a "safe space" in which all produced final product batches will have the anticipated *in vivo* performance.[160]

The ultimate goal is to be able to predict clinical effects by combining biorelevant *in vitro* tools – PBPK models with pharmacodynamics (PD) models, thus being able to connect the early stages of pharmaceutical development directly to the later clinical stages, not only for healthy volunteers, but also for the concerned patient populations.

5.3   German Summary

Die Forschung beschrieben in dieser Dissertation ist ein Teil der "European Research and Innovation Programme - PEARRL", und wurde von Horizon 2020 Marie Sklodowska-Curie actions der Europäischen Union, unter Förderungsnummer 674909 unterstützt. Dies ist ein internationales Programm, das die Akademiker, Regulierungsbehörden und pharmazeutische Industrie zusammenbringt und zum Ziel die Entwicklung und Förderung der Werkzeuge zur Charakterizierung innovativer Wirkstoffformulierungen hat, nämlich "bio-enabling" Formulierungen, um den Patienten einen frühen Zugang zu Durchbruchstherapien zu ermöglichen.

In den letzten Jahren, wurde Senkung der Intensität der pharmazeutischen Forschung und Entwicklung beobachtet, da die Weiterentwicklung der Wirkstoffmolekülen hinzu einer "handlichen" Formulierung viele Schwierigkeiten aufweist.[64]

Meiste der neuen Wirkstoffkandidaten, die sich in Entwicklung befinden, haben suboptimale Eigenschaften in Bezug zur Löslichkeit und Auflösung[66] und zeigen schlechte Bioverfügbarkeit, wenn eingenommen.

Deswegen verlangen meiste neue Wirkstoffkandidate einen besonderen Ansatz in Bezug auf Formulierung, um akzeptable orale Bioverfügbarkeit zu erreichen. Diese neue Formulierungen werden meistens als bio-enabling Formulierungen bezeichnet und werden in Heilmittelentwicklung immer häufiger verwendet. Das Verstehen davon ist dennoch mangelhaft

Hauptziel dieser Dissertation ist zu erforschen ob, durch Verbinden von biorelevanten *in vitro* Werkzeugen mit *in silico* Modelling und Simulationen, die *in vitro* Löslichkeit und Auflösung von bio-enabling Formulierungen mechanistisch erkläert und besser verstanden werden kann und somit eine erfolgreiche Simulation von *in vivo* Leistung erreicht werden kann.

Zuerst wird ein ausführlicher Überblick über die physiologische Faktoren und Prozessen, die am wahrscheinlichsten die *in vivo* Aufnahme solcher Formulierungen beeinflüssen werden, vorgestellt. Desweiteren, um die *in vivo* Leistung bio-enabling Formulierungen zu charakterisieren und zu beurteilen, *in vitro* biorelevante Werkzeuge, d.h. Apparaturen und

Methoden, die die gastrointestinale Umbebung so genau wie möglich darstellen, waren notwendig. Je genauer die gastrointesinale Physiologie mithilfe eines *in vitro* Werkzeugs dargestellt werden kann, desto besser ist die Chance, dass es die in vivo Auflösungsprozesse der bio-enabling Formulierungen simuliert.

Die mithilfe biorelevanten *in vitro* Werkzeugen neben den Literaturdaten erhaltenen Ergebnisse, können in *in silico* Modelle und Simulationsprogramme eingegeben werden. Dadurch können physiologisch begründete Pharmakokinetik (engl. Physiologically Based Pharmacokinetic (PBPK) Modelle fur jeden Wirkstoff erbaut werden und, weiterhin, die *in vivo* Leistung des Heilmittels simuliert werden.

Als Erstes wurden die physiologische Parameter, die die pharmakokinetik oraler Formulierungen beeinflüssen, identifiziert, indem die Auswirkung der Wirkstoffe, die zur Behandlung Magen-Darm-Krankheiten genutzt werden, sowie deren Pharmakokinetik, beurteilt wurde. Unter anderem wurde pH als einer der entscheinenden physiologischen Parameter erkannt, da es die Pharmakokinetik peroral verabreichter Stoffe signifikant beeinflüssen kann. Desweiteren, die meisten pharmakokinetische Wechselwirkungen zwischen zwei Wirkstoffe, die mit Aufnahme eines Wirkstoffs gekoppelt sind, treten bei beleitender Therapie mit Säurereduktionsmitteln auf.

Als zweiter Schritt, mit besonderer Beachtung auf die Verwendung der biorelevanten *in vitro* Werkzeugen für die Erforschung der *in vivo* Auflösungsprozesse von bio-enabling Formulierungen, Fokus auf die biorelevante Medien und *in vitro* Apparaturen, die mögliche Prezipitationskinetik einschätzen können, wurde gesetzt. Biorelevante Medien sind wässrige Flüssigkeiten, die die Zusammensetzung der gastrointestinaler Flüssigkeiten nachmachen und für die Auflösungsuntersuchungen genutzt werden.

Bis heute beinhalten die Aspirationsstudien die wichtigsten Hinweise und Informationen für den Design biorelevanter Medien. Es wurde beobachtet, dass die berichteten Werte mancher phyisiologisher Parameter erhebliche Unterschiede zwischen den Aspirationsstudien zeigen. Deswegen wurde untersucht, ob die Ergebnisse durch die Auswahl an Methodologie, die für die Entnahme und die Auswertung der Proben genutzt worden sind, beeinflusst werden können, wobei besondere Aufmerksamkeit den pH und der Pufferkapazität geschenkt wurde. Es wurde

gezeigt, dass Unterschiede im Prozess der Probenhandhabung, z.B. Zentrifugieren und Lagerung einen deutlichen Einfluss auf die gemessenen Werte haben kann. Beispielsweise führt ein einziger Einfrieren-Auftauen-Zyklus zu signifikanter Verringerung gemessener Werte des pH und der Pufferkapazität von Aspiraten, die aus dem Magen u.o. dem oberen Dünndarm gesunder Freiwilligen entnommen wurden. Es wurde daher der Schluss gezogen, dass der physiologische pH-Wert und die Pufferkapazität von Flüssigkeiten im nüchternen oberen gastrointestinalen Lumen unmittelbar nach der Probenaspiration ohne zusätzliche Probenhandhabung u.o. vorherige Lagerung gemessen werden sollen.

Bio-enabling Formulierungen enthalten schwerlösliche Wirkstoffe, die üblicherweise in einem thermodynamisch instabilen Zustand formuliert sind und daher eine hohe Neigung zur Ausfällung aufweisen. Die Bewertung einer möglichen Übersättigung u.o. Prezipitation im Magen-Darm-Trakt ist entscheidend für die Vorhersage der *in vivo* Leistung solcher Formulierungen. Es besteht dennoch ein Mangel an mechanistischem Verständnis für die Aufrechterhaltung eines übersättigten Zustands intralumenal.[110] Daher ist es von großer Bedeutung, zuverlässige *in vitro* Methoden zu verwenden, um den Übergang des Arzneimittels vom Magen in den oberen Dünndarm zu simulieren und die *in vivo* Prezipitationseigenschaften/ -kinetik genau vorherzusagen.[110] In dieser Arbeit wurden die *in vitro* Setups, die bisher in der Literatur zur Beurteilung der Übersättigung u.o. Ausfällung von Arzneimitteln im oberen Magen-Darm-Trakt vorgeschlagen wurden, überprüft und ihre Nützlichkeit und aktuelle Anwendung bewertet.

Zwei Fallbeispielformulierungen wurden ausgewählt, um die Haupthypothese zu untersuchen, d. h. um die *in vivo* Leistung von biofähigenden Formulierungen durch das Verknüpfen von biorelevanten *in vitro* Experimenten mit *in silico* PBPK Modelling vorherzusagen. Die erste Formulierung ist auf den Markt unter dem Namen EMEND® und enthält den Wirkstoff in Nanoform. Die zweite Formulierung wird als INTELENCE® vermarktet und ist eine amorphe feste Dispersion des Wirkstoffs Etravirin. Durch die Wahl zwei unterschiedlicher Formulierungsansätzen konnten unterschiedliche Fallszenarien untersucht werden, wodurch umfassendere Vorschläge für die Bewältigung der Herausforderungen bei *in vitro* Experimenten und *in silico* Modelling mit bio-enabling Formulierungen möglich waren.

Im ersten Fallbeispiel, EMEND® Kapseln, zeigten die *in vitro* Experimente, die mit biorelevanten Methoden durchgeführt wurden, dass Aprepitant, das aus der Auflösung von EMEND® Kapseln resultiert, über die gesamte Dauer der Experimente eine Übersättigung aufweist. Darüber hinaus zeigten die *in vitro* Experimente eine große Auswirkung nativer Tenside auf die Löslichkeit von Aprepitant. Die Kopplung der *in vitro* Ergebnisse mit dem PBPK Modell führte zu einer passenden Simulation der Plasmakonzentrationen von Aprepitant nach dem Verabreichen von EMEND® Kapseln sowohl im nüchternen als auch im Zustand nach einer Mahlzeit. Es ist interessant festzustellen, dass eine erfolgreiche Simulation der Wirkstoffplasmaprofile nach Verabreichung der EMEND® Kapseln nur unter Verwendung der Werte des gelösten Arzneimittels erreicht wurde, die aus den Auflösungsexperimenten stammen, während die Implementierung der Löslichkeit des kristallinen Arzneimittels für die Plasmaspiegel-Vorhersage zu signifikanter Untervorhersagen führte.

Für das zweite Fallbeispiel, INTELENCE® Tabletten, wurden ähnliche Beobachtungen gemacht. Insbesondere zeigten die *in vitro* Experimente einen großen Effekt von natürlich vorkommenden Lösungsvermittlern auf die Löslichkeit von Etravirin. Interessanterweise wurde verlängerte Übersättigung von Etravirin über die gesamte Dauer der Auflösungsexperimente an INTELENCE® Tabletten beobachtet. Die Kopplung der *in vitro* Ergebnisse mit dem PBPK Modell bot die Möglichkeit, zwei mögliche Absorptionsszenarien zu untersuchen, mit und ohne Berücksichtigung der Prezipitationsprozesse. Die Ergebnisse der Simulationen legen nahe, dass ein Szenario, in dem Etravirin nicht ausfällt, repräsentativer für die *in vivo* Daten ist. Auch in diesem Fall führte die Implementierung der Löslichkeit des kristallinen Arzneimittels als Ausgangspunkt für die Vorhersage des Plasmaspiegels zu einer signifikanten Untervorhersage.

Trotz intensiver Forschung zu bio-enabling Formulierungen mangelt es immer noch an grundlegendem Verständnis hinsichtlich ihrer *in vivo* Leistung, der Änderungen, die in den physikochemischen Eigenschaften des Wirkstoffs auftreten können (z. B. Bildung eines amorphen oder nanokristallinen Arzneimittels), Wechselwirkungen mit Polymeren, die als Fällungsinhibitoren wirken usw.) und wie diese Informationen *in silico* PBPK Modellen implementiert werden könnten. Bisher war die Anwendung von PBPK und Absorptionsmodellen zur Vorhersage der *in vivo* Leistung von bio-enabling Formulierungen aufgrund der komplexen *in*

vitro und *in vivo* Auflösungsprozesse nur begrenzt.[92–94] Dennoch, einige frühe Versuche und Ansetze wurden bereits veröffentlicht und weitere Studien dieser Art sind erforderlich, um unser Verständnis auf diesem Gebiet zu verbessern. [92–94] Bezogen auf den in dieser Dissertation beschriebenen Ansatz, ein mechanistisches Verständnis des *in vivo* Absorptionsprozesses, sowie eine erfolgreiche Simulation der nach der Verabreichung resultierenden Plasmaprofile einer bio-enabling-Formulierung der Nanoskala- und einer amorphen festen Dispersion wurde erreicht. Darüber hinaus wurden mögliche Wege vorgeschlagen, um einige Herausforderungen im Hinblick auf die Entwicklung von PBPK Modellen für biofähige Formulierungen anzugehen. Diese Arbeit zeigt die mögliche Anwendung und Bedeutung der Absorptionsmodellierung für die rationale Formulierungsentwicklung und für die Stärkung des Wissens über Bio-Heilmittel in Bezug auf bio-enabling Formulierungen. Mithilfe dieses Ansatzes können die wesentlichen Parameter identifiziert werden, die das pharmakokinetische Verhalten schwerlöslicher Wirkstoffe beeinflussen, die als bio-enabling Formulierungen formuliert sind, und ermöglichen wiederum eine robuste Vorhersage der klinischen Ergebnisse.

References

1. FDA. Novel Drug Approvals for 2019. Available at: https://www.fda.gov/drugs/new-drugs-fda-cders-new-molecular-entities-and-new-therapeutic-biological-products/novel-drug-approvals-2019. Accessed February 19, 2020.

2. Selen A *et al.* The biopharmaceutics risk assessment roadmap for optimizing clinical drug product performance. *J Pharm Sci* 2014; 103(11): 3377–3397. doi:10.1002/jps.24162.

3. Mudie DM *et al.* Physiological parameters for oral delivery and in vitro testing. *Mol Pharm* 2010; 7(5): 1388–1405. doi:10.1021/mp100149j.

4. Pentafragka C *et al.* The impact of food intake on the luminal environment and performance of oral drug products with a view to *in vitro* and *in silico* simulations: a PEARRL review. *J Pharm Pharmacol* 2019; 71(4): 557–580. doi:10.1111/jphp.12999.

5. Allen A, Garner A. Mucus and bicarbonate secretion in the stomach and their possible role in mucosal protection. *Gut* 1980; 21(3): 249–62. Available at: http://www.ncbi.nlm.nih.gov/pubmed/6995243. Accessed September 10, 2018.

6. Järbur K *et al.* Quantitative assessment of motility-associated changes in gastric and duodenal luminal pH in humans. *Scand J Gastroenterol* 2003; 38(4): 392–8. Available at: http://www.ncbi.nlm.nih.gov/pubmed/12739711. Accessed September 10, 2018.

7. Feldman M *et al.* Effect of proximal gastric vagotomy on calculated gastric HCO3- and nonparietal volume secretion in man. Studies during basal conditions and gastrin-17 infusion. *J Clin Invest* 1987; 79(6): 1615–20. doi:10.1172/JCI112997.

8. Feldman M. Gastric bicarbonate secretion in humans. Effect of pentagastrin, bethanechol, and 11,16,16-trimethyl prostaglandin E2. *J Clin Invest* 1983; 72(1): 295–303. doi:10.1172/JCI110969.

9. Lindahl A *et al.* Characterization of Fluids from the Stomach and Proximal Jejunum in Men and Women. *Pharm Res* 1997; 14(4): 497–502. doi:10.1023/A:1012107801889.

10.   Pedersen PB *et al.* Characterization of fasted human gastric fluid for relevant rheological parameters and gastric lipase activities. *Eur J Pharm Biopharm* 2013; 85(3): 958–965. doi:10.1016/j.ejpb.2013.05.007.

11.   Kalantzi L *et al.* Characterization of the Human Upper Gastrointestinal Contents Under Conditions Simulating Bioavailability/Bioequivalence Studies. *Pharm Res* 2006; 23(1): 165–176. doi:10.1007/s11095-005-8476-1.

12.   Litou C *et al.* Characteristics of the Human Upper Gastrointestinal Contents in the Fasted State Under Hypo- and A-chlorhydric Gastric Conditions Under Conditions of Typical Drug – Drug Interaction Studies. *Pharm Res* 2016; 33(6): 1399–1412. doi:10.1007/s11095-016-1882-8.

13.   Hens B *et al.* Low Buffer Capacity and Alternating Motility along the Human Gastrointestinal Tract: Implications for *in Vivo* Dissolution and Absorption of Ionizable Drugs. *Mol Pharm* 2017; 14(12): 4281–4294. doi:10.1021/acs.molpharmaceut.7b00426.

14.   Allen A, Flemström G. Gastroduodenal mucus bicarbonate barrier: protection against acid and pepsin. *Am J Physiol Physiol* 2005; 288(1): C1–C19. doi:10.1152/ajpcell.00102.2004.

15.   Hogan DL *et al.* Review article: gastroduodenal bicarbonate secretion. *Aliment Pharmacol Ther* 1994; 8(5): 475–488. doi:10.1111/j.1365-2036.1994.tb00319.x.

16.   Seidler U, Sjöblom M. Gastroduodenal Bicarbonate Secretion. In: *Physiology of the Gastrointestinal Tract*. Academic Press, 2012: 1311–1339. doi:10.1016/B978-0-12-382026-6.00048-8.

17.   Novak I *et al.* Pancreatic Bicarbonate Secretion Involves Two Proton Pumps. *J Biol Chem* 2011; 286(1): 280–289. doi:10.1074/jbc.M110.136382.

18.   Bucher GR *et al.* The action of the human small intestine in altering the composition of physiological saline. *J Biol Chem* 1944; 155: 305–313. Available at: https://www.cabdirect.org/cabdirect/abstract/19441403289. Accessed September 10, 2018.

19. Repishti M *et al.* Human duodenal mucosal brush border Na $^+$/H $^+$ exchangers NHE2 and NHE3 alter net bicarbonate movement. *Am J Physiol Liver Physiol* 2001; 281(1): G159–G163. doi:10.1152/ajpgi.2001.281.1.G159.

20. McGee LC, Hastings BA. The carbon dioxide tension and acid-base balance of jejunal secretions in man. *J Biol Chem* 1942; 142: 893–904. Available at: http://www.jbc.org/content/142/2/893.citation. Accessed September 10, 2018.

21. Isenberg JI *et al.* Impaired Proximal Duodenal Mucosal Bicarbonate Secretion in Patients with Duodenal Ulcer. *N Engl J Med* 1987; 316(7): 374–379. doi:10.1056/NEJM198702123160704.

22. Dressman JB *et al.* Upper Gastrointestinal (GI) pH in Young, Healthy Men and Women. *Pharm Res An Off J Am Assoc Pharm Sci* 1990; 7(7): 756–761. doi:10.1023/A:1015827908309.

23. Fadda HM *et al.* Drug solubility in luminal fluids from different regions of the small and large intestine of humans. *Mol Pharm* 2010; 7(5): 1527–32. doi:10.1021/mp100198q.

24. Dressman JB, Soederlind E. Physiological Factors Affecting Drug Release and Absorption in the Gastrointestinal Tract. In: Dressman JB, Reppas C, eds. *Oral Drug Absorption Prediction and Assessment*, 2nd ed. CRC Press, 2016: 1–20. doi:10.3109/9781420077346-2.

25. Persson EM *et al.* The Effects of Food on the Dissolution of Poorly Soluble Drugs in Human and in Model Small Intestinal Fluids. *Pharm Res* 2005; 22(12): 2141–2151. doi:10.1007/s11095-005-8192-x.

26. Perez de la Cruz Moreno M *et al.* Characterization of fasted-state human intestinal fluids collected from duodenum and jejunum. *J Pharm Pharmacol* 2006; 58(8): 1079–89. doi:10.1211/jpp.58.8.0009.

27. Fuchs A, Dressman JB. Composition and Physicochemical Properties of Fasted-State Human Duodenal and Jejunal Fluid: A Critical Evaluation of the Available Data. *J Pharm Sci* 2014; 103(11): 3398–3411. doi:10.1002/jps.24183.

28. FDA. Guidance for Industry Food-Effect Bioavailability and Fed Bioequivalence Studies. 2002. Available at: https://www.fda.gov/files/drugs/published/Food-Effect-Bioavailability-and-Fed-Bioequivalence-Studies.pdf. Accessed February 21, 2020.

29. EMA - Committee for Medicinal Products For Human Use (CHMP). *Guidline on the Investigation of Bioequivalence*., 2010. Available at: https://www.ema.europa.eu/en/documents/scientific-guideline/guideline-investigation-bioequivalence-rev1_en.pdf. Accessed February 21, 2020.

30. Malagelada JR *et al.* Different gastric, pancreatic, and biliary responses to solid-liquid or homogenized meals. *Dig Dis Sci* 1979; 24(2): 101–110. doi:10.1007/BF01324736.

31. Koziolek M *et al.* Intragastric pH and pressure profiles after intake of the high-caloric, high-fat meal as used for food effect studies. *J Control Release* 2015; 220(Pt A): 71–78. doi:10.1016/j.jconrel.2015.10.022.

32. Riethorst D *et al.* Characterization of Human Duodenal Fluids in Fasted and Fed State Conditions. *J Pharm Sci* 2016; 105(2): 673–681. doi:10.1002/jps.24603.

33. Vertzoni M *et al.* Luminal lipid phases after administration of a triglyceride solution of danazol in the fed state and their contribution to the flux of danazol across Caco-2 cell monolayers. *Mol Pharm* 2012; 9(5): 1189–1198. doi:10.1021/mp200479f.

34. Clarysse S *et al.* Postprandial evolution in composition and characteristics of human duodenal fluids in different nutritional states. *J Pharm Sci* 2009; 98(3): 1177–1192. doi:10.1002/jps.21502.

35. Wiedmann TS *et al.* Solubilization of drugs by physiological mixtures of bile salts. *Pharm Res* 2002; 19(8): 1203–8. doi:10.1023/a:1019858428449.

36. Armand M *et al.* Physicochemical characteristics of emulsions during fat digestion in human stomach and duodenum. *Am J Physiol - Gastrointest Liver Physiol* 1996; 271(1 34-1). doi:10.1152/ajpgi.1996.271.1.g172.

37. Hasler WL. The Physiology of Gastric Motility and Gastric Emptying. In: *Textbook of*

Gastroenterology, Fifth Edition, Vol 1. Blackwell Publishing Ltd., 2009: 207–230. doi:10.1002/9781444303254.ch10.

38. Wilson CG *et al.* Gastrointestinal Transit and Drug Absorption. In: Dressman JB, Reppas C, eds. *Oral Drug Absorption Prediction and Assessment*, 2nd ed. CRC Press, 2016: 41–65. doi:10.3109/9781420077346.

39. Davis SS *et al.* A comparative study of the gastrointestinal transit of a pellet and tablet formulation. *Int J Pharm* 1984; 21(2): 167–177. doi:10.1016/0378-5173(84)90091-7.

40. Abrahamsson B *et al.* Drug absorption from nifedipine hydrophilic matrix extended-release (ER) tablet-comparison with an osmotic pump tablet and effect of food. *J Control Release* 1998; 52(3): 301–310. doi:10.1016/S0168-3659(97)00267-8.

41. Bevernage J *et al.* Evaluation of gastrointestinal drug supersaturation and precipitation: Strategies and issues. *Int J Pharm* 2013; 453(1): 25–35. doi:10.1016/j.ijpharm.2012.11.026.

42. Mitra A, Fadda HM. Effect of surfactants, gastric emptying, and dosage form on supersaturation of dipyridamole in an in vitro model simulating the stomach and duodenum. *Mol Pharm* 2014; 11(8): 2835–2844. doi:10.1021/mp500196f.

43. Cecil JE *et al.* Comparison of the effects of a high-fat and high-carbohydrate soup delivered orally and intragastrically on gastric emptying, appetite, and eating behaviour. *Physiol Behav* 1999; 67(2): 299–306. doi:10.1016/s0031-9384(99)00069-4.

44. Collins PJ *et al.* Gastric emptying in normal subjects - a reproducible technique using a single scintillation camera and computer system. *Gut* 1983; 24(12): 1117–1125. doi:10.1136/gut.24.12.1117.

45. Schwizer W *et al.* Magnetic resonance imaging for the assessment of gastrointestinal function. *Scand J Gastroenterol* 2006; 41(11): 1245–1260. doi:10.1080/00365520600827188.

46. Weitschies W *et al.* Magnetic Marker Monitoring: High resolution real-time tracking of oral solid dosage forms in the gastrointestinal tract. *Eur J Pharm Biopharm* 2010; 74(1): 93–

101. doi:10.1016/j.ejpb.2009.07.007.

47. Markopoulos C *et al.* In-vitro simulation of luminal conditions for evaluation of performance of oral drug products: Choosing the appropriate test media. 2015; 93: 173–182. doi:10.1016/j.ejpb.2015.03.009.

48. Vertzoni M *et al.* Simulation of fasting gastric conditions and its importance for the in vivo dissolution of lipophilic compounds. *Eur J Pharm Biopharm* 2005; 60(3): 413–417. doi:10.1016/j.ejpb.2005.03.002.

49. Klein S. The use of biorelevant dissolution media to forecast the in vivo performance of a drug. *AAPS J* 2010; 12(3): 397–406. doi:10.1208/s12248-010-9203-3.

50. Dressman JB *et al.* Dissolution testing as a prognostic tool for oral drug absorption: Immediate release dosage forms. *Pharm Res* 1998; 15(1): 11–22. doi:10.1023/A:1011984216775.

51. Jantratid E *et al.* Dissolution media simulating conditions in the proximal human gastrointestinal tract: An update. *Pharm Res* 2008; 25(7): 1663–1676. doi:10.1007/s11095-008-9569-4.

52. Fuchs A *et al.* Advances in the design of fasted state simulating intestinal fluids: FaSSIF-V3. *Eur J Pharm Biopharm* 2015; 94: 229–240. doi:10.1016/j.ejpb.2015.05.015.

53. Macheras P *et al.* Drug dissolution studies in milk using the automated flow injection serial dynamic dialysis technique. *Int J Pharm* 1986; 33(1–3): 125–136. doi:10.1016/0378-5173(86)90046-3.

54. Diakidou A *et al.* Estimation of intragastric drug solubility in the fed state: comparison of various media with data in aspirates. *Biopharm Drug Dispos* 2009; 30(6): 318–325. doi:10.1002/bdd.670.

55. Andreas CJ *et al.* Mechanistic investigation of the negative food effect of modified release zolpidem. *Eur J Pharm Sci* 2017; 102: 284–298. doi:10.1016/j.ejps.2017.03.011.

56. Galia E *et al.* Evaluation of various dissolution media for predicting In vivo performance of

class I and II drugs. *Pharm Res* 1998; 15(5): 698–705. doi:10.1023/A:1011910801212.

57.   Jantratid E, Dressman J. Biorelevant Dissolution Media Simulating the Proximal Human Gastrointestinal Tract: An Update. 2007. doi:10.14227/DT160309P21.

58.   Jamei M. Recent Advances in Development and Application of Physiologically-Based Pharmacokinetic (PBPK) Models: a Transition from Academic Curiosity to Regulatory Acceptance. *Curr Pharmacol Reports* 2016; 2(3): 161–169. doi:10.1007/s40495-016-0059-9.

59.   Jamei M *et al.* A framework for assessing inter-individual variability in pharmacokinetics using virtual human populations and integrating general knowledge of physical chemistry, biology, anatomy, physiology and genetics: A tale of "bottom-up" vs "top-down" recognition of covariates. *Drug Metab Pharmacokinet* 2009; 24(1): 53–75. Available at: http://www.ncbi.nlm.nih.gov/pubmed/19252336. Accessed April 17, 2019.

60.   European Medicines Agency. Guideline on the qualification and reporting of physiologically based pharmacokinetic (PBPK) modelling and simulation Guideline on the qualification and reporting of physiologically based pharmacokinetic (PBPK) modelling and simulation. 2016; 44(July): 1–18.

61.   Physiologically Based Pharmacokinetic Analyses — Format and Content Guidance for Industry. 2016. Available at: http://www.fda.gov/Drugs/GuidanceComplianceRegulatoryInformation/Guidances/default.htm. Accessed September 21, 2017.

62.   Formulation Development - A Call for Collaboration to Meet the Bioavailability Challenge. Available at: https://drug-dev.com/formulation-development-a-call-for-collaboration-to-meet-the-bioavailability-challenge/. Accessed February 26, 2020.

63.   The EFPIA view. Available at: https://www.efpia.eu/news-events/the-efpia-view/#/. Accessed February 26, 2020.

64.   Scannell JW *et al.* Diagnosing the decline in pharmaceutical R&D efficiency. *Nat Rev Drug*

Discov 2012; 11(3): 191–200. doi:10.1038/nrd3681.

65.   Bergström CAS *et al.* Early pharmaceutical profiling to predict oral drug absorption: Current status and unmet needs. *Eur J Pharm Sci* 2014; 57(1): 173–199. doi:10.1016/j.ejps.2013.10.015.

66.   Butler JM, Dressman JB. The Developability Classification System: Application of Biopharmaceutics Concepts to Formulation Development. *J Pharm Sci* 2010; 99(12): 4940–4954. Available at: http://www.ncbi.nlm.nih.gov/pubmed/20821390. Accessed May 2, 2019.

67.   Raman S, Polli JE. Prediction of positive food effect: Bioavailability enhancement of BCS class II drugs. *Int J Pharm* 2016; 506(1–2): 110–115. doi:10.1016/j.ijpharm.2016.04.013.

68.   Paul SM *et al. How to improve RD productivity: The pharmaceutical industry's grand challenge.*, 2010:203–214. doi:10.1038/nrd3078.

69.   Amidon GL *et al.* A Theoretical Basis for a Biopharmaceutic Drug Classification: The Correlation of in Vitro Drug Product Dissolution and in Vivo Bioavailability. *Pharm Res An Off J Am Assoc Pharm Sci* 1995; 12(3): 413–420. doi:10.1023/A:1016212804288.

70.   FDA. *Guidance for Industry - Waiver of In Vivo Bioavailability and Bioequivalence Studies for Immediate-Release Solid Oral Dosage Forms Based on a Biopharmaceutics Classification System* ., 2017. Available at: https://www.fda.gov/media/70963/download. Accessed February 28, 2020.

71.   Dressman JB *et al.* The BCS: Where Do We Go from Here? *Pharm Technol* 2001; 25: 68–76. Available at: www.pharmaportal.com. Accessed February 29, 2020.

72.   Sheng JJ, Amidon GL. The Biopharmaceutics Classification System: Recent Applications in Pharmaceutical Discovery, Development, and Regulation. In: Dressman J, Reppas C, eds. *Oral Drug Absorption Prediction and Assessment*, 2nd ed. CRC Press, 2016: 154–170. doi:10.3109/9781420077346-9.

73.   Rosenberger J *et al.* A Refined Developability Classification System. *J Pharm Sci* 2018;

107(8): 2020–2032. doi:10.1016/j.xphs.2018.03.030.

74.   Guzmán HR *et al.* Combined Use of Crystalline Salt Forms and Precipitation Inhibitors to Improve Oral Absorption of Celecoxib from Solid Oral Formulations. *J Pharm Sci* 2007; 96(10): 2686–2702. doi:10.1002/jps.20906.

75.   Xua S, Dai WG. Drug precipitation inhibitors in supersaturable formulations. *Int J Pharm* 2013; 453(1): 36–43. doi:10.1016/j.ijpharm.2013.05.013.

76.   Williams HD *et al.* Strategies to address low drug solubility in discovery and development. *Pharmacol Rev* 2013; 65(1): 315–499. doi:10.1124/pr.112.005660.

77.   Rabinow BE. Nanosuspensions in drug delivery. *Nat Rev Drug Discov* 2004; 3(9): 785–796. doi:10.1038/nrd1494.

78.   Noyes AA, Whitney WR. The rate of solution of solid substances in their own solutions. *J Am Chem Soc* 1897; 19(12): 930–934. doi:10.1021/ja02086a003.

79.   Dokoumetzidis A, Macheras P. A century of dissolution research: From Noyes and Whitney to the Biopharmaceutics Classification System. *Int J Pharm* 2006; 321(1–2): 1–11. doi:10.1016/j.ijpharm.2006.07.011.

80.   Junghanns JUAH, Müller RH. Nanocrystal technology, drug delivery and clinical applications. *Int J Nanomedicine* 2008; 3(3): 295–309.

81.   Kesisoglou F, Mitra A. Crystalline Nanosuspensions as Potential Toxicology and Clinical Oral Formulations for BCS II/IV Compounds. *AAPS J* 2012; 14(4): 677–687. doi:10.1208/s12248-012-9383-0.

82.   Shono Y *et al.* Forecasting in vivo oral absorption and food effect of micronized and nanosized aprepitant formulations in humans. *Eur J Pharm Biopharm* 2010; 76(1): 95–104. doi:10.1016/j.ejpb.2010.05.009.

83.   Kaptay G. On the size and shape dependence of the solubility of nano-particles in solutions. *Int J Pharm* 2012; 430(1–2): 253–257. doi:10.1016/j.ijpharm.2012.03.038.

84. Letellier P *et al.* Solubility of nanoparticles: nonextensive thermodynamics approach. *J Phys Condens Matter* 2007; 19(43): 436229. doi:10.1088/0953-8984/19/43/436229.

85. Leuner C, Dressman J. Improving drug solubility for oral delivery using solid dispersions. *Eur J Pharm Biopharm* 2000; 50(1): 47–60. doi:10.1016/S0939-6411(00)00076-X.

86. Newman A *et al.* Assessing the performance of amorphous solid dispersions. *J Pharm Sci* 2012; 101(4): 1355–1377. doi:10.1002/jps.23031.

87. Newman A *et al.* Amorphous solid dispersions: a robust platform to address bioavailability challenges. *Ther Deliv* 2015; 6(2): 247–61. doi:10.4155/tde.14.101.

88. Gao P. Amorphous pharmaceutical solids: Characterization, stabilization, and development of marketable formulations of poorly soluble drugs with improved oral absorption. *Mol Pharm* 2008; 5(6): 903–904. doi:10.1021/mp800203k.

89. Klein CE *et al.* The tablet formulation of lopinavir/ritonavir provides similar bioavailability to the soft-gelatin capsule formulation with less pharmacokinetic variability and diminished food effect. *J Acquir Immune Defic Syndr* 2007; 44(4): 401–10. doi:10.1097/QAI.0b013e31803133c5.

90. Mellaerts R *et al.* Increasing the oral bioavailability of the poorly water soluble drug itraconazole with ordered mesoporous silica. *Eur J Pharm Biopharm* 2008; 69(1): 223–30. doi:10.1016/j.ejpb.2007.11.006.

91. Sager JE *et al.* Physiologically based pharmacokinetic (PBPK) modeling and simulation approaches: A systematic review of published models, applications, and model verification. *Drug Metab Dispos* 2015; 43(11): 1823–1837. doi:10.1124/dmd.115.065920.

92. Mitra A *et al.* Physiologically Based Absorption Modeling for Amorphous Solid Dispersion Formulations. *Mol Pharm* 2016; 13(9): 3206–3215. doi:10.1021/acs.molpharmaceut.6b00424.

93. Purohit HS *et al.* Investigating the Impact of Drug Crystallinity in Amorphous Tacrolimus Capsules on Pharmacokinetics and Bioequivalence Using Discriminatory In Vitro

Dissolution Testing and Physiologically Based Pharmacokinetic Modeling and Simulation. *J Pharm Sci* 2018; 107(5): 1330–1341. doi:10.1016/j.xphs.2017.12.024.

94. Emami Riedmaier A *et al.* Mechanistic Physiologically Based Pharmacokinetic Modeling of the Dissolution and Food Effect of a Biopharmaceutics Classification System IV Compound—The Venetoclax Story. *J Pharm Sci* 2018. doi:10.1016/j.xphs.2017.09.027.

95. EMA. Guideline on the investigation of drug interactions. *Guid Doc* 2012; 44(June): 59. doi:10.1093/deafed/ens058.

96. Huang S-M. Clinical Drug Interaction Studies — Study Design, Data Analysis, and Clinical Implications Guidance for Industry. *FDA Guid* 2009. Available at: http://www.fda.gov/Drugs/GuidanceComplianceRegulatoryInformation/Guidances/default.htm. Accessed January 10, 2018.

97. Litou C *et al.* Effects of medicines used to treat gastrointestinal diseases on the pharmacokinetics of coadministered drugs: a PEARRL Review. *J Pharm Pharmacol* 2018. doi:10.1111/jphp.12983.

98. Jaruratanasirikul S, Sriwiriyajan S. Effect of omeprazole on the pharmacokinetics of itraconazole. *Eur J Clin Pharmacol* 1998; 54(2): 159–61. Available at: http://www.ncbi.nlm.nih.gov/pubmed/9626921. Accessed August 29, 2017.

99. Johnson MD *et al.* A randomized comparative study to determine the effect of omeprazole on the peak serum concentration of itraconazole oral solution. *J Antimicrob Chemother* 2003; 51(2): 453–7. Available at: http://www.ncbi.nlm.nih.gov/pubmed/12562722. Accessed September 1, 2017.

100. DIFLUCAN ® (Fluconazole Tablets) (Fluconazole for Oral Suspension). Available at: https://www.accessdata.fda.gov/drugsatfda_docs/label/2014/019949s060,020090s044lbl.pdf. Accessed August 29, 2017.

101. LIM SG *et al.* Short report: the absorption of fluconazole and itraconazole under conditions of low intragastric acidity. *Aliment Pharmacol Ther* 2007; 7(3): 317–321.

doi:10.1111/j.1365-2036.1993.tb00103.x.

102. Hörter D, Dressman J. Influence of physicochemical properties on dissolution of drugs in the gastrointestinal tract. *Adv Drug Deliv Rev* 2001; 46(1–3): 75–87. doi:10.1016/S0169-409X(00)00130-7.

103. Thorpe JE *et al.* Effect of Oral Antacid Administration on the Pharmacokinetics of Oral Fluconazole. *Antimicrob Agents Chemother* 1990; 34(10): 2032–3. Available at: http://www.ncbi.nlm.nih.gov/pubmed/2291673. Accessed August 31, 2017.

104. Budha NR *et al.* Drug Absorption Interactions Between Oral Targeted Anticancer Agents and PPIs: Is pH-Dependent Solubility the Achilles Heel of Targeted Therapy? *Clin Pharmacol Ther* 2012; 92(2): 203–213. doi:10.1038/clpt.2012.73.

105. Cristofoletti R *et al.* Assessment of Bioequivalence of Weak Base Formulations Under Various Dosing Conditions Using Physiologically Based Pharmacokinetic Simulations in Virtual Populations. Case Examples: Ketoconazole and Posaconazole. *J Pharm Sci* 2017; 106(2): 560–569. doi:10.1016/J.XPHS.2016.10.008.

106. Doki K *et al.* Virtual bioequivalence for achlorhydric subjects: The use of PBPK modelling to assess the formulation-dependent effect of achlorhydria. *Eur J Pharm Sci* 2017; 109: 111–120. doi:10.1016/J.EJPS.2017.07.035.

107. Establishing Bioequivalence in Virtual Space: Are We Really There? | AAPS Blog. Available at: https://aapsblog.aaps.org/2016/09/29/establishing-bioequivalence-in-virtual-space-are-we-really-there/. Accessed January 25, 2018.

108. Litou C *et al.* Measuring pH and Buffer Capacity in Fluids Aspirated from the Fasted Upper Gastrointestinal Tract of Healthy Adults. *Pharm Res* 2020; 37(3): 42. doi:10.1007/s11095-019-2731-3.

109. Psachoulias D *et al.* Precipitation in and supersaturation of contents of the upper small intestine after administration of two weak bases to fasted adults. *Pharm Res* 2011; 28(12): 3145–3158. doi:10.1007/s11095-011-0506-6.

110. O'Dwyer PJ *et al. In vitro* methods to assess drug precipitation in the fasted small intestine - a PEARRL review. *J Pharm Pharmacol* 2018. doi:10.1111/jphp.12951.

111. Kostewicz ES *et al.* Predicting the precipitation of poorly soluble weak bases upon entry in the small intestine. *J Pharm Pharmacol* 2004; 56(1): 43–51. doi:10.1211/0022357022511.

112. Ruff A *et al.* Prediction of Ketoconazole absorption using an updated in vitro transfer model coupled to physiologically based pharmacokinetic modelling. *Eur J Pharm Sci* 2017; 100: 42–55. doi:10.1016/j.ejps.2016.12.017.

113. Berlin M *et al.* Prediction of oral absorption of cinnarizine – A highly supersaturating poorly soluble weak base with borderline permeability. *Eur J Pharm Biopharm* 2014; 88(3): 795–806. doi:10.1016/j.ejpb.2014.08.011.

114. Hens B *et al. In Silico* Modeling Approach for the Evaluation of Gastrointestinal Dissolution, Supersaturation, and Precipitation of Posaconazole. *Mol Pharm* 2017: acs.molpharmaceut.7b00396. doi:10.1021/acs.molpharmaceut.7b00396.

115. Kambayashi A *et al.* Prediction of the precipitation profiles of weak base drugs in the small intestine using a simplified transfer ("dumping") model coupled with in silico modeling and simulation approach. *Eur J Pharm Biopharm* 2016; 103: 95–103. doi:10.1016/j.ejpb.2016.03.020.

116. Sjögren E *et al. In Silico* Modeling of Gastrointestinal Drug Absorption: Predictive Performance of Three Physiologically Based Absorption Models. *Mol Pharm* 2016; 13(6): 1763–1778. doi:10.1021/acs.molpharmaceut.5b00861.

117. Wagner C *et al.* Predicting the oral absorption of a poorly soluble, poorly permeable weak base using biorelevant dissolution and transfer model tests coupled with a physiologically based pharmacokinetic model. *Eur J Pharm Biopharm* 2012; 82(1): 127–138. doi:10.1016/j.ejpb.2012.05.008.

118. Kesisoglou F *et al.* Physiologically Based Absorption Modeling of Salts of Weak Bases Based on Data in Hypochlorhydric and Achlorhydric Biorelevant Media. *AAPS PharmSciTech*

2018; 19(7): 2851–2858. doi:10.1208/s12249-018-1059-3.

119. EMA. EMEND: Summary of product characteritics. Available at: http://www.ema.europa.eu/docs/en_GB/document_library/EPAR_-_Product_Information/human/000527/WC500026537.pdf. Accessed October 25, 2017.

120. FDA-Emend Capsules Pharmacology Review Part 1.pdf. Available at: https://www.accessdata.fda.gov/drugsatfda_docs/nda/2003/21-549_Emend.cfm.

121. Wu Y *et al.* The role of biopharmaceutics in the development of a clinical nanoparticle formulation of MK-0869: A Beagle dog model predicts improved bioavailability and diminished food effect on absorption in human. *Int J Pharm* 2004; 285(1–2): 135–146. doi:10.1016/j.ijpharm.2004.08.001.

122. Georgaka D *et al.* Evaluation of Dissolution in the Lower Intestine and Its Impact on the Absorption Process of High Dose Low Solubility Drugs. *Mol Pharm* 2017; 14(12): 4181–4191. doi:10.1021/acs.molpharmaceut.6b01129.

123. Söderlind E *et al.* Simulating Fasted Human Intestinal Fluids: Understanding the Roles of Lecithin and Bile Acids. *Mol Pharm* 2010; 7(5): 1498–1507. doi:10.1021/mp100144v.

124. Takano R *et al.* Rate-limiting steps of oral absorption for poorly water-soluble drugs in dogs; prediction from a miniscale dissolution test and a physiologically-based computer simulation. *Pharm Res* 2008; 25(10): 2334–2344. doi:10.1007/s11095-008-9637-9.

125. EMEND® Clinical Pharmacology and Biopharmaceutics Review. Available at: https://www.accessdata.fda.gov/drugsatfda_docs/nda/2003/21-549_Emend_biopharmr.pdf. Accessed August 31, 2017.

126. Majumdar AK *et al.* Pharmacokinetics of aprepitant after single and multiple oral doses in healthy volunteers. *J Clin Pharmacol* 2006; 46(3): 291–300. doi:10.1177/0091270005283467.

127. Deeks ED, Keating GM. Etravirine. *Drugs* 2008; 68(16): 2357–2372.

128. EMA. Intelence: Summary of Product Characteristics. Available at:

https://www.ema.europa.eu/en/documents/product-information/intelence-epar-product-information_en.pdf. Accessed July 24, 2019.

129. FDA. Intelence Drug Approval Package. Available at: https://www.accessdata.fda.gov/drugsatfda_docs/nda/2008/022187TOC.cfm. Accessed July 24, 2019.

130. Weuts I *et al.* Physicochemical properties of the amorphous drug, cast films, and spray dried powders to predict formulation probability of success for solid dispersions: Etravirine. *J Pharm Sci* 2011; 100(1): 260–274. doi:10.1002/jps.22242.

131. EMA. INTELENCE: Etravirine CHMP Assessment Report. *43952* 2008: 1–52. Available at: http://www.ema.europa.eu/docs/en_GB/document_library/EPAR_-_Public_assessment_report/human/000900/WC500034183.pdf.

132. Bevernage J *et al.* Supersaturation in human gastric fluids. *Eur J Pharm Biopharm* 2012; 81(1): 184–189. doi:10.1016/j.ejpb.2012.01.017.

133. Moltó J. Physiologically based pharmacokinetic model to predict drug-drug interaction in patients receiving antiretroviral and antineoplastic therapies. In: *16th HIVHEPPK*. Alexandria, VA, 2015.

134. Schöller-Gyüre M *et al.* Effects of different meal compositions and fasted state on the oral bioavailability of etravirine. *Pharmacotherapy* 2008; 28(10): 1215–1222. doi:10.1592/phco.28.10.1215.

135. Rajoli RKR *et al.* Physiologically Based Pharmacokinetic Modelling to Inform Development of Intramuscular Long-Acting Nanoformulations for HIV. *Clin Pharmacokinet* 2015; 54(6): 639–650. doi:10.1007/s40262-014-0227-1.

136. Litou C *et al.* Combining biorelevant in vitro and in silico tools to simulate and better understand the in vivo performance of a nano-sized formulation of aprepitant in the fasted and fed states. *Eur J Pharm Sci* 2019; 138: 105031. doi:10.1016/j.ejps.2019.105031.

137. Andreas CJ *et al.* In vitro biorelevant models for evaluating modified release mesalamine

products to forecast the effect of formulation and meal intake on drug release. *Eur J Pharm Biopharm* 2015; 97: 39–50. doi:10.1016/j.ejpb.2015.09.002.

138.   Niederquell A, Kuentz M. Biorelevant Drug Solubility Enhancement Modeled by a Linear Solvation Energy Relationship. *J Pharm Sci* 2018; 107(1): 503–506. doi:10.1016/j.xphs.2017.08.017.

139.   Zhou Z *et al.* Statistical investigation of simulated fed intestinal media composition on the equilibrium solubility of oral drugs. *Eur J Pharm Sci* 2017; 99: 95–104. doi:10.1016/j.ejps.2016.12.008.

140.   Sanchez RI *et al.* Cytochrome P450 3A4 Is the Major Enzyme Involved in the Metabolism of the Substance P Receptor Antagonist Aprepitant Abstract : 2004; 32(11): 1287–1292. doi:10.1124/dmd.104.000216.given.

141.   EMA. EMEND® - Scientific Discussion. 2004; (June): 1–30. Available at: http://www.ema.europa.eu/docs/en_GB/document_library/EPAR_-_Scientific_Discussion/human/000527/WC500026534.pdf.

142.   Bubalo JS *et al.* Aprepitant pharmacokinetics and assessing the impact of aprepitant on cyclophosphamide metabolism in cancer patients undergoing hematopoietic stem cell transplantation. *J Clin Pharmacol* 2012; 52(4): 586–594. doi:10.1177/0091270011398243.

143.   Rowland M, Tozer TN. *Clinical pharmacokinetics : concepts and applications*. Williams & Wilkins, 1995. Available at: https://openlibrary.org/books/OL1101417M/Clinical_pharmacokinetics. Accessed August 7, 2018.

144.   Jamei M *et al.* Population-based mechanistic prediction of oral drug absorption. *AAPS J* 2009; 11(2): 225–37. doi:10.1208/s12248-009-9099-y.

145.   S. Darwich A *et al.* Interplay of Metabolism and Transport in Determining Oral Drug Absorption and Gut Wall Metabolism: A Simulation Assessment Using the "Advanced Dissolution, Absorption, Metabolism (ADAM)" Model. *Curr Drug Metab* 2010; 11(9): 716–

729. doi:10.2174/138920010794328913.

146. Litou C *et al.* Combining biorelevant in vitro and in silico tools to investigate the in vivo performance of the amorphous solid dispersion formulation of etravirine in the fed state. *Eur J Pharm Sci* 2020: 105297. doi:10.1016/j.ejps.2020.105297.

147. Bevernage J *et al.* Drug Supersaturation in Simulated Human Intestinal Fluids Representing Different Nutritional States. *J Pharm Sci* 2010; 99(11): 4525–4534. doi:10.1002/jps.22154.

148. Elkhabaz A *et al.* Variation in Supersaturation and Phase Behavior of Ezetimibe Amorphous Solid Dispersions upon Dissolution in Different Biorelevant Media. *Mol Pharm* 2018; 15(1): 193–206. doi:10.1021/acs.molpharmaceut.7b00814.

149. Siccardi M *et al.* Prediction of Etravirine Pharmacogenetics using a Physiologically Based Pharmacokinetic approach. *20th Conf Retroviruses Opportunistic Infect Atlanta, USA* 2013.

150. Green B *et al.* Evaluation of Concomitant Antiretrovirals and CYP2C9/CYP2C19 Polymorphisms on the Pharmacokinetics of Etravirine. *Clin Pharmacokinet* 2017; 56(5): 525–536. doi:10.1007/s40262-016-0454-8.

151. Lubomirov R *et al.* Pharmacogenetics-based population pharmacokinetic analysis of etravirine in HIV-1 infected individuals. *Pharmacogenet Genomics* 2013; 23(1): 9–18. doi:10.1097/FPC.0b013e32835ade82.

152. Kakuda TN *et al.* Pharmacokinetics and Pharmacodynamics of the Non-Nucleoside Reverse-Transcriptase Inhibitor Etravirine in Treatment-Experienced HIV-1-Infected Patients. *Clin Pharmacol Ther* 2010; 88(5): 695–703. doi:10.1038/clpt.2010.181.

153. Yanakakis LJ, Bumpus NN. Biotransformation of the antiretroviral drug etravirine: Metabolite identification, reaction phenotyping, and characterization of autoinduction of cytochrome P450-dependent metabolism. *Drug Metab Dispos* 2012; 40(4): 803–814. doi:10.1124/dmd.111.044404.

154. Moltó J *et al.* Use of a physiologically based pharmacokinetic model to simulate drug–drug interactions between antineoplastic and antiretroviral drugs. *J Antimicrob Chemother*

2016; (December 2016): dkw485. doi:10.1093/jac/dkw485.

155. Kakuda TN *et al.* Single-dose pharmacokinetics of pediatric and adult formulations of etravirine and swallowability of the 200-mg tablet: results from three Phase 1 studies. *Int J Clin Pharmacol Ther* 2013; 51(9): 725–737. doi:10.5414/CP201770.

156. Schöller-Gyüre M *et al.* A pharmacokinetic study of etravirine (TMC125) co-administered with ranitidine and omeprazole in HIV-negative volunteers. *Br J Clin Pharmacol* 2008; 66(4): 508–516. doi:10.1111/j.1365-2125.2008.03214.x.

157. Schöller-Gyüre M *et al.* Effects of hepatic impairment on the steady-state pharmacokinetics of etravirine 200 mg BID: An open-label, multiple-dose, controlled Phase I study in adults. *Clin Ther* 2010; 32(2): 328–337. doi:10.1016/j.clinthera.2010.02.013.

158. Park K. Different phase behaviors of enzalutamide amorphous solid dispersions. *J Control Release* 2018; 292: 277–278. doi:10.1016/j.jconrel.2018.11.021.

159. Wilson V *et al.* Relationship between amorphous solid dispersion in vivo absorption and in vitro dissolution: phase behavior during dissolution, speciation, and membrane mass transport. *J Control Release* 2018; 292: 172–182. doi:10.1016/j.jconrel.2018.11.003.

160. Dickinson PA *et al.* Optimizing Clinical Drug Product Performance: Applying Biopharmaceutics Risk Assessment Roadmap (BioRAM) and the BioRAM Scoring Grid. *J Pharm Sci* 2016; 105(11): 3243–3255. doi:10.1016/j.xphs.2016.07.024.

A. Appendix

A.1 Publication List

Peer-reviewed papers

1. O'Dwyer PJ, <u>Litou C</u>, Box KJ, Dressman JB, Kostewicz ES, Kuentz M, et al. *In vitro* methods to assess drug precipitation in the fasted small intestine - a PEARRL review. Journal of Pharmacy and Pharmacology. 2018 Jun 28; Available from: http://www.ncbi.nlm.nih.gov/pubmed/29956338
    (equal first author)

2. <u>Litou C</u>, Effinger A, Kostewicz ES, Box KJ, Fotaki N, Dressman JB. Effects of medicines used to treat gastrointestinal diseases on the pharmacokinetics of coadministered drugs: a PEARRL Review. Journal of Pharmacy and Pharmacology. 2018 Jul 30; Available from: http://www.ncbi.nlm.nih.gov/pubmed/30062750
    (equal first author)

3. <u>Litou C</u>, Patel N, Turner DB, Kostewicz E, Kuentz M, Box KJ, et al. Combining biorelevant in vitro and in silico tools to simulate and better understand the in vivo performance of a nano-sized formulation of aprepitant in the fasted and fed states. Vol. 138, European Journal of Pharmaceutical Sciences. 2019 Oct 1;138:105031. Available from: http://www.ncbi.nlm.nih.gov/pubmed/31386891

4. <u>Litou C</u>, Psachoulias D, Vertzoni M, Dressman J, Reppas C. Measuring pH and Buffer Capacity in Fluids Aspirated from the Fasted Upper Gastrointestinal Tract of Healthy Adults. Vol. 37, Pharmaceutical Research. 2020 Mar 1;37(3):42. Available from: http://www.ncbi.nlm.nih.gov/pubmed/31989335

5. <u>Litou C</u>, Turner DB, Holmstock N, Ceulemans J, Box KJ, Kostewicz E, et al. Combining biorelevant in vitro and in silico tools to investigate the in vivo performance of the amorphous solid dispersion formulation of etravirine in the fed state. European Journal of Pharmaceutical Sciences. 2020 Mar 6;105297. Available from: https://linkinghub.elsevier.com/retrieve/pii/S0928098720300865

A.2 Personal contributions

Publication 1: Effects of medicines used to treat gastrointestinal diseases on the pharmacokinetics of coadministered drugs: a PEARRL Review.

My personal contributions to this work were: i) writing of the abstract, introduction, conclusion and future perspectives, ii) writing of paragraphs "Agents affecting gastrointestinal motility", "Prokinetic agents", "Anticholinergic agents", "Dietary Fibers", "Antiemetics", "Proton pump inhibitors", "H_2 receptor antagonists", "Antacids", "Probiotics", iii) improving the whole manuscript according to the suggestions of the co-authors and reviewers, iv) submitting the article and handling correspondence with the reviewers.

The paragraphs "Laxatives", "Antidiarrheal agents", "Antibiotics used for gastrointestinal infections", "Anti-inflammatory drugs for inflammatory bowel disease", "Immunosuppressive agents for inflammatory bowel disease" and "Bile acid sequestrants" were written by my co-author Angela Effinger.

Publication 2: Measuring pH and Buffer Capacity in Fluids Aspirated from the Fasted Upper Gastrointestinal Tract of Healthy Adults.

My personal contributions to this work were: i) planning and conducting all *in vitro* experiments, ii) acquiring all the relevant information needed from all published aspiration studies, iii) the statistical analysis and interpretation of the data, iv) writing the manuscript, and v) handling correspondence and improving the manuscript according to the suggestions of the co-authors and reviewers.

Publication 3: *In vitro* methods to assess drug precipitation in the fasted small intestine - a PEARRL review.

My personal contributions to this work were: i) writing of the introduction, as well as the paragraph "Coupling full scale *in vitro* testing with physiologically based pharmacokinetic modelling", ii) writing all paragraphs regarding the full scale methods to address drug precipitation (i.e. Compendial apparatus and methods- USP I and USP II dissolution apparatus and methods, the "dumping" test-, Compartment methods not addressing intestinal absorption-closed systems, open systems-, Compartment methods which attempt to account of absorption-Using appropriate flow rates to take into account both absorption and transit process, Simulating the intestinal epithelial barrier-), iii) writing the paragraph entitled "Compartmental methods using cellular membranes" from the small scale methods to address drug precipitation and iv) improving the manuscript according to the suggestions of the co-authors and reviewers, regarding the parts which I have written.

The conclusion and the rest paragraphs of the small scale methods to address drug precipitation (i.e. Single media tests, Tests with medium shift, Tests with medium and pH shifts, Two-stage tests, Methods addressing intestinal absorption-Biphasic dissolution test, Compartmental methods using non-cellular biomimetic membranes-) were written by my co-author Patrick

O'Dwyer. The abstract of the paper was written together with my co-author Patrick O'Dwyer. The submission of article and the correspondence with the reviewers was handled by my co-author Patrick O'Dwyer.

Publication 4: Combining biorelevant *in vitro* and *in silico* tools to simulate and better understand the *in vivo* performance of a nano-sized formulation of aprepitant in the fasted and fed states.

My personal contributions to this work were: i) planning and conducting all *in vitro* experiments, ii) acquiring all the relevant information needed for building the PBPK model, for simulation and interpretation, iii) building the mechanistic PBPK models under fasted and fed state conditions, iv) writing the manuscript, and v) handling correspondence and improving the manuscript according to the suggestions of the co-authors and reviewers.

Publication 5: Combining biorelevant *in vitro* and *in silico* tools to investigate the *in vivo* performance of the amorphous solid dispersion formulation of etravirine in the fed state.

My personal contributions to this work were: i) planning and conducting all *in vitro* experiments, ii) acquiring all the relevant information needed for building the PBPK model, for simulation and interpretation, iii) building the mechanistic PBPK models under fed state conditions, iv) writing the manuscript, and v) handling correspondence and improving the manuscript according to the suggestions of the co-authors and reviewers.

A.3 Publication manuscripts

Review

Effects of medicines used to treat gastrointestinal diseases on the pharmacokinetics of coadministered drugs: a PEARRL Review

Chara Litou[a,†] (iD), Angela Effinger[b,†], Edmund S. Kostewicz[a], Karl J. Box[c], Nikoletta Fotaki[b] (iD) and Jennifer B. Dressman[a]

[a]Institute of Pharmaceutical Technology, Goethe University, Frankfurt am Main, Germany, [b]Department of Pharmacy and Pharmacology, Faculty of Science, University of Bath, Bath, UK and [c]Pion Inc. (UK) Ltd., Forest Row, East Sussex, UK

Abstract

Objectives Drugs used to treat gastrointestinal diseases (GI drugs) are widely used either as prescription or over-the-counter (OTC) medications and belong to both the 10 most prescribed and 10 most sold OTC medications worldwide. The objective of this review article is to discuss the most frequent interactions between GI and other drugs, including identification of the mechanisms behind these interactions, where possible.

Key findings Current clinical practice shows that in many cases, these drugs are administered concomitantly with other drug products. Due to their metabolic properties and mechanisms of action, the drugs used to treat gastrointestinal diseases can change the pharmacokinetics of some coadministered drugs. In certain cases, these interactions can lead to failure of treatment or to the occurrence of serious adverse events. The mechanism of interaction depends highly on drug properties and differs among therapeutic categories. Understanding these interactions is essential to providing recommendations for optimal drug therapy.

Summary Interactions with GI drugs are numerous and can be highly significant clinically in some cases. While alterations in bioavailability due to changes in solubility, dissolution rate, GI transit and metabolic interactions can be (for the most part) easily identified, interactions that are mediated through other mechanisms, such as permeability or microbiota, are less well-understood. Future work should focus on characterising these aspects.

Introduction

It is estimated that 60–70 million US-Americans suffer annually from various types of gastrointestinal (GI) diseases, with GI diseases being the underlying cause of approximately 10% of all deaths in the USA.[1,2] In fact, statistical data on global sales of prescription medication from 2014 indicate that sales of drug products for the treatment of GI diseases rank 12th with regard to sales of prescription medication worldwide.[3]

The term gastrointestinal diseases covers a wide range of disorders, which can be either acute or chronic. Non-ulcer or functional dyspepsia, for example, is usually an acute condition that affects the upper GI tract and is expressed by symptoms such as nausea, vomiting, heartburn, bloating and stomach discomfort. The treatment of functional dyspepsia can involve various drug classes depending on the symptoms as well as the possible causative factors.[4–6] Crohn's disease, by contrast, is a chronic inflammatory disorder that can affect any part of the GI tract from the mouth to the anus. Although as of yet there is no cure for Crohn's disease, there are several treatment options which can relieve the symptoms and prevent relapse.[7] As illustrated by these two examples, it is evident that a diversity of drugs with different mechanisms of action is required to address the various targets across the spectrum of GI diseases.

Frequently, patients are prescribed several drugs concomitantly. Drug–drug interactions (DDIs) are a common problem during drug treatment and can sometimes lead to

failure of treatment, or can cause serious or even fatal adverse events.[8]

Medications used for the treatment of GI diseases can alter the GI physiology and thus interact with the absorption of concomitant medications, but they can also alter the metabolism and/or elimination of coadministered drugs, potentially resulting, on the one hand, in a lack of efficacy of the coadministered drug or, on the other hand, in adverse drug reactions. From a regulatory perspective, studies of potential DDIs which lead to changes in absorption are required for the marketing authorisation of medicinal products in the European Union and United States.[8,9] In particular, these studies are designed to evaluate the effect of increased GI pH, the possibility of complexation and alterations in GI transit time.[8] Understanding the effect of GI drugs on the physiology of the GI tract and achieving a mechanistic understanding of the interaction(s) involved are key to successfully managing concomitant drug therapy.

In clinical trials, drug performance is determined under controlled conditions (e.g. with strict inclusion/exclusion criteria, under absence of, or controlled comedication and with monitoring of compliance). But, in clinical practice, where a much wider variety of patient characteristics, disease states and multimorbidity is usual, the potential for DDIs is much greater. In fact, statistics show that one in a hundred hospital admissions occurs as a result of a drug–drug interaction.[10] The number of unreported/less severe interactions is probably far greater.

In addition to potential interactions with prescription drugs, one must also consider the possibility of interactions with over-the-counter medication (OTC). FDA publishes information leaflets for consumers about the most typical drug interactions that occur with specific OTC medications. It is interesting to note that four out of the 12 drugs discussed by FDA in these leaflets involve drugs used to treat gastrointestinal diseases.[11] European statistics indicate that there may be similar issues with concomitant use of OTC medication in the European Union, since 20–70% of those surveyed reported using OTC medicines.[12]

Keeping in mind these statistics, as well as the fact that medications used to treat GI diseases count among the 10 most prescribed medicines – and also fall within the top 10 in terms of sales of OTC medications – worldwide,[3,13] it is evident that there is a high potential for DDIs with these medications.

The objective of this review was first to present and discuss the effects of drugs used to treat GI diseases, both prescription and OTC, on the pharmacokinetics and bioavailability of coadministered drugs and second, to identify the mechanisms behind these interactions insofar as possible. The review is organised according to the therapeutic indication of the drug (see Figure 1 for an overview) and covers drugs used to prevent/treat all major GI diseases. Although several reviews concerning DDIs of specific GI drug classes, for example proton-pump inhibitors (PPIs), are available in the literature, to the best of these authors' knowledge, this is the first to provide an overview of interactions that are likely to occur across the range of drugs used to treat GI diseases.
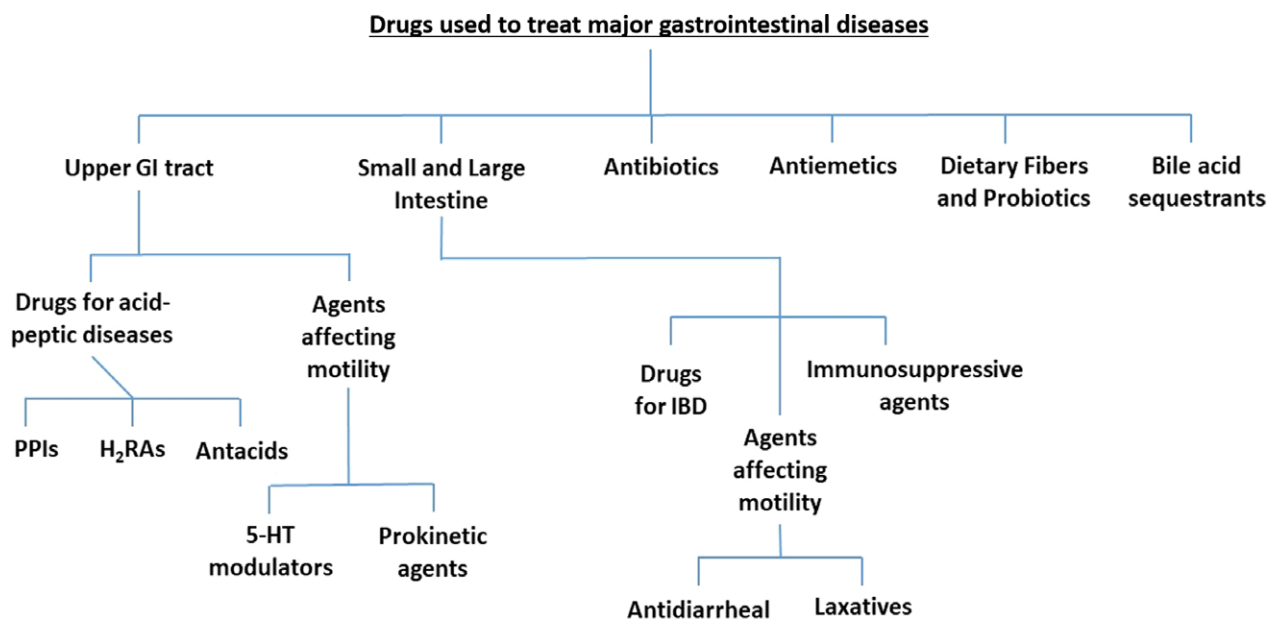
Figure 1 Gastrointestinal drugs discussed in this review. [Colour figure can be viewed at wileyonlinelibrary.com]

Medicines used to treat gastrointestinal diseases and their effect on coadministered drugs

Agents affecting gastrointestinal motility

Various neurotransmitters have an effect on GI motility and its coordination. Dopamine, for example, is present in significant amounts in the GI wall and has an inhibitory effect on motility.[14,15] Dopamine receptor antagonists are currently being used for motor disorders of the upper GI tract, gastroesophageal reflux disease, chronic dyspepsia and gastroparesis and have also been investigated for therapy of motility disorders of the lower GI tract.[16,17] Acetylcholine, by contrast, stimulates GI motility through increased contractile activity by the smooth muscle.[18,19] Serotonin, which is mainly present in the enterochromaffin cells in the enteric epithelium and colon, has a wide range of effects on the GI tract. The diversity of effects can be explained by the presence of multiple subtypes of 5-HT receptors, located on different types of cells. Both agonists and antagonists of 5-HT receptors are used for the treatment of GI diseases.[20,21]

Prokinetic agents

Prokinetic agents promote gut wall contractions and increase their coordination, thus enhancing GI motility. However, they do not disrupt the normal physiological pattern of motility.[16,17]

Metoclopramide. Metoclopramide is a first-generation prokinetic agent with antidopaminergic properties (D1 and D2 receptor antagonist). In addition, metoclopramide is a 5-HT$_3$ receptor antagonist and a 5-HT$_4$ receptor agonist. Metoclopramide promotes the response to acetylcholine in the upper GI tract and therefore accelerates gastric emptying and increases the tone of the lower oesophageal sphincter.[22] The effect is observed in both healthy volunteers and those with GI diseases.[23–25] For example, Fink *et al.*[25] demonstrated that metoclopramide accelerates gastric emptying in patients with gastroesophageal reflux disease independent of their gastric emptying status (Figure 2a and 2b). Metoclopramide is used for the symptomatic treatment of postoperative or chemotherapy-induced nausea and vomiting, gastroesophageal reflux disease and gastroparesis.[23] A summary of the effects of concomitant use of metoclopramide on the absorption of several APIs is presented in Table 1, and mechanistic explanations for the observed effects are presented in the following text.

It is known that migraine attacks are often accompanied by delayed gastric emptying.[26] Tokola *et al.*,[27] investigated the effect of metoclopramide on the absorption of
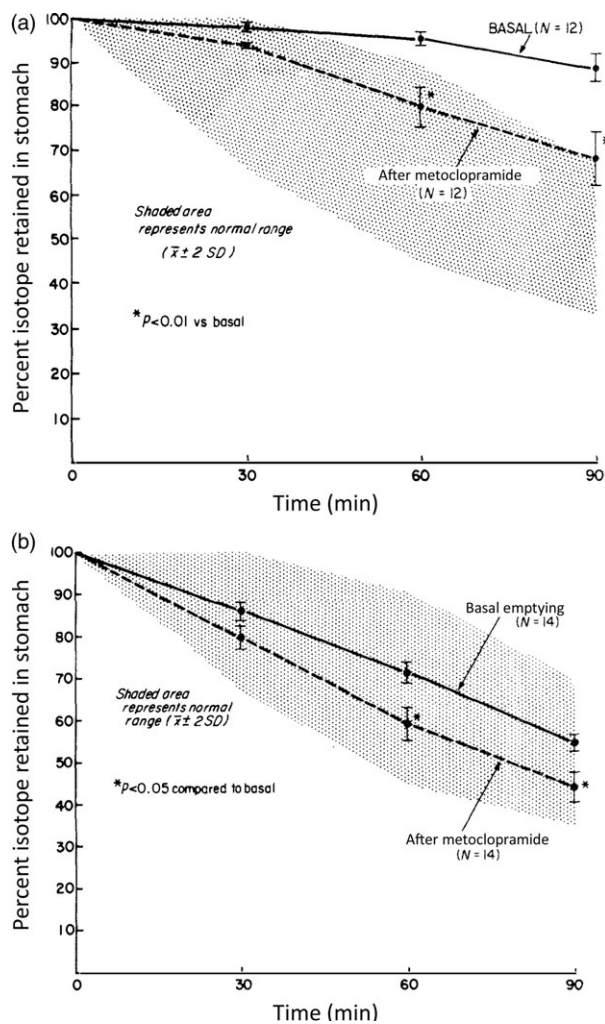
Figure 2 Gastric emptying results in 12 gastroesophageal reflux patients with delayed basal emptying rates (a) and in 14 gastroesophageal reflux patients with normal basal emptying rates (b), in a two-way crossover design consisting of a control phase and a phase in which 10 mg metoclopramide was ingested orally. The data are expressed as the mean percent (±1 SEM) isotope remaining in the stomach for a period of 90 min after ingestion of an isotope-labelled test meal.[25] Figure reprinted from Fink *et al.* with permission from Springer Nature.

tolfenamic acid in patients diagnosed with migraine. According to the protocol, the volunteers took part in the absorption studies twice in the absence of migraine and twice as soon as possible after the beginning of a migraine attack. After rectal administration of metoclopramide, the absorption of the tolfenamic acid was accelerated compared to control (rectal administration of placebo) in all subjects. However, the total bioavailability of tolfenamic acid did not change significantly.[27] A similar study had been conducted in 1975 by Volans, in which the effect of

100

Table 1 Reported pharmacokinetic interactions with metoclopramide

		Effect				
	Interaction with	Rate of absorption	C_{max}	T_{max}	AUC	References
Drug–drug interactions with metoclopramide	Acetaminophen	↑	↑	↓		Nimmo et al. (1973)[30]
	Cimetidine		↓		↓	Gugler et al. (1981)[36]
			↓			Lee et al. (2000)[341]
	Cyclosporine		↑	↓	↑	Wadhwa et al. (1986)[42]
	Digoxin			↓	↓ (only for tablet)	Johnson et al. (1984)[41]
			↓			Manninen et al. (1973)[40]
	Droxicam	–		↓	–	Sánchez et al. (1989)[33]
	Levodopa	↑	↑	↓		Morris et al. (1976)[35]
	Lithium			↓		Crammer et al. (1974)[32]
	Methotrexate				↓ (paediatrics)	Mahony et al. (1984)[37]
	Mexiletine	↑			–	Wing et al. (1980)[31]
	Morphine		–	↓	–	Manara et al. (1988)[34]
	Salicylic acid		↑ plasma levels (in patients with migraine attacks)			Volans et al. (1975)[28]
	Tetracycline			↓	–	Gothoni et al. (1972)[29]
	Tolfenamic acid	↑			–	Tokola et al. (1984)[27]

metoclopramide on the absorption of aspirin during migraine attacks was investigated.[28] In that study, the delayed gastric emptying during a migraine attack was confirmed. In addition, it was shown that the plasma levels of salicylate achieved during a migraine attack, after intramuscular administration of metoclopramide, were higher in comparison with those achieved without metoclopramide pretreatment.

Gothoni et al.[29] reported an earlier time to achieve maximum plasma concentration (t_{max}) and elevated serum tetracycline concentrations in six healthy volunteers after coadministration of tetracycline with intramuscular metoclopramide. Nonetheless, the total area under the curve (AUC) remained unaltered. In the same study, an increase in the rate of absorption of oral pivampicillin was reported when administered along with metoclopramide.[29]

Concomitant administration of metoclopramide has also been shown to increase the absorption rate of acetaminophen, mexiletine, lithium, droxicam and morphine. Nimmo et al.[30] studied the absorption of acetaminophen with and without coadministration of metoclopramide in five healthy volunteers. The mean t_{max} was reduced from 120 to 48 min while the mean maximum plasma concentration (C_{max}) increased from 125 to 205 μg/ml. The urinary excretion of acetaminophen was not influenced. Given the fact that t_{max} is a function of both absorption and elimination rates, the shortened t_{max} after pretreatment with metoclopramide indicates an enhanced absorption rate.[30] Similar results were obtained in the study of Wing et al.,[31] in which the authors demonstrated an increased absorption rate of mexiletine after coadministration of metoclopramide. Here too, it was observed that the bioavailability of mexiletine was unaltered, indicating that during chronic

dosing of mexiletine, the antiarrhythmic effect is unlikely to change after concomitant use of metoclopramide.[31] In a further study by Crammer et al.,[32] it was shown that metoclopramide reduced the t_{max} of coadministered lithium by 2 h. Sánchez et al.,[33] investigated the effect of intravenous metoclopramide on the absorption of droxicam (a piroxicam prodrug) and Manara et al.,[34] investigated the effect of oral metoclopramide after concomitant administration of an oral controlled release formulation of morphine. In both cases, a significant reduction in t_{max} was observed, but other pharmacokinetic parameters were not significantly different.[33,34] Thus, in most studies, it has been demonstrated that although concomitant administration of metoclopramide increases absorption rate, there is little or no effect on AUC, or clinical efficacy.

In a study by Morris et al.,[35] it was likewise observed that the coadministration of metoclopramide resulted in an increased rate of absorption of levodopa and higher peak plasma concentrations, consistent with the earlier t_{max}. In this case, though, the authors emphasised the fact that higher peak concentrations of levodopa may result in dyskinetic movements, and therefore, this should be taken into consideration when metoclopramide is coadministered with levodopa.

Considering the properties of metoclopramide and the fact that besides promoting gastric emptying, it also increases the upper small intestinal motility, administration of metoclopramide could also decrease the time available for absorption in the small intestine and thus lead to a reduction in total bioavailability. Gugler et al.,[36] explored this hypothesis by studying the absorption of cimetidine when given concomitantly with antacids or metoclopramide. The study was conducted in eight healthy volunteers and showed that there was a

tendency to a shorter time to reach maximum plasma concentrations when metoclopramide was coadministered. Additionally, a decrease in AUC of approximately 22% was observed, although in neither case did the difference reach statistical significance.[36] On the other hand, Mahony *et al.*,[37] conducted a clinical study with children with leukaemia and reported that concomitant administration of methotrexate tablets with oral metoclopramide led to significantly lower AUC. Consistent with these findings, Pearson *et al.*,[38] demonstrated that a very fast or slow small intestinal transit in children with leukaemia reduces the C_{max} of methotrexate.[37,38]

In the studies conducted by Manninen *et al.*,[39,40] coadministration of metoclopramide with digoxin in eight healthy adults or in 11 patients on digoxin therapy resulted in reduced serum digoxin concentrations. The lower bioavailability of digoxin was attributed to its dissolution rate-limited absorption, as the changes were only observed when digoxin was given as a tablet and not when it was given as a solution. For this reason, authors suggested that fast dissolving tablets of digoxin would be less affected by coadministration of drugs which alter the GI motility. Supporting this hypothesis, Johnson *et al.*,[41] demonstrated that digoxin was absorbed completely and more quickly when it was given as soft-gelatine capsules rather as a tablet. Oral metoclopramide reduced the t_{max} for both formulations, but only reduced the AUC of the tablet formulation.[41] From these two studies, it is apparent that coadministration of metoclopramide may result in impaired drug absorption and decreased bioavailability in cases when a poorly soluble API exhibits dissolution rate-limited absorption.

In contrast to the results discussed above, Wadhwa *et al.*,[42] conducted a clinical study in 14 kidney transplant patients with the aim of increasing the bioavailability of cyclosporine. Cyclosporine is incompletely absorbed in the small intestine with a dose-dependent rate and extent of absorption. The authors reasoned the concomitant administration of cyclosporine with metoclopramide would increase the absorption rate and possibly the bioavailability of this immunosuppressive. Due to accelerated gastric emptying, there was a very significant increase in the C_{max} of cyclosporine, as well as a decrease in t_{max}. Furthermore, an average increase of 29% in the AUC was observed ($P = 0.003$). However, the authors concluded that further studies would be required to determine whether metoclopramide can reproducibly increase the absorption of cyclosporine on a long-term basis.[42]

Overall, it appears that coadministration of metoclopramide leads to a decreased t_{max} of the coadministered drugs, indicating a faster rate of absorption. However, the effect of concomitant use of metoclopramide on the AUC of the coadministered drug is variable. Although the reported examples are limited, it appears that after coadministration of metoclopramide small intestinal transit may be too fast for poorly permeable (e.g. cimetidine) or poorly dissolving (e.g. digoxin) drugs to be adequately absorbed. Thus, in this case, BCS classification may be helpful in identifying potential problems in bioavailability when metoclopramide is coadministered.

Anticholinergic agents

Propantheline is an anticholinergic agent which reduces gastrointestinal motility and prolongs gastric emptying rate. It is usually used in combination with other medicines to treat stomach ulcers. As for metoclopramide, propantheline has been investigated with respect to its potential effect on the absorption of concomitant medications. As one would anticipate, propantheline decreased the absorption rate of acetaminophen and lithium when given concurrently.[30,32] Coadministration of propantheline with a rapidly and a slowly dissolving tablet of digoxin resulted in increased serum digoxin concentrations only for the slowly dissolving formulation.[39,40]

Laxatives

Laxatives promote defecation and are often used OTC for the treatment of constipation. They can be grouped in osmotic, stimulant and bulk laxatives (Table 2).[43] An overview of the effects of laxatives and antidiarrheal agents on gastrointestinal physiology is given in Table 3. Osmotic laxatives (indigestible disaccharides, sugar alcohols, synthetic macromolecules, saline laxatives) attract and retain water in the intestinal lumen by increasing the luminal osmotic pressure. Stimulant laxatives (such as bisacodyl, senna and sodium picosulfate) act locally by increasing colonic motility and decreasing water absorption in the large intestine.[44] Bulk laxatives such as bran, isphagula and sterculia adsorb and retain luminal fluids and increase the faecal mass. For constipation linked with specific diseases, additional treatment options are available: linaclotide, an agonist of guanylate cyclase-C, stimulates fluid secretion, accelerates intestinal transit and is used for constipation-predominant irritable bowel syndrome.[45]

In general, laxatives shorten GI transit time, but depending on the type of laxative, the extent of the effect on transit time through specific GI compartments may vary (Figure 3). Studies have been conducted with a variety of methods including radiopaque markers,[46–48] following transit of a single metal sphere (diameter 6 m, density 1.4 g/ml) using a metal detector,[49] [13C]-octanoate and lactose-[13C] ureide breath tests[50] and scintigraphy.[45,51–54]

For healthy subjects, the following observations have been reported: the total GI transit time was reduced in 13

Table 2 Classification of laxatives and antidiarrheal agents[43–45]

	Class	Subgroup	Examples
Laxatives	Osmotic laxatives	Indigestible disaccharides	Lactulose
		Sugar alcohols	Sorbitol
		Synthetic macromolecules	Polyethylene glycol 4000
		Saline laxatives	Sodium sulphate
			Magnesium sulphate
	Stimulant laxatives		Bisacodyl
			Senna
			Phenolphthalein
			Casanthranol
			Sodium picosulfate
	Bulk laxatives		Wheat bran
			Isphagula
			Sterculia
	Others		Linaclotide
Antidiarrheal agents	Opioids		Loperamide
			Diphenoxylate
			Codeine phosphate
	Adsorbents/Bulking agents		Kaolin
			Isphagula
			Methylcellulose
	Miscellaneous		Racecadotril

Table 3 Effects of laxatives and antidiarrheal agents on gastrointestinal conditions[45,46,49,51–54,58–60,65,342,343]

Drug category	Effect on GI physiology	
Laxatives	↓ Gastrointestinal transit time	Small intestinal transit time (bisacodyl)
		Colonic transit time (bisacodyl, linaclotide, lactulose, polyethylene glycol)
		Whole gastrointestinal transit time (wheat bran, senna, bisacodyl)
	pH in the colon	↓ pH (lactulose, senna, wheat bran, sodium sulphate)
		↑ pH (magnesium sulphate)
	Faecal short chain fatty acids	↑ (bisacodyl, senna, wheat bran)
	Differences in gut microbiota	↑ Anaerobes, Bifidobacteria (lactulose)
		↓ Bifidobacteria (polyethylene glycol-4000)
	Haustra (small pouches in the colon)	↓ (chronic use of stimulant laxatives)
Antidiarrheal agents	↑ Gastrointestinal transit time	↑ intestinal transit time (loperamide)
	Faecal short chain fatty acids	↑ (loperamide)

subjects after treatment for 9 days with either the bulk laxative wheat bran (39.0 h vs 69.0 h) or the stimulant laxative senna (41.0 h. vs. 69.0 h) compared to the baseline value.[46] Small intestinal transit time was reduced by bisacodyl (dose 10 mg) from approximately 2.5 to 1.5 h in 10 subjects,[49] while the osmotic laxatives polyethylene glycol and lactulose had a minimum effect (if any) on the small intestinal transit time after being administered at a dose of 10 g twice daily for 5 days.[51] Administration of an isosmotic solution containing 40 g polyethylene glycol 3350 resulted in a significant decrease in oro-caecal transit time from 423.8 ± 28.1 min to 313.8 ± 17.2 min in 12 subjects.[50] In another study, administration of 5 mg bisacodyl in 25 subjects significantly accelerated the transit through the ascending colon (median 6.5 h vs 11.0 h).[54] Similarly, 10–20 ml of lactulose (Duphalac; Duphar

Laboratories Ltd., West End, Southampton, UK) three times daily for 5 days resulted in a significant decrease of the mean proximal colon transit time from 12.9 ± 3.7 h to 7.0 ± 2.5 h in 11 subjects.[53] The total colonic transit time was reduced to a greater extent after administration of 10 mg bisacodyl (from 31 ± 14 h to 7 ± 8 h) than by treatment with 30 g lactulose (from 34 ± 12 h to 30 ± 19 h) in 10 subjects.[49]

In patient populations, the following observations have been reported: in 12 subjects with constipation-predominant irritable bowel syndrome, treatment with linaclotide (dose 100 μg or 1000 μg) did not affect the gastric or small intestinal transit time.[45] However, the ascending colon transit time was decreased by 54% at a high dose of 1000 μg of linaclotide. At a lower dose of 100 μg, there was a decrease of 33%, although this was not statistically
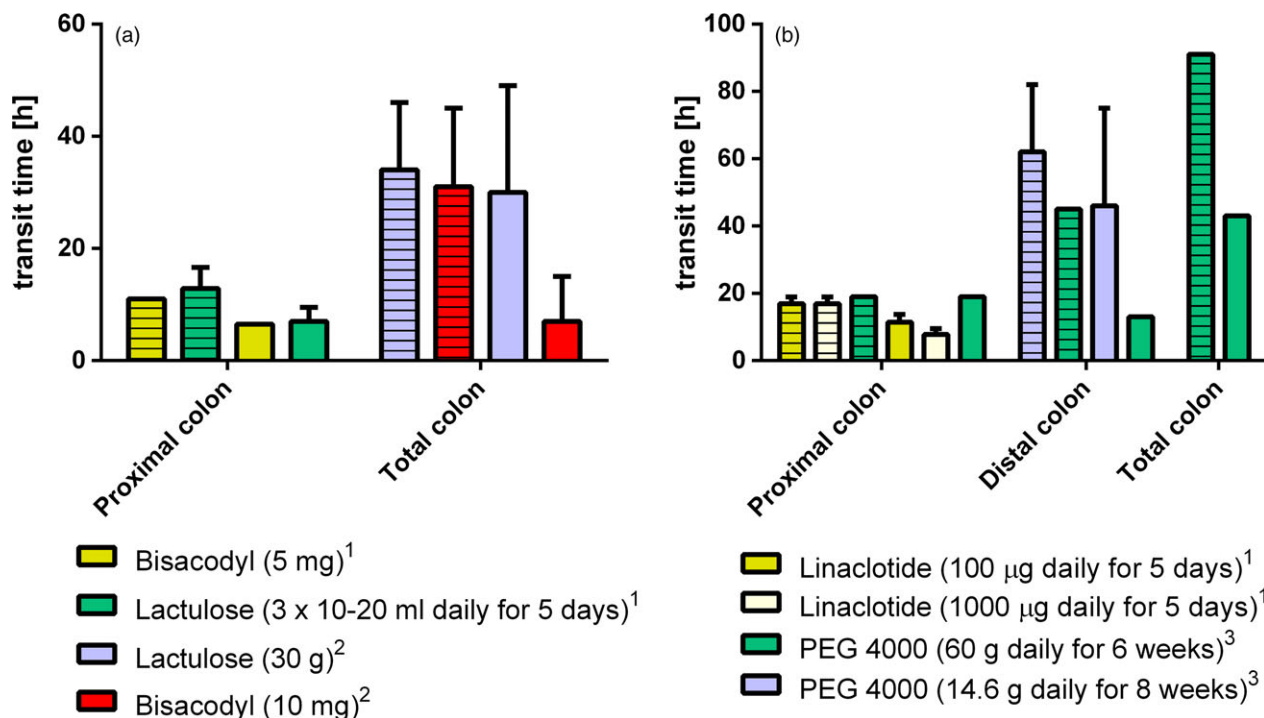
Figure 3 Impact of laxatives on colonic transit times of (a) healthy subjects and (b) patients, measured by scintigraphy (1), metal detector (2) or radiopaque markers (3); patterned bars represent controls.[45,47–49,53,54] [Colour figure can be viewed at wileyonlinelibrary.com]

significant. In line with these observations, the total colonic transit time was only significantly accelerated by the higher dose.[45] In nine subjects with chronic non-organic constipation, treatment with an isosmotic electrolyte solution containing polyethylene glycol 4000 (14.6 g) for 8 weeks did not significantly alter the transit time through the proximal colon, while the transit through the left colon and rectum was significantly accelerated (46 ± 29 h vs 62 ± 20 h and 37 ± 42 vs 78 ± 21 h, respectively).[48] The results in eight patients with slow transit constipation were similar after administration of 60 g polyethylene glycol 4000 daily for 6 weeks; the right colon transit time was not significantly different compared to placebo, while the transit time through the left colon was significantly accelerated (13 h vs 45 h) resulting in a reduction in total colonic transit time from 91 h to 43 h.[47] In summary, laxatives decrease transit times in healthy subjects throughout the GI tract, while in constipated patients, the effects are mainly limited to the colon.

Changes in GI transit times induced by laxatives can lead to changes in bioavailability. For example, coadministration of senna (20 ml of Liquidepur; Fa. Nattermann, Cologne, Germany) with a sustained-release quinidine formulation (0.5 g every 12 h) reduced quinidine plasma levels by 25% in nine patients with cardiac arrhythmia on long-term treatment, resulting in reoccurrence of

supraventricular extrasystoles.[55] Similarly, polyethylene glycol 4000 reduced the absorption of digoxin by 30% when coadministered with digoxin tablets (dose 0.5 mg) in 18 healthy subjects.[56] However, it is not clear whether the same effect would be observed in cardiac patients or what the clinical ramifications would be. Further, a trend (although not statistically significant) to decreased AUC of oestradiol glucuronide (dose 1.5 mg) was observed when coadministered for 10 days with the maximum tolerated dose of wheat bran (−13%) and senna (−10%) in 20 healthy postmenopausal women.[57]

Many laxatives have been shown to alter the production of short-chain fatty acids (SCFA). SCFA are usually associated with a decrease in luminal pH. After treatment with senna or wheat bran, faecal SCFA concentrations were increased in healthy subjects ($n = 13$) by 82% and 19%, respectively.[46] After administration of senna, the pH in the middle and distal colon was decreased (6.39 vs 6.85, 6.66 vs 7.14).[46] Lactulose significantly acidified the contents in the lower small intestine as well as in the right colon.[58–60] Sodium sulfate also decreased the pH, with the greatest effect in the left colon.[58] By contrast, wheat bran reduced the pH in the distal colon of 13 healthy subjects only slightly (6.88 vs 7.08).[46] But mechanisms other than via SCFA can also be at play. For example, the increase in the pH in the lower small intestine, colon and

104

rectum observed after administration of magnesium sulphate is postulated to be the result of gastric conversion to magnesium chloride and subsequent reconversion to insoluble magnesium carbonate in the colon prompted by increased colonic bicarbonate secretion.[58] The possible pH changes observed with laxatives are not clearly associated with changes in drug product performance. For example, mesalazine release from a delayed-release, pH-dependent formulation of mesalazine (Asacol®, SmithKline Beecham, Brentford, UK) was not affected by the coadministration of ispaghula husk or lactulose despite their known pH-lowering effect in the colon.[61,62] Nonetheless, the UK manufacturers of delayed-release mesalazine formulations (Asacol®, Allergan Ltd, Bucks, UK and Salofalk® granules, Dr. Falk Pharma UK Ltd, Bourne End, UK) suggest that drug release might be impaired by preparations with pH-lowering effect.[63,64]

With respect to the gut microbiota, the faecal microbiota of patients with chronic idiopathic constipation ($n = 65$) treated with lactulose over 28 days was increased in Anaerobes by 3% and Bifidobacteria by 8%, while treatment with polyethylene glycol 4000 resulted in a reduced faecal amount of Bifidobacteria (-14%).[65] Lactulose administration in patients taking coumarins (acenocoumarol, phenprocoumon) increased their risk of over-anticoagulation, as assessed in a population-based cohort study, because of changes in the vitamin K production of the colonic bacterial flora. By contrast, concomitant intake of isphagula with coumarins did not alter the risk of over-anticoagulation.[66]

The importance of the gut microbiota on oral pharmacotherapy is discussed further in the section on 'Antibiotics'.

Antidiarrheal agents

Antidiarrheal agents provide symptomatic relief of diarrhoea by decreasing fluid loss, by slowing down the passage of the gastrointestinal contents through the digestive tract, by increasing fluid absorption and/or by reducing intestinal secretions.[67] They can be classified according to their mechanism of action (Table 2). Opioids (such as loperamide, diphenoxylate and codeine phosphate) inhibit intestinal transit by activating μ-opioid receptors. Adsorbents and bulking agents (kaolin, isphagula, methylcellulose) adsorb water and increase the faecal mass, while the antisecretory action of racecadotril, an enkephalinase inhibitor, is linked to reducing chloride and fluid flux into the GI lumen.

Differences in the GI transit time have been observed after oral loperamide administration (Figure 4). The total GI transit time was increased after loperamide administration in healthy subjects (74.0 h vs 50.3 h, $n = 11$), as measured by radiopaque marker pellets, presumably due to reduced, irregular motor activity and therefore prolonged transit time in the jejunum.[46,68,69] Gastric emptying time was not significantly different in 24 healthy subjects treated with 4 mg loperamide compared to placebo as measured with a radio-labelled meal.[70] However, gastric residence time measured with a radiotelemetry capsule was increased twofold in five healthy subjects treated with 8 mg loperamide (four doses, every 6 h).[71] Small intestinal transit time, as measured with the hydrogen breath test, was increased by 80–130% in healthy subjects receiving 4–8 mg of loperamide.[70–72]

With respect to the composition of GI fluids, loperamide has been shown to decrease prostaglandin-E2 induced water and electrolyte secretion in the jejunum of healthy volunteers and reduce postprandial secretion of trypsin and bilirubin by more than 50% in patients with short bowel syndrome.[69,73,74] Similarly, basal and amino acid stimulated gallbladder motility was decreased by loperamide (dose 8 mg) in eight healthy subjects as measured by ultrasonography and bilirubin output in the duodenum.[75] After loperamide administration, faecal SCFA concentrations were decreased in healthy subjects (82.0 μmol/g wet weight vs 152.0 μmol/g wet weight; $n = 13$).[46]
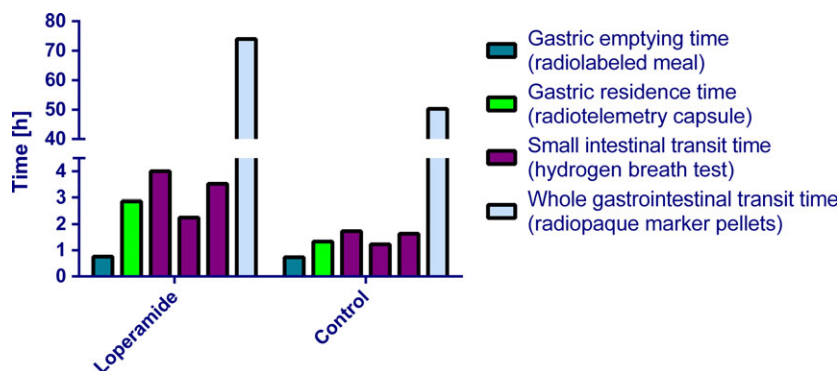

Figure 4 Effect of loperamide on gastrointestinal transit time after oral administration in healthy subjects.[46,70–72] [Colour figure can be viewed at wileyonlinelibrary.com]

In terms of DDIs, administration of 4 mg loperamide 24, 12 and 1 h before desmopressin administration increased the bioavailability of desmopressin in 18 healthy subjects (AUC 3.1-fold, C_{max} 2.3-fold) and prolonged the time to reach the maximum plasma concentration (2 h vs 1.3 h) without affecting the elimination half-life.[76] These effects could be explained by the decrease in GI motility. Desmopressin is highly soluble but poorly permeable (bioavailability approximately 0.1%), so longer transit times are expected to lead to a longer contact time of the drug with the absorptive mucosa.[77] Coadministration of loperamide at the maximum tolerated dose over 10–12 days also increased the AUC of estradiol glucuronide (dose 1.5 mg) by 15% in 20 healthy postmenopausal women, although the difference did not reach statistical significance.[57]

On the other hand, a single dose of loperamide (16 mg) decreased the bioavailability of the poorly soluble drug saquinavir (dose 600 mg) by 54% in 12 healthy subjects when administered concomitantly. This could be explained by the decreased motility and/or a reduction in electrolyte and fluid secretion both of which could hinder dissolution.[78] Additionally, it is possible that a decreased secretion of bile salts secondary to reduced gallbladder motility[75] impeded the solubilisation of saquinavir.

On the other hand, loperamide coadministration (8 mg every 6 h) in 12 healthy male subjects decreased the absorption rate of theophylline from a sustained-release 600 mg formulation (C_{max} 3.2 mg/l vs 4.6 mg/l, t_{max} 20 h vs 11 h), which could be explained by impeded release from the formulation due to a decrease in hydrodynamics (decreased motility) or perhaps a prolonged gastric residence time of the formulation/released drug. However, the AUC was not affected.[72]

Last but not least, the surface of bulk laxatives and bulking agents offers a site for drug adsorption. Concomitant administration of kaolin-pectin decreased the absorption of tetracycline (20%), aspirin (5–10%), procainamide (30%), quinidine (58%), trimethoprim (12–20%), lincomycin (90%), chloroquine (29%) and digoxin (15–62%), which is most likely the result of adsorption of the drugs onto kaolin.[79–87] Drug adsorption is also observed onto dietary fibres, and therefore, similar DDIs to those observed with dietary fibres are further considered in the section on 'Dietary Fibres.'

An overview of the effects of antidiarrheal agents on gastrointestinal physiology is given in Table 3.

Dietary fibres

The use of dietary fibres in the treatment of various diseases, such as diabetes, hypercholesterolemia, obesity, chronic constipation and gastrointestinal motility disorders, has increased over the last years. However, there are few studies that have investigated the impact of concomitant use of dietary fibres with other drugs. From the studies available, it seems that the effect of the concomitant use of dietary fibres depends on the type of fibre used.

The interaction of levothyroxine with dietary fibres is well-established. Concomitant use of dietary fibres, such as oat bran, soy fibre and ispaghula husk, result in decreased bioavailability of levothyroxine, due to adsorption of the drug to the fibres in the GI tract.[88] The authors commented that the adsorption of levothyroxine to soluble fibres and the consequent reduction in bioavailability might be greater than its adsorption to insoluble fibres. The interaction with levothyroxine is also noted by FDA in a consumers' information leaflet regarding drug interactions with food.[89]

In a case study reported by Perlman, the blood levels of lithium were decreased by 48%, when a patient was treated simultaneously with lithium and ispaghula husk.[90] There is also some evidence that fibres interact with some tricyclic antidepressants. The clinical effectiveness of tricyclic antidepressants appears usually after an administration period of 2–6 weeks. During this period, due to anticholinergic effects of the drugs, constipation is a common side effect. Therefore, patients receiving antidepressant medication often ingest dietary fibres. Already in 1992, Stewart observed a decrease in plasma concentrations of three tricyclic antidepressants (amitriptyline, doxepin and imipramine) in three patients, who concurrently ingested a diet rich in fibres.[91]

There are conflicting inputs in the literature about the interaction of dietary fibres and digoxin. Brown *et al.*,[92] reported a significant decrease in the bioavailability of digoxin when given concomitantly to 12 healthy volunteers ingesting a regular or high fibre diet, as opposed to administering digoxin alone in the fasted state. Albert *et al.*,[84] reported that when kaolin-pectin suspension was given simultaneously with digoxin, the total amount of digoxin absorbed was decreased by 62%. However, no significant interactions were observed when digoxin was given 2 h before the administration of the fibre suspension.[84] However, studies by Lembcke *et al.*, and Kasper *et al.*, found no effect on the bioavailability of digoxin when it was administered together with guar gum or other fibres.[93,94] In a later study Huupponen *et al.*,[95] investigated the effect of guar gum on the absorption of digoxin in 10 healthy volunteers. It was demonstrated that coadministration of guar gum with digoxin resulted in reduced plasma concentrations of digoxin and a decrease of 15% of the AUC for the first 6 h ($P < 0.05$).[95]

Holt *et al.*,[96] investigated the effect of coadministration of the soluble fibres guar gum and pectin on the absorption of acetaminophen. Concomitant administration with these

fibres resulted in delayed absorption and decreased C_{max}. However, the total absorption of acetaminophen was not significantly reduced. The authors attributed their results to delayed gastric emptying. Moreover, they argued that because guar gum, when hydrated, forms a viscous colloidal suspension, the high viscosity of this suspension could be a possible reason for the observed delay in gastric emptying.[96] The results from this study correlate well with the study conducted by Reppas *et al.*,[97] in mongrel dogs, in which the effect of elevated luminal viscosity on the absorption of acetaminophen, hydrochlorothiazide, cimetidine and mefenamic acid was investigated. Elevated luminal viscosity was achieved by administering saline solutions of the water-soluble guar gum. When given concurrently with the guar gum solutions, the C_{max} and AUC of the highly soluble acetaminophen and hydrochlorothiazide were significantly decreased, suggesting that the decreased rate of dissolution, due to the higher luminal viscosity, led to lower concentrations at the absorption sites. In the case of cimetidine, concurrent administration of the guar gum solution led only to a decrease in C_{max} and not AUC. For the poorly soluble but highly permeable mefenamic acid, neither the C_{max} nor the AUC were significantly affected by the concomitant administration of the guar gum in dogs.[97] Huupponen *et al.*,[95] reported a decrease in C_{max} and AUC of penicillin when given together with guar gum. Finally, Astarloa *et al.*,[98] investigated the effect of a diet rich in insoluble fibre on the pharmacokinetics of levodopa. Consumption of 2 months of the dietary supplement with the usual dose of levodopa led to elevated plasma levels of levodopa especially at 30 and 60 min after oral administration.[98,99]

It is evident from these studies that it is currently not possible to make any generalisations about DDIs with dietary fibres although it seems that there is a tendency for decreased maximum plasma concentrations of the coadministered drug. These events are likely attributable to slower gastric emptying, higher viscosity and, perhaps in some cases, adsorption phenomena.[100] It also seems that the type of interaction, if any, is highly dependent on the type of dietary fibre used. It remains to be investigated whether these interactions, such as they exist, lead to clinically significant differences.

Antiemetics

Antiemetics are classified according to their mechanism of action. There are five receptors that play a key role in the vomiting reflex; muscarinic, dopaminergic, histaminic, serotoninergic and substance P/neurokinin receptors.

Aprepitant is a very potent neurokinin-1 receptor antagonist used for the prevention of acute and delayed chemotherapy-induced nausea and vomiting.[101,102]

Aprepitant is metabolised primarily by CYP3A4 and secondarily by CYP1A2 and CYP2C19. It also acts as a moderate inhibitor of CYP1A2, CYP2C9, CYP2C19, CYP2E1 and as a weak inducer of CYP2C.[101,102] Caution is therefore necessary, especially when administered concomitantly with chemotherapy agents that are metabolised primarily by CYP3A4, as inhibition by aprepitant may lead to higher plasma levels and toxic side effects. According to the Public Assessment Report, EMEND® capsules (which contain aprepitant as API) should not be concomitantly administered with ergot alkaloid derivatives, pimozide, terfenadine, astemizole or cisapride, as the competitive inhibition of the CYP3A4 by aprepitant results in elevated plasma concentrations, leading to adverse effects.[102] Further pharmacokinetic interactions that have been reported for aprepitant in the literature are those with midazolam, warfarin, dexamethasone and methylprednisolone.[22,103]

Majumdar *et al.*,[104] investigated the effect of aprepitant on the pharmacokinetics of single dose midazolam on day 1 and on day 5 during daily administration of aprepitant for 5 days. In this study, two dose regimens of aprepitant were used: 125/80 and 40/25 mg. It was concluded that coadministration of midazolam with the 125/80 mg regimen (125 mg on day 1 and 80 mg on days 2–5) resulted in a 2.3-fold increase in midazolam AUC on day 1 and a 3.3-fold increase on day 5. The plasma concentrations achieved 1 h after dosing (C_{1h}) and the half-life ($t_{1/2}$) were also increased due to the inhibition of first pass and systemic metabolism and subsequent reduction in clearance. Although coadministration of midazolam with the 40/25 mg dose regimen did not result in any significant change in the pharmacokinetics of midazolam, this lower dose is not used in clinical practice.[104] Majumdar *et al.*,[105] later investigated the effect of aprepitant on intravenously administered midazolam and the findings were consistent with the first study, but with an increase in AUC of 1.47-fold. The authors suggested that the lower increase in AUC observed after intravenous administration of midazolam might be due to circumvention of the presystemic metabolic interaction when midazolam is given intravenously.[105]

In an analogous study by McCrea *et al.*,[106] the effect of a 5-day administration of 125/80 mg aprepitant regimen on the pharmacokinetics of orally administered methylprednisolone and dexamethasone was evaluated. Due to the inhibition of CYP3A4 by aprepitant, the C_{max} of methylprednisolone was increased 1.5-fold while the AUC increased 2.5-fold. An increase of 2.2-fold in AUC was observed for dexamethasone.[106] Clinically, unnecessary high exposure to corticosteroids should be avoided due to the potential risk of adverse effects such as hyperglycaemia and increased susceptibility to infections. For these reasons, it is suggested that the oral doses of dexamethasone and

methylprednisolone should be reduced by half when used for the management of chemotherapy-induced nausea and vomiting concurrently with aprepitant.[106] The interaction of aprepitant with warfarin is less clear.[107] In a study by Takaki *et al.*, a decrease in warfarin plasma levels was observed, but no significant interaction between warfarin and aprepitant was established. One possible reason for the lack of interaction could be the fact that the volunteers who took part in this clinical study were also receiving several other chemotherapeutic agents. In any case, careful monitoring of patients on chronic warfarin therapy is required.[103,108]

Serotonin plays an important role in various body functions. Most serotonin is synthesised in the GI tract, and it affects various aspects of intestinal physiology. Multiple subtypes of 5-HT receptors exist on various types of cells, such as smooth muscle and enterocytes, and agonists or antagonists of 5-HT receptors are used in the treatment of different gastrointestinal disorders.[21] 5-HT$_3$ receptor antagonists, for example ondansetron and granisetron, have been successfully used in the treatment of chemotherapy-induced nausea and vomiting. Recommendations, published by the American Society of Clinical Oncology (ASCO) for the use of the 5-HT$_3$ receptor antagonists, do not distinguish among them with regard to their safety and efficacy. Nonetheless, these compounds differ significantly in their pharmacokinetic properties and especially with respect to their potential to interact with CYP enzymes.[109,110] Granisetron, for example, does not inhibit any of the CYP enzymes which are commonly involved in drug metabolism, whereas ondansetron inhibits both CYP1A2 and CYP2D6 and can thus interact with various concurrently used drugs.

However, the interactions reported in the literature are not solely attributed to their enzyme inhibitory properties. Concomitant use of ondansetron with cyclophosphamide resulted in reduced systemic exposure, probably due to increased systemic clearance.[111,112] In any case, there is a need for more studies to increase knowledge about drug interactions of chemotherapeutic agents with commonly used antiemetics, as even a slight change in the pharmacokinetic parameters or pharmacodynamics of the anti-cancer medication could jeopardise the effectiveness of chemotherapy.[111]

Gastric acid reducing agents and antacids

Proton-pump inhibitors, H$_2$-receptor antagonists (H$_2$RAs) and antacids are widely used in the treatment of various gastric acid-related disorders, such as peptic ulcers and gastroesophageal reflux disease. In fact, PPIs and H$_2$RAs are classified among the three most prescribed drug classes for the years 2011–2014 and the situation is similar today.[113]

Indeed, esomeprazole, a PPI, ranks among the top five most prescribed medications worldwide.[114] Of particular concern for these drugs is their increasing OTC use. Despite the fact that gastric antisecretory agents or antacids are tolerated well, with a low overall frequency of adverse reactions,[115] their concurrent use with other medications can have a great effect on drug absorption. If prescribed, identification of potential interactions by the prescribing physician and/or dispensing pharmacist is possible, but this control mechanism is largely lost if the drugs are obtained OTC or via e-pharmacies.

Proton pump inhibitors

Proton-pump inhibitors are a group of substituted benzimidazole sulfoxide drugs with strong inhibitory effects on gastric acid secretion from the parietal cells in the stomach. At present, six PPIs (dexlansoprazole, esomeprazole, lansoprazole, omeprazole, pantoprazole and rabeprazole) are available on the market.[116] PPIs are used in the treatment of acid-related disorders and for the prevention of gastrointestinal bleeding in patients receiving dual antiplatelet therapy of clopidogrel and aspirin. Furthermore, they are used as a component of combination therapy for the eradication of H. pylori, because their properties enhance the anti-H. pylori activity of the coadministered antibacterials (clarithromycin and amoxicillin).[117] PPIs can affect the absorption of the coadministered drugs to a great extent, mainly due to the increase in gastric pH. In a recent study, the effect of 40 mg of pantoprazole administered orally once per day for 4 days and 20 mg of the H$_2$RA famotidine administered orally twice within 12 h, on the GI physiology of eight healthy male volunteers was investigated.[118] In both cases, the gastric pH differed significantly in comparison to the control group (Figure 5). However, PPIs can also affect the pharmacokinetics of coadministered drugs through other mechanisms,[119] and several excellent reviews have been written regarding the DDIs of PPIs.[120–122]

As already mentioned, gastric pH is an important parameter that can affect absorption of drugs, especially these which are poorly soluble weak bases. For example, Jaruratanasirikul *et al.*,[123] investigated the effect of 40 mg oral omeprazole on the pharmacokinetics of a single 200 mg capsule of itraconazole in 11 healthy volunteers. Concomitant use of omeprazole resulted in reduction of the mean AUC and C_{max} of itraconazole by 64% and 66%, respectively. No interaction due to omeprazole's inhibition of CYP3A4 was reported.[123] On the other hand, Johnson *et al.*,[124] investigated the effect of concomitant use of 40 mg oral omeprazole with a 40 mg dose oral solution of itraconazole in 20 volunteers. It was reported that there was no statistically significant difference on the AUC, t_{max} and
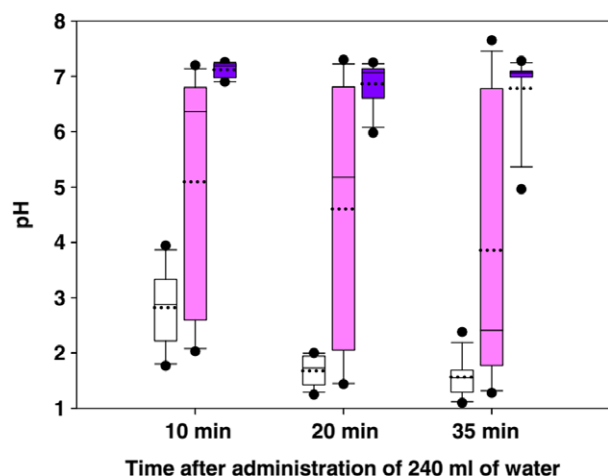
Figure 5 pH in the stomach of fasted healthy adults as a function of time, after administration of 240 ml table water into the antrum of the stomach. Key: (From left to right boxes) White boxes, Phase 1 (control phase); Light pink boxes, Phase 2 (pantoprazole phase); Dark blue boxes, Phase 3 (famotidine phase). Each box was constructed using 7–8 individual values.[118] [Colour figure can be viewed at wile yonlinelibrary.com]

C_{max} with the coadministration of omeprazole.[124] The results of these two clinical studies (one with a solid dosage form, one with itraconazole in solution) suggest that coadministration of omeprazole and elevation of gastric pH affects the dissolution of itraconazole capsules rather than the permeability of itraconazole. The results regarding ketoconazole are similar. In 1995, Chin *et al.*, conducted a clinical study with nine healthy volunteers, in which the effects of 60 mg oral omeprazole or an acidic beverage on the pharmacokinetics of orally administered 200 mg ketoconazole were investigated. Pretreatment with omeprazole resulted in significantly lower AUC and C_{max} and a prolongation of t_{max}.[125] Ketoconazole and itraconazole are both practically insoluble at pH > 4. Coadministration of PPIs with poorly soluble imidazole antifungal agents when given as capsules or tablets is therefore not recommended.[126] Interestingly, the elevated gastric pH does not affect the bioavailability of fluconazole tablets.[127] This lack of interaction is explained by the high solubility of fluconazole over the whole pH range of the GI tract. Thus, stomach acidity does not limit the dissolution rate of fluconazole or its absorption.[128,129]

The increase in the gastric pH caused by PPIs can also greatly affect the bioavailability and effectiveness of antiretroviral agents, depending on their pH/solubility profiles. Tappouni *et al.*,[130] conducted a clinical study with 16 patients, in which the effect of omeprazole on indinavir was evaluated. With pre-treatment and coadministration of 20 mg oral omeprazole, the C_{max} of indinavir decreased by 29% and the AUC by 34%, whereas at a higher dose of 40 mg omeprazole, the C_{max} and AUC of indinavir

decreased by 41% and 47%, respectively.[130] Coadministration of omeprazole resulted in reduction to the systemic exposure to both nelfinavir and its metabolite. In particular, the AUC of nelfinavir was decreased by 36%.[131] Tomilo *et al.*,[132] reported a 94% and 91% decrease in AUC and C_{max}, respectively, of 400 mg oral atazanavir, when coadministered with 60 mg lansoprazole in 10 healthy volunteers. The results were similar when omeprazole was coadministered.[133] However, the clinical impact of this drug–drug interaction on the clinical effect of atazanavir is not clear.[134,135] It seems that coadministration of PPIs with an atazanavir/ritonavir regimen does not affect the ability of atazanavir to achieve the minimum plasma concentration necessary for the virologic response, that is the concomitant use of atazanavir/ritonavir regimen and PPIs was not associated with higher virologic failure rate.[134] Nonetheless, further studies, in which both the pharmacokinetic parameters and the clinical response rates are simultaneously investigated, are needed to understand the interaction and its consequences more fully.

In contrast to the results mentioned so far, in the study of Winston *et al.*,[136] coadministration of 40 mg oral omeprazole with 1000 mg saquinavir (given orally as 1000 mg saquinavir/100 mg ritonavir combination) resulted in an 82% increase in the mean AUC of saquinavir in 18 healthy volunteers. The increase did not result in an increase in adverse effects. The authors commented that further work is necessary in order to understand the mechanism of this DDI and to address whether the effects of omeprazole on saquinavir's pharmacokinetics would be the same even in the absence of ritonavir. The authors also raised the possibility of whether the increase could be the result of inhibition of transmembrane-transporters, such as P-gp or MRP by omeprazole.[136]

As for most of the antifungal and antiviral drugs, the absorption of mycophenolate mofetil is impaired by concomitant administration of PPIs. Kofler *et al.*,[137] measured the levels of mycophenolic acid (active metabolite) in 33 patients concurrently receiving 40 mg oral pantoprazole. C_{max} and AUC of mycophenolic acid were significantly lower when patients were pretreated with pantoprazole.[137] As anticipated, coadministration of pantoprazole with an enteric coated formulation of mycophenolic acid had no significant effect on its pharmacokinetics.[138]

Apart from lowering the solubility of APIs in the stomach, an increase in the gastric pH can jeopardise the bioavailability of formulations with pH-dependent release. The effect of concomitant administration of esomeprazole on the bioavailability of risedronate sodium DR was evaluated in a clinical study involving 87 postmenopausal women. The results showed that esomeprazole administration 1 h before dinner or 1 h before breakfast resulted in 32% and 48% reduction in the bioavailability of risedronate

sodium DR, respectively. In the report, it was suggested that an increase in the gastric pH may compromise the enteric coating of risedronate delayed release formulation, thus resulting in release of risedronate sodium in the stomach, where it could convert to the less soluble free acid.[139] However, as it has been shown that PPIs (pantoprazole) decrease buffer capacity as well as increase gastric pH,[118] a premature release due to enteric coating failure appears unlikely.

A review of all the available clinical data from literature describing the effect of the administration of various gastric acid reducing agents on the absorption and bioavailability of coadministered weakly basic anticancer drugs was published by Budha *et al.*[140] The authors attempted to correlate the physicochemical properties and pH-solubility profiles of the different anticancer drugs with the observed effect on the absorption caused by the elevation of the gastric pH after the administration of the acid reducing agents (PPIs, H$_2$RAs and antacids). It was concluded that the impact of the elevation of gastric pH is more prominent for the anticancer drugs which exhibit an exponentially decreasing solubility in the pH range 1–4 and for which the maximum dose strength is not soluble in 250 ml of water. Elevation of gastric pH is expected to substantially decrease the dissolution rate of these drug products, thus leading to incomplete dissolution of the dose and impaired absorption.

In 2013, Mitra and Kesisoglou described strategies to minimise or avoid reduced absorption of weakly basic drugs resulting from elevated gastric pH.[141]

The observed DDIs with PPIs occur not only because of their elevation of gastric pH, but can also arise from other properties. It has been shown that concurrent administration of 10 mg of nifedipine with 20 mg of omeprazole for 8 days (short-term treatment) resulted in an AUC increase of 26%, whereas no increase was observed after coadministration of a single 20 mg dose of omeprazole.[142] The authors hypothesise that the higher levels might be due to inhibition of CYP3A4, but they note that this increase is not likely to have major clinical relevance, especially when taking into account the intra- and inter-individual variability observed for nifedipine.[142] In contrast, in the study by Bliesath *et al.*,[143] coadministration of 20 mg of nifedipine with 40 mg of pantoprazole for 10 days had no effect on the pharmacokinetics of nifedipine. This apparent discrepancy in DDI tendency might be due to the different CYP-isoenzymes inhibitory properties of the two PPIs. It is believed that among all PPIs, omeprazole is the one which has the greatest potential for drug interactions, as it has a high affinity for CYP2C19 and CYP3A4.[144–147]

Another example of a non-pH-related DDI with PPIs is the delayed elimination of plasma methotrexate, independent of renal function.[148]

Last, but not least, there has been an increasing interest in investigating the mechanism of drug interactions of PPIs with clopidogrel. Clopidogrel is a prodrug that requires activation via cytochrome P450 isozymes (CYP2C19, CYP3A4, CYP3A5) in order to transform to its pharmacologically active form. Therefore, inhibition of the cytochrome isoenzymes, which are involved in the metabolic pathway of clopidogrel, may reduce its antiplatelet activity and potentially increase the risk of thrombosis. In fact, in 2009 FDA published a warning note on the drug label of Plavix® (clopidogrel; Sanofi Clir SNC, Paris, France) and continues to warn the public against concomitant use of clopidogrel and omeprazole. It should be noted that, although studies have demonstrated that concomitant use of clopidogrel and PPIs, especially omeprazole, reduces the antiplatelet effect of clopidogrel, the mechanism behind this interaction and the clinical importance (cardiovascular risk) has not yet been clearly established.[149–154]

H$_2$ receptor antagonists

The H$_2$RAs are another drug class used to treat gastric acid-related disorders. These compounds bind to histamine H$_2$ receptors on parietal cells and antagonise the action of histamine, which is the major transmitter for stimulation of acid secretion.[155] As with the PPIs, there are DDIs with different classes of drugs and these are mainly attributed to the elevation of the gastric pH (see Figure 5). For example, ketoconazole and itraconazole demonstrate impaired drug absorption when they are concomitantly used with H$_2$RAs as well as with PPIs. Piscitelli *et al.*,[156] investigated the effect of 150 mg orally administered ranitidine on 400 mg oral ketoconazole in six healthy volunteers. The decreased C_{max} and AUC and bioavailability of ketoconazole in this study was attributed to the elevated gastric pH, which resulted in a decreased and incomplete ketoconazole dissolution.[156] The results were similar when the effect of cimetidine on the absorption and pharmacokinetics of ketoconazole was investigated.[121] Lim *et al.*,[157] investigated the effect of famotidine on the absorption of fluconazole and itraconazole. Twenty healthy volunteers received orally 40 mg famotidine with 200 mg itraconazole or 100 mg fluconazole. Coadministration of famotidine resulted in a 52.9% decrease in C_{max} and a 51.1% decrease in the AUC of itraconazole, but no difference was observed in the pharmacokinetics of fluconazole.[157] This different behaviour of fluconazole had previously been observed by Blum *et al.*,[158] and can be explained by its much higher solubility (see the section on 'Proton pump inhibitors').

The situation is similar with antiretroviral medications.[159] Analogous to the PPIs/saquinavir interaction, coadministration of cimetidine resulted in increased exposure to saquinavir.[136,160]

Russell *et al.*, investigated the effect of a single dose of 40 mg of famotidine on the pharmacokinetics of the weak base dipyridamole in 11 elderly adults with normal gastric acid secretion. After coadministration of famotidine, the C_{max} and absorption constant (k_a) of dipyridamole decreased significantly. The total AUC decreased by 37%, but this decrease was not found to be statistically significant. The authors attributed the observed differences to slower dissolution rate of dipyridamole tablets at elevated gastric pH.[161] In other studies, coadministration of ranitidine with two weak bases, enoxacin and cefpodoxime, resulted in decreased bioavailability, which was again attributed to decreased solubility in the gastric environment at elevated pH.[162,163]

As with the PPIs, DDIs with H₂RAs can occur not only because of their elevation of gastric pH, but can also arise from their other properties. In particular, it has been shown that, among the various H₂RAs, cimetidine is the most potent inhibitor of the CYP450 enzymes. The inhibition is attributable to the imidazole ring in its structure and results in changes in the metabolism of various coadministered drugs.[164] In cases where a clinical significant interaction is suspected, other H₂RAs (e.g. ranitidine, famotidine) are preferred over cimetidine.[165,166] Among the various metabolic interactions that have been reported after coadministration of cimetidine,[164] the metabolic interactions observed with warfarin and propranolol have been most intensively studied and the clinical significance of these interactions has also been evaluated. Toon *et al.*, investigated the effect of a 9-day short treatment of cimetidine and ranitidine (800 mg oral dose daily and 300 mg oral dose daily respectively) on the pharmacokinetics of 25 mg of racemic warfarin, administered orally starting on the fourth day of cimetidine treatment and continuing for the next 5 days, in nine healthy volunteers.[167] The prothrombin time and Factor VII clotting time were also evaluated. While ranitidine had no effect on the pharmacokinetics of either of the two enantiomers of warfarin, cimetidine significantly increased the elimination half-life and decreased the clearance of the (R)-enantiomer of warfarin. In contrast, the pharmacokinetics of the (S)-enantiomer of warfarin were not affected by coadministration of cimetidine. Nonetheless, coadministration of either ranitidine or cimetidine did not result in a clinically significant difference in terms of the anticoagulation effect of warfarin.[167] These results were further confirmed by a later study from Niopas *et al.*[168] It should be noted, however, that both studies were conducted in healthy volunteers, and therefore, the clinical effects on patient populations could differ.

The effect of a daily oral dose of 1000 mg cimetidine on the steady-state plasma levels of propranolol, administered as a 160-mg sustained-release formulation daily, was evaluated in seven healthy volunteers during a 13-day treatment (administration of cimetidine started on the eighth day).[169] It was concluded that coadministration of cimetidine resulted in decreased clearance of propranolol and thus increased propranolol plasma levels at steady state. In a similar study, Reimann *et al.*[170] investigated the effect of cimetidine (1000 mg daily, 1 day oral pretreatment) and ranitidine (300 mg daily oral dose, 1 and 6 days pretreatment) on the steady-state propranolol plasma levels (160 mg sustained-release capsule, once daily) of five healthy volunteers. It was shown that 1-day pretreatment with cimetidine resulted in elevated propranolol plasma levels at steady state, while ranitidine pretreatment for 1 or 6 days did not affect significantly the propranolol plasma levels at steady state. However, the authors stated that the elevated plasma levels of propranolol observed after pretreatment with cimetidine did not lead to a clinically significant effect.[170] Again, the study was conducted in healthy volunteers and the clinical effects on patient populations could differ. Nonetheless, it should be noted that the companies are required by the regulatory authorities to inform the patients that there is a potentially clinically significant DDI of cimetidine and propranolol in the patient information leaflets.[171]

It is obvious that there are many interactions of PPIs and H₂RAs with other concomitantly used drugs, especially poorly soluble weak bases, and that their use should be monitored, particularly in cases where the DDI is well-established. Besides the elevation of gastric pH and the interactions with metabolic pathways, it should be noted that PPIs and H₂RAs can also affect other aspects of the physiology in the GI tract. Recent data in the literature suggest that administration of PPIs or H₂RAs can be accompanied by reduced buffer capacity, chloride ion concentration, osmolality and surface tension in stomach and an increase in the pH of the upper small intestine of up to 0.7 units, an increase that would be especially relevant for compounds (basic or acidic) with pKas between 6 and 7.[118] Carefully designed DDI studies, in terms of dosing and duration of treatment, are needed in order to accurately determine the effect of H₂RAs or PPIs on the pharmacokinetics of coadministered drugs and investigate the clinical consequences of these interactions.

Antacids

The term 'antacids' describe a category of salts, formulated as the combination of polyvalent cations such as calcium, aluminium or magnesium with a base, such as hydroxide, trisilicate or carbonate. Aluminium hydroxide alone, or in combination with magnesium hydroxide, is the main ingredient of many antacid products. Owing to the introduction of PPIs and H₂RAs, which are more potent drugs and can be used for a wide variety of gastrointestinal disorders,

antacids are now mainly marketed as OTC medications. However, the concomitant use of antacids with other drugs can significantly affect their absorption or even their therapeutic effect. Considering the fact that the use of OTC antacids is widespread, there is a particular need for appropriate information for patients, doctors and pharmacists. Besides interactions associated with increased pH, the major DDIs with antacids involve chelation reactions. Various categories of drugs, such as quercetin, catechol derivatives and tetracyclines, are known to form drug/metal chelates.[172–174] Fluoroquinolones also interact with multivalent cations and this interaction can lead to reduced antimicrobial activity.[175]

Deppermann *et al.*,[176] and Garty *et al.*,[177] investigated the effect of H_2RAs or antacids (mixture of aluminium hydroxide and magnesium hydroxide) on the oral absorption of various tetracycline antibiotics. The antacids resulted in reduction of the oral bioavailability of tetracyclines by 80% or more, whereas coadministration of the H_2RAs did not affect the pharmacokinetic parameters of tetracyclines.[176,177] For this reason, it was concluded that chelation rather than elevation of gastric pH is the probable mechanism of this DDI. The complexes that are formed by chelation are insoluble and therefore they precipitate, preventing absorption. The results are similar with coadministration of antacids and fluoroquinolones. Aluminium ions form a stable and insoluble complex with quinolones, thus preventing their intestinal absorption and reducing their bioavailability.[178,179] By contrast, concomitant administration of an H_2RA did not have a significant effect on the AUC of ciprofloxacin.[176] As the formation of the chelate complex is the limiting factor to absorption of quinolone antibiotics, many studies have been conducted in order to establish an optimal interval of antacid dosing before or after the administration of the antimicrobial agents. With regard to fluoroquinolones, it has been concluded that administration of antacids 4 h earlier or 2 h later than the administration of the antibiotic would circumvent the interaction.[162,180–183]

As with the PPIs and H_2RAs, the elevation of gastric pH that is observed after administration of antacids could also impact the dissolution or oral solid formulations and change their pharmacokinetics. Indeed, coadministration of itraconazole with antacids resulted in decreased AUC.[184] However, in a pilot study by Brass *et al.*[185] ($n = 4$), the absorption of ketoconazole was not significantly decreased.

The interaction of antacids and NSAIDs is also an interesting case. NSAIDs are among the most popular OTC and frequently prescribed medications for acute or short-term pain and chronic inflammatory diseases. As NSAIDs cause dyspepsia and damage in the upper gastrointestinal mucosa, they are often given with antacids. Interactions of antacids with NSAIDs are not clearly established and no general recommendations can be made for this drug category. However, there are studies indicating that coadministration with antacids containing magnesium hydroxide or sodium bicarbonate could enhance the rate and possibly the extent of absorption of some NSAIDs, for example ibuprofen, tolfenamic and mefenamic acid, diflunisal and naproxen.[186–189] This has been attributed to the fact that magnesium hydroxide, in addition to increasing gastric pH, also accelerates gastric emptying. Such effects have not been observed for aluminium hydroxide, which in contrast to magnesium hydroxide prolongs gastric emptying[190]

There have been many further studies investigating the interactions of antacids with APIs from various drug classes, including corticosteroids, cardiovascular agents and antidiabetic agents. However, it has not been possible to make any generalisations about the observed interactions. Furthermore, in some cases, there is no evidence that differences in pharmacokinetic parameters translate into clinically significant differences.[190]

Probiotics

It is well-known that the intestinal microflora plays a key role in physiological, metabolic, immunological and nutritional processes in the human body. For this reason, there is currently great interest in influencing the composition of the microflora and its activity using probiotics for both the prevention and treatment of various diseases.[191] According to WHO, probiotics are 'live microorganisms which, when administered in adequate amounts, confer a health benefit on the host'.[192] There are several clinical studies that have illustrated their beneficial effects on gastrointestinal disorders such as diarrhoea and irritable bowel syndrome. The gram-negative bacterium *Escherichia coli* Nissle 1917, for example, has been used since 1920 for the treatment or prevention of irritable bowel syndrome, chronic constipation, non-ulcer dyspepsia and other gastrointestinal disorders.[193] The mechanism of action of the probiotics is not yet fully understood. It seems that they may modulate the intestinal epithelial barrier and transport across it, noting that in inflammatory bowel diseases (IBDs), for example ulcerative colitis and Crohn's disease, the barrier properties of the epithelium are compromised due to secreted cytokines and/or medication.[194]

Despite the wealth of evidence regarding their advantageous and well-tolerated use, the literature on interactions between concomitantly administered probiotics and drugs with respect to drug pharmacokinetics is mainly limited to animal experiments. In the study of Mikov *et al.*,[195] the effect of coadministration of probiotics (oral 2 g dose of freeze dried powder of a mixture of the strains Lactobacillus acidophilus L10, Bifidobacterium lactis B94 and

Streptococcus salivarius K12 every 12 h for 3 days) on sul-fasalazine metabolism (sulfasalazine administered as an oral dose of 100 mg/kg dissolved in saline via gavage 6 h after completing the 3 day treatment with probiotics) in the rat gut lumen was investigated. The authors showed that administration of probiotics significantly increased the con-version of sulfasalazine to sulfapyridine and 5-aminosa-licylic acid by increasing azoreductase activity. This could possibly enhance sulfasalazine therapy, which would be important in patients with reduced gut microflora, subse-quent to antibiotic therapy, or in severe diarrhoea.[195] Lee et al.,[196] confirmed an increase in azoreductase activity in ex vivo colon rat fluids. However, no differences were found in the pharmacokinetic parameters of sulfasalazine and sul-fapyridine.[196] Kunes et al.,[197] investigated the effect of E. coli Nissle 1917 probiotic medication on the absorption kinetics of 5-aminosalicylic acid in rats. The results showed that there was no difference in the pharmacokinetics of 5-aminosalicylic acid and that E. coli Nissle 1917 medication did not affect the absorption of 5-aminosalicylic acid.[197] Al Salami et al.,[198] investigated the effect of a mixture of three probiotics in diabetic rats on gliclazide pharmacoki-netics. They observed that gliclazide's absorption and bioavailability were reduced in healthy rats. The authors attributed this change to several possible causes, most of which had to do with intestinal efflux drug trans-porters.[198] Saksena et al.,[199] reported that Lactobacilli or their soluble factors significantly enhanced P-gp expression and function under normal and inflammatory conditions in mice. Finally, Matuskova et al.,[200] investigated the effect of administration of E. coli Nissle 1917 on amio-darone absorption in rats. This resulted in 43% increase in the AUC of amiodarone. Interestingly, this effect was not observed when E. coli Nissle 1917 was replaced by a refer-ence non-probiotic E. coli strain, suggesting that the increase in AUC of amiodarone was due to the administra-tion of the probiotic.[200]

Clearly, studies in humans are needed in order to investi-gate whether these results can be extrapolated well to patients with altered intestinal microflora.

Antibiotics used for gastrointestinal infections

Antibiotics aim to attack targets specific to bacterial organ-isms such as bacterial cell walls, bacterial cell membranes, bacterial metabolism or replication, in order to avoid dam-age to human cells. However, antibiotics are not 100% selective for bacteria that are pathogenic for the host organ-ism. As a result, the GI microbiota is frequently disturbed after treatment with antibiotics.[201,202] In fact, depending on the antibiotic, 5–25% of patients treated experience diarrhoea.[203,204]

Sullivan et al.[202] reviewed the effect of various antibi-otics on the abundance of bacterial types and species. Dif-ferences in the composition of the microbiota could alter the composition of colonic fluids and permeability of the gut wall as well as the abundance of bacterial enzymes.

Colonic bacteria are involved in the cleavage of dietary fibres to oligosaccharides and monosaccharides and their further fermentation to SCFAs such as acetate, propionate and butyrate.[205] Patients treated with antibiotics showed a decreased colonic carbohydrate fermentation and conse-quently lower faecal concentrations of SCFAs.[206–210] In other studies, it was shown that SCFAs stimulate ileal and colonic motility.[211–213] The inhibition of gastric emptying by nutrients that reach the ileo-colonic junction, the so-called ileocolonic brake, is also associated with SCFAs.[214] But GI transit times can also be affected by certain antibi-otics through other mechanisms: for example, erythromycin accelerates gastric emptying (−25% to −77%) by acting as a motilin agonist, while prolonging small intestinal transit time (+20% to +45%) for liquids and solids in healthy vol-unteers and patients.[215–220] For example, when ery-thromycin was coadministered with a controlled-release formulation of pregabalin, designed to remain for a pro-longed time in the stomach, in 18 healthy subjects there was a reduction of AUC and C_{max} by 17% and 13%, respectively, due to erythromycin's prokinetic action.[221] As the prega-balin exposure was still in the range calculated for patients receiving an immediate release formulation of pregabalin, the interaction was deemed not to be clinically relevant.

If bacterial enzymes are involved in the biotransforma-tion of a drug, the intake of antibiotics can affect its meta-bolism by changing the composition of the microbiota and thus altering the bacterial enzyme activity.[222,223] At least 30 commercially available drugs have been reported to be metabolised by bacterial enzymes in the gastrointestinal tract.[222] The serum concentrations of digoxin, which is partly metabolised by gut microbiota, increased twofold after administration of erythromycin or tetracycline for 5 days in four healthy volunteers.[224] In another report, toxic digoxin plasma levels were observed in a patient after cotreatment with erythromycin, possibly due to the inhibi-tion of Eubacterium lentum which converts digoxin to its reduced derivatives.[225] Incubation of flucytosine with fae-cal specimens of neutropenic patients before and after treatment with antibiotics (ciprofloxacin, penicillin, cotri-moxazole) and antimycotics (amphotericin B, fluconazole, nystatin) indicated that the transformation of flucytosine to its active metabolite, fluorouracil, was reduced.[226] Sim-ilarly, concomitant administration with ampicillin (250 mg four times daily for 5 days) with sulfasalazine (single dose 2 g) led to a decrease in the AUC of sulfapyridine by 35% in five healthy subjects suggesting a decrease in azoreduc-tase activity and prodrug activation.[227]

An altered colonic microflora could also adversely affect the drug release from colon-targeting formulations coated with water-insoluble polysaccharides.[228] As polysaccharides such as guar gum, pectin and chitosan are degraded by bacterial enzymes in the colon, release of the drug relies on the abundance and activity of the polysaccharide-specific bacterial enzymes. Samples (faecal slurries) from volunteers treated with antibiotics within the last 3 months should be excluded from the evaluation of such formulations in in-vitro dissolution tests.[228]

The microbiota is also involved in the modification of primary bile acids to secondary bile acids, such as deoxycholic acid and lithocholic acid, via microbial 7α-dehydroxylase and in the deconjugation of conjugated bile acids.[229] Unconjugated bile acids are less likely to be reabsorbed in the terminal ileum and therefore, bacterial action promotes the excretion of bile acids.[230] Thus, antibiotic treatment may cause changes in the bile acid pool. Indeed, treatment with oral vancomycin decreased faecal levels of secondary bile acids and increased faecal levels of primary bile acids in healthy volunteers ($n = 10$). By contrast, treatment with oral amoxicillin showed no such effect.[231] It has also been hypothesised that antibiotic-induced differences in the bile acid composition could affect the solubilisation of lipophilic drugs. However, a recent study evaluating the differences in the solubilisation capacity of primary and secondary bile acids for nine poorly water-soluble drugs revealed at most minor differences between conjugated and unconjugated bile acids. Only dehydroxylation at C-7 improved drug solubilisation significantly for the compounds investigated.[232]

With regard to DDIs at the level of metabolism, the effect of antibiotics on metabolic enzymes is often specific to the antibiotic agent. Macrolide antibiotics interact with substrates metabolised by CYP3A4 (i.e. carbamazepine, terfenadine, cyclosporine) depending on the macrolide's specific affinity for CYP3A4. The interaction potential can be high (troleandomycin, erythromycin), moderate (clarithromycin, roxithromycin) or low (azithromycin).[233] For example, concomitant administration of erythromycin (500 mg three times daily for 7 days) with midazolam (single dose 15 mg) resulted in a fourfold increase of the AUC of midazolam in 15 healthy subjects.[234] Similarly, when administered with clarithromycin (500 mg twice daily for 7 days), the bioavailability of midazolam (single dose 4 mg) was increased 2.4-fold in 16 healthy subjects.[235] But, after pretreatment with azathioprine (500 mg daily for 3 days), no significant effect on the pharmacokinetics of midazolam (single dose 15 mg) was observed in 12 healthy subjects.[236]

For the fluoroquinolones, depending on the fluoroquinolone's specific affinity for CYP1A2, interactions with CYP1A2 substrates (i.e. clozapine, theophylline) have been observed.[237] Concomitant oral administration of enoxacin (400 mg twice daily for 6 days) with theophylline (250 mg twice daily for 11 days) resulted in a reduction in total clearance of theophylline by 74% in six healthy subjects,[238] while ciprofloxacin (500 mg twice daily for two and a half days) reduced theophylline's total clearance by 19% after a single oral dose of theophylline syrup (3.4 mg/kg) in nine healthy subjects.[239] In contrast, concomitant administration of norfloxacin (400 mg twice daily for 4 days) with theophylline (200 mg three times daily for 4 days) had no significant effect on theophylline's total clearance in 10 healthy subjects.[240] For more detailed information, the reader is referred to several review articles.[233,237,241]

Anti-inflammatory drugs for inflammatory bowel disease

Anti-inflammatory agents, such as aminosalicylates and corticosteroids, are the most commonly used drugs in IBD. Treatment with aminosalicylates includes a range of prodrugs (sulfasalazine, olsalazine, balsalazine) or modified release formulations to deliver aminosalicylates to their target site in the intestine. If remission cannot be achieved with aminosalicylates, the next treatment option consists of different corticosteroids ranging from locally acting drugs (budesonide) to systemic acting ones (hydrocortisone, prednisolone, dexamethasone).

Aminosalicylates have shown to alter the GI physiology. In terms of GI transit time, olsalazine accelerated transit, with a mean gastric emptying time of 45.3 ± 24.2 min vs 67.3 ± 33.1 min, a mouth to caecum transit time of 242 ± 41 min vs 325 ± 33 min and whole gut transit time of 37.8 ± 17.8 h vs 60.5 ± 26 h in six patients with ulcerative colitis whereas intake of sulfasalazine had no effect in six healthy subjects (measured by scintigraphy of a solid radio-labelled meal or hydrogen breath test).[242–244] The authors commented that this may be the result of a direct action of olsalazine on contractile activity in the small intestine, inducing hypersecretion or decreasing fluid absorption.[243]

With respect to luminal pH, treatment with sulfasalazine in patients with ulcerative colitis in remission resulted in a decrease in colonic pH to 4.90 ± 1.3 compared to treatment with Asacol® (mesalazine) with a colonic pH of 5.52 ± 1.13 or Dipentum® (olsalazine) with a pH of 5.51 ± 0.37.[245] Nugent *et al.*[246] postulated that reduced colonic pH may impair drug release from delayed-release formulations targeting the terminal ileum/colon (trigger pH for release is >6–7) or alter bacterial enzyme activity.

Regarding permeability, jejunal perfusion studies showed a decreased absorption of water, sodium, potassium and chloride in the presence of olsalazine or sulfasalazine.[247] In ileal perfusion studies, reduced absorption of water and

glucose was observed, when olsalazine was present, which in turn could explain the higher volume of ileostomy fluid observed after oral administration of this drug.[247,248] By contrast, no changes in absorption or volume of fluids was observed in ileal perfusion studies in the presence of sulfasalazine.[247] With regard to specific uptake mechanisms, sulfasalazine reduced the uptake of folic acid and methotrexate by folate transporters in biopsy specimens taken from the duodenojejunal region while olsalazine only decreased folic acid uptake.[249] In an intervention study, sulfasalazine treatment was discontinued in rheumatoid arthritis patients who had previously received a combination of sulfasalazine and methotrexate. The discontinuation of sulfasalazine resulted in a more than twofold increase of methotrexate serum concentrations, in line with the ability of sulfasalazine to compete with methotrexate for the folic acid transporter.[250]

After treatment with sulfasalazine the faecal microbiota of patients with rheumatoid arthritis was richer in Bacillus, whereas decreased numbers of aerobic bacteria, *E. coli*, Clostridium perfringens and Bacteroides were observed.[251–253] Treatment with mesalazine resulted in a decreased diversity of the intestinal microbiota and also reduced the quantity of faecal bacteria in patients with diarrhoea-predominant irritable bowel syndrome.[254,255] These changes in colonic bacteria may have ramifications for drugs like digoxin, which are partly metabolised by bacterial enzymes (see the section on 'Antibiotics').[256–258]

With regard to DDIs, pretreatment with sulfasalazine (500 mg for 6 days) in 10 healthy subjects decreased the AUC of digoxin by 25% after being administered as oral solution (dose 0.5 mg).[256] The mechanism of the interaction is not yet understood. Differences in bioavailability could possibly be attributed to a direct action of sulfasalazine on the intestinal mucosa or induced differences in the gut microbiota enhancing digoxin metabolism. For a patient on concomitant treatment with cyclosporin (480 mg daily) and sulfasalazine (1.5 g daily), increased plasma concentrations of cyclosporine were observed 5 days after the treatment of sulfasalazine was stopped, making it necessary to reduce the dose of cyclosporine by 60%.[259] While the interaction is not yet understood, an induction of metabolic enzymes is plausible considering the time course of the observation. For 6-mercaptopurine (50–75 mg), a metabolic interaction was observed with concomitantly administered olsalazine (1000–1750 mg) in a patient with Crohn's disease, resulting in bone marrow suppression and requiring dose reduction of 6-mercaptopurine.[260] This interaction may be caused by the inhibition of thiopurine methyltransferase, which is responsible for 6-mercaptopurine metabolism; inhibition of this enzyme by aminosalicylates has been demonstrated in invitro enzyme kinetic studies.[261]

After treatment with corticosteroids, the phospholipid mucus layer can be fluidised, resulting in a thinner mucus barrier.[262] Impairment of membrane integrity can cause side effects such as gastrointestinal bleeding and bowel perforation.[263] The corticosteroids can also affect active transport mechanisms such as bile salt reuptake and exo-transport. Treatment with budesonide results in upregulation of the apical sodium-dependent bile acid transporter in the terminal ileum, which enhances bile acid absorption in both healthy controls and patients with Crohn's disease.[264,265] Consequently, lower luminal bile salt concentrations may impede solubilisation and absorption of lipophilic poorly soluble drugs from the ileum.[266] In terms of transporters, budesonide and prednisone are substrates of the efflux transporter P-glycoprotein.[267] However, it is unclear whether these alterations result in clinically significant DDIs.

The main elimination pathway of corticosteroids is the metabolism by intestinal and hepatic CYP3A4 which is especially important for high-clearance corticosteroids such as budesonide and prednisone.[268] Coadministration of prednisone with metronidazole in six patients with Crohn's disease reduced the bioavailability of metronidazole by 31%, most likely attributed to the induction of liver enzymes responsible for metabolising metronidazole.[269] Likewise, cotreatment with prednisone resulted in decreased serum concentrations of salicylates in a 11-year-old child with juvenile rheumatoid arthritis due to the induction of salicylate clearance by prednisone.[270] On the other hand, drugs inhibiting CYP3A4 in the intestinal wall and liver such as ketoconazole, itraconazole, clarithromycin and HIV-protease inhibitors reduce the metabolism of corticosteroids and increase their bioavailability.[271–274]

Immunosuppressive agents for inflammatory bowel disease

Immunosuppressive agents are frequently used in gastroenterology for the treatment of IBD, autoimmune hepatitis, autoimmune pancreatitis, sclerosing cholangitis and in the post-transplantation setting.[275] In particular, in IBD, therapy with immunosuppressive agents has gained in importance over the last few years.[276] Immunosuppressive agents can be classified in immunomodulators (e.g. thiopurines (6-mercaptopurine, azathioprine), methotrexate, tacrolimus, sirolimus, everolimus, cyclosporine A) and biologics (e.g. monoclonal antibodies: infliximab, adalimumab, vedolizumab, golimumab).[276] Depending on the specific immunosuppressive agent, gastrointestinal transit time, bile flow and/or permeability can be altered, which could further affect drug product performance of coadministered drugs.

Regarding transit time, gastric emptying time (as measured with magnetic markers after a standardised meal

using Alternating Current Biosusceptometry) was decreased in patients treated with tacrolimus after kidney transplant (47 ± 34 min) compared to healthy subjects (176 ± 42 min) or patients treated with cyclosporine A (195 ± 42 min).[277]

In terms of drug absorption, immunosuppressants can result in increased permeability on the one hand, but decreased surface area on the other hand. Intestinal permeability was increased (75% of median value; indicated by an increased lactulose/L-rhamnose excretion ratio) in liver graft recipients treated with tacrolimus (*n* = 12) compared to healthy subjects (*n* = 9) and by 48% compared to untreated liver transplant patients (*n* = 5).[278] Only the permeability via the transcellular pathway seems to be increased by tacrolimus, as indicated by an increased lactulose/L-rhamnose ratio (+160%) and unchanged excretion of lactulose in treated orthotopic liver transplantation patients.[278,279]

Another side effect of immunosuppressive therapy, especially with methotrexate (including low-dose therapy) is GI mucositis resulting in the loss of villi in the duodenum, crypts in the colon and enterocytes.[280–284] Oral mucositis is a side effect of azathioprine therapy.[285] In patients with oral mucositis, bupivacaine absorption from lozenges was increased and a trend to higher fentanyl absorption administered with a sublingual spray was observed but did not reach statistical significance.[286,287] The effect may be due to impairment of the barrier function of the mucosa.

In terms of transporter systems and metabolism, immunosuppressants (cyclosporine A, tacrolimus, everolimus and sirolimus) are substrates of P-glycoprotein and CYP3A4.[288–290] As a result, various drug interactions with P-gp substrates such as aliskiren and anthracyclines have been reported for cyclosporine A.[291–293] Additionally, concomitant administration of inhibitors (e.g. azole antifungal drugs, macrolide antibiotics) and inducers (e.g. anticonvulsants, rifampicin) of CYP3A4 can modify therapeutic response and toxicity of the above-mentioned immunosuppressants.[294–296] Methotrexate intramuscular or subcutaneous cotreatment in patients with Crohn's disease or oral cotreatment in patients with rheumatoid arthritis resulted in increased infliximab concentrations, most likely due to a decrease in the development of infliximab antibodies.[297,298] Coadministration of azathioprine in patients treated with warfarin resulted in higher warfarin doses needed to reach therapeutic anticoagulant effects but the mechanism of the interaction is unclear.[299–301]

Bile acid sequestrants

Bile acid sequestrants (BAS) such as cholestyramine, colesevelam and colestipol are used for the treatment of primary hyperlipidaemia, as monotherapy or in combination with statins or ezetimibe, and in the treatment of gastrointestinal diseases.[302] Cholestyramine is indicated for diarrhoea associated with Crohn's disease, ileal resection, vagotomy, diabetes, diabetic vagal neuropathy and radiation.[303] While colesevelam is not licensed for the treatment of bile acid malabsorption, several clinical trials have demonstrated positive outcomes which has provoked its off-label use in this indication.[304–306]

Bile acid sequestrants are positively charged ion-exchange resins which bind bile acids in the intestine to form insoluble complexes and as a consequence reduce the bile acid pool.[303] As a result of decreased luminal bile acid concentrations, BAS are expected to interfere with the bioavailability of lipophilic, low-soluble compounds by impeding their solubilisation. For several drugs, such as rifaximin[307] and troglitazone,[308] the presence of bile acids was shown to increase drug solubility, and therefore, their absorption may be impeded by cotherapy with BAS.

The positive charge of BAS leads to a high affinity for deprotonated acidic drugs in the intestine. Binding of these anions increases the excretion and impedes the absorption of acidic coadministered drugs. Drugs that are known to be affected by this mechanism are furosemide,[309] warfarin,[310] phenprocoumon,[311,312] sulindac,[313] cerivastatin,[314] levothyroxine,[315] glipizide,[316] mycophenolic acid,[317] folic acid[318] and valproate.[319] The binding affinity for coadministered drugs can vary among the different BAS, for example, cholestyramine, which has a high affinity for hydrophobic compounds,[302,320] decreased ibuprofen and diclofenac absorption to a higher extent than colestipol; while colesevelam has a favourable DDI-profile compared to other BAS.[321–323]

High-molecular lipophilic drugs are typical substrates for enterohepatic recirculation.[324] By binding drugs or drug metabolites that undergo enterohepatic recirculation, BAS can enhance drug elimination of the victim drug even if the administration was not concomitant. Drugs affected by this mechanism include oral anticoagulants,[310–312] cardiac glycosides[325] and mycophenolate mofetil.[317] It is difficult to predict which drugs that undergo enterohepatic recirculation will be affected by BAS, as various factors such as polarity, ionisation properties and metabolism by liver and microbiota all influence biliary excretion.[326] Prolonging the interval between administration of BAS and comedication often reduces the potential for drug interactions and must be adapted for extended-release formulations.

Bile acid sequestrants can also affect GI transit time: cholestyramine prolonged the transit time in the transverse colon by up to 8 h in 13 patients with idiopathic bile acid diarrhoea (as measured with radiopaque markers), while total colonic transit was not altered.[327] After concomitant administration of a sustained-release formulation of verapamil (dose 240 mg) with colesevelam (dose 4.5 g), a

reduction in AUC of 11% and decreased plasma levels of verapamil were observed in 31 healthy subjects.[328] This interaction was deemed not to be clinically relevant.[328]

An overview of DDIs of bile acid sequestrants and their mechanism is given in Table 4.

Conclusions and future perspectives

Gastrointestinal events and conditions play a key role in the bioavailability of an orally administered drug and its therapeutic action. Concomitant use of various medications can affect the absorption and the pharmacokinetics of the administered drugs and therefore their performance. As presented in this review article, various interactions between drugs used to treat gastrointestinal diseases and coadministered drugs have been identified. These interactions are of particular concern, as GI drugs are commonly prescribed and many of them are also available OTC. Prescribing physicians and pharmacists need to be aware of and monitor these potential interactions. Furthermore, information involving interactions with GI drugs should be made available not only to clinical practitioners, but also to patients, in order to prevent the appearance of adverse effects, on the one hand, and failure of treatment on the other hand.

It should be noted, however, that despite the large number of DDI studies with GI drugs reported in literature, most studies have only investigated the effects of short-term treatment and little is known about the ramifications of long-term administration on DDIs. Furthermore, most DDI studies have been conducted in healthy volunteers and may not necessarily reflect the degree of interaction in patients. As most of the DDIs have been based on changes in pharmacokinetics, it is also not clear in all cases whether the DDI has any ramifications for the therapeutic effect. Indeed, some studies have suggested that even quite significant changes in pharmacokinetics do not always lead to a change in the clinical response. More work on pharmacokinetics/pharmacodynamics (PK/PD) relationships and the

influence of DDIs on them will be necessary to tease out the clinical implications of DDIs.

However, the number of studies that can be conducted to test for potentially clinically relevant DDIs is limited, due to both ethical and cost-related issues. So there is a need for innovative evaluation methods to address knowledge gaps and provide key information on safe and effective drug use.[329] In the last 10 years, there has been an increasing use of Physiologically Based Pharmacokinetic (PBPK) modelling and simulation at different stages of drug development.[330] To date, PBPK modelling and simulation has been mostly used for predicting enzyme interactions which, as mentioned in this article, can also occur with concomitant administration of GI drugs.[331–336] PBPK modelling is gaining acceptance at the various regulatory agencies as a tool to qualitatively and quantitatively predict DDIs and, in some cases, the simulation results may even be used to support labelling, depending on the clinical importance of the interaction.[8]

One of the advantages of PBPK modelling is that it is able to account for both formulation characteristics and physiological parameters. As such, it can be used to help define a 'safe space' by identifying the range of dosing conditions under which the pharmacokinetic parameters will not be significantly affected by changes in the release properties of the dosage form. This approach, which is sometimes referred to as 'virtual bioequivalence', has already been used to explore whether bioequivalence decisions based on clinical trials in healthy adults can be extrapolated to special populations, such as the hypochlorhydric or achlorhydric population, in whom the gastrointestinal physiology differs from that of healthy adults.[337–339]

The same approach could be extended to predict preabsorptive DDIs with GI drugs, as these are intended to modify gastrointestinal physiology. First attempts have already been made for acid reducing agents, with results from in-vitro dissolution experiments, which are tailored to mimic the changes in the upper gastrointestinal tract after the administration of these drugs, combined with PBPK

Table 4 Drug–drug interactions with concomitant administration of bile acid sequestrants

Implications for comedication	Associated risk for comedication	Reported interactions
Binding of weakly acidic drugs	↓ Bioavailability of coadministered drug	Furosemide[309] warfarin,[310] phenprocoumon,[311,312] sulindac,[313] cerivastatin,[314] levothyroxine,[315] glipizide,[316] mycophenolic acid,[317] folic acid,[318] valproate[319]
Disruption of enterohepatic recirculation of drugs	↑ Excretion of coadministered drug	Anticoagulants,[310–312] cardiac glycosides,[325] mycophenolate mofetil[317]
Possible impact on gastrointestinal transit time	↓↑ Time available at gastrointestinal absorption site, effect on t_{max}	Sustained-release formulation of verapamil[328]a
Reduced concentrations of bile acids for drug solubilisation	↓ Absorption of low-soluble compounds	

aNot clinically significant due to high variability in the pharmacokinetics of verapamil.

models for healthy adults.[337,338,340] This approach should be broadened to encompass other classes of GI drugs. Possible future steps include tailoring dissolution tests and PBPK models to the physiological conditions observed in special populations, thus allowing for predictions of the *in vivo* performance of drug products in special populations (paediatrics, geriatrics, ethnic groups, the obese, hepatically impaired, etc.) who concomitantly receive GI drugs. This approach will provide the way forward to predicting pharmacokinetic differences resulting from these combinations and, especially when coupled with PK/PD relationships, whether these are likely to be clinically significant, in a wide variety of populations and dosing conditions.

Declaration

Acknowledgement

References

1. Everhart JE, Ruhl CE. Burden of digestive diseases in the United States part I: overall and upper gastrointestinal diseases. *Gastroenterology* 2009; 136: 376–386.

2. Peery A *et al.* Burden of gastrointestinal disease in the United States: 2012 update. *Gastroenterology* 2012; 143: 1179–1187.

3. Lindsley CW. 2014 global prescription medication statistics: strong growth and CNS well represented. *ACS Chem Neurosci* 2015; 6: 505–506.

4. Quigley EMM. Prokinetics in the management of functional gastrointestinal disorders. *Curr Gastroenterol Rep* 2017; 19: 53.

5. Enck P *et al.* Functional dyspepsia. *Nat Rev Dis Primers* 2017; 3: 17081.

6. Pinto-Sanchez MI *et al.* Proton pump inhibitors for functional dyspepsia. *Cochrane Database Syst Rev* 2017; (3): CD011194.

7. Ford AC *et al.* Efficacy of 5-aminosalicylates in Crohn's disease: systematic review and meta-analysis. *Am J Gastroenterol* 2011; 106: 617–629.

8. EMA. Guideline on the investigation of drug interactions. *Guid Doc* 2012; 44(June): 59. https://doi.org/10.1093/deafed/ens058

9. Huang S-M. Clinical drug interaction studies—study design, data analysis, and clinical implications guidance for industry. *FDA Guid* 2009. Available at: http://www.fda.gov/Drugs/GuidanceComplianceRegulatoryInformation/Guidances/default.htm. Accessed January 10, 2018.

10. Dechanont S *et al.* Hospital admissions/visits associated with drug-drug interactions: a systematic review and meta-analysis. *Pharmacoepidemiol Drug Saf* 2014; 23: 489–497.

11. Center for Drug Evaluation and Research. Resources for you – drug interactions: what you should know. Available at: https://www.fda.gov/drugs/resourcesforyou/ucm163354.htm. Accessed October 25, 2017.

12. Eurostat. File:Self-reported use of non-prescribed medicines by sex, 2014 (%).png – statistics explained. Available at: http://ec.europa.eu/eurostat/statistics-explained/index.php/File:Self-reported_use_of_non-prescribed_medicines_by_sex,_2014_(%25).png. Accessed October 25, 2017.

13. Connelly D. Sales of over-the-counter medicines in 2015 by clinical area and top 50 selling brands. *Pharm J* 2016. https://doi.org/10.1211/PJ.2016.20200923.

14. Holzbauer M, Sharman DF. The distribution of catecholamines in vertebrates. In: Blaschko H, Muscholl E, eds. *Catecholamines*. Berlin, Heidelberg: Springer Berlin Heidelberg, 1972: 110–185. https://doi.org/10.1007/978-3-642-65249-3_5

15. Orloff LA *et al.* Dopamine and norepinephrine in the alimentary tract changes after chemical sympathectomy and surgical vagotomy. *Life Sci* 1985; 36: 1625–1631.

16. Longo WE, Vernava AM. Prokinetic agents for lower gastrointestinal motility disorders. *Dis Colon Rectum* 1993; 36: 696–708.

17. Tonini M. Recent advances in the pharmacology of gastrointestinal prokinetics. *Pharmacol Res* 1996; 33: 217–226.

18. Ehrlein HJ, Schemann M. Gastrointestinal motility. Available at: http://humanbiology.wzw.tum.de/motvid01/tutorial.pdf. Accessed January 15, 2018.

19. Mandl P, Kiss JP. Role of presynaptic nicotinic acetylcholine receptors in the regulation of gastrointestinal motility. *Brain Res Bull* 2007; 72: 194–200.

20. Gershon MD. Review article: serotonin receptors and transporters – roles in normal and abnormal gastrointestinal motility. *Aliment Pharmacol Ther* 2004; 20: 3–14.

21. Halpert A, Drossman D. 5-HT modulators and other antidiarrheal agents and cathartics. In: Wolfe MM, Lowe RC, eds. *Pocket Guide to Gastrointestinal Drugs*. Chichester, UK: John Wiley & Sons, Ltd, 2014: 57–81.

22. Kale H, Fass R. Prokinetic agents and antiemetics. In: Wolfe MM, Lowe RC, eds. *Pocket Guide to Gastrointestinal Drugs*. Chichester, UK: John Wiley & Sons, Ltd, 2014: 1–14.

23. Lee A, Kuo B. Metoclopramide in the treatment of diabetic gastroparesis. *Expert Rev Endocrinol Metab* 2010; 5: 653–662.

24. McCallum RW *et al.* Effects of metoclopramide and bethanechol on delayed gastric emptying present in

gastroesophageal reflux patients. *Gastroenterology* 1983; 84: 1573–1577.

25. Fink SM *et al.* Effect of metoclopramide on normal and delayed gastric emptying in gastroesophageal reflux patients. *Dig Dis Sci* 1983; 28: 1057–1061.

26. Parkman HP. Migraine and gastroparesis from a gastroenterologist's perspective. *Headache* 2013; 53: 4–10.

27. Tokola R, Neuvonen P. Effects of migraine attack and metoclopramide on the absorption of tolfenamic acid. *Br J Clin Pharmacol* 1984; 17: 67–75.

28. Volans GN. The effect of metoclopramide on the absorption of effervescent aspirin in migraine. *Br J Clin Pharmacol* 1975; 2: 57–63.

29. Gothoni G *et al.* Absorption of antibiotics: influence of metoclopramide and atropine on serum levels of pivampicillin and tetracycline. *Ann Clin Res* 1972; 4: 228–232.

30. Nimmo J *et al.* Pharmacological modification of gastric emptying: effects of propantheline and metoclopromide on paracetamol absorption. *Br Med J* 1973; 1: 587–589.

31. Wing LM *et al.* The effect of metoclopramide and atropine on the absorption of orally administered mexiletine. *Br J Clin Pharmacol* 1980; 9: 505–509.

32. Crammer JL *et al.* Blood levels and management of lithium treatment. *Br Med J* 1974; 3: 650–654.

33. Sánchez J *et al.* The influence of gastric emptying on droxicam pharmacokinetics. *J Clin Pharmacol* 1989; 29: 739–745.

34. Manara AR *et al.* The effect of metoclopramide on the absorption of oral controlled release morphine. *Br J Clin Pharmacol* 1988; 25: 518–521.

35. Morris JGL *et al.* Plasma dopa concentrations after different preparations of levodopa in normal subjects. *Br J Clin Pharmacol* 1976; 3: 983–990.

36. Gugler R *et al.* Impaired cimetidine absorption due to antacids and metoclopramide. *Eur J Clin Pharmacol* 1981; 20: 225–228.

37. Mahony MJ *et al.* Modification of oral methotrexate absorption in children with leukemia. *Cancer Chemother Pharmacol* 1984; 12: 131–133.

38. Pearson ADJ *et al.* Small intestinal transit time affects methotrexate absorption in children with acute lymphoblastic leukemia. *Cancer Chemother Pharmacol* 1985; 14: 211–215.

39. Manninen V *et al.* Altered absorption of digoxin in patients given propantheline and metoclopramide. *Lancet* 1973; 1: 398–400.

40. Manninen V *et al.* Effect of propantheline and metoclopramide on absorption of digoxin. *Lancet* 1973; 1: 1118–1119.

41. Johnson BF *et al.* Effect of metoclopramide on digoxin absorption from tablets and capsules. *Clin Pharmacol Ther* 1984; 36: 724–730.

42. Wadhwa NK *et al.* The effect of oral metoclopramide on the absorption of cyclosporine. *Transplantation* 1987; 43: 211–213.

43. Cash BD, Lacy BE. Systematic review: FDA-approved prescription medications for adults with constipation. *Gastroenterol Hepatol (N Y)* 2006; 2: 736–749.

44. Tack J *et al.* Diagnosis and treatment of chronic constipation – a European perspective. *Neurogastroenterol Motil* 2011; 23: 697–710.

45. Andresen V *et al.* Effect of 5 days linaclotide on transit and bowel function in females with constipation-predominant irritable bowel syndrome. *Gastroenterology* 2007; 133: 761–768.

46. Lewis SJ, Heaton KW. Increasing butyrate concentration in the distal colon by accelerating intestinal transit. *Gut* 1997; 41: 245–251.

47. Klauser AG *et al.* Polyethylene glycol 4000 for slow transit constipation. *Z Gastroenterol* 1995; 33: 5–8.

48. Corazziari E *et al.* Small volume isosmotic polyethylene glycol electrolyte balanced solution (PMF-100) in treatment of chronic nonorganic constipation. *Dig Dis Sci* 1996; 41: 1636–1642.

49. Ewe K *et al.* Effect of lactose, lactulose and bisacodyl on gastrointestinal transit studied by metal detector. *Aliment Pharmacol Ther* 1995; 9: 69–73.

50. Coremans G *et al.* Small doses of the unabsorbable substance polyethylene glycol 3350 accelerate oro-caecal transit, but slow gastric emptying in healthy subjects. *Dig Liver Dis* 2005; 37: 97–101.

51. Jouët P *et al.* Effects of therapeutic doses of lactulose vs. polyethylene glycol on isotopic colonic transit. *Aliment Pharmacol Ther* 2008; 27: 988–993.

52. Fritz E *et al.* Effects of lactulose and polyethylene glycol on colonic transit. *Aliment Pharmacol Ther* 2005; 21: 259–268.

53. Barrow L *et al.* Scintigraphic demonstration of lactulose-induced accelerated proximal colon transit. *Gastroenterology* 1992; 103: 1167–1173.

54. Manabe N *et al.* Effects of bisacodyl on ascending colon emptying and overall colonic transit in healthy volunteers. *Aliment Pharmacol Ther* 2009; 30: 930–936.

55. Guckenbiehl W *et al.* Effect of laxatives and metoclopramide on plasma quinidine concentration during prolonged administration in patients with heart rhythm disorders. *Med Welt* 1976; 26: 1273–1276. [in German]

56. Ragueneau I *et al.* Pharmacokinetic and pharmacodynamic drug interactions between digoxin and macrogol 4000, a laxative polymer, in healthy volunteers. *Br J Clin Pharmacol* 1999; 48: 453–456.

57. Lewis SJ *et al.* Intestinal absorption of oestrogen: the effect of altering transit-time. *Eur J Gastroenterol Hepatol* 1998; 10: 33–39.

58. Bown RL *et al.* Effects of lactulose and other laxatives on ileal and colonic pH as measured by a radiotelemetry device. *Gut* 1974; 15: 999–1004.

59. Agostini L *et al.* Faecal ammonia and pH during lactulose administration in man: comparison with other cathartics. *Gut* 1972; 13: 859–866.

60. Mann NS *et al.* Effect of lactulose, neomycin and antacid on colonic pH recorded continuously with an implanted electrode. *Am J Gastroenterol* 1979; 72: 141–145.

61. Hussain FN *et al.* Mesalazine release from a pH dependent formulation: effects of omeprazole and lactulose co-administration. *Br J Clin Pharmacol* 1998; 46: 173–175.

62. Riley SA *et al.* Mesalazine release from coated tablets: effect of dietary fibre. *Br J Clin Pharmacol* 1991; 32: 248–250.

63. Medicines.org.uk. Asacol 400 mg MR tablets- summary of product characteristics (SPC) – (eMC). 2018. Available at: https://www.medicines.org.uk/emc/product/2217/smpc. Accessed June 3, 2018.

64. Medicines.org.uk. Salofalk 1000 mg gastro-resistant prolonged-release granules- summary of product characteristics (SPC) – (eMC). 2018. Available at: https://www.medicines.org.uk/emc/product/140/smpc. Accessed June 3, 2018.

65. Bouhnik Y *et al.* Prospective, randomized, parallel-group trial to evaluate the effects of lactulose and polyethylene glycol-4000 on colonic flora in chronic idiopathic constipation. *Aliment Pharmacol Ther* 2004; 19: 889–899.

66. Visser LE *et al.* Overanticoagulation associated with combined use of lactulose and acenocoumarol or phenprocoumon. *Br J Clin Pharmacol* 2004; 57: 522–524.

67. Ippoliti C. Antidiarrheal agents for the management of treatment-related diarrhea in cancer patients. *Am J Health Syst Pharm* 1998; 55: 1573–1580.

68. Kachel G *et al.* Human intestinal motor activity and transport: effects of a synthetic opiate. *Gastroenterology* 1986; 90: 85–93.

69. Press AG *et al.* Effect of loperamide on jejunal electrolyte and water transport, prostaglandin E 2-induced secretion and intestinal transit time in man. *Eur J Clin Pharmacol* 1991; 41: 239–243.

70. Sninsky CA *et al.* Effect of lidamidine hydrochloride and loperamide on gastric emptying and transit of the small intestine: a double-blind study. *Gastroenterology* 1986; 90: 68–73.

71. Kirby MG *et al.* Effect of metoclopramide, bethanechol, and loperamide on gastric residence time, gastric emptying, and mouth-to-cecum transit time. *Pharmacotherapy* 1989; 9: 226–231.

72. Bryson JC *et al.* Effect of altering small bowel transit time on sustained release theophylline absorption. *J Clin Pharmacol* 1989; 29: 733–738.

73. Hughes S *et al.* Loperamide has antisecretory activity in the human jejunum in vivo. *Gut* 1984; 25: 931–935.

74. Remington M *et al.* Inhibition of postprandial pancreatic and biliary secretion by loperamide in patients with short bowel syndrome*. *Gut* 1982; 23: 98–101.

75. Thimister PWL *et al.* Inhibition of pancreaticobiliary secretion by loperamide in humans. *Hepatology* 1997; 26: 256–261.

76. Callréus T *et al.* Changes in gastrointestinal motility influence the absorption of desmopressin. *Eur J Clin Pharmacol* 1999; 55: 305–309.

77. Fredholt K *et al.* alpha-Chymotrypsin-catalyzed degradation of desmopressin (dDAVP): influence of pH, concentration and various cyclodextrins. *Int J Pharm* 1999; 178: 223–229.

78. Mikus G *et al.* Reduction of saquinavir exposure by coadministration of loperamide. *Clin Pharmacokinet* 2004; 43: 1015–1024.

79. Wafik Gouda M. Effect of an antidiarrhoeal mixture on the bioavailability of tetracycline. *Int J Pharm* 1993; 89: 75–77.

80. Juhl RP. Comparison of kaolin-pectin and activated charcoal for inhibition of aspirin absorption. *Am J Hosp Pharm* 1979; 36: 1097–1098.

81. Al-Shora HI *et al.* Interactions of procainamide, verapamil, guanethidine and hydralazine with adsorbent antacids and antidiarrhoeal mixtures. *Int J Pharm* 1988; 47: 209–213.

82. Gupta KC *et al.* Effect of pectin and kaolin on bioavailability of co-trimoxazole suspension. *Int J Clin Pharmacol Ther Toxicol* 1987; 25: 320–321.

83. Albert KS *et al.* Influence of kaolin–pectin suspension on digoxin bioavailability. *J Pharm Sci* 1978; 67: 1582–1586.

84. Albert KS *et al.* Pharmacokinetic evaluation of a drug interaction between kaolin–pectin and clindamycin. *J Pharm Sci* 1978; 67: 1579–1582.

85. Albert KS *et al.* Influence of kaolin-pectin suspension on steady-state plasma digoxin levels. *J Clin Pharmacol* 1981; 21: 449–455.

86. Brown DD *et al.* Decreased bioavailability of digoxin due to antacids and kaolin-pectin. *N Engl J Med* 1976; 295: 1034–1037.

87. Moustafa MA *et al.* Decreased bioavailability of quinidine sulphate due to interactions with adsorbent antacids and antidiarrhoeal mixtures. *Int J Pharm* 1987; 34: 207–211.

88. Liel Y *et al.* Evidence for a clinically important adverse effect of fiber-enriched diet on the bioavailability of levothyroxine in adult hypothyroid patients. *J Clin Endocrinol Metab* 1996; 81: 857–859.

89. FDA. Avoid food and drug interactions. Available at: https://www.fda.gov/downloads/drugs/resourcesforyou/consumers/buyingusingmedicinesafely/ensuringsafeuseofmedicine/generaluseofmedicine/ucm229033.pdf. Accessed September 6, 2017.

90. Perlman B. Interaction between lithium salts and ispaghula husk. *Lancet* 1990; 335: 416.

91. Stewart DE. High-fiber diet and serum tricyclic antidepressant levels. *J Clin Psychopharmacol* 1992; 12: 438–440.

92. Brown DD *et al.* Decreased bioavailability of digoxin due to hypocholesterolemic interventions. *Circulation* 1978; 58: 164–172.

93. Lembcke B *et al.* Plasma digoxin concentrations during administration of dietary fibre (guar gum) in man. *Z Gastroenterol* 1982; 20: 164–167.

94. Kasper H *et al.* The effect of dietary fiber on postprandial serum digoxin concentration in man. *Am J Clin Nutr* 1979; 32: 2436–2438.

95. Huupponen R *et al.* Effect of guar gum, a fibre preparation, on digoxin and penicillin absorption in man.

Eur J Clin Pharmacol 1984; 26: 279–281.

96. Holt S *et al.* Effect of gel fibre on gastric emptying and absorption of glucose and paracetamol. *Lancet* 1979; 1: 636–639.

97. Reppas C *et al.* Effect of elevated viscosity in the upper gastrointestinal tract on drug absorption in dogs. *Eur J Pharm Sci* 1998; 6: 131–139.

98. Astarloa R *et al.* Clinical and pharmacokinetic effects of a diet rich in insoluble fiber on Parkinson disease. *Clin Neuropharmacol* 1992; 15: 375–380.

99. González Canga A *et al.* Dietary fiber and its interaction with drugs. *Nutr Hosp* 2010; 25: 535–539.

100. Reppas C *et al.* Effect of hydroxypropylmethylcellulose on gastrointestinal transit and luminal viscosity in dogs. *Gastroenterology* 1991; 100: 1217–1223.

101. FDA-emend capsules pharmacology review part 1.pdf. Available at: https://www.accessdata.fda.gov/drugsatfda_docs/nda/2003/21-549_Emend.cfm.

102. EMA. Emend: summary of product characteristics. Available at: http://www.ema.europa.eu/docs/en_GB/document_library/EPAR_-_Product_Information/human/000527/WC500026537.pdf. Accessed October 25, 2017.

103. Blower P *et al.* Drug-drug interactions in oncology: why are they important and can they be minimized? *Crit Rev Oncol Hematol* 2005; 55: 117–142.

104. Majumdar AK *et al.* Effects of aprepitant on cytochrome P450 3A4 activity using midazolam as a probe. *Clin Pharmacol Ther* 2003; 74: 150–156.

105. Majumdar AK *et al.* Effect of aprepitant on the pharmacokinetics of intravenous midazolam. *J Clin Pharmacol* 2007; 47: 744–750.

106. McCrea JB *et al.* Effects of the neurokinin1 receptor antagonist aprepitant on the pharmacokinetics of dexamethasone and methylprednisolone. *Clin Pharmacol Ther* 2003; 74: 17–24.

107. Takaki J *et al.* Assessment of drug-drug interaction between warfarin and aprepitant and its effects on PT-INR of patients receiving anticancer

chemotherapy. *Biol Pharm Bull* 2016; 39: 863–868.

108. EMEND®. Clinical pharmacology and biopharmaceutics review. Available at: https://www.accessdata.fda.gov/drugsatfda_docs/nda/2003/21-549_Emend_biopharmr.pdf. Accessed August 31, 2017.

109. Blower PR. Granisetron: relating pharmacology to clinical efficacy. *Support Care Cancer* 2003; 11: 93–100.

110. Gralla RJ *et al.* Recommendations for the use of antiemetics: evidence-based, clinical practice guidelines. *J Clin Oncol* 1999; 17: 2971–2994.

111. Cagnoni PJ *et al.* Modification of the pharmacokinetics of high-dose cyclophosphamide and cisplatin by antiemetics. *Bone Marrow Transplant* 1999; 24: 1–4.

112. Gilbert CJ *et al.* Pharmacokinetic interaction between ondansetron and cyclophosphamide during high-dose chemotherapy for breast cancer. *Cancer Chemother Pharmacol* 1998; 42: 497–503.

113. Speaks M. Health United States report 2016. 2016. Available at: https://www.cdc.gov/nchs/data/hus/hus16.pdf#080. Accessed August 28, 2017.

114. 100 best-selling, most prescribed branded drugs through March. Available at: http://www.medscape.com/viewarticle/844317#vp_1. Accessed August 28, 2017.

115. Arnold R. Safety of proton pump inhibitors–an overview. *Aliment Pharmacol Ther* 1994; 8(Suppl 1): 65–70.

116. Blanton WP, Wolfe MM. Proton pump inhibitors. In: Wolfe MM, Lowe RC, eds. *Pocket Guide to Gastrointestinal Drugs*. Chichester, UK: John Wiley & Sons, Ltd, 2014: 15–30.

117. Sugimoto M *et al.* Treatment strategy to eradicate *Helicobacter pylori* infection: impact of pharmacogenomics-based acid inhibition regimen and alternative antibiotics. *Expert Opin Pharmacother* 2007; 8: 2701–2717.

118. Litou C *et al.* Characteristics of the human upper gastrointestinal

contents in the fasted state under hypo- and A-chlorhydric gastric conditions under conditions of typical drug – drug interaction studies. *Pharm Res* 2016; 33: 1399–1412.

119. Meyer UA. Interaction of proton pump inhibitors with cytochromes P450: consequences for drug interactions. *Yale J Biol Med* 1996; 69: 203–209.

120. Ogawa R, Echizen H. Drug-drug interaction profiles of proton pump inhibitors. *Clin Pharmacokinet* 2010; 49: 509–533.

121. Lahner E *et al.* Systematic review: impaired drug absorption related to the co-administration of antisecretory therapy. *Aliment Pharmacol Ther* 2009; 29: 1219–1229.

122. Wedemeyer R-S, Blume H. Pharmacokinetic drug interaction profiles of proton pump inhibitors: an update. *Drug Saf* 2014; 37: 201–211.

123. Jaruratanasirikul S, Sriwiriyajan S. Effect of omeprazole on the pharmacokinetics of itraconazole. *Eur J Clin Pharmacol* 1998; 54: 159–161.

124. Johnson MD *et al.* A randomized comparative study to determine the effect of omeprazole on the peak serum concentration of itraconazole oral solution. *J Antimicrob Chemother* 2003; 51: 453–457.

125. Chin TW *et al.* Effects of an acidic beverage (Coca-Cola) on absorption of ketoconazole. *Antimicrob Agents Chemother* 1995; 39: 1671–1675.

126. Nexium®. Clinical pharmacology and biopharmaceutics review. Available at: https://www.accessdata.fda.gov/drugsatfda_docs/nda/2001/21154_Nexium_biopharmr_P1.pdf. Accessed August 29, 2017.

127. DIFLUCAN® (Fluconazole tablets) (fluconazole for oral suspension). Available at: https://www.accessdata.fda.gov/drugsatfda_docs/label/2014/019949s060,020090s044lbl.pdf. Accessed August 29, 2017.

128. Hörter D, Dressman J. Influence of physicochemical properties on dissolution of drugs in the gastrointestinal tract. *Adv Drug Deliv Rev* 2001; 46: 75–87.

129. Thorpe JE *et al.* Effect of oral antacid administration on the pharmacokinetics of oral fluconazole. *Antimicrob Agents Chemother* 1990; 34: 2032–2033.

130. Tappouni HL *et al.* Effect of omeprazole on the plasma concentrations of indinavir when administered alone and in combination with ritonavir. *Am J Health Syst Pharm* 2008; 65: 422–428.

131. Fang AF *et al.* Significant decrease in nelfinavir systemic exposure after omeprazole coadministration in healthy subjects. *Pharmacotherapy* 2008; 28: 42–50.

132. Tomilo DL *et al.* Inhibition of atazanavir oral absorption by lansoprazole gastric acid suppression in healthy volunteers. *Pharmacotherapy* 2006; 26: 341–346.

133. Klein CE *et al.* Effects of acid-reducing agents on the pharmacokinetics of lopinavir/ritonavir and ritonavir-boosted atazanavir. *J Clin Pharmacol* 2008; 48: 553–562.

134. Furtek KJ *et al.* Proton pump inhibitor therapy in atazanavir-treated patients: contraindicated? *J Acquir Immune Defic Syndr* 2006; 41: 394–396.

135. Sahloff EG, Duggan JM. Clinical outcomes associated with concomitant use of atazanavir and proton pump inhibitors. *Ann Pharmacother* 2006; 40: 1731–1736.

136. Winston A *et al.* Effect of omeprazole on the pharmacokinetics of saquinavir-500 mg formulation with ritonavir in healthy male and female volunteers. *AIDS* 2006; 20: 1401–1406.

137. Kofler S *et al.* Proton pump inhibitor co-medication reduces mycophenolate acid drug exposure in heart transplant recipients. *J Hear Lung Transplant* 2009; 28: 605–611.

138. Rupprecht K *et al.* Bioavailability of mycophenolate mofetil and enteric-coated mycophenolate sodium is differentially affected by pantoprazole in healthy volunteers. *J Clin Pharmacol* 2009; 49: 1196–1201.

139. Actonel®. Clinical pharmacology and biopharmaceutics review. Available at: https://www.accessda ta.fda.gov/drugsatfda_docs/nda/98/20835_Actonel_biopharmr.pdf. Accessed August 29, 2017.

140. Budha NR *et al.* Drug absorption interactions between oral targeted anticancer agents and ppis: is pH-dependent solubility the Achilles heel of targeted therapy? *Clin Pharmacol Ther* 2012; 92: 203–213.

141. Mitra A, Kesisoglou F. Impaired drug absorption due to high stomach pH: a review of strategies for mitigation of such effect to enable pharmaceutical product development. *Mol Pharm* 2013; 10: 3970–3979.

142. Soons PA *et al.* Influence of single- and multiple-dose omeprazole treatment on nifedipine pharmacokinetics and effects in healthy subjects. *Eur J Clin Pharmacol* 1992; 42: 319–324.

143. Bliesath H *et al.* Pantoprazole does not interact with nifedipine in man under steady-state conditions. *Int J Clin Pharmacol Ther* 1996; 34: 51–55.

144. Zvyaga T *et al.* Evaluation of six proton pump inhibitors as inhibitors of various human cytochromes P450: focus on cytochrome P450 2C19. *Drug Metab Dispos* 2012; 40: 1698–1711.

145. Li X-Q *et al.* Comparison of inhibitory effects of the proton pump-inhibiting drugs omeprazole, esomeprazole, lansoprazole, pantoprazole, and rabeprazole on human cytochrome P450 activities. *Drug Metab Dispos* 2004; 32: 821–827.

146. Ko JW *et al.* Evaluation of omeprazole and lansoprazole as inhibitors of cytochrome P450 isoforms. *Drug Metab Dispos* 1997; 25: 853–862.

147. Blume H *et al.* Pharmacokinetic drug interaction profiles of proton pump inhibitors. *Drug Saf* 2006; 29: 769–784.

148. Suzuki K *et al.* Co-administration of proton pump inhibitors delays elimination of plasma methotrexate in high-dose methotrexate therapy. *Br J Clin Pharmacol* 2009; 67: 44–49.

149. Drug safety and availability – FDA reminder to avoid concomitant use of Plavix (clopidogrel) and omeprazole. Available at: https://www.fda.gov/Drugs/DrugSafety/uc m231161.htm. Accessed August 29, 2017.

150. Stockl KM *et al.* Risk of rehospitalization for patients using clopidogrel with a proton pump inhibitor. *Arch Intern Med* 2010; 170: 704.

151. Evanchan J *et al.* Recurrence of acute myocardial infarction in patients discharged on clopidogrel and a proton pump inhibitor after stent placement for acute myocardial infarction. *Clin Cardiol* 2010; 33: 168–171.

152. Gaglia MA *et al.* Relation of proton pump inhibitor use after percutaneous coronary intervention with drug-eluting stents to outcomes. *Am J Cardiol* 2010; 105: 833–838.

153. Chua D *et al.* Clopidogrel and proton pump inhibitors: a new drug interaction? *Can J Hosp Pharm* 2010; 63: 47–50.

154. Bundhun PK *et al.* Is the concomitant use of clopidogrel and Proton Pump Inhibitors still associated with increased adverse cardiovascular outcomes following coronary angioplasty?: a systematic review and meta-analysis of recently published studies (2012–2016). *BMC Cardiovasc Disord* 2017; 17: 3.

155. Sugano K. Histamine H$_2$-receptor antagonists. In: Wolf MM, Lowe RC, eds. *Pocket Guide to Gastrointestinal Drugs*. Chichester, UK: John Wiley & Sons, Ltd, 2014: 31–43.

156. Piscitelli SC *et al.* Effects of ranitidine and sucralfate on ketoconazole bioavailability. *Antimicrob Agents Chemother* 1991; 35: 1765–1771.

157. Lim SG *et al.* Short report: the absorption of fluconazole and itraconazole under conditions of low intragastric acidity. *Aliment Pharmacol Ther* 2007; 7: 317–321.

158. Blum RA *et al.* Increased gastric pH and the bioavailability of fluconazole and ketoconazole. *Ann Intern Med* 1991; 114: 755–757.

159. Ford SL *et al.* Effect of antacids and ranitidine on the single-dose pharmacokinetics of fosamprenavir. *Antimicrob Agents Chemother* 2005; 49: 467–469.

160. Boffito M *et al.* Pharmacokinetics of saquinavir co-administered with cimetidine. *J Antimicrob Chemother* 2002; 50: 1081–1084.

161. Russell TL *et al.* pH-Related changes in the absorption of dipyridamole in the elderly. *Pharm Res* 1994; 11: 136–143.

162. Grasela TH *et al.* Inhibition of enoxacin absorption by antacids or ranitidine. *Antimicrob Agents Chemother* 1989; 33: 615–617.

163. Hughes GS *et al.* The effects of gastric pH and food on the pharmacokinetics of a new oral cephalosporin, cefpodoxime proxetil. *Clin Pharmacol Ther* 1989; 46: 674–685.

164. Gerber MC *et al.* Drug interactions with cimetidine: an update. *Pharmacol Ther* 1985; 27: 353–370.

165. Berardi RR *et al.* Comparison of famotidine with cimetidine and ranitidine. *Clin Pharm* 1988; 7: 271–284.

166. O'Reilly RA. Comparative interaction of cimetidine and ranitidine with racemic warfarin in man. *Arch Intern Med* 1984; 144: 989–991.

167. Toon S *et al.* Comparative effects of ranitidine and cimetidine on the pharmacokinetics and pharmacodynamics of warfarin in man. *Eur J Clin Pharmacol* 1987; 32: 165–172.

168. Niopas I *et al.* The effect of cimetidine on the steady-state pharmacokinetics and pharmacodynamics of warfarin in humans. *Eur J Clin Pharmacol* 1999; 55: 399–404.

169. Reimann IW *et al.* Cimetidine increases steady state plasma levels of propranolol. *Br J Clin Pharmacol* 1981; 12: 785–790.

170. Reimann IW *et al.* Effects of cimetidine and ranitidine on steady-state propranolol kinetics and dynamics. *Clin Pharmacol Ther* 1982; 32: 749–757.

171. Medicines.org.uk. Propranolol film-coated tablets- Patient Information Leaflet (PIL) – (eMC). 2018. Available at: https://www.medicines.org.uk/emc/files/pil.2904.pdf. Accessed June 3, 2018.

172. Cornard J, Merlin J. Spectroscopic and structural study of complexes of quercetin with Al(III). *J Inorg Biochem* 2002; 92: 19–27.

173. Türkel N *et al.* Potentiometric and spectroscopic studies on aluminium (III) complexes of some catechol derivatives. *Chem Pharm Bull (Tokyo)* 2004; 52: 929–934.

174. Khan MA *et al.* Differential binding of tetracyclines with serum albumin and induced structural alterations in drug-bound protein. *Int J Biol Macromol* 2002; 30: 243–249.

175. Córdoba-Díaz M *et al.* Modification of fluorescent properties of norfloxacin in the presence of certain antacids. *J Pharm Biomed Anal* 1998; 18: 565–571.

176. Deppermann KM *et al.* Influence of ranitidine, pirenzepine, and aluminum magnesium hydroxide on the bioavailability of various antibiotics, including amoxicillin, cephalexin, doxycycline, and amoxicillin-clavulanic acid. *Antimicrob Agents Chemother* 1989; 33: 1901–1907.

177. Garty M, Hurwitz A. Effect of cimetidine and antacids on gastrointestinal absorption of tetracycline. *Clin Pharmacol Ther* 1980; 28: 203–207.

178. Timmers K, Sternglanz R. Ionization and divalent cation dissociation constants of nalidixic and oxolinic acids. *Bioinorg Chem* 1978; 9: 145–155.

179. Radandt JM *et al.* Interactions of fluoroquinolones with other drugs: mechanisms, variability, clinical significance, and management. *Clin Infect Dis* 1992; 14: 272–284.

180. Nix DE *et al.* Effects of aluminum and magnesium antacids and ranitidine on the absorption of ciprofloxacin. *Clin Pharmacol Ther* 1989; 46: 700–705.

181. Krishna G *et al.* Effect of an aluminum- and magnesium-containing antacid on the bioavailability of garenoxacin in healthy volunteers. *Pharmacotherapy* 2007; 27: 963–969.

182. Lober S *et al.* Pharmacokinetics of gatifloxacin and interaction with an antacid containing aluminum and magnesium. *Antimicrob Agents Chemother* 1999; 43: 1067–1071.

183. Allen A *et al.* Effect of Maalox on the bioavailability of oral gemifloxacin in healthy volunteers. *Chemotherapy* 1999; 45: 504–511.

184. Lohitnavy M *et al.* Reduced oral itraconazole bioavailability by antacid suspension. *J Clin Pharm Ther* 2005; 30: 201–206.

185. Brass C *et al.* Disposition of ketoconazole, an oral antifungal, in humans. *Antimicrob Agents Chemother* 1982; 21: 151–158.

186. Neuvonen PJ. The effect of magnesium hydroxide on the oral absorption of ibuprofen, ketoprofen and diclofenac. *Br J Clin Pharmacol* 1991; 31: 263–266.

187. Tobert JA *et al.* Effect of antacids on the bioavailability of diflunisal in the fasting and postprandial states. *Clin Pharmacol Ther* 1981; 30: 385–389.

188. Neuvonen PJ, Kivistö KT. Effect of magnesium hydroxide on the absorption of tolfenamic and mefenamic acids. *Eur J Clin Pharmacol* 1988; 35: 495–501.

189. Segre EJ *et al.* Transport of organic acids across cell membrane. *N Engl J Med* 1974; 291: 582.

190. Ogawa R, Echizen H. Clinically significant drug interactions with antacids: an update. *Drugs* 2011; 71: 1839–1864.

191. Gareau MG *et al.* Probiotics and the gut microbiota in intestinal health and disease. *Nat Rev Gastroenterol Hepatol* 2010; 7: 503–514.

192. Guidelines for the evaluation of probiotics in food report. Joint FAO/WHO Working Group report on drafting guidelines for the evaluation of probiotics in food. 2002. Available at: http://www.who.int/foodsafety/fs_management/en/probiotic_guidelines.pdf. Accessed September 5, 2017.

193. Westendorf AM *et al.* Intestinal immunity of *Escherichia coli* NISSLE 1917: a safe carrier for therapeutic molecules. *FEMS Immunol Med Microbiol* 2005; 43: 373–384.

194. Resta-Lenert SC, Barrett KE. Modulation of intestinal barrier properties by probiotics: role in reversing colitis. *Ann N Y Acad Sci* 2009; 1165: 175–182.

195. Mikov M *et al.* The influence of probiotic treatment on sulfasalazine

metabolism in rat gut contents. *Asian J Pharmacodyn Pharmacokinet* 2006; 6: 337–342.

196. Lee HJ *et al.* The influence of probiotic treatment on sulfasalazine metabolism in rat. *Xenobiotica* 2012; 42: 791–797.

197. Kunes M *et al.* Absorption kinetics of 5-aminosalicylic acid in rat: influence of indomethacin-induced gastrointestinal lesions and *Escherichia coli* Nissle 1917 medication. *Neuro Endocrinol Lett* 2011; 32(Suppl 1): 46–52.

198. Al-Salami H *et al.* Probiotic treatment reduces blood glucose levels and increases systemic absorption of gliclazide in diabetic rats. *Eur J Drug Metab Pharmacokinet* 2008; 33: 101–106.

199. Saksena S *et al.* Upregulation of P-glycoprotein by probiotics in intestinal epithelial cells and in the dextran sulfate sodium model of colitis in mice. *Am J Physiol Gastrointest Liver Physiol* 2011; 300: G1115–G1123.

200. Matuskova Z *et al.* Administration of a probiotic can change drug pharmacokinetics: effect of *E. coli* Nissle 1917 on amidarone absorption in rats. *PLoS One* 2014; 9: 3–7.

201. Fröhlich EE *et al.* Cognitive impairment by antibiotic-induced gut dysbiosis: analysis of gut microbiota-brain communication. *Brain Behav Immun* 2016; 56: 140–155.

202. Sullivan Å *et al.* Effect of antimicrobial agents on the ecological balance of human microflora. *Lancet Infect Dis* 2001; 1: 101–114.

203. Edlund C, Nord CE. Effect on the human normal microflora of oral antibiotics for treatment of urinary tract infections. *J Antimicrob Chemother* 2000; 46(Suppl 1): 41–48; discussion 63–5.

204. Beaugerie L, Petit J-C. Antibiotic-associated diarrhoea. *Best Pract Res Clin Gastroenterol* 2004; 18: 337–352.

205. Tremaroli V, Bäckhed F. Functional interactions between the gut microbiota and host metabolism. *Nature* 2012; 489: 242–249.

206. Clausen MR *et al.* Colonic fermentation to short-chain fatty acids is decreased in antibiotic-associated diarrhea. *Gastroenterology* 1991; 101: 1497–1504.

207. Edwards CA *et al.* Effect of clindamycin on the ability of a continuous culture of colonic bacteria to ferment carbohydrate. *Gut* 1986; 27: 411–417.

208. Gustafsson A *et al.* Faecal short-chain fatty acids in patients with antibiotic-associated diarrhoea, before and after faecal enema treatment. *Scand J Gastroenterol* 1998; 33: 721–727.

209. Mellon AF *et al.* Effect of oral antibiotics on intestinal production of propionic acid. *Arch Dis Child* 2000; 82: 169–172.

210. Høverstad T *et al.* Influence of oral intake of seven different antibiotics on faecal short-chain fatty acid excretion in healthy subjects. *Scand J Gastroenterol* 1986; 21: 997–1003.

211. Kamath PS *et al.* Short-chain fatty acids stimulate ileal motility in humans. *Gastroenterology* 1988; 95: 1496–1502.

212. Fich A *et al.* Stimulation of ileal emptying by short-chain fatty acids. *Dig Dis Sci* 1989; 34: 1516–1520.

213. Aguilera M *et al.* Antibiotic-induced dysbiosis alters host-bacterial interactions and leads to colonic sensory and motor changes in mice. *Gut Microbes* 2015; 6: 10–23.

214. Cherbut C *et al.* Effects of short-chain fatty acids on gastrointestinal motility. *Scand J Gastroenterol* 1997; 32: 58–61.

215. Edelbroek MA *et al.* Effects of erythromycin on gastric emptying, alcohol absorption and small intestinal transit in normal subjects. *J Nucl Med* 1993; 34: 582–588.

216. Mantides A *et al.* The effect of erythromycin in gastric emptying of solids and hypertonic liquids in healthy subjects. *Am J Gastroenterol* 1993; 88: 198–202.

217. Landry C *et al.* Effects of erythromycin on gastric emptying, duodeno-caecal transit time, gastric and biliopancreatic secretion during continuous gastric infusion of a liquid diet in healthy volunteers. *Eur J Gastroenterol Hepatol* 1995; 7: 797–802.

218. Caron F *et al.* Effects of two oral erythromycin ethylsuccinate formulations on the motility of the small intestine in human beings. *Antimicrob Agents Chemother* 1996; 40: 1796–1800.

219. Annese V *et al.* Erythromycin accelerates gastric emptying by inducing antral contractions and improved gastroduodenal coordination. *Gastroenterology* 1992; 102: 823–828.

220. Leung WK *et al.* Effect of oral erythromycin on gastric and small bowel transit time of capsule endoscopy. *World J Gastroenterol* 2005; 11: 4865–4868.

221. Chew ML *et al.* Effect of the gastrointestinal prokinetic agent erythromycin on the pharmacokinetics of pregabalin controlled-release in healthy individuals: a phase I, randomized crossover trial. *Clin Drug Investig* 2015; 35: 299–305.

222. Sousa T *et al.* The gastrointestinal microbiota as a site for the biotransformation of drugs. *Int J Pharm* 2008; 363: 1–25.

223. Saad R *et al.* Gut pharmacomicrobiomics: the tip of an iceberg of complex interactions between drugs and gut-associated microbes. *Gut Pathog* 2012; 4: 16.

224. Lindenbaum J *et al.* Inactivation of digoxin by the gut flora: reversal by antibiotic therapy. *N Engl J Med* 1981; 305: 789–794.

225. Morton MR, Cooper JW. Erythromycin-induced digoxin toxicity. *DICP* 1989; 23: 668–670.

226. Vermes A *et al.* An in vitro study on the active conversion of flucytosine to fluorouracil by microorganisms in the human intestinal microflora. *Chemotherapy* 2003; 49: 17–23.

227. Houston JB *et al.* Azo reduction of sulphasalazine in healthy volunteers. *Br J Clin Pharmacol* 1982; 14: 395–398.

228. Singh SK *et al.* A novel dissolution method for evaluation of polysaccharide based colon specific delivery systems: a suitable alternative to animal sacrifice. *Eur J Pharm Sci* 2015; 73: 72–80.

229. Hofmann AF, Hagey LR. Bile acids: chemistry, pathochemistry, biology, pathobiology, and therapeutics. *Cell Mol Life Sci* 2008; 65: 2461–2483.

230. Brestoff JR, Artis D. Commensal bacteria at the interface of host metabolism and the immune system. *Nat Immunol* 2013; 14: 676–684.

231. Vrieze A *et al.* Impact of oral vancomycin on gut microbiota, bile acid metabolism, and insulin sensitivity. *J Hepatol* 2014; 60: 824–831.

232. Söderlind E *et al.* Simulating fasted human intestinal fluids: understanding the roles of lecithin and bile acids. *Mol Pharm* 2010; 7: 1498–1507.

233. von Rosensteil NA, Adam D. Macrolide antibacterials. Drug interactions of clinical significance. *Drug Saf* 1995; 13: 105–122.

234. Olkkola KT *et al.* A potentially hazardous interaction between erythromycin and midazolam. *Clin Pharmacol Ther* 1993; 53: 298–305.

235. Gorski JC *et al.* The contribution of intestinal and hepatic CYP3A to the interaction between midazolam and clarithromycin. *Clin Pharmacol Ther* 1998; 64: 133–143.

236. Yeates RA *et al.* Interaction between midazolam and clarithromycin: comparison with azithromycin. *Int J Clin Pharmacol Ther* 1996; 34: 400–405.

237. Douros A *et al.* Safety issues and drug–drug interactions with commonly used quinolones. *Expert Opin Drug Metab Toxicol* 2014; 11: 1–15.

238. Beckmann J *et al.* Enoxacin–a potent inhibitor of theophylline metabolism. *Eur J Clin Pharmacol* 1987; 33: 227–230.

239. Batty KT *et al.* The effect of ciprofloxacin on theophylline pharmacokinetics in healthy subjects. *Br J Clin Pharmacol* 1995; 39: 305–311.

240. Bowles SK *et al.* Effect of norfloxacin on theophylline pharmacokinetics at steady state. *Antimicrob Agents Chemother* 1988; 32: 510–512.

241. Pai MP *et al.* Antibiotic drug interactions. *Med Clin North Am* 2006; 90: 1223–1255.

242. Rao SS *et al.* Influence of olsalazine and sulphasalazine on

gastrointestinal transit influence of olsalazine and sulphasalazine on gastrointestinal transit. *Scand J Gastroenterol* 1988; 23: 148–196.

243. Rao SS *et al.* Influence of olsalazine on gastrointestinal transit in ulcerative colitis. *Gut* 1987; 28: 1474–1477.

244. Staniforth DH. Comparison of orocaecal transit times assessed by the lactulose/breath hydrogen and the sulphasalazine/sulphapyridine methods. *Gut* 1989; 30: 978–982.

245. Raimundo A *et al.* Gastrointestinal pH profiles in ulcerative colitis. *Gastroenterology* 1992; 4: A681.

246. Nugent SG *et al.* Intestinal luminal pH in inflammatory bowel disease: possible determinants and implications for therapy with aminosalicylates and other drugs. *Gut* 2001; 48: 571–577.

247. Raimundo AH *et al.* Effects of olsalazine and sulphasalazine on jejunal and ileal water and electrolyte absorption in normal human subjects. *Gut* 1991; 32: 270–274.

248. Sandberg-Gertzén H *et al.* Azodisal sodium in the treatment of ulcerative colitis. A study of tolerance and relapse-prevention properties. *Gastroenterology* 1986; 90: 1024–1030.

249. Zimmerman J. Drug interactions in intestinal transport of folic acid and methotrexate. Further evidence for the heterogeneity of folate transport in the human small intestine. *Biochem Pharmacol* 1992; 44: 1839–1842.

250. Okada M *et al.* Drug interaction between methotrexate and salazosulfapyridine in Japanese patients with rheumatoid arthritis. *J Pharm Health Care Sci* 2017; 3: 7.

251. Kanerud L *et al.* Effect of sulphasalazine on gastrointestinal microflora and on mucosal heat shock protein expression in patients with rheumatoid arthritis. *Br J Rheumatol* 1994; 33: 1039–1048.

252. Neumann VC *et al.* Effects of sulphasalazine on faecal flora in patients with rheumatoid arthritis: a comparison with penicillamine. *Br J Rheumatol* 1987; 26: 334–337.

253. Bradley SM *et al.* Sequential study of bacterial antibody levels and faecal flora in rheumatoid arthritis patients taking sulphasalazine. *Br J Rheumatol* 1993; 32: 683–688.

254. Xue L *et al.* The possible effects of mesalazine on the intestinal microbiota. *Aliment Pharmacol Ther* 2012; 36: 813–814.

255. Andrews CN *et al.* Mesalazine (5-aminosalicylic acid) alters faecal bacterial profiles, but not mucosal proteolytic activity in diarrhoea-predominant irritable bowel syndrome. *Aliment Pharmacol Ther* 2011; 34: 374–383.

256. Juhl RP *et al.* Effect of sulfasalazine on digoxin bioavailability. *Clin Pharmacol Ther* 1976; 20: 387–394.

257. Marcus FI. Pharmacokinetic interactions between digoxin and other drugs. *J Am Coll Cardiol* 1985; 5(5 Suppl A): 82A–90A.

258. Haiser HJ *et al.* Mechanistic insight into digoxin inactivation by *Eggerthella lenta* augments our understanding of its pharmacokinetics. *Gut Microbes* 2014; 5: 233–238.

259. Du Cheyron D *et al.* Effect of sulfasalazine on cyclosporin blood concentration. *Eur J Clin Pharmacol* 1999; 55: 227–228.

260. Lewis LD *et al.* Olsalazine and 6-mercaptopurine-related bone marrow suppression: a possible drug-drug interaction. *Clin Pharmacol Ther* 1997; 62: 464–475.

261. Lowry PW *et al.* Balsalazide and azathiprine or 6-mercaptopurine: evidence for a potentially serious drug interaction. *Gastroenterology* 1999; 116: 1505–1506.

262. Bengmark S, Jeppsson B. Gastrointestinal surface protection and mucosa reconditioning. *JPEN J Parenter Enteral Nutr* 1995; 19: 410–415.

263. Narum S *et al.* Corticosteroids and risk of gastrointestinal bleeding: a systematic review and meta-analysis. *BMJ Open* 2014; 4: e004587.

264. Jung D *et al.* Human ileal bile acid transporter gene ASBT (SLC10A2) is transactivated by the glucocorticoid receptor. *Gut* 2004; 53: 78–84.

265. Bajor A *et al.* Budesonide treatment is associated with increased bile acid

absorption in collagenous colitis. *Aliment Pharmacol Ther* 2006; 24: 1643–1649.

266. Fleisher D *et al.* Drug, meal and formulation interactions influencing drug absorption after oral administration. *Clin Pharmacokinet* 1999; 36: 233–254.

267. Dilger K *et al.* Identification of budesonide and prednisone as substrates of the intestinal drug efflux pump P-glycoprotein. *Inflamm Bowel Dis* 2004; 10: 578–583.

268. Schwab M, Klotz U. Pharmacokinetic considerations in the treatment of inflammatory bowel disease. *Clin Pharmacokinet* 2001; 40: 723–751.

269. Eradiri O *et al.* Interaction of metronidazole with phenobarbital, cimetidine, prednisone, and sulfasalazine in Crohn's disease. *Biopharm Drug Dispos* 1988; 9: 219–227.

270. Koren G *et al.* Corticosteroids-salicylate interaction in a case of juvenile rheumatoid arthritis. *Ther Drug Monit* 1987; 9: 177–179.

271. Seidegård J. Reduction of the inhibitory effect of ketoconazole on budesonide pharmacokinetics by separation of their time of administration. *Clin Pharmacol Ther* 2000; 68: 13–17.

272. Raaska K *et al.* Plasma concentrations of inhaled budesonide and its effects on plasma cortisol are increased by the cytochrome P4503A4 inhibitor itraconazole. *Clin Pharmacol Ther* 2002; 72: 362–369.

273. De Wachter E *et al.* Inhaled budesonide induced Cushing's syndrome in cystic fibrosis patients, due to drug inhibition of cytochrome P450. *J Cyst Fibros* 2003; 2: 72–75.

274. Gray D *et al.* Adrenal suppression and Cushing's syndrome secondary to ritonavir and budesonide. *S Afr Med J* 2010; 100: 296.

275. Orlicka K *et al.* Prevention of infection caused by immunosuppressive drugs in gastroenterology. *Ther Adv Chronic Dis* 2013; 4: 167–185.

276. Zenlea T, Peppercorn MA. Immunosuppressive therapies for inflammatory bowel disease. *World J Gastroenterol* 2014; 20: 3146–3152.

277. Teixeira Mdo CB *et al.* Influence of post-transplant immunosuppressive therapy on gastrointestinal transit using biomagnetic method: a pilot study. *Dig Dis Sci* 2015; 60: 174–180.

278. Gabe SM *et al.* The effect of tacrolimus (FK506) on intestinal barrier function and cellular energy production in humans. *Gastroenterology* 1998; 115: 67–74.

279. Parrilli G *et al.* Effect of chronic administration of tacrolimus and cyclosporine on human gastrointestinal permeability. *Liver Transpl* 2003; 9: 484–488.

280. Helderman JH, Goral S. Gastrointestinal complications of transplant immunosuppression. *J Am Soc Nephrol* 2002; 13: 277–287.

281. Deeming GMJ *et al.* Methotrexate and oral ulceration. *Br Dent J* 2005; 198: 83–85.

282. Kalantzis A *et al.* Oral effects of low-dose methotrexate treatment. *Oral Surg Oral Med Oral Pathol Oral Radiol Endod* 2005; 100: 52–62.

283. Troeltzsch M *et al.* Oral mucositis in patients receiving low-dose methotrexate therapy for rheumatoid arthritis: report of 2 cases and literature review. *Oral Surg Oral Med Oral Pathol Oral Radiol* 2013; 115: e28–e33.

284. Fijlstra M *et al.* Reduced absorption of long-chain fatty acids during methotrexate-induced gastrointestinal mucositis in the rat. *Clin Nutr* 2013; 32: 452–459.

285. Chun JY *et al.* Adverse events associated with azathioprine treatment in Korean pediatric inflammatory bowel disease patients. *Pediatr Gastroenterol Hepatol Nutr* 2013; 16: 171.

286. Mogensen S *et al.* Absorption of bupivacaine after administration of a lozenge as topical treatment for pain from oral mucositis. *Basic Clin Pharmacol Toxicol* 2017; 120: 71–78.

287. Parikh N *et al.* A single-dose pharmacokinetic study of fentanyl sublingual spray in cancer patients with and without oral mucositis. *J Pain* 2013; 14: S73.

288. Amundsen R *et al.* Cyclosporine A-and tacrolimus-mediated inhibition of CYP3A4 and CYP3A5 in vitro. *Drug Metab Dispos* 2012; 40: 655–661.

289. Moes DJAR *et al.* Sirolimus and everolimus in kidney transplantation. *Drug Discov Today* 2015; 20: 1243–1249.

290. Finch A, Pillans P. P-glycoprotein and its role in drug-drug interactions. *Aust Prescr* 2014; 37: 137–139.

291. Rebello S *et al.* Effect of cyclosporine on the pharmacokinetics of aliskiren in healthy subjects. *J Clin Pharmacol* 2011; 51: 1549–1560.

292. Rushing DA *et al.* The effects of cyclosporine on the pharmacokinetics of doxorubicin in patients with small cell lung cancer. *Cancer* 1994; 74: 834–841.

293. Eising EG *et al.* Does the multidrug-resistance modulator cyclosporin A increase the cardiotoxicity of high-dose anthracycline chemotherapy? *Acta Oncol* 1997; 36: 735–740.

294. Galetin A *et al.* Maximal inhibition of intestinal first-pass metabolism as a pragmatic indicator of intestinal contribution to the drug-drug interactions for CYP3A4 cleared drugs. *Curr Drug Metab* 2007; 8: 685–693.

295. Yee GC, McGuire TR. Pharmacokinetic drug interactions with cyclosporin (Part II). *Clin Pharmacokinet* 1990; 19: 400–415.

296. Yee GC, McGuire TR. Pharmacokinetic drug interactions with cyclosporin (Part I). *Clin Pharmacokinet* 1990; 19: 319–332.

297. Vermeire S *et al.* Effectiveness of concomitant immunosuppressive therapy in suppressing the formation of antibodies to infliximab in Crohn's disease. *Gut* 2007; 56: 1226–1231.

298. Maini RN *et al.* Therapeutic efficacy of multiple intravenous infusions of anti-tumor necrosis factor? Monoclonal antibody combined with low-dose weekly methotrexate in rheumatoid arthritis. *Arthritis Rheum* 1998; 41: 1552–1563.

299. Havrda DE *et al.* A case report of warfarin resistance due to azathioprine and review of the literature. *Pharmacotherapy* 2001; 21: 355–357.

300. Joo Ng H, Crowther MA. Azathioprine and inhibition of the anticoagulant effect of warfarin: evidence from a case report and a literature review. *Am J Geriatr Pharmacother* 2006; 4: 75–77.

301. Vazquez SR *et al.* Azathioprine-induced warfarin resistance. *Ann Pharmacother* 2008; 42: 1118–1123.

302. Scaldaferri F *et al.* Use and indications of cholestyramine and bile acid sequestrants. *Intern Emerg Med* 2013; 8: 205–210.

303. Joint Formulary Committee. Colestyramine. In: *Joint Formulary Committee.* British National Formulary London: BMJ Group and Pharmaceutical Press [online] 2017. Available at: https://bnf.nice.org.uk/drug/colestyramine.html. Accessed June 26, 2017.

304. Bile acid malabsorption: colesevelam | Guidance and guidelines | NICE. Available at: https://www.nice.org.uk/advice/esuom22/chapter/Key-points-from-the-evidence. Accessed September 28, 2017.

305. Wedlake L *et al.* Effectiveness and tolerability of colesevelam hydrochloride for bile-acid malabsorption in patients with cancer: a retrospective chart review and patient questionnaire. *Clin Ther* 2009; 31: 2549–2558.

306. Odunsi-Shiyanbade ST *et al.* Effects of chenodeoxycholate and a bile acid sequestrant, colesevelam, on intestinal transit and bowel function. *Clin Gastroenterol Hepatol* 2010; 8: 159–165.e5.

307. Darkoh C *et al.* Bile acids improve the antimicrobial effect of rifaximin. *Antimicrob Agents Chemother* 2010; 54: 3618–3624.

308. Young MA *et al.* Concomitant administration of cholestyramine influences the absorption of troglitazone. *Br J Clin Pharmacol* 1998; 45: 37–40.

309. Neuvonen PJ *et al.* Effects of resins and activated charcoal on the absorption of digoxin, carbamazepine and frusemide. *Br J Clin Pharmacol* 1988; 25: 229–233.

310. Jähnchen E *et al.* Enhanced elimination of warfarin during treatment with cholestyramine. *Br J Clin Pharmacol* 1978; 5: 437–440.

311. Meinertz T *et al.* Interruption of the enterohepatic circulation of phenprocoumon by cholestyramine. *Clin Pharmacol Ther* 1977; 21: 731–735.

312. Balmelli N *et al.* Fatal drug interaction between cholestyramine and phenprocoumon. *Eur J Intern Med* 2002; 13: 210–211.

313. Malloy MJ *et al.* Influence of cholestyramine resin administration on single dose sulindac pharmacokinetics. *Int J Clin Pharmacol Ther* 1994; 32: 286–289.

314. Mück W *et al.* Influence of cholestyramine on the pharmacokinetics of cerivastatin. *Int J Clin Pharmacol Ther* 1997; 35: 250–254.

315. Kaykhaei MA *et al.* Low doses of cholestyramine in the treatment of hyperthyroidism. *Endocrine* 2008; 34: 52–55.

316. Kivistö KT, Neuvonen PJ. The effect of cholestyramine and activated charcoal on glipizide absorption. *Br J Clin Pharmacol* 1990; 30: 733–736.

317. Bullingham RES *et al.* Clinical pharmacokinetics of mycophenolate mofetil. *Clin Pharmacokinet* 1998; 34: 429–455.

318. West RJ, Lloyd JK. The effect of cholestyramine on intestinal absorption. *Gut* 1975; 16: 93–98.

319. Malloy MJ *et al.* Effect of cholestyramine resin on single dose valproate pharmacokinetics. *Int J Clin Pharmacol Ther* 1996; 34: 208–211.

320. Zhu XX *et al.* Bile salt anion sorption by polymeric resins: comparison of a functionalized polyacrylamide resin with cholestyramine. *J Colloid Interface Sci* 2000; 232: 282–288.

321. He L *et al.* Lack of effect of colesevelam HCl on the single-dose pharmacokinetics of aspirin, atenolol, enalapril, phenytoin, rosiglitazone, and sitagliptin. *Diabetes Res Clin Pract* 2014; 104: 401–409.

322. al-Meshal MA *et al.* The effect of colestipol and cholestyramine on ibuprofen bioavailability in man. *Biopharm Drug Dispos* 1994; 15: 463–471.

323. al-Balla SR *et al.* The effects of cholestyramine and colestipol on the absorption of diclofenac in man. *Int J Clin Pharmacol Ther* 1994; 32: 441–445.

324. Weaver R, Jochemsen R. Nonclinical pharmacokinetics and toxicokinetics. In: Cartwright AC, Matthews BR, eds. *International Pharmaceutical Product Registration*, 2nd edn. Boca Raton, FL: CRC Press, 2009: 336–376.

325. Caldwell JH, Greenberger NJ. Interruption of the enterohepatic circulation of digitoxin by cholestyramine. *J Clin Invest* 1971; 50: 2626–2637.

326. Malik MY *et al.* Role of enterohepatic recirculation in drug disposition: cooperation and complications. *Drug Metab Rev* 2016; 48: 281–327.

327. Stotzer P-O *et al.* Effect of cholestyramine on gastrointestinal transit in patients with idiopathic bile acid diarrhea: a prospective, open-label study. *Neuroenterology* 2013; 2: 5.

328. Donovan JM *et al.* Drug interactions with colesevelam hydrochloride, a novel, potent lipid-lowering agent. *Cardiovasc Drugs Ther* 2000; 14: 681–690.

329. Sinha V *et al.* Physiologically based pharmacokinetic modeling: from regulatory science to regulator policy. *Clin Pharmacol Ther* 2014; 95: 478–480.

330. Kesisoglou F *et al.* Physiologically based absorption modeling to impact biopharmaceutics and formulation strategies in drug development—industry case studies. *J Pharm Sci* 2016; 105: 2723–2734.

331. Duan P *et al.* Physiologically based pharmacokinetic (PBPK) modeling of pitavastatin and atorvastatin to predict drug-drug interactions (DDIs). *Eur J Drug Metab Pharmacokinet* 2017; 42: 689–705.

332. Chen Y *et al.* Development of a physiologically based pharmacokinetic model for itraconazole pharmacokinetics and drug-drug interaction prediction. *Clin Pharmacokinet* 2016; 55: 735–749.

333. Min JS *et al.* Application of physiologically based pharmacokinetic modeling in predicting drug-drug interactions for sarpogrelate hydrochloride in humans. *Drug Des Devel Ther* 2016; 10: 2959–2972.

334. Grillo JA *et al.* Utility of a physiologically-based pharmacokinetic (PBPK) modeling approach to quantitatively predict a complex drug-drug-disease interaction scenario for rivaroxaban during the drug review process: implications for clinical practice. *Biopharm Drug Dispos* 2012; 33: 99–110.

335. Mitra A *et al.* Using absorption simulation and gastric pH modulated dog model for formulation development to overcome achlorhydria effect. *Mol Pharm* 2011; 8: 2216–2223.

336. Qi F *et al.* Influence of different proton pump inhibitors on the pharmacokinetics of voriconazole. *Int J Antimicrob Agents* 2017; 49: 403–409.

337. Cristofoletti R *et al.* Assessment of bioequivalence of weak base formulations under various dosing conditions using physiologically based pharmacokinetic simulations in virtual populations. Case examples: ketoconazole and posaconazole. *J Pharm Sci* 2017; 106: 560–569.

338. Doki K *et al.* Virtual bioequivalence for achlorhydric subjects: the use of PBPK modelling to assess the formulation-dependent effect of achlorhydria. *Eur J Pharm Sci* 2017; 109: 111–120.

339. Establishing bioequivalence in virtual space: are we really there? | AAPS Blog. Available at: https://aapsblog.aaps.org/2016/09/29/establishing-bioequivalence-in-virtual-space-are-we-really-there/. Accessed January 25, 2018.

340. Litou C *et al.* The impact of reduced gastric acid secretion on dissolution of salts of weak bases in the fasted upper gastrointestinal lumen: data in biorelevant media and in human aspirates. *Eur J Pharm Biopharm* 2017; 115: 94–101.

341. Lee HT *et al.* Effect of prokinetic agents, cisapride and metoclopramide, on the bioavailability in humans and intestinal permeability in rats of ranitidine, and intestinal charcoal transit in rats. *Res Commun Mol Pathol Pharmacol* 2000; 108: 311–323.

342. Bustos D *et al.* Effect of loperamide and bisacodyl on intestinal transit time, fecal weight and short chain fatty acid excretion in the rat. *Acta Gastroenterol Latinoam* 1991; 21: 3–9.

343. Joo JS *et al.* Alterations in colonic anatomy induced by chronic stimulant laxatives: the cathartic colon revisited. *J Clin Gastroenterol* 1998; 26: 283–286.

Measuring pH and Buffer Capacity in Fluids Aspirated from the Fasted Upper Gastrointestinal Tract of Healthy Adults

Chara Litou[1] • Dimitrios Psachoulias[2,3] • Maria Vertzoni[2] • Jennifer Dressman[1,4] • Christos Reppas[2] iD

ABSTRACT

Purpose The design of biorelevant conditions for *in vitro* evaluation of orally administered drug products is contingent on obtaining accurate values for physiologically relevant parameters such as pH, buffer capacity and bile salt concentrations in upper gastrointestinal fluids.

Methods The impact of sample handling on the measurement of pH and buffer capacity of aspirates from the upper gastrointestinal tract was evaluated, with a focus on centrifugation and freeze-thaw cycling as factors that can influence results. Since bicarbonate is a key buffer system in the fasted state and is used to represent conditions in the upper intestine *in vitro*, variations on sample handling were also investigated for bicarbonate-based buffers prepared in the laboratory.

Results Centrifugation and freezing significantly increase pH and decrease buffer capacity in samples obtained by aspiration from the upper gastrointestinal tract in the fasted state and in bicarbonate buffers prepared *in vitro*. Comparison of data suggested that the buffer system in the small intestine does not derive exclusively from bicarbonates.

Conclusions Measurement of both pH and buffer capacity immediately after aspiration are strongly recommended as "best practice" and should be adopted as the standard procedure for measuring pH and buffer capacity in aspirates from the gastrointestinal tract. Only data obtained in this way provide a valid basis for setting the physiological parameters in physiologically based pharmacokinetic models.

KEYWORDS Bicarbonates · buffer capacity · human intestinal fluid · pH · small intestine · stomach

INTRODUCTION

The design of biorelevant conditions for the *in vitro* evaluation of orally administered drug products is contingent on obtaining accurate values for physiologically relevant parameters such as pH, buffer capacity and bile salt concentrations. For this purpose, samples are often aspirated from the upper gastrointestinal (GI) tract. As values that have been reported for these parameters differ substantially among studies reported in the literature, the question arises as to whether the results may be influenced by the methodology used to collect and process the samples. If so, the aspiration study design needs to be harmonized to "best practices" in order to assure that meaningful and comparable results are reported. While Fuchs and Dressman [1] have discussed in general how various aspects of sampling can affect results (e.g. pooling of aspirates, location of aspiration etc.), in this study we focus specifically on the question of how sample handling procedures can influence pH and buffer capacity measurements in aspirates collected in the upper GI tract.

The buffer capacity of GI fluids, i.e. their resistance to change in pH, can be important to the *in vivo* dissolution of ionizable active pharmaceutical ingredients (APIs) and the

✉ Jennifer Dressman
dressman@em.uni-frankfurt.de

✉ Christos Reppas
reppas@pharm.uoa.gr

1 Institute of Pharmaceutical Technology, Biocenter, Johann Wolfgang Goethe University, Max von Laue St. 9, 60438 Frankfurt am Main, Germany

2 Department of Pharmacy, School of Health Sciences, National and Kapodistrian University of Athens, Panepistimiopolis, 157 84 Zografou, Greece

3 Present address: Drug Products and MDD III, Lavipharm S.A., Athens, Greece

4 Fraunhofer IME, Theodor Stern Kai 7, 60590 Frankfurt am Main, Germany

 Springer

release of APIs from pharmaceutical products with pH-dependent release mechanisms (2–4). The buffer capacity of GI fluids is determined by the physiological pH-regulating agents that are present in the region of interest as well as any food and drink that is ingested by the patient. Further, the impact of the transfer of gastric contents to the small intestine and the contribution of various protein-based pancreatic secretions to the buffer capacity of the fluids in the upper intestine should be taken into consideration.

The intragastric pH in fasted, healthy adults is mainly regulated by the concentration of hydrochloric acid. Using perfusion techniques, hydrogen ion concentrations have been measured to range from 56 to 160 mM (5–8). There is also a potential contribution of pepsin, lipase, or other protein-based components to the buffer capacity of bulk gastric contents. Under conditions of reduced gastric acid secretion there may also be some contribution from bicarbonate ions. Bicarbonate concentrations in the acid-suppressed stomach using the carbon dioxide partial pressure and pH (pCO_2/pH) method (which is based on the Henderson-Hasselbalch equation and in which the total concentration of bicarbonates is considered to be the sum of carbon dioxide and free bicarbonates) have been reported to range from 1 to 20 mM (9,10).

In the fasted small intestine, on the other hand, the pH is considered to be mainly controlled by bicarbonates, which are secreted by the pancreas and the enterocytes and are also present in the bile (11–14). Using the pCO_2/pH method, the bicarbonate concentration in the upper intestine (duodenum and jejunum) of fasted adults has been measured to range between 2 and 20 mM, and the influx of hydrochloric acid into the upper small intestine has been shown to result in a significant increase in bicarbonate secretion rates (6,15–18). Here it should be mentioned that pCO_2/pH measurements have been criticized as sometimes leading to an underestimation of bicarbonate concentration (19), in which case values at the upper end of the reported ranges for the stomach and upper intestine are likely to be closer to the true intraluminal values.

The buffer capacity of the GI contents can be estimated by aspirating the luminal contents from the region of interest and titrating the sample with a strong acid or base. Handling of aspirates and any storage prior to titration appear to have an impact on the measured value, since both sample handling techniques and reported values for pH and buffer capacity vary widely among studies. It has been reported that the pH of samples aspirated from the upper intestine drifts to higher values when the samples remain on the bench at room temperature (20). The authors attributed the drift to the transformation of bicarbonates to carbon dioxide (20). Moreover, Litou et al. demonstrated that subjecting the samples to a freeze-thaw cycle significantly reduces the measured buffer capacity values in both the stomach and in the upper intestine (21).

To resolve the various issues described above and thus assist in achieving a standardized methodology for sample handling of GI aspirates, this study had three specific objectives: First, to investigate the impact of sample handling on values of pH and buffer capacity measured in gastric and intestinal aspirates. In several studies reported in the literature, the pH and buffer capacity values were determined after centrifugation of the aspirated samples and/or after subjecting the aspirates to a freeze-thaw cycle (22–26), while in others these measurements were made immediately after obtaining the sample (20,21). Second, to evaluate the impact of drug administration on buffer capacity via locally and/or systemically mediated mechanisms, based on literature data (21,23). Third, to compare the impact of freeze-thaw cycling and centrifugation on the pH and buffer capacity of bicarbonate solutions prepared in the laboratory with the impact of these sample handling procedures on aspirated samples.

METHODS

Data from Published Human Intubation Studies that Were Considered in the Present Work

For each clinical study published to date, the protocol as well as the aspirate collection and handling procedures prior to the *ex vivo* measurements are summarized in Table I. In this work, data from the studies of Litou et al. (21), Pedersen et al. (24), Kalantzi et al. (20) and Persson et al. (26) were used to evaluate the impact of a freeze-thaw cycle on the buffer capacity values in gastric aspirates and in aspirates from the upper small intestine. In all these studies, the adult volunteers were healthy, had fasted overnight prior to the study day and had received no treatment prior to the aspirations. In each of these studies the buffer capacity was measured with NaOH in gastric aspirates and with HCl in aspirates from the upper small intestine. In the study by Kalantzi et al. (20) 10 mg/mL PEG 4000 was used as a non-absorbable marker. Data from the studies of Kalantzi et al. and Litou et al. were reported as individual values (20,21). Data from the study of Pedersen et al. (24) were reported as mean (SD) values, resulting from six measurements in one pooled sample of gastric contents aspirated from three healthy volunteers, whereas data from the study of Persson et al. (26) were reported as a single value corresponding to one pooled sample of intestinal fluids aspirated from six healthy volunteers.

Individual data from the study of Litou et al. (21) were used to evaluate the impact of a freeze-thaw cycle on the estimated buffer capacity values in the stomach after treatment with famotidine to elevate the gastric pH. In that study the adult volunteers were healthy, had fasted overnight prior to the study day, and had received a treatment with famotidine prior to aspiration. In this case, the buffer capacity in the stomach

Table I Published Median pH and Average Buffer Capacity Values for the Gastric Contents and the Contents of Upper Intestine of Fasted Adults, Clinical Study Protocols and Aspirate Storage Conditions and Handling Procedures

	H$_2$O volume (mL)	Drug pretreatment	Sample handling				Time of sample aspiration after water administration (min)	Median/Mean pH (range/±SD)*	Average buffer capacity (±SD) (mmol/L/ΔpH)	Titrant	Reference
			Immediate measurement	Pooling	Centrifugation	Freezing					
Stomach	250	800 mg ibuprofen			✓	✓	0–420	2.6 (1.8–3.7)	4.7 (1.3)	NaOH	(23)
	240	–	✓				10	2.7 (1.9–3.9)	4.7 (4.6)	NaOH	(21)
							20	1.7 (1.3–2.0)	21.3 (11.4)		
							35	1.6 (1.1–2.4)	27.6 (15.7)		
	240	40 mg famotidine	✓				10	7.2 (6.9–7.3)	0.5 (0.2)	NaOH	(21)
							20	7.1 (6.0–7.2)	0.7 (0.2)		
							35	7.1 (4.7–7.3)	1.3 (0.7)		
	–	–		✓		✓	N/A	2.5 (1.40)	14.3 (9.5)	NaOH	(24)
	250	–	✓				20	2.4	7.0	NaOH	(20)
							40–60	1.7	18.0		
Duodenum	250	800 mg ibuprofen			✓	✓	0–420	5.1 (4.5–5.8)	1.4 (0.4)	HCl	(23)
	240	–	✓				5	6.8 (6.4–7.2)	8.4 (2.9)	HCl	(21)
							15	6.2 (2.3–7.1)	19.2 (33.7)		
							30	6.3 (3.0–7.0)	9.0 (3.8)		
							50	6.5 (2.7–7.7)	14.2 (10.5)		
	240	40 mg famotidine	✓				5	7.2 (7.1–7.6)	6.1 (0.8)	HCl	(21)
							15	7.2 (7.0–7.7)	9.0 (3.8)		
							30	7.1 (6.6–8.4)	7.7 (2.8)		
							50	7.3 (6.2–8.0)	6.9 (2.7)		
Jejunum	N/A	–		✓		✓	N/A	N/A	4.0–13.0 (range)	N/A	(22)
	250	–	✓				30	6.2	5.60	HCl	(20)
	250	800 mg ibuprofen			✓	✓	0–420	5.6 (4.9–6.1)	0.8 (0.3)	HCl	(23)
	N/A	N/A	N/A	N/A	N/A	N/A	N/A	N/A	4.0	N/A	(28)
	N/A	–	✓	✓		✓	N/A	7.1 (0.5)	3.2 (1.3)	HCl	(25)
	–	–		✓		✓	0–150	7.5	2.4	HCl	(26)
	–	–		✓		✓	0–150	7.5	2.8	NaOH	(26)

N/A: not available

*In the Hens et al. (23), Litou et al. (21), Pedersen et al. (24) and Kalantzi et al. (20) studies pH was measured immediately upon aspiration. In the studies of Persson et al. (26) and Fadda et al. (25) the exact timepoint of the measurement of the pH is not specified

was estimated immediately upon aspiration by titrating with NaOH and additionally after one freeze-thaw cycle by titrating with NaOH and by titrating with HCl (i.e. in both directions).

Data from the study of Hens *et al.* (23) were used to evaluate the impact of administration of ibuprofen (a weak acid), prior to initiation of aspiration, on the pH and buffer capacity in the stomach and upper small intestine. In that study aspirates collected from another study by the same group were used (27). In the Koeningsknecht *et al.* study (27) the healthy adult volunteers fasted overnight prior to the study day and received 800 mg ibuprofen prior to aspiration. 25 mg of phenol red was used as a non-absorbable marker. Buffer capacity was measured with NaOH in aspirates collected from the stomach and with HCl in aspirates collected from the upper intestine, after centrifuging at 21000 g for 5 min and then freezing the samples at −80°C. At an undisclosed time-point during the sample handling and the buffer capacity measurement, pure mineral oil was added to the sample. In the Hens *et al.* study the mean buffer capacity and pH values were reported at each aspiration time. Relevant data from this study were digitalized from the published figures using WebPlotDigitizer (v. 4.0, Texas, USA).

Bergström *et al.* reported a median value for jejunal buffer capacity, but provided no information about either the protocol of the clinical study or of the sample handling procedures (28). Perez de la Cruz Moreno *et al.* did not clarify whether the titrations were performed with NaOH or HCl (22). Fadda *et al.* did not clarify which samples were measured immediately upon aspiration and which after freezing and thawing (25). Therefore, data from those three studies could not be used in the present analysis.

Pairwise statistical comparisons were performed in all cases using parametric or distribution-free tests, depending on the results of the normality and equal variance tests, using SigmaPlot 11.0 (Systat Software Inc. Chicago, IL, USA) and setting the Type I error at 0.05.

Impact of Centrifugation on the pH of Aspirates from the Fasted Upper Small Intestine

In a further study (29), eight successive aspirates were collected from the upper intestine of a fasted volunteer between 5 and 70 min after administration of 30 mg dipyridamole as an aqueous solution. The aspirates were centrifuged at 37°C for 10 min and 12,560 g immediately after aspiration, and the pH after centrifugation was compared with the pH measured immediately upon aspiration. On a separate occasion, eight successive aspirates were collected over 5–70 min from the same volunteer after administration of 90 mg dipyridamole as an aqueous solution. These samples were placed in centrifuge vials, which were immediately sealed and then centrifuged at 37°C for 10 min and 12,560 g: here, too, the

pH values after centrifugation were compared with the pH measured immediately upon aspiration. The comparative data are presented in this work for the first time. The differences between the pH values before and after centrifugation were evaluated using either the paired t-test or Wilcoxon Signed-Rank test, depending on the results of normality and equal variances testing, with the Type I error set at 0.05. The statistical analysis of the data was performed using the SigmaPlot 11.0 software (Systat Software Inc., Chicago, IL, USA).

Titration Methodologies for Determining Buffer Capacity

In all studies identified in the literature the buffer capacity of samples aspirated from the stomach was determined by titration with NaOH. In the case of samples aspirated from the upper small intestine, most published buffer capacity values were determined by titration with hydrochloric acid. It should be noted that the contents of the upper intestine are more resistant to a decrease in pH value when a strong acid is added than to an increase in pH when an equivalent molar amount of a strong base is added (21,26).

In Vitro **Experiments with Bicarbonate Solutions**

Bicarbonate buffers of 10, 20, 30, 50 and 100 mM were prepared using the appropriate amount of sodium hydrogen carbonate (Alfa Aesar, LOT: Z07C065, ThermoFisher GmBH, Kandel, Germany) and adjusting the final pH of the buffer to 6.5 with HCl with the aid of a pH electrode (pHenomenal®, VWR Int. Leuven, Belgium). Buffer capacity measurements were performed by dropwise addition of HCl after various storage conditions and sample handling procedures, as follows:

a) immediately upon buffer preparation,
b) after freezing the sample in a sealed vial (−20°C, 10 d),
c) after centrifuging (20°C, 21000 g, 5 min) and freezing the sample in a sealed vial (−20°C, 10 d), and
d) after leaving the sample in a sealed vial on the bench for 4 or for 24 h.

Frozen samples were allowed to thaw on the bench at room temperature for about 1 h before measuring the pH and buffer capacity. Experiments were performed at least in triplicate. The statistical evaluation of differences was performed with one-way ANOVA or the Kruskal-Wallis test, depending on the results of normality and equal variance testing, and post hoc comparisons were carried out using the Tukey test (SigmaPlot 11.0, Systat Software Inc., Chicago, IL, USA). The Type I error was set at 0.05 in all cases.

RESULTS

The impact of Sample Handling on pH and Buffer Capacity of Aspirates from the Upper Gastrointestinal Tract of Healthy Adult Volunteers in the Fasted State

Gastric Aspirates

For aspirates collected from the fasted healthy adult stomach (20,21,24), measurements immediately after aspiration or after one freeze-thaw cycle indicate that the pH is not significantly different (pH 1.73, $n = 60$ (20,21) *vs.* pH 1.92, $n = 16$ (21,24), Mann-Whitney, $p = 0.078$). There appears to be a relation between the buffer capacity and gastric pH (Fig. 1). As can be observed from the insert graphs in Fig. 1, there is a linear correlation between the measured buffer capacity value and the hydrogen ion concentration (calculated according to the measured pH value), independent of whether the measurement was performed immediately after aspiration ($R^2 = 0.85$) or after one freeze-thaw cycle ($R^2 = 0.82$). The outlying datum for buffer capacity after one freeze-thaw cycle (Fig. 1b) from the study of Pedersen *et al.* (24) could be related to the fact that no water was administered in that study prior to aspiration, unlike in the studies by Kalantzi *et al.* (20) and Litou *et al.* (21), in which 240 mL of water had been administered prior to aspiration (see Table I).

The median buffer capacity of gastric fluids measured immediately upon aspiration (17.4 mmol/L/ΔpH, $n = 60$ (20,21)) was far higher than after one freeze-thaw cycle (6.6 mmol/L/ΔpH, $n = 16$ (21,24); Mann-Whitney, $p = 0.007$).

Data measured in aspirates collected from the stomach after pretreatment with famotidine indicated that one freeze-thaw cycle did not affect the pH significantly (paired t-test, $p = 0.301$). The absence of a clear relationship between pH and buffer capacity in this case can be attributed to the lack of HCl and the presence of other components in the gastric aspirates (Fig. 2) (30–32).

The mean buffer capacity of gastric fluids after treatment with famotidine was significantly higher when measured immediately after aspiration (0.62 mmol/L/ΔpH), than after one freeze-thaw cycle (0.21 mmol/L/ΔpH; paired t-test, $n = 16$, $p < 0.001$).

Intestinal Aspirates

When vials containing aspirates from the fasted upper small intestine were not sealed prior to centrifugation, the centrifugation procedure (37°C, 12560 g, 10 min) increased the median (range) pH values significantly from 6.11 (2.67–6.74) to 6.70 (2.67–7.29) ($p = 0.008$) (29). When the vials were sealed prior to centrifugation, the effect was reduced, with the pH rising from 5.84 (4.38–7.03) to 5.89 (4.38–7.48), but still statistically significant ($p = 0.031$) (29).
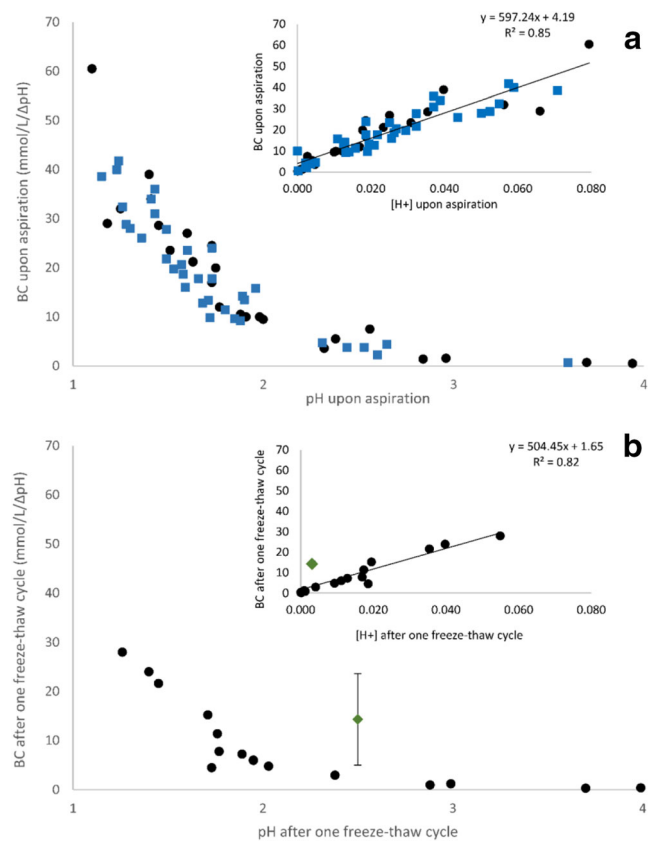

Fig. 1 Data on the buffer capacity of gastric contents in fasted healthy adults *vs.* the corresponding pH values previously published by Litou *et al.* (21) (● , individual data), by Kalantzi *et al.* (20) (■, individual data), and by Pedersen *et al.* (24) (◆, mean ± SD data). (**a**) Data measured immediately upon aspiration; (**b**) data measured after one freeze-thaw cycle. The inserts in the Figure represent the linear relationship between the buffer capacity, measured immediately upon aspiration or after one freeze-thaw cycle, with the concentration of hydrogen ions.

pH values of aspirates from upper intestine were not significantly affected by one freeze-thaw cycle (6.35, $n = 47$ *vs* 6.86, $n = 18$, Mann-Whitney, $p = 0.168$) (20,21,26). The median buffer capacity measured immediately upon aspiration (7.0 mmol/L/ΔpH, $n = 45$ (20,21)) was significantly higher than that after one freeze-thaw cycle (4.8 mmol/L/ΔpH, $n = 17$ (21,26)) (Mann-Whitney, $p = 0.019$) (Fig. 3).

The Impact of Ibuprofen on the pH and Buffer Capacity in Aspirates from the Upper Gastrointestinal Tract of Healthy Adult Volunteers in the Fasted State

Gastric Aspirates

Gastric pH value was significantly different after administration of 800 mg ibuprofen; median pH values were 1.73 ($n = 60$) (20,21) measured immediately upon aspiration without prior drug administration compared with pH 2.63 ($n = 13$) (23)
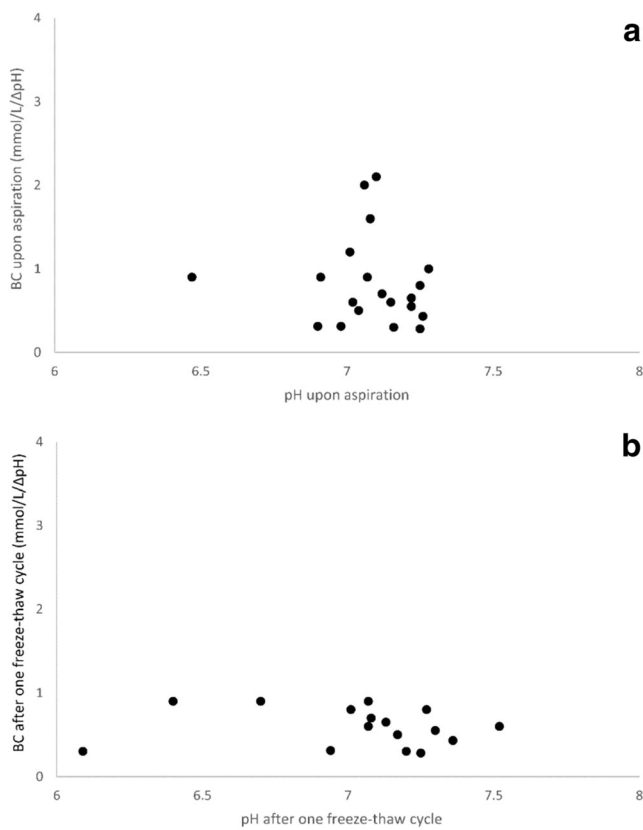
Fig. 2 Data on the buffer capacity of gastric contents of fasted healthy adults after pretreatment with famotidine *vs.* the corresponding pH values previously published by Litou *et al.* (21) (**a**) data measured immediately upon aspiration; (**b**) data measured after one freeze-thaw cycle.

Fig. 3 Data on the buffer capacity of contents of upper intestine of fasted healthy adults *vs.* the corresponding pH values published previously by Litou *et al.* (21) (●), by Kalantzi *et al.* (20) (■), and by Persson *et al.* (26) (✕). (**a**) data measured immediately upon aspiration; (**b**) data measured after one freeze-thaw cycle.

measured immediately upon aspiration after administration of ibuprofen (Mann-Whitney, $p < 0.001$). However, the buffer capacity of the gastric contents measured after administration of ibuprofen and after centrifuging/ freezing the samples was not significantly affected. In aspirates that were obtained from volunteers who had not received ibuprofen and which underwent a freeze-thaw cycle prior to measurement the median value was 6.6 mmol/L/ΔpH ($n = 16$) (21,24), whereas in aspirates that were obtained from another set of volunteers who had received ibuprofen and which had undergone both centrifugation and a freeze-thaw cycle, the median value was 4.7 mmol/L/ΔpH ($n = 13$) (23) ($p = 0.283$, Mann-Whitney) (Fig. 4a).

Intestinal Aspirates

The pH values measured immediately upon aspiration in samples collected from the upper small intestine after administration of 800 mg ibuprofen (median 5.51, $n = 26$ (23)) were significantly lower than those measured immediately upon aspiration with no prior drug administration (median 6.35, $n = 47$ (20,21)) ($p = 0.002$, Mann-Whitney). The observation is in line with data reported by Hoffman *et al.* (33) who measured the intestinal pH with a Heidelberg capsule in eight healthy volunteers. In that
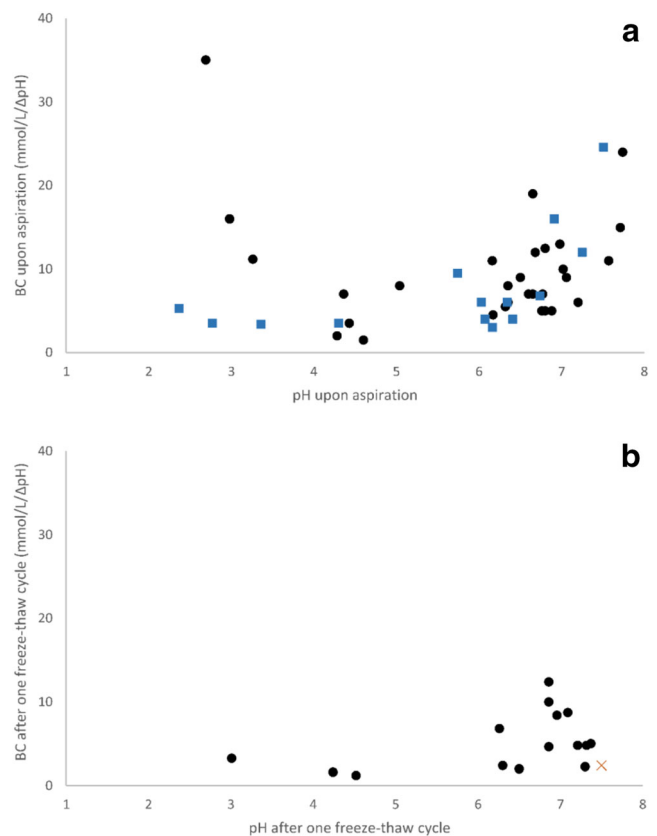
study, values reported after administration of an ibuprofen suspension at various infusion rates were lower than average population data. However, the exact region of the upper small intestine at which the pH was measured was not confirmed in that study (33).

Given that the pH values in aspirates collected from the upper small intestine are significantly lowered by prior administration of ibuprofen and/or centrifuging of aspirates, the buffer capacity values are also expected to be affected. Indeed, the buffer capacity measured in aspirates under ibuprofen administration combined with centrifugation/freezing sample handling (median 1.0 mmol/L/ΔpH, $n = 26$ (23)) was significantly lower than in other studies in which no ibuprofen was administered and the samples were frozen without having been centrifuged (median 4.72 mmol/L/ΔpH, $n = 16$ (21,26)) ($p < 0.001$, Mann-Whitney) (Fig. 4b).

The Impact of Handling and Storage on Buffer Capacity of Bicarbonate Solutions Prepared in the Laboratory

Data with respect to the impact of sample handling procedures and storage conditions on the buffer capacity of
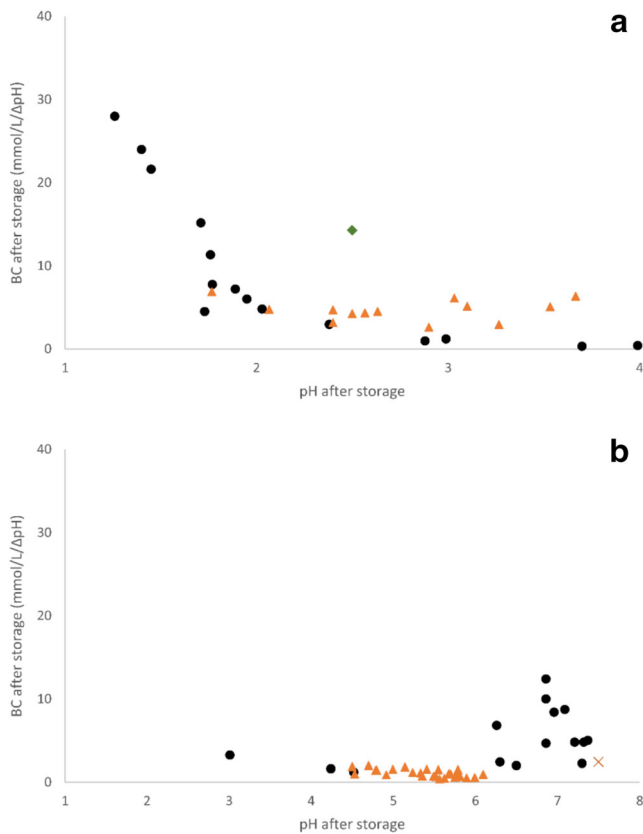
Fig. 4 (**a**) Data on the buffer capacity of fasted adult gastric contents *vs.* the corresponding pH values collected without prior treatment [Litou *et al.* (21) (●),and Pedersen *et al.* (24) (◆)], and after administration of 800 mg ibuprofen just before initiation of aspirations [Hens *et al.* (23) (▲)]

(**b**) Data on the buffer capacity of fasted adult contents of upper intestine *vs.* the corresponding pH values collected without prior treatment of the volunteers [Litou *et al.* (21) (●),and Persson *et al.* (26) (✗)] and after administration of 800 mg ibuprofen just before initiation of aspirations [Hens *et al.* (23) (▲)].

All data were collected after one freeze-thaw cycle and/or centrifugation and a freeze-thaw cycle.

solutions of bicarbonate prepared in the laboratory at concentrations of 10 mM to 100 mM are presented in Tables II and III.

At a 10 mM concentration of bicarbonate, subjecting the samples to centrifugation followed by one freeze–thaw cycle increased the pH (Kruskall-Wallis, $p = 0.004$) and decreased the buffer capacity (one-way ANOVA, $p = 0.021$) significantly. By contrast, subjecting the samples to just the freeze–thaw cycle (without centrifugation) did not affect either the pH or the buffer capacity significantly (Table II). Keeping the sample on the bench for 4 h or 24 h (Table III) led to a statistically significant increase in pH with an attendant decrease in buffer capacity (one-way ANOVA, $p < 0.001$ for both parameters, all pairwise comparisons were significantly different for both parameters).

At a bicarbonate concentration of 30 mM buffer, centrifuging and/or freezing the sample significantly increased the pH and decreased the buffer capacity (one-way ANOVA, $p < 0.001$, for both parameters). Keeping the sample on the bench for 24 h significantly increased the pH (one-way ANOVA, $p < 0.001$, all pairwise comparisons) and decreased the buffer capacity (one-way ANOVA, $p = 0.012$).

At a very high bicarbonate concentration of 100 mM buffer, centrifuging and/or freezing the sample did not affect the pH or the buffer capacity (one-way ANOVA, $p = 0.197$). While keeping the sample on the bench for 24 h significantly increased the pH (6.50 *vs.* 7.04, (Kruskal – Wallis, $p = 0.004$), the buffer capacity was not significantly altered (one-way ANOVA, $p = 0.123$).

Overall, it was observed that keeping the sample on the bench for 4 h leads to a significant increase in the pH and to a significant decrease in the buffer capacity at bicarbonate concentrations up to 30 mM. Likewise, freezing and/or centrifuging the sample affects the pH and buffer capacity significantly at concentrations of up to 30 mM (i.e. within the physiological range of bicarbonate concentrations that

Table II   The Impact of Freezing and of Centrifuging and Freezing on the pH and Buffer Capacity of Bicarbonate Buffer Systems as a Function of Concentration

Buffer concentration (mM)	pH			Buffer capacity		
	Upon preparation	After freezing	After centrifugation and freezing	Upon preparation	After freezing	After centrifugation and freezing
10	6.50	7.08 $p > 0.05$	7.28 $p < 0.05$	5.83	5.33 $p = 0.140$	4.67 $p = 0.004$
20	6.50	7.22 $p < 0.001$	7.23 $p < 0.001$	11.4	10.93 $p > 0.05$	10.13 $p > 0.05$
30	6.50	7.28 $p < 0.001$	7.32 $p < 0.001$	17.33	15.27 $p < 0.001$	14.67 $p < 0.001$
50	6.50	7.30 $p = 0.071$	7.33 $p = 0.071$	27.2	23.60 $p = 0.05$	24.00 $p = 0.05$
100	6.50	7.30 $p = 0.05$	7.36 $p = 0.05$	51.44	44.30 $p > 0.05$	42.33 $p > 0.05$

Table III   The Impact of Keeping the Sample on the Bench for 4 or 24 h on the pH and Buffer Capacity of Bicarbonate Buffer Systems as a Function of Concentration

Buffer concentration (mM)	pH			Buffer capacity		
	Upon preparation	After 4 h	After 24 h	Upon preparation	After 4 h	After 24 h
10	6.50	6.78 $p < 0.001$	7.10 $p < 0.001$	5.83	5.57 $p < 0.001$	5.83 vs 4.70 0.005
20	6.50	6.99 $p < 0.001$	7.15 $p < 0.001$	11.4	11.20 $p > 0.05$	9.70 $p > 0.05$
30	6.50	6.89 $p < 0.001$	7.04 $p < 0.001$	17.33	17.27 $p > 0.05$	15.13 $p = 0.008$
50	6.50	6.87 $p < 0.001$	7.03 $p < 0.001$	27.2	26.80 $p > 0.05$	21.07 $p < 0.001$
100	6.50	6.89 $p > 0.05$	7.04 $p = 0.004$	51.44	50.80 $p > 0.05$	49.67 $p > 0.05$

have been observed). The observed differences are greater when the sample has been both centrifuged and frozen than when it is simply frozen before storage. The results are in general agreement with the study of Leijssen *et al.*, in which the "loss of label" (i.e. decrease in concentration) of bicarbonate solutions was investigated *in vitro*. The authors reported that different stirring rates (when the bicarbonate solution was placed in a beaker) resulted in a loss of label up to 58% in one hour and that that the percentage loss could be reduced by increasing the bicarbonate buffer concentration from 1 to 10 mM [34].

In summary, at bicarbonate concentrations in the physiological range of values observed in the fasted state in the small intestine, both the pH and buffer capacity are very sensitive to the sample handling procedure, so it is imperative to ensure that the sample handling procedure is closely controlled.

DISCUSSION

A general comment on the studies with aspirates from the stomach and upper intestine is that the sample handling, use of marker compounds and pretreatment with drugs all vary from study to study. Although this is to be expected to some extent because of the different aims of the studies, it impedes a straightforward comparison of the results. At least for the purposes of determining inter-subject variability in parameters like pH and buffer capacity (and other relevant upper GI parameters such as bile salt concentrations), it would be extremely helpful to have a harmonized protocol.

pH in Aspirates

It can be concluded that the pH of the samples aspirated from the fasted stomach and upper small intestine is not significantly affected by a single freeze-thaw cycle. By contrast, centrifugation of intestinal aspirates upon collection increases the pH of the sample. It has been reported that the pH of samples aspirated from the upper small intestine drifted to higher values when the samples were kept on the bench at room temperature. The authors attributed the drift to the transformation of bicarbonates to carbon dioxide [20]. Taken together, these observations suggest that different sample handling procedures can have an effect on the measured intestinal pH values.

Buffer Capacity in Aspirates

The data presented here show that the buffer capacity of samples aspirated from the either the fasted stomach or the fasted small intestine is lowered significantly by subjecting the sample to a freeze-thaw cycle. Further, comparing studies in which ibuprofen was administered and the samples were centrifuged before freezing with studies in which no drug was administered and samples were frozen without having been centrifuged, it appears that centrifugation also leads to a decrease in buffer capacity. Thus, it is evident that the accuracy of the buffer capacity measurements of fluids aspirated from the upper GI tract is compromised when they are not performed immediately upon aspiration. Since centrifugation or leaving the sample on the laboratory bench for several hours both affect the pH, these sample handling procedures are expected to have a knock-on effect on the accuracy of the measurement of the buffer capacity as well.

Similar concerns with respect to the effects of sample handling on pH and buffer capacity have been made for other body fluids. For example, Gittings *et al.* performed pH and buffer capacity measurements in human saliva collected from healthy volunteers, immediately upon collection and after storing the samples at $-80°C$, respectively [35]. The authors recognized that bicarbonate buffer is a dynamic system and

opined that in saliva samples carbon dioxide may be lost from the system.

In Vitro **Testing**

Comparison of the *in vivo* and *in vitro* observations provides experimental evidence for non-exclusivity of bicarbonates in the regulation of pH in the fasted upper small intestine as well as in the fasted stomach at elevated pH. The results from the *in vitro* experiments indicated that both the buffer capacity and the pH of bicarbonate solutions up to 30 mM are affected by subjecting the samples to a freeze-thaw cycle. Since subjecting the samples to a freeze-thaw cycle does not significantly affect the pH of aspirates from the upper small intestine or from the stomach when the subjects are pretreated with famotidine, the question of whether bicarbonate is the sole contributor to the buffer system in the upper gastrointestinal tract arises. It appears that in these aspirates, species other than bicarbonates e.g. enzymes and/or mucin glycoproteins, may play an important role in regulating the intraluminal pH. This possibility is also supported by recent data concerning the importance of bicarbonates in biorelevant media simulating the conditions in the stomach under elevated gastric pH conditions and in the upper small intestine in the fasted state (21,36).

Proteins are present both in gastric and intestinal fluids. Lindahl *et al.* reported, among others, concentrations of proteins in the fasted gastric fluids of 2.1 ± 1.2 mg/mL (37). This value is in general agreement with the study of Litou *et al.*, where concentrations of 0.27 ± 0.14, 0.53 ± 0.18 and 0.71 ± 0.35 mg/mL at 10, 20 and 35 min after administration of 240 mL of water, respectively, were reported (21). With regard to the upper small intestine, Lindahl *et al.* reported protein concentrations in jejunal fluids of 1.8 ± 0.7 mg/mL (37). Similar values were reported by Kalantzi *et al.* for the fasted duodenum (3.1 mg/mL) (20), Persson *et al.* (1 ± 0.1 mg/mL) (26) and Litou *et al.* (1.00 ± 0.37, 1.8 ± 1.2, 2.7 ± 1.7 and 3.7 ± 0.11 mg/mL at 5, 10, 30 and 50 min after administration of 240 mL of water) (21). Since the freeze-thawing process can denature or destabilize proteins (38), it is important to measure their contributions to buffer capacity by titrating immediately after collection of the aspirate. From the observations in this study as well as the literature data on other physiological fluids (39–44), it seems that bicarbonates may not be the only contributors to the buffer system of the luminal fluids in the upper gastrointestinal tract and that proteins likely have an important role.

Effects of Drug Administration on pH and Buffer Capacity

Some authors have administered a drug prior to aspirating samples from the upper GI tract and it is quite clear that the administration of some drugs prior to the initiation of aspirations can have an effect on the measured pH and/or buffer capacity of the luminal aspirates.

A case in point is famotidine, a histamine 2 receptor antagonist, which like proton pump inhibitors is often used to elevate the gastric pH. In the Litou *et al.* study (21) it was shown that a 40 mg dose of famotidine (20 mg famotidine 14 h and 2 h prior to aspirations) elevates the gastric pH to values of pH 7 or more. Under these conditions the buffer capacity is reduced to a very low value (mean 0.62 mmol/L/ΔpH) due to the suppression of gastric acid secretion combined with the intake of a glass of water prior to aspiration. Interestingly, even at these extremely low buffer capacities, subjecting the sample to a freeze-thaw cycle prior to measurement resulted in a further decrease of the buffer capacity.

Hens *et al.* reported that the buffer capacity decreased after administration of 800 mg ibuprofen (23). This can be partly explained by the decrease in pH when ibuprofen dissolves in the intestinal lumen to a value far lower than the pKa of the bicarbonate buffer system, thus weakening the buffer capacity of the bicarbonate. However, the pharmacological effect of ibuprofen should be also taken into consideration when interpreting its effects on pH and buffer capacity in the gastrointestinal tract. It has been suggested that bicarbonate secretion from the duodenal mucosa is regulated through cephalic-vagal stimulation, non-humoral mediators activated by the presence of acid in the stomach, as well as locally produced prostaglandins of the E-type (PGEs), which stimulate the bicarbonate secretion in the proximal and distal duodenum and are released by the presence of acid in the intestinal fluids (12,13,45–48). The suppression of proximal and distal duodenal bicarbonate secretion after administration of an non-steroidal anti-inflammatory drug (NSAID) has been investigated in healthy subjects (50 mg of indomethacin orally administered 13 h and 1 h prior to the study, or 50 mg of indomethacin rectally administered at identical time intervals, $n = 10$) (49). In that study, the authors concluded that administration of NSAIDs could cause duodenal mucosal bicarbonate injury at least partly by decreasing mucosal prostaglandin generation (49). It seems, therefore, that the decrease in luminal pH and buffer capacity induced by ibuprofen is mediated via both physicochemical interactions in the lumen and systemic pharmacological effects.

CONCLUSIONS

Data collected from aspiration studies comprise the most valuable source of information with respect to characterizing the gastrointestinal environment and the properties of the gastrointestinal fluids, as well as the inter-subject variability in the associated parameters.

This study showed that sample handling procedures can significantly affect the pH and buffer capacity measurements of samples aspirated from the fasted upper gastrointestinal tract. It is therefore recommended that reporting of the physiological pH and buffer capacity values of fluids in the fasted upper gastrointestinal lumen should rely exclusively on data collected immediately upon aspiration, without prior drug treatment of the volunteers and without any additional sample handling.

There is a clear need for a standardized aspiration study protocol based on best practices to enable accuracy of the measurements and comparability of results across aspiration studies. Only data obtained in this way provide a valid basis for designing biorelevant test conditions and setting the physiological parameters in Physiologically Based Pharmacokinetic (PBPK) models.

Since both pH and buffer capacity of bicarbonate solutions up to 30 mM are more sensitive to a freeze-thaw cycle than in aspirates, in addition to hydrochloric acid and bicarbonates, other substances may play a role in regulation of pH in the upper GI tract in the fasted state. In particular, further studies are needed in order to better define the role of proteins, and possibly other components, in the buffer capacity of the luminal fluids.

REFERENCES

1. Fuchs A, Dressman JB. Composition and physicochemical properties of fasted-state human duodenal and jejunal fluid: a critical evaluation of the available data. Vol. 103. Journal of Pharmaceutical Sciences. 2014 Nov;103(11):3398–411. Available from: http://www.ncbi.nlm.nih.gov/pubmed/25277073.

2. Cristofoletti R, Dressman JB. FaSSIF-V3, but not compendial media, appropriately detects differences in the peak and extent of exposure between reference and test formulations of ibuprofen. Eur J Pharm Biopharm 2016 Aug;105:134–140. Available from: http://linkinghub.elsevier.com/retrieve/pii/S0939641116302107

3. Liu F, Merchant HA, Kulkarni RP, Alkademi M, Basit AW. Evolution of a physiological pH 6.8 bicarbonate buffer system: application to the dissolution testing of enteric coated products. Eur J Pharm Biopharm 2011 May 1;78(1):151–157. Available from: https://www.sciencedirect.com/science/article/pii/S0939641111000087

4. EMA. Guideline on quality of oral modified release products [Internet]. 2014. Available from: https://www.ema.europa.eu/documents/scientific-guideline/guideline-quality-oral-modified-release-products_en.pdf Accessed 11 Jan 2019

5. Allen A, Garner A. Mucus and bicarbonate secretion in the stomach and their possible role in mucosal protection. Vol. 21, Gut. 1980 Mar;21(3):249–62. Available from: http://www.ncbi.nlm.nih.gov/pubmed/6995243.

6. Järbur K, Dalenbäck J, Sjövall H. Quantitative assessment of motility-associated changes in gastric and duodenal luminal pH in humans. Vol. 38. Scandinavian journal of gastroenterology. 2003 Apr;38(4):392–8. Available from: http://www.ncbi.nlm.nih.gov/pubmed/12739711.

7. Feldman M, Blair AJ, Richardson CT, Richardson CT. Effect of proximal gastric vagotomy on calculated gastric HCO3- and non-parietal volume secretion in man. Studies during basal conditions and gastrin-17 infusion. Vol. 79. The Journal of clinical investigation. 1987 Jun;79(6):1615–20. Available from: http://www.ncbi.nlm.nih.gov/pubmed/3584462.

8. Feldman M. Gastric bicarbonate secretion in humans. Effect of pentagastrin, bethanechol, and 11,16,16-trimethyl prostaglandin E2. Vol. 72. The Journal of clinical investigation. 1983 Jul;72(1):295–303. Available from: http://www.ncbi.nlm.nih.gov/pubmed/6135708.

9. Rees WDW, Botham D, Turnberg LA. A demonstration of bicarbonate production by the normal human stomach in vivo. Vol. 27, Digestive Diseases and Sciences. 1982 Nov;27(11):961–6. Available from: https://link.springer.com/article/10.1007/BF01391739

10. Okosdinossian ET, El Munshid HA. Composition of the alkaline component of human gastric juice: effect of swallowed saliva and Duodeno-gastric reflux. Scand J Gastroenterol 1977 Dec 23;12(8):945–950. Available from: http://www.tandfonline.com/doi/full/10.3109/00365527709181354

11. Allen A, Flemström G. Gastroduodenal mucus bicarbonate barrier: protection against acid and pepsin. Vol. 288. American Journal of Physiology-Cell Physiology. 2005 Jan;288(1):C1–19. Available from: http://www.ncbi.nlm.nih.gov/pubmed/15591243.

12. Hogan DL, Ainsworth MA, Isenberg JI. Review article: gastroduodenal bicarbonate secretion. Vol. 8, Alimentary Pharmacology & Therapeutics. 1994 Oct;8(5):475–88. Available from: http://www.ncbi.nlm.nih.gov/pubmed/7865639.

13. Seidler U, Sjöblom M. Gastroduodenal bicarbonate secretion. In: Physiology of the Gastrointestinal Tract. Academic Press; 2012. p. 1311–39. Available from: https://www.sciencedirect.com/science/article/pii/B9780123820266000488

14. Novak I, Wang J, Henriksen KL, Haanes KA, Krabbe S, Nitschke R, *et al.* Pancreatic Bicarbonate Secretion Involves Two Proton Pumps. Vol. 286, Journal of Biological Chemistry. 2011 Jan 7;286(1):280–9. Available from: http://www.ncbi.nlm.nih.gov/pubmed/20978133.

15. Bucher GR, Flynn JC, Robinson CS. The action of the human small intestine in altering the composition of physiological saline. Vol. 155, Journal of Biological Chemistry. 1944;155:305–13. Available from: https://www.cabdirect.org/cabdirect/abstract/19441403289

16. Repishti M, Hogan DL, Pratha V, Davydova L, Donowitz M, Tse CM, *et al.* Human duodenal mucosal brush border Na $^+$/H $^+$ exchangers NHE2 and NHE3 alter net bicarbonate movement. Vol. 281, American Journal of Physiology-Gastrointestinal and Liver Physiology. 2001 Jul;281(1):G159–63. Available from: http://www.ncbi.nlm.nih.gov/pubmed/11408268.

17. McGee LC, Hastings BA. The carbon dioxide tension and acid-base balance of jejunal secretions in man. J Biol Chem. 1942;142:893–904 Available from: http://www.jbc.org/content/142/2/893.citation.

18. Isenberg JI, Selling JA, Hogan DL, Koss MA. Impaired proximal duodenal mucosal bicarbonate secretion in patients with duodenal ulcer, N Engl J Med 1987 Feb 12;316(7):374–379. Available from: http://www.nejm.org/doi/abs/10.1056/NEJM198702123160704

19. Odes HS, Hogan DL, Steinbach JH, Ballesteros MA, Koss MA, Isenberg JI. Measurement of gastric bicarbonate secretion in the human stomach: different methods produce discordant results. Vol. 27, Scandinavian journal of gastroenterology. 1992

Oct;27(10):829–36. Available from: http://www.ncbi.nlm.nih.gov/pubmed/1332183.

20. Kalantzi L, Goumas K, Kalioras V, Abrahamsson B, Dressman JB, Reppas C. Characterization of the Human Upper Gastrointestinal Contents Under Conditions Simulating Bioavailability/Bioequivalence Studies. Vol. 23, Pharmaceutical Research. 2006 Jan 1;23(1):165–76. Available from: http://www.ncbi.nlm.nih.gov/pubmed/16308672.

21. Litou C, Vertzoni M, Goumas C, Vasdekis V, Xu W, Kesisoglou F, Reppas C. Characteristics of the human upper gastrointestinal contents in the fasted state under hypo- and A-chlorhydric gastric conditions under conditions of typical drug – drug interaction studies. Pharm Res 2016 Jun 14;33(6):1399–1412. Available from: http://link.springer.com/10.1007/s11095-016-1882-8

22. Perez de la Cruz Moreno M, Oth M, Deferme S, Lammert F, Tack J, Dressman J, et al. Characterization of fasted-state human intestinal fluids collected from duodenum and jejunum. Vol. 58, The Journal of pharmacy and pharmacology. 2006 Aug;58(8):1079–89. Available from: http://doi.wiley.com/10.1211/jpp.58.8.0009

23. Hens B, Tsume Y, Bermejo M, Paixao P, Koenigsknecht MJ, Baker JR, et al. Low Buffer Capacity and Alternating Motility along the Human Gastrointestinal Tract: Implications for in Vivo Dissolution and Absorption of Ionizable Drugs. Vol. 14, Molecular Pharmaceutics. 2017 Dec 4;14(12):4281–94. Available from: http://www.ncbi.nlm.nih.gov/pubmed/28737409.

24. Pedersen PB, Vilmann P, Bar-Shalom D, Müllertz A, Baldursdottir S. Characterization of fasted human gastric fluid for relevant rheological parameters and gastric lipase activities. Vol. 85, European Journal of Pharmaceutics and Biopharmaceutics. 2013 Nov;85(3):958–65. Available from: http://www.ncbi.nlm.nih.gov/pubmed/23727368.

25. Fadda HM, Sousa T, Carlsson AS, Abrahamsson B, Williams JG, Kumar D, Basit AW. Drug solubility in luminal fluids from different regions of the small and large intestine of humans. Mol Pharm 2010 Oct 4;7(5):1527–1532. Available from: http://pubs.acs.org/doi/abs/10.1021/mp100198q

26. Persson EM, Gustafsson A-S, Carlsson AS, Nilsson RG, Knutson L, Forsell P, et al. The effects of food on the dissolution of poorly soluble drugs in human and in model small intestinal fluids. Pharmaceutical Research. 2005 Dec 30;22(12):2141–51. Available from: http://www.ncbi.nlm.nih.gov/pubmed/16247711.

27. Koenigsknecht MJ, Baker JR, Wen B, Frances A, Zhang H, Yu A, et al. In Vivo Dissolution and Systemic Absorption of Immediate Release Ibuprofen in Human Gastrointestinal Tract under Fed and Fasted Conditions., Molecular Pharmaceutics. 2017 Dec 4;14(12):4295–304. Available from: http://www.ncbi.nlm.nih.gov/pubmed/28937221.

28. Bergström CAS, Holm R, Jørgensen SA, Andersson SBE, Artursson P, Beato S, et al. Early pharmaceutical profiling to predict oral drug absorption: Current status and unmet needs. Vol. 57, European Journal of Pharmaceutical Sciences. 2014 Jun 16;57(1):173–99. Available from: http://www.ncbi.nlm.nih.gov/pubmed/24215735.

29. Psachoulias D, Vertzoni M, Goumas K, Kalioras V, Beato S, Butler J, et al. Precipitation in and supersaturation of contents of the upper small intestine after administration of two weak bases to fasted adults. Vol. 28. Pharm Res. 2011;28(12):3145–58.

30. Urbansky ET, Schock MR. Understanding, Deriving, and Computing Buffer Capacity. Vol. 77, Journal of Chemical Education. 2000;77(12). Available from: https://www.researchgate.net/publication/231265068

31. Mioni R, Mioni G. A mathematical model of pH, based on the total stoichiometric concentration of acids, bases and ampholytes dissolved in water. Vol. 75, Scandinavian Journal of Clinical and Laboratory Investigation. 2015 Aug 18;75(6):452–69. Available from: http://www.ncbi.nlm.nih.gov/pubmed/26059505.

32. Karow AR, Bahrenburg S, Garidel P. Buffer capacity of biologics-from buffer salts to buffering by antibodies. Vol. 29, Biotechnology Progress. 2013 Mar;29(2):480–92. Available from: http://www.ncbi.nlm.nih.gov/pubmed/23296746.

33. Hofmann M, Thieringer F, Nguyen MA, Månsson W, Galle PR, Langguth P. A novel technique for intraduodenal administration of drug suspensions/solutions with concurrent pH monitoring applied to ibuprofen formulations. Vol. 136, European Journal of Pharmaceutics and Biopharmaceutics. 2019 Mar;136:192–202. Available from: http://www.ncbi.nlm.nih.gov/pubmed/30659894.

34. Leijssen DP, Elia M. Recovery of 13CO2 and 14CO2 in human bicarbonate studies: a critical review with original data. Vol. 91, Clinical science (London, England : 1979). 1996;91(6):665–77.

35. Gittings S, Turnbull N, Henry B, Roberts CJ, Gershkovich P. Characterisation of human saliva as a platform for oral dissolution medium development. Vol. 91, European Journal of Pharmaceutics and Biopharmaceutics. 2015 Apr;91:16–24. Available from: http://www.ncbi.nlm.nih.gov/pubmed/25603197.

36. Litou C, Vertzoni M, Xu W, Kesisoglou F, Reppas C. The impact of reduced gastric acid secretion on dissolution of salts of weak bases in the fasted upper gastrointestinal lumen: Data in biorelevant media and in human aspirates. Vol. 115, European Journal of Pharmaceutics and Biopharmaceutics. 2017 Jun;115:94–101. Available from: http://www.ncbi.nlm.nih.gov/pubmed/28214603.

37. Lindahl A, Ungell A, Knutson L, Lennernäs H. Characterization of fluids from the stomach and proximal jejunum in men and women. Pharm Res. 1997;14(4):497–502 Available from: http://link.springer.com/10.1023/A:1012107801889.

38. Arakawa T, Prestrelski SJ, Kenney WC, Carpenter JF. Factors affecting short-term and long-term stabilities of proteins, Adv Drug Deliv Rev 2001 Mar 1;46(1–3):307–326. Available from: https://www.sciencedirect.com/science/article/pii/S0169409X00001447

39. Lilienthal B. An Analysis of the Buffer Systems in Saliva. Vol. 34, Journal of Dental Research. 1955 Aug 9;34(4):516–30. Available from: http://www.ncbi.nlm.nih.gov/pubmed/13242718.

40. Holma B, Hegg PO. pH- and protein-dependent buffer capacity and viscosity of respiratory mucus. Their interrelationships and influence on health. Vol. 84, The Science of the total environment. 1989 Aug;84:71–82. Available from: http://www.ncbi.nlm.nih.gov/pubmed/2772626.

41. Bardow A, Moe D, Nyvad B, Nauntofte B. The buffer capacity and buffer systems of human whole saliva measured without loss of CO2. Vol. 45, Archives of oral biology. 2000 Jan;45(1):1–12. Available from: http://www.ncbi.nlm.nih.gov/pubmed/10669087.

42. Carney LG, Mauger TF, Hill RM. Buffering in human tears: pH responses to acid and base challenge. Vol. 30, Investigative ophthalmology & visual science. 1989 Apr;30(4):747–54. Available from: http://www.ncbi.nlm.nih.gov/pubmed/2703317.

43. Izutsu KT, Madden PR. Evidence for the Presence of Carbamino Compounds in Human Saliva. Vol. 57, Journal of Dental Research. 1978 Feb 8;57(2):319–25. Available from: http://www.ncbi.nlm.nih.gov/pubmed/277528.

44. Kim D, Liao J, Hanrahan JW. The buffer capacity of airway epithelial secretions. Vol. 5, Frontiers in physiology. 2014;5:188. Available from. http://www.ncbi.nlm.nih.gov/pubmed/24917822.

45. Isenberg JI, Smedfors B, Johansson C. Effect of Graded Doses of Intraluminal H+, Prostaglandin E2, and Inhibition of Endogenous Prostaglandin Synthesis on Proximal Duodenal Bicarbonate

Secretion in Unanesthetized Rat. Gastroenterology. 1985. p. 303–7.

46.   Wallace JL. Prostaglandins, NSAIDs, and gastric mucosal protection: why Doesn't the stomach digest itself? Physiol Rev 2008 Oct;88(4):1547–1565. Available from: http://www.physiology.org/doi/10.1152/physrev.00004.2008

47.   Isenberg JI, Hogan DL, Selling JA, Koss MA. Duodenal bicarbonate secretion in humans - Role of prostaglandins. Vol. 31, Digestive Diseases and Sciences. 1986;31(2 Supplement):2116.

48.   Konturek P., Konturek S., Hahn E. Duodenal alkaline secretion: its mechanisms and role in mucosal protection against gastric acid. Vol. 36, Digestive and Liver Disease. 2004 Aug;36(8):505–12. Available from: http://www.ncbi.nlm.nih.gov/pubmed/15334769.

49.   Selling JA, Hogan DL, Aly A, Koss MA, Isenberg JI. Indomethacin inhibits duodenal mucosal bicarbonate secretion and endogenous prostaglandin E2 output in human subjects. Vol. 106, Annals of internal medicine. 1987 Mar;106(3):368–71. Available from: http://www.ncbi.nlm.nih.gov/pubmed/3468819.

PUBLISHER'S NOTE

Review

In vitro methods to assess drug precipitation in the fasted small intestine – a PEARRL review

Patrick J. O'Dwyer[a,b,]*, Chara Litou[c,]*, Karl J. Box[a], Jennifer B. Dressman[c], Edmund S. Kostewicz[c], Martin Kuentz[d] and Christos Reppas[b]

[a]Pion Inc. (UK) Ltd., Forest Row, East Sussex, UK, [b]Department of Pharmacy, School of Health Sciences, National and Kapodistrian University of Athens, Zografou, Greece, [c]Institute of Pharmaceutical Technology, Goethe University, Frankfurt am Main, Germany and [d]University of Applied Sciences and Arts Northwestern Switzerland, Muttenz, Switzerland

Abstract

Objectives Drug precipitation *in vivo* poses a significant challenge for the pharmaceutical industry. During the drug development process, the impact of drug supersaturation or precipitation on the *in vivo* behaviour of drug products is evaluated with *in vitro* techniques. This review focuses on the small and full scale *in vitro* methods to assess drug precipitation in the fasted small intestine.

Key findings Many methods have been developed in an attempt to evaluate drug precipitation in the fasted state, with varying degrees of complexity and scale. In early stages of drug development, when drug quantities are typically limited, small-scale tests facilitate an early evaluation of the potential precipitation risk *in vivo* and allow rapid screening of prototype formulations. At later stages of formulation development, full-scale methods are necessary to predict the behaviour of formulations at clinically relevant doses. Multicompartment models allow the evaluation of drug precipitation after transfer from stomach to the upper small intestine. Optimisation of available biopharmaceutics tools for evaluating precipitation in the fasted small intestine is crucial for accelerating the development of novel breakthrough medicines and reducing the development costs.

Summary Despite the progress from compendial quality control dissolution methods, further work is required to validate the usefulness of proposed setups and to increase their biorelevance, particularly in simulating the absorption of drug along the intestinal lumen. Coupling results from *in vitro* testing with physiologically based pharmacokinetic modelling holds significant promise and requires further evaluation.

Introduction

Oral drug absorption is a complex process that can be affected by a range of parameters, related to the drug, the formulation and the underlying physiology of the gastrointestinal tract (GIT). Molecular size, degree of ionisation, dissolution, precipitation, gastrointestinal (GI) transit times, luminal viscosity, pH, bile salt and phospholipid concentrations, cellular permeation and intestinal drug transport and metabolism are some examples of the factors which can affect absorption of a drug and, therefore, its bioavailability.

Possible supersaturation or precipitation are important parameters to consider, as they can significantly affect the bioavailability of an active pharmaceutical ingredient (API). Assessment of potential supersaturation and precipitation is critical, especially in cases where the API is a weak base with low aqueous solubility or a bio-enabling formulation is implemented.

Under fasting conditions, weakly basic drugs usually have higher solubility values in the acidic environment of the stomach compared with the small intestine. Due to the variability in pH values along the human GIT, weakly basic drugs have a propensity to precipitate. In particular, for weakly basic compounds, supersaturation can occur after transfer from the stomach to the small intestine. However, supersaturated states are thermodynamically unstable and the degree of supersaturation is the driving force for

precipitation. Precipitation and drug absorption are competing processes in the GIT and excipient effects can be of critical importance. From 1981 until the end of 2006, 38% of the APIs approved in the U.S.A. for oral administration were basic molecules[1] and as new drug entities in current pipelines tend to be somewhat larger molecules (>500 Daltons) and more lipophilic, there is a need to develop reliable *in vitro* methods to simulate the transfer of the drug through the GIT and accurately predict their precipitation characteristics/kinetics *in vivo*.

The ultimate goal of bio-enabling formulations is enhanced intestinal absorption. To achieve this, pharmaceutical scientists often develop formulations, which are aimed at achieving and maintaining supersaturation, that is the so-called spring and parachute approach.[2,3] In this way, a greater amount of drug is in solution for a longer period of time in the upper small intestine and therefore, available for absorption. Common methods to improve dissolution and achieve supersaturation include solid phase dispersions, lipid-based formulations and formulating with cyclodextrins.[4–6] Despite the increasing interest in producing these formulations, there is still a lack of mechanistic understanding about how to achieve and maintain a supersaturated state intraluminally. Therefore, design of these formulations remains a challenge.[7]

In every case, precipitation of drug particles can result in impaired absorption of the API and reduced bioavailability. Consequently, it can jeopardise both the therapeutic efficacy and safety of the drug. Precipitation can further contribute to the large intra- and inter-individual variability in drug exposure often detected during development of new drug products[8] and can impair the chances of proving efficacy in clinical trials.[9]

Currently, apparent supersaturation or precipitation of drug *in vivo* is assessed directly in the human lumen or indirectly using plasma profiles (from humans or animals), *ex vivo* methods, or *in vitro* methods. Luminal studies in humans provide the best source of information regarding the supersaturation or precipitation of different compounds.[10–14] Despite the valuable information obtained from luminal and *in vivo* methods in humans, as well as from *ex vivo* studies,[15] they are expensive, time-consuming and can raise ethical issues. Animal pharmacokinetic studies are also a valuable source of information,[16] but differences in the GI conditions between humans and the animal model can be an important source of error when assessing supersaturation or precipitation. Animal studies may also raise ethical issues and are costly to conduct. Methodologies for assessing drug supersaturation or precipitation *in vitro* allow for understanding and predicting the behaviour of an API/formulation and can facilitate the development of more efficient and safe drug products for patients. Assessing the supersaturation and precipitation

kinetics of a compound is important in early development stages, before first in human studies, as well as in the later stages of formulation development. In early stage of drug development, usually a small amount of the candidate-API is available and, therefore, small-scale techniques are necessary. On the other hand, robust full scale *in vitro* setups are needed at the stage of formulation development for the evaluation of precipitation and supersaturation after administration of clinically relevant doses, as well as understanding supersaturation and precipitation kinetics in the presence of various excipients.

The purpose of this review article is to present an up-to-date overview of the *in vitro* tools which have been proposed to predict *in vivo* precipitation, to understand their rationale and to outline strengths and weaknesses. This will highlight areas for optimisations and guide the evolution of the methodology.

Small-scale methods to assess drug precipitation

Small-scale *in vitro* setups facilitate the use of small quantities of the API available in the early stages of drug development. They may also be useful for the evaluation of prototype formulations.[17] In addition, the use of small-scale experiments allows for reducing the quantity of biorelevant media required, which helps to reduce expenses.

Smaller versions of the USP II dissolution apparatus have been developed.[18,19] The mini-paddle vessels use 250 ml, instead of at least 500 ml used in the full-sized apparatus. Some of these downscaled apparatus have been shown to produce dissolution results comparable to the standard USP II apparatus.[19] However, in pharmaceutical profiling and early formulation development, an even smaller scale can be beneficial.

Single media tests

In early stage of drug development, evaluation of potential drug precipitation can be inferred by comparing solubility in simulated gastric with intestinal media. Solubility information can be obtained rapidly using high-throughput 96 well-based solubility screening tests.[20,21] For example, the solubility of ketoconazole, as measured by the PASS (partially automated solubility screening) test, in Level II fasted state simulated intestinal fluid (FaSSIF)[22] (0.017 mg/ml) is much lower than in Level 0 simulated gastric fluid (SGF) (418.3 mg/ml)[20], indicating possible precipitation upon transition from gastric to intestinal environment. Subsequent *in vivo* studies have shown precipitation of ketoconazole in the upper small intestine up to 16% of the administered dose.[10]

Many of the high-throughput solubility tests use a solvent casting procedure, which raises concerns on potential changes of drug crystallinity upon removal of the solvent in the excipient matrix.[21] Another potential problem is that traces of solvent could also lead to an overestimation of solubility when the medium is added. While not attempting to capture the full complexity of the *in vivo* supersaturation or precipitation process, these high-throughput solubility screening tests provide useful information about solubility 'gaps' and thus, potential precipitation at an early stage under given conditions using only microgram quantities of drug.

Chandran *et al.*,[23] proposed a small-scale approach using a turbidimetric spectrophotometry method to quickly evaluate the precipitation potential of a drug. With this method, a stock solution of drug was prepared using polyethylene glycol (PEG) 400 as a vehicle and precipitation inhibitors were added. Drug stock solution (100 µl) was added to a 96-well plate and mixed with an equal volume of deionised water. This setup measured absorbance at 500 nm, which is well above the absorbance range of any of the molecules tested, but provides a measure of light scattering due to the precipitation of drug, leading essentially to a turbidimetric endpoint. The authors hypothesised that the initial precipitation of fine particles caused a strong scattering of light, before agglomeration of particles resulted. A resulting increase in effective particle size and settling allows for increased transmission through the well, thus leading to decreasing absorption. The qualitative results using this method correlated well with traditional UPLC methods when examining the efficacy of different precipitation inhibitors, as both methods found that the 5% (w/w) d-alpha tocopheryl polyethylene glycol 1000 succinate (TPGS) in PEG 400 formulation was the most effective at preventing camphor precipitation.[23] Benefits of using the UV spectrometer include the simple and rapid analysis of drug precipitation at multiple time points, without the requirement of extra sample preparation or sample wastage. This test could be a useful tool to rapidly assess drug precipitation and the impact of excipients in early formulation development.

Tests with medium shift (solvent shift)

Yamashita *et al.*,[24] used a solvent shift experiment to evaluate drug precipitation. In this method drug is initially dissolved in DMSO to produce a highly concentrated stock solution. The highly concentrated stock solution is diluted in Level II FaSSIF in a 96-well plate and drug precipitation is monitored by HPLC/UV analysis. This method is useful for comparing the effectiveness of different precipitation inhibitors, which can be added to FaSSIF. Yamashita *et al.*, used this test to assess the efficacy of precipitation

inhibitors with itraconazole. Results were found to correlate well with the full scale paddle dissolution experiment, as both methods identified HPMC-AS (hydroxypropyl methylcellulose-acetate succinate) as the most effective precipitation inhibitor.

Petrusevska *et al.*,[25] used DMSO to deliver dissolved drug in a high-throughput test. McIlvaine's buffer (pH 6.8) with excipient concentrations of 0.001%, 0.01% and 0.1% (w/v) were initially dispensed into each well. The concentrated stock solution of drug in DMSO was added and the plate was shaken for 5 s to ensure adequate mixing. The plate was incubated and samples were removed at various time points up to 360 min. Experimental factors such as the shaking frequency, incubation temperature and effect of various DMSO concentrations in the setup were investigated. A DMSO concentration of ≤1% (v/v) in the assay was found to be acceptable. The efficacy of 23 different excipients to prevent precipitation of two poorly soluble neutral drugs, carbamazepine and fenofibrate, was examined. Distinct results were found for the two compounds, highlighting the case-specific nature of precipitation inhibitor effects. The authors concluded that this high-throughput test provided a reasonable starting point to select appropriate excipients to help prevent precipitation of drugs.

Petrusevska *et al.*,[26] carried out a follow-up study investigating the use of light scattering and turbidity to evaluate drug precipitation and the efficacy of precipitation inhibitors. Light scattering was measured using a nephelometer, whereas turbidity was measured using a UV plate reader at 500 nm. Stock solutions of dipyridamole and fenofibrate in DMSO were tested using similar conditions as outlined in the previous experiment. Results were compared to those obtained using standard quantification methods, such as UPLC, to evaluate drug precipitation. The authors expressed a preference for using the light scattering method over the turbidity as it produced less false positives (4 vs 5) and less false negatives (0 vs 2) when examining the efficacy of different precipitation inhibitors.

Christfort *et al.*,[27] developed a video-microscopic tool to assess the precipitation of tadalafil and the efficacy of precipitation inhibitors. Using a 96-well microplate, 30 µl of a tadalafil DMSO stock solution was added to FaSSIF with varying concentrations (0.0–5.0% w/v) of HPMC, acting as a precipitation inhibitor. Micrographs were obtained using the oCelloScope system™ (Philips Biocell A/S, Allerød, Denmark). The development of precipitation was monitored by both single and multi-particle analysis. Single particle analysis determined the induction time for precipitation to occur as the time taken for the first well-defined particle to appear into focus. Using single particle analysis, the effect of varying HPMC concentrations on the induction time for crystal growth and the growth in area of a

single crystal was observed over time. As single particle analysis only focuses on the growth of a single crystal, it may not be representative of the total population of crystals. In contrast, multi-particle analysis enabled the analysis of the total population of particles by examining all areas of crystal growth within the field of view. Crystal growth was quantified by determining the percentage of the area of the microscopic field of view that is covered by particles and by counting the number of particles. Results of single and multi-particle analysis correlated with each other as both found that a 0.01% (w/v) concentration of HPMC was required to observe inhibition of precipitation, with maximum inhibition occurring at a concentration of 0.1% (w/v). This visual method of assessing precipitation has significant potential to increase the understanding of the precipitation kinetics in the intestine.

The μDiss system (Pion Inc., Billerica, MA, USA) employs UV fibre optics to obtain real-time experimental information about drug solubility and dissolution. Information about drug supersaturation and precipitation can also be inferred using the μDiss and can be used to study dissolution from drug powder or a miniaturised disc.[28,29] Up to eight experiments can be run in parallel using volumes of media ranging from 1 to 10 ml. This method was employed to study dissolution for a wide variety of compounds, including poorly soluble drugs.[28] Palmelund *et al.*,[30] developed an *in vitro* standardised supersaturation and precipitation method (SSPM) using the μDiss system. High concentration stock solutions of the model drugs were prepared using DMSO, and aliquots (200 μl) were added into 10 ml of Level II FaSSIF at 37 °C. The model drugs tested were albendazole, aprepitant, danazol, felodipine, fenofibrate, and tadalafil. After each addition of stock

solution, UV absorbance was measured using the *in situ* UV probes for 60 min or, if no precipitation was observed, for longer. Precipitation was detected by a shift in the baseline UV spectrum and decrease in drug concentration. Plum *et al.*,[31] investigated the inter-lab reproducibility of the SSPM method, with testing carried out at seven different sites. Values obtained for three model drugs (aprepitant, felodipine, fenofibrate) for apparent drug supersaturation (aDS) and the induction time for detectable precipitation (t_{ind}) were compared across the various laboratories. While a direct comparison for aDS and t_{ind} values between sites was not possible, it was found that 80% of the partners who submitted a full data set found the same rank-ordering of drugs (aprepitant > felodipine ≈ fenofibrate) when comparing β-values, which was defined as the slope of the $\ln(t_{ind})$ vs $\ln(aDS)^{-2}$ plot.[31]

Tests with medium and pH shifts

Klein *et al.*,[32] investigated the feasibility of creating a miniaturised transfer model system to model the transition from gastric to intestinal environment. Two different experimental setups were tested: a 96-well plate model and a mini-paddle apparatus model. In the 96-well model experiment, the drug is initially dissolved in Level 0 SGF (donor phase) before 30 μl of the donor phase is pipetted into the acceptor phase, consisting of 170 μl of either Level II FaSSIF or Level II FeSSIF. Drug concentration was measured every 2 min with a UV microplate reader. In the mini-paddle setup, the drug is initially dissolved in 10 ml of Level 0 SGF and is added to 40 ml of either Level II FeSSIF or Level II FaSSIF, as shown in Figure 1. Drug concentration
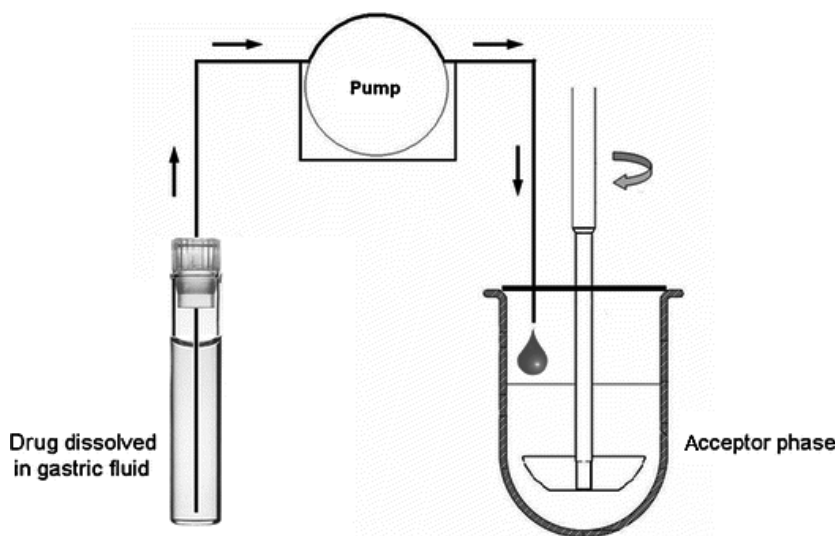

Figure 1 Schematic of miniaturised transfer model system proposed by Klein *et al.*[32] Reproduced with permission from Springer.

was determined by HPLC. Hydroxybutenyl-β-cyclodextrin complexes of both tamoxifen and itraconazole were tested using both setups and the results were consistent between platforms; tamoxifen was not found to precipitate in either setup, whereas itraconazole precipitated by approximately 90% in both methods.

The miniaturised intrinsic dissolution screening (MIND-ISS) setup uses minidiscs of compacted drug, typically 2–5 mg, to deliver drug into a 96-well plate.[33] The minidiscs are prepared in a custom-made holder, resulting in a drug surface area of 3 mm^2. Dissolution medium (0.35 ml) is added into the wells and stirred. The minidiscs are added to the wells so that the drug is immersed in the dissolution media. After a set period of time, the minidiscs are transferred into a new well. This transfer into new media enables a pH shift, which may help to improve the biorelevance of the test by mimicking the changing environment along the GIT.[17] Drug concentrations are determined using UPLC, while Raman spectroscopy is used to analyse the solid state characteristics of the disc. The disc intrinsic dissolution rates (DIDR) calculated from the MINDISS setup, were closely correlated ($R^2 = 0.9292$) to larger scale drug disc dissolution tests.

Using the MINDISS setup, the DIDR of diclofenac sodium and diclofenac potassium in SGF, pH 1.2, was found to be identical to the free acid.[33] When testing both salt forms in Level 0 SGF, a layer of free diclofenac acid was formed on the surface of the disc which controlled the DIDR. This precipitation was thought to be due to the conversion of the salt forms of the drug to the less soluble free acid. A free base would be expected to demonstrate the converse behaviour that is to rapidly dissolve in acidic gastric conditions and precipitate in the more neutral intestinal environment.

Two-stage tests

The Sirius T3 instrument (Pion Inc.) is an automated titration system as shown in Figure 2.[34] Gravestock *et al.*,[35] used it to monitor precipitation of a wide range of acidic, basic and neutral drugs. It uses a fibre optic UV dip probe connected to a diode array UV spectrometer to obtain a real-time measurement of drug concentration. When examining dissolution and precipitation of drug, off-line sample analysis is susceptible to potential errors due to sample ageing. Real-time analytical technology, by contrast, avoids such errors. Drug dissolution and precipitation in 15 ml of buffered 0.15 M KCl was measured at four pHs: 1.9, 3.8, 5.2 and 7.2. The pH was initially 1.9 and increased every 30 min. The effect of pH on the dissolution and precipitation of drugs was observed; dissolution rates of acidic compounds increased with increasing pH, whereas neutral compounds had a relatively constant dissolution rate across
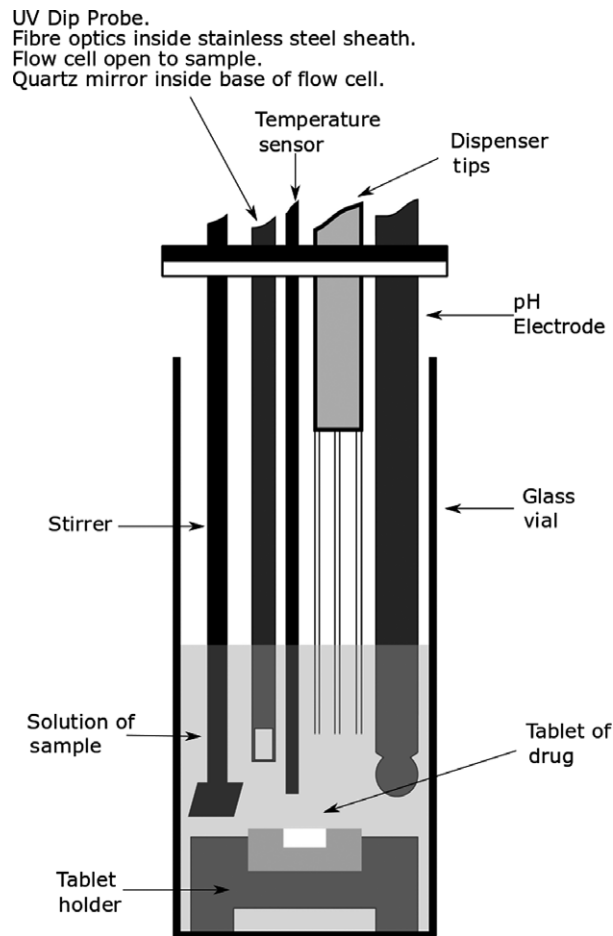

Figure 2 Schematic of the Sirius T3 instrument.[34] Reproduced with permission from Springer.

the four pHs. Some basic drugs, such as dipyridamole, chlorpromazine HCl and clopidogrel bisulfate, precipitated as the pH was increased. Other basic drugs, such as haloperidol, maprotiline and propranolol, did not precipitate as the pH was increased. Jakubiak *et al.*[9] used dissolution data from the T3 to develop a dissolution and precipitation model. In their studies, the dissolution testing on the T3 was carried out using two different pH values (pH 2 and pH 6.5) to simulate gastric and intestinal conditions, respectively. Level II FaSSIF was used for simulating the conditions in the upper small intestine, while a simple phosphate buffer at pH 2 was used for simulating the conditions in the stomach. After 10 min at pH 2, concentrated FaSSIF was added to simulate the transfer from the gastric to the intestinal environment. The drug plasma profiles estimated using their model for dipyridamole and erlotinib showed a strong correlation to the human *in vivo* plasma profile, obtained from previous clinical studies.

Mathias *et al.*,[36] developed a micro-dissolution test to examine the effect of changing media and pH on the

dissolution, supersaturation and precipitation behaviour of drugs under conditions which aim to replicate the transit through the GI tract, as shown in Figure 3. Drug, either as powder or suspension, was initially added to 7 ml of Level 0 SGF. After 20 min, 14 ml of a 1.5 times concentrated Level II FaSSIF solution was added to simulate the changes in conditions due to transfer from the stomach to the intestine. The pH of the resulting FaSSIF solution was 6.5 and the drug was incubated for a further 160 min. The weakly basic drugs ketoconazole and erlotinib were among the evaluated drugs using this test. Ketoconazole remained supersaturated for 55 min upon transition from gastric to intestinal conditions, before precipitating slowly over the next 75 min. Erlotinib precipitated rapidly to its equilibrium crystalline solubility upon addition of Level II FaSSIF.

Methods addressing intestinal absorption

Biphasic dissolution tests

A method to simulate the absorption step in dissolution tests is through the use of an organic layer on top of the aqueous donor layer. Drug partitioning from the aqueous to the organic layer helps to generate sink conditions in the donor layer, which can have a significant effect on drug precipitation. The disadvantage of biphasic experiments is that the organic layer is in direct contact with the aqueous layer; this can lead to effects which differ from *in vivo* drug absorption. For example, some of the organic layer may be solubilised and an emulsification could occur as a result. This issue can be especially pronounced if surface-active compounds are present in the biphasic experiments, which is rather common in bio-enabling formulations.

The miBldi-pH (miniscale biphasic dissolution model with pH-shift) is a small-scale biphasic dissolution test which incorporates a pH shift to evaluate drug release and precipitation, as shown in Figure 4.[37,38] The organic lipid layer acts as an absorptive sink as drug partitions from the aqueous phase into the organic phase. The system consists of 50 ml of aqueous media covered by a 15 ml octanol layer, which acts as an absorptive sink, in a miniaturised USP dissolution apparatus II. Drug concentration is determined by online UV-spectrometry. Frank *et al.*,[37] investigated the utility of this system to predict the *in vivo* dissolution processes of two weakly basic drugs: dipyridamole and BIXX. Precipitation was observed for both drugs upon shift of the pH from an acidic gastric environment to the neutral intestinal environment. The correlation to *in vivo* data for both drugs was greatly improved using the biphasic dissolution model compared to single phase dissolution experiments. A level A IVIVC (*in vitro–in vivo* correlation) was established ($R^2 = 0.95$) between the fraction absorbed *in vivo* and the fraction dissolved in octanol for the BIXX formulations tested, whereas the single phase dissolution tests were not found to be predictive of *in vivo* performance.

The inForm (Pion Inc.) has also been proposed for biphasic dissolution experiments to study precipitation. The inForm setup employs a fibre optic UV dip probe to measure drug concentration in real time, and uses a potentiometric pH probe to monitor pH of the media in real time to facilitate *in situ* pH control. Biphasic experiments have been carried out using the inForm on a range of acidic, basic and neutral compounds using a solvent shift process.[39] Drugs were initially dissolved using DMSO to prepare a concentrated stock solution and samples were
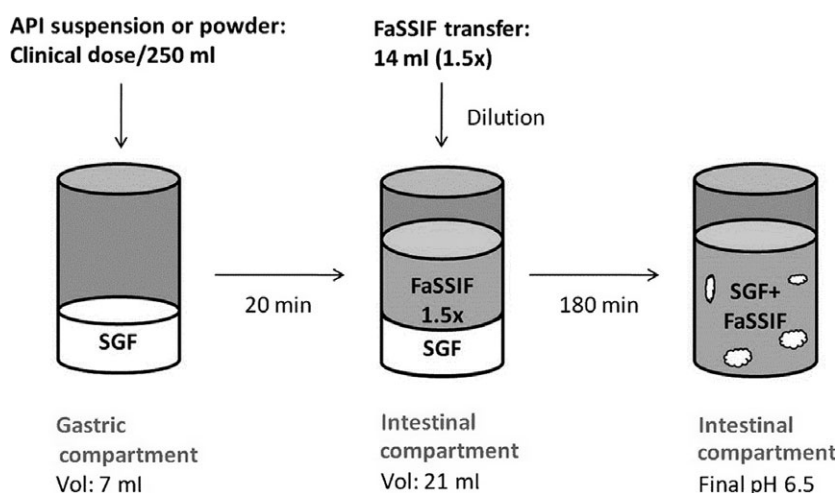

Figure 3 Schematic of the experiment carried out by Mathias *et al.*[36] Reprinted (adapted) with permission from Mathias *et al.* Copyright 2013 American Chemical Society.
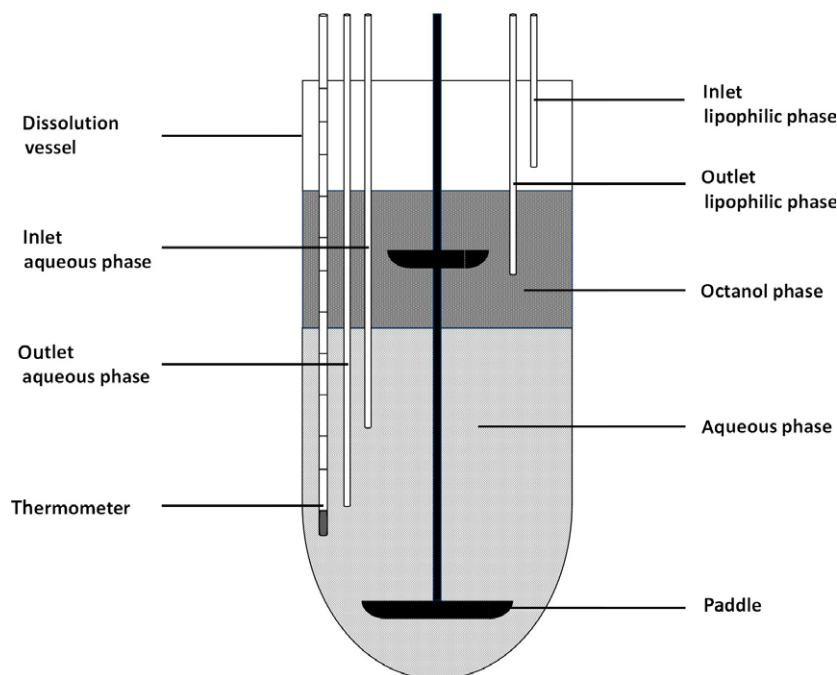
Figure 4 Schematic of the miBldi-pH apparatus.[38] Reproduced with permission from Elsevier.

added using an automatic liquid handling needle into the aqueous layer. The aqueous layer consisted of 40 ml of an acetate-phosphate buffer at pH 6.5, while the organic layer consisted of 30 ml of decanol. All the neutral and basic drugs were found to precipitate when injected into the aqueous layer at a dose level of 10 mg. Fenofibrate, a neutral compound, was added at two dose levels: 5 and 10 mg. Precipitation was observed at both dosing levels and the quantity of drug which partitioned into the lipid layer, was the same after 1 h. This indicated that in both cases fenofibrate rapidly precipitated to its equilibrium solubility in the aqueous layer and only dissolved fenofibrate was able to partition across from the aqueous into the lipid layer. To date, published data with respect to biphasic dissolution experiments using the inForm setup with a pH shift is very limited.[40]

Compartmental methods using non-cellular biomimetic membranes

A two-chamber system has been proposed by Pion Inc. called the µFlux.[41] Drug concentrations in both the donor and acceptor chambers can be measured by fibre optic UV probes. A membrane separates the two chambers and a biomimetic membrane coated with lipids, which is a scaled-up version of the parallel artificial membrane permeability assay (PAMPA) membrane, is typically used. Uptake through the membrane into the acceptor chamber aims to represent drug absorption *in vivo*. Incorporation of an absorption step helps

to improve the biorelevance compared with single chamber systems, as drug absorption can generate sink conditions in the donor chamber, which is beneficial when assessing drug precipitation. Zhu *et al.*,[42] used the µFlux apparatus to study the effect of an increased gastric pH on the kinetic profiles of many drugs, including ketoconazole and nilotinib, as shown in Figure 5. Initially 400 µl of drug suspension was added to 7 ml of SGF in the donor chamber. The pH of SGF was either at pH 2 or pH 6, simulating typical gastric pH and acid suppression, respectively. The acceptor chamber was filled with 21 ml of an acceptor sink buffer (ASB). After 20 min, 14 ml of 1.5 times concentrated Level II FaSSIF solution was added to the donor chamber and the concentrations in both chambers were monitored for 160 min. The resulting FaSSIF solution in the donor chamber had a pH of 6.5. In the experiment simulating normal gastric pH, ketoconazole maintained a supersaturated state for at least 20 min after addition of the concentrated FaSSIF and readily partitioned across the membrane into the acceptor compartment. In contrast, nilotinib was only transiently supersaturated after the addition of the FaSSIF solution in the experiment simulating normal gastric pH and appeared to precipitate quickly. The smaller surface area of the biomimetic membrane compared with the human intestine hampers the transfer of drug from the donor into the acceptor chamber. Therefore, precipitation may be overestimated in the donor chamber. This limitation must be considered when mimicking the relationship between absorption and precipitation using the µFlux.
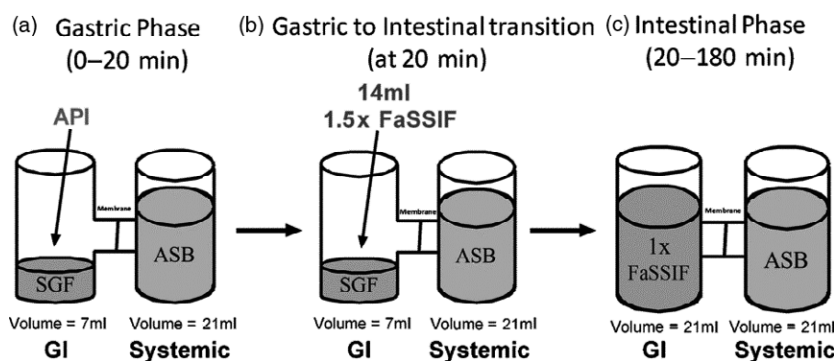
Figure 5 Schematic of dissolution-permeation experimental setup (μFlux apparatus) used by Zhu *et al.*[42] ASB, Acceptor Sink Buffer. Reproduced with permission from Springer.

Sironi *et al.*,[43] investigated a dissolution/permeation system using an Ussing chamber with a Permeapad® acting as an intestinal barrier between the acceptor and donor side. Permeapad® consists of a thin layer of soy phosphatidylcholine on a hydrophilic support sheet. A good correlation has been achieved between the permeability coefficients found using Permeapad® with those using Caco-2 cells ($R^2 = 0.75$)[44] and the PAMPA membrane ($R^2 = 0.76$). The volume of media in donor and acceptor compartments was 7 and 6 ml, respectively. Phosphate-buffered saline (pH 7.35–7.45) was used as both acceptor and donor media. Hydrocortisone (BCS class II) suspension and hydrocortisone methanolate tablets were tested using this setup. For the suspension, a constant rate of permeation into the acceptor chamber was observed. This constant flux indicated that permeation through the membrane was the rate-limiting step. In contrast, the tablets had a variable rate of permeation through the membrane for the initial 3 h of the experiment. As the concentration plateaued in the donor chamber approaching equilibrium solubility after 3 h, a linear increase of drug was subsequently observed in the acceptor chamber. The area to volume ratio (0.25 cm^2/ml) in this experiment was a limiting factor when trying to achieve a substantial decrease in donor chamber drug concentrations within a reasonable period of time. The authors calculated that it would take an area to volume ratio of 5.9 cm^2/ml to achieve a 90% permeation of hydrocortisone into the acceptor chamber within 4 h. The inter-laboratory variability of these biomimetic membranes needs to be further investigated. The compatibility of the Permeapad® membrane with surfactants, co-solvents and biorelevant media,[45] and ability to be used over a long duration, up to 94.5 h in the experiment, are advantages compared with cellular membranes, such as Caco-2. To evaluate this setup's usefulness in assessing drug precipitation in the upper fasted small intestine, further

studies must be carried out incorporating a pH shift from gastric to intestinal media.

Compartmental methods using cellular membranes

Ginski *et al.*,[46] proposed a 'two-step' dissolution/Caco-2 system with the aim of simulating simultaneous dissolution and absorption in the GIT. This would enable prediction of the dissolution-absorption relationship for different compounds and allow a comparison with results from clinical studies. This continuous system consisted of a dissolution apparatus and a side-by-side diffusion cell. The drug is dissolved in the dissolution compartment and, after a filtration with a 10 μm filter, is transferred with a pump to a donor compartment, containing the Caco-2 monolayer. In this particular study, fast and slow dissolving formulations of piroxicam, metoprolol tartrate and ranitidine hydrochloride were tested. Generally, this two-step setup was able to reflect the qualitative dissolution-absorption relationships. This setup can be considered as a first attempt to couple dissolution with permeation through Caco-2 cell lines, although it is obvious that several more factors would need to be considered. For example, the lack of appropriate first-order gastric emptying, GI transfer and the level of biorelevance of the media need to be taken into account to better simulate the *in vivo* drug absorption and accurately predict plasma concentrations.

Kobayashi *et al.*,[47] proposed a system for predicting drug absorption using Caco-2 cells, which also accounted for the pH change from the stomach to the intestine. The drug was dissolved in a vessel that simulates the stomach (pH 1.0, volume of medium 3 ml) and a pump transferred the dissolved drug to a vessel (pH 6.0, volume of medium 3 ml) for pH adjustment. The solution with the adjusted pH was then transferred

to the compartment containing the Caco-2 monolayer. The same setup was also used by Sugawara *et al.*,[48] where additionally the effect of pH change in the 'gastric vessel' (i.e. simulating achlorhydria or patients administered with proton pump Inhibitors or H2-receptor antagonists) was evaluated. Significant differences were found in the cumulative permeation of two albendazole formulations at raised and normal gastric pH in this experiment. These results qualitatively agreed with a previous rabbit study carried out using the same albendazole formulations.[49] However, the culturing time required for the Caco-2 cells limits the throughput capacity of this method. Issues concerning the poor reproducibility of results, and incompatibility with some solubilising excipients (e.g. surfactants) and some media (e.g. Level II FeSSIF) also further limit the use of Caco-2 cell monolayers as intestinal barriers in studies examining intestinal precipitation.[45]

In the same logic of assessing simultaneously dissolution and permeation through cell monolayers, Kataoka *et al.*,[50] introduced a dissolution/permeation system (D/P), which consisted of an apical and basolateral compartment mounted with a Caco-2 monolayer. The volume of apical and basolateral compartments was 8 and 5.5 ml, respectively. Magnetic stirrers were placed in both compartments and Hanks balanced salt solution issued in both sides as a transport medium. Kataoka *et al.*,[51] utilised the same technique but improved its biorelevance using a modified Hank's balanced salt solution containing sodium taurocholate (3 mM) and lecithin (0.75 mM) as a transfer medium. Overall, the D/P system was proposed to be a useful tool for formulation selection during drug development.[52] Nonetheless, it is mainly used for powders or suspensions and despite the use of a more biorelevant transfer medium, the D/P system is far from properly mimicking *in vivo* conditions, such as hydrodynamics, fluid volumes, GI transfer etc. Furthermore, to the best of our knowledge, it has not been used to study precipitation or supersaturation kinetics.

Full-scale methods to assess drug precipitation

In late stages of formulation development, where larger amounts of the API are available, full-scale methods and setups are required to accurately characterise and predict the behaviour of the formulation, after administration of clinically relevant doses. These full-scale techniques aim to evaluate the supersaturation or precipitation of the drug product and to help understand the effect of different excipients on its kinetics. The main goal is to link the bioavailability of the drug product to the amount of drug

which is in solution in the upper small intestine, where absorption mainly takes place.

Compendial apparatus and methods

USP I and USP II dissolution apparatus and methods

The basket (USP I) and paddle (USP II) apparatus were first introduced into the United States Pharmacopeia in the 1970s for evaluating the dissolution characteristics of oral drug products.[53] They have primarily been used to fulfil a QC function for testing a variety of oral dosage forms[54] and provide a large volume of media for a dosage form to dissolve in a well-stirred environment.[55] Dissolution testing using either the USP I or USP II apparatus is conducted under various parameters and conditions, including variations in hydrodynamics, type and volume of dissolution medium.[56] Typically the volumes used in the basket/paddle apparatus range from 500 to 1000 ml and these large volumes are often useful to generate sink conditions required to achieve complete dissolution. However, they are far in excess of volumes in the human stomach and intestine, which do not typically exceed 250 ml in the fasted stomach and 30–100 ml in the fasted upper small intestine.[57,58]

The simple aqueous buffers typically used in the USP methods reflect the composition of the GI contents to a limited extent. This can lead to a misinterpretation of the *in vivo* dissolution profile, where supersaturation, precipitation and re-dissolution might occur. Apart from the pharmacopoeial buffers, different levels of biorelevant media can be used for simulating the composition of the GI fluids. Biorelevant media have demonstrated advantages over compendial media when assessing drug performance *in vivo*.[22,59,60] Wagner *et al.*,[60] carried out an experiment comparing the use of compendial and biorelevant media with the USP II apparatus for Compound A, a basic BCS class IV drug. It was found to have a much greater solubility and dissolution rate constant (*z* value) in biorelevant media representing the upper fasting intestine, compared with simple media at the same pH. The STELLA® software was used to model the predicted drug plasma profiles from the dissolution data and a stronger correlation to the human *in vivo* data was observed from the profiles predicted from the dissolution experiments using biorelevant media.

The transfer process from the stomach through different parts of the intestine is not taken into consideration when using the compendial USP I and USP II dissolution methods. This process is important for IR formulations of weak bases, as the drug might precipitate as it enters the small intestine, and for MR formulations, which are commonly designed to deliver the drug to distal, as well as proximal sites of the GIT.
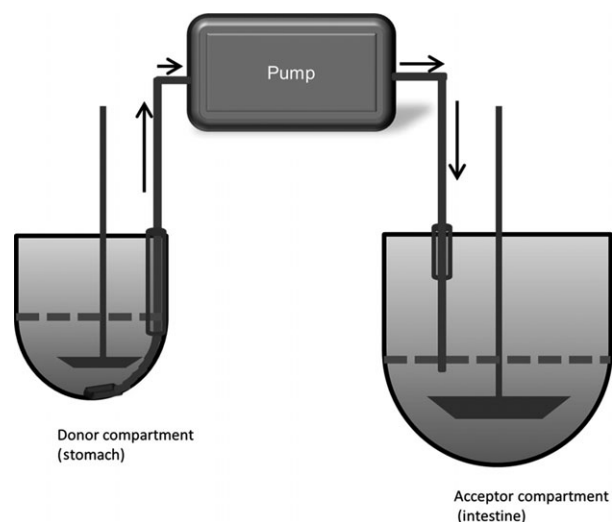
Figure 6 The 'transfer model' proposed by Ruff *et al.*[64] Reproduced with permission from Elsevier.

The 'dumping test'

Kambayashi *et al.*,[61] proposed a simple pH-shift test, the so-called dumping test, in which 50 ml solutions of two weak bases, dipyridamole and ketoconazole, in 0.02 N HCl at various concentrations were 'dumped' into 450 ml of FaSSIF-V2. In this case, Level II FaSSIF-V2 had higher concentration of sodium taurocholate and lecithin, so after 'dumping' of the drug solutions, the final concentrations of sodium taurocholate and lecithin in the dissolution vessel corresponded to the composition of Level II FaSSIF-V2. The results from this *in vitro* setup were successfully coupled with STELLA® software and a predictive model for the total and dissolved concentration in small intestine for both drugs, after oral administration in the fasted state was established. The advantage of this simple approach is that it could be used as an early assessment and pre-screening tool for drug precipitation during early stages in drug product development to facilitate the design and development of new drug products. The performance of this method as a screening tool and its possible preference over the more complicated transfer methods should be further investigated, especially when solid dosage forms are considered.

Compartment methods not addressing intestinal absorption

Closed systems

It was Kostewicz *et al.*,[62] who first introduced the so-called transfer model, which simulates the transfer of drug from the stomach to the upper small intestine. This setup is a two compartment compendial dissolution

method where contents of the vessel, in which dosage form's performance under simulated gastric conditions (donor compartment) is evaluated, are transferred with a pump into another vessel, where the conditions in the small intestine are simulated (acceptor compartment) (Figure 6). In that study, the donor compartment containing the dissolved drug in 125 ml SGF was transferred at a constant rate between 0.5 and 9.0 ml/min (values within the observed physiological range) into the acceptor compartment 500 ml Level II FaSSIF. The results indicated that a combination of data collected with the transfer model, solubility data and dissolution data should lead to better prediction of the *in vivo* behaviour of poorly soluble weak bases. Furthermore, it was clear that gastric emptying rates may play an important role on the precipitation kinetics. Such effects of the transfer rate can be considered by mathematical modelling as it has been proposed for the *in vitro* transfer test by Arnold *et al.*[63] The classical transfer test was here used together with an on-line particle analyser and in-line Raman spectroscopy to study the kinetics of drug precipitation. A nucleation and growth model was used at two transfer rates (4 and 9 ml/min) and experimental results for dipyridamole were in good agreement with the model.

Due to the shortcomings of the initial transfer model, such as the zero order rate of drug pumping from the donor compartment to the acceptor compartment, Ruff *et al.*,[64] attempted to optimise the experimental conditions of the originally proposed transfer model, using ketoconazole as model compound. In this study, the 'average' physiological GI conditions were taken into consideration, while the impact of extreme conditions was also evaluated. To reflect fasting gastric emptying behaviour *in vivo,* a first-order transfer rate with half-life of 9 min was used. Generally, the optimised transfer model by Ruff *et al.* was successful in simulating the *in vivo* dosage form performance. Nonetheless, one disadvantage of this model is that it fails to take the absorption process into consideration, which might be crucial to whether precipitation occurs or not, and thus also in determining drug plasma concentrations. It was concluded that this *in vitro* model over-predicted the precipitation behaviour of ketoconazole. The authors also mention that for BCS Class II compounds, which have high or moderate permeability values, *in vivo* precipitation may be reduced due to the continuous *in vivo* absorption of the drug through the intestinal mucosa. This may not apply to BCS Class IV drugs with low permeability characteristics, where possible precipitation seriously affects the amount of drug available for absorption. To circumnavigate the lack of absorption in the *in vitro* model, the authors coupled the results obtained with the transfer model to a PBPK model, where absorption was taken into account. With

this approach not only was precipitation shown not to occur in the intestinal compartment, but the plasma profile was accurately simulated in humans.

Open systems

The artificial stomach duodenal (ASD) model has two chambers representing the stomach and the duodenum. In the standard setup, the gastric and duodenal chambers have a maximum capacity of 400 and 50 ml, respectively,[65] with fluid transfer controlled by a series of five pumps, accounting for stomach and duodenal secretions and chamber emptying. The initial starting volumes in the chambers, the flow rate of fresh media into the chambers and the emptying rate from the chambers can all be adjusted to fit the experimental requirements (e.g. *in vitro* modelling of fasted/fed state, human or dog model).[65–68] Dilute HCl and Level II FaSSIF are typically used as gastric and duodenal fluid, respectively. Dissolution is the primary process which occurs in the ASD's gastric and duodenal chambers. However, concurrent precipitation can also occur in these chambers. The ASD model has been used to examine the relative bioavailability of various drugs.[65,66,69] When assessing the performance of the weakly basic drug galunisertib, the ASD showed that the formulations maintained supersaturation upon transition into the duodenal chamber and that no significant precipitation occurred throughout the experiment (150 min).[67] To account for the information obtained from the ASD model in the absorption modelling, a precipitation time of 11 h was estimated by the GastroPlus® software. This estimate exceeds the usual small intestine transit times which are observed *in vivo* and confirms that galunisertib could maintain supersaturation in the small intestine for a longer period than 15 min, which is the default value used in GastroPlus® when no experimental data are available. Combining the ASD data and other biopharmaceutical results (e.g. permeability) as inputs for GastroPlus®, the simulated plasma concentration profiles for the three tablet formulations were found to have AUCs of between 90% and 105% of the observed human clinical data. The model was able to successfully rank the *in vivo* bioavailability of the different formulations of galunisertib used in the clinical trials. The ASD model was also used to check the effect of gastric pH on LY2157299, a weakly basic BCS class II drug, which had showed variability of absorption in early studies carried out in dogs.[68] Compared with humans, dogs have a larger variability of basal gastric pHs, which can be a source of error when assessing the *in vivo* performance of drugs with a pH-dependent solubility in dogs. To model the variability in dog gastric pH, experiments were carried out in the ASD using gastric fluid at pH 2 and pH 4.5, using 10^{-2} N HCl

or 10^{-4} N HCl, respectively. While the ASD model was able to qualitatively predict the effect of variability of stomach pH on the bioavailability of LY2157299, it overestimated the influence of the raised gastric pH on the absorption of LY2157299.

Takeuchi *et al.*,[70] evaluated the performance of a three-compartment setup (Gastrointestinal Simulator-GIS) for predicting *in vivo* dissolution and precipitation. The three compartments of the GIS represent the stomach, the duodenum and the jejunum, where different buffer species, volumes and pH values were used to mimic the *in vivo* conditions. The fluid transfer rate from the gastric to the duodenal compartment was set at a first-order rate with a half-life between 5 and 10 min. In this particular setup, paddles were adjusted to give a high-speed burst at certain intervals to simulate the contractions in the stomach and the duodenum. Gastroplus® software was used to determine the *in vitro* gastric emptying time, which provided the best fit to *in vivo* data for two BCS Class I drugs, propranolol and metoprolol. Overall, the GIS was able to predict the *in vivo* performance of the investigated compounds. The GIS setup was also used by Matsui *et al.*,[71] to investigate the impact of elevated gastric pH. When coupled with *in silico* modelling GIS could be useful for assessing *in vivo* precipitation of BCS Class II weakly basic compounds, but incorporation of an absorptive site, to mimic the continuous drug removal from the intestine, might be beneficial for enhancing its *in vivo* predictability.

A slightly modified form of the GIS (mGIS), was used by Tsume *et al.*,[72] to investigate the absorption kinetics of the weakly basic drug dasatinib. In this study, the *in vitro* results from the dissolution experiments performed in the USP apparatus II and mGIS, were coupled with Gastroplus® to predict plasma concentrations. The predicted plasma profiles were compared with clinical data. The dissolution profiles of dasatinib acquired with the USP apparatus II did not indicate precipitation and resulted in absorption profiles, which did not match the human data. On the other hand, the dissolution profiles acquired with the mGIS exhibited supersaturation and precipitation of dasatinib and, when coupled with Gastroplus®, resulted in better plasma concentration predictions. Despite the fact that the PBPK model underestimated the overall Cmax and AUC, something that could be partially attributed to underestimated permeability values, the study clearly demonstrated the benefit of assessing drug supersaturation or precipitation with a more complex setup. Tsume *et al.*,[73] have used also the GIS to assess the supersaturation/precipitation kinetics of the two weakly basic compounds; dipyridamole and ketoconazole. For both compounds, and in accordance to previous studies,[10,62,64,74] the precipitation rates observed in the

intestinal compartments of GIS were overestimated, most likely due to lack of an absorptive compartment. This study highlighted once more the importance of accounting also for the absorption process when assessing precipitation with various setups *in vitro*.

Compartment methods which attempt to account of absorption

Although models which do not account for the intestinal absorption process can be useful in predicting *in vivo* drug supersaturation or precipitation, the *in vivo* performance of a drug product is highly dependent not only on the GI transfer, but also on other important parameters, such as the intestinal permeability. As mentioned previously, for drugs with high or moderate permeability values, *in vitro* setups can overpredict *in vivo* precipitation as the sink conditions created by continuous removal of the drug through the gut wall are not simulated *in vitro*. To account for drug absorption in the *in vitro* experiment, a number of models have been setup.

Using appropriate flow rates to take into account both absorption and transit process

These methods have been proposed primarily for evaluating products of highly permeable APIs.

Psachoulias *et al.*,[74] introduced a three-compartment setup for the prediction of intraluminal precipitation of

ketoconazole and dipyridamole. This setup consisted of a gastric, a duodenal and a reservoir compartment. The reservoir compartment contained concentrated Level II biorelevant medium with the purpose of keeping pH values, lecithin and bile salt concentrations constant in the duodenal compartment, thereby compensating for the dilution that occurs when the simulating gastric fluid is pumped into the duodenal compartment. During each experiment, the volume of the medium in the duodenal compartment was kept constant at 60 ml. The flow rates between the compartments were regulated by a multi-channel peristaltic pump and a first order gastric emptying rate of 15 min was used. The contents of the duodenal compartment were completely renewed with fresh medium every 15 min. Using this experimental setup the measured *in vitro* duodenal compartment concentrations were in line with the luminal concentrations measured in healthy volunteers in previously performed clinical studies.[10,75] Dose-dependent *in vitro* precipitation was observed for ketoconazole. However, XRPD studies indicated differences in the solid state characteristics of the precipitates; *in vitro* the precipitate of ketoconazole was crystalline, but *in vivo* it was amorphous. Despite the good results presented with this methodology, the equipment is not commercially available, thus restricting its application in the pharmaceutical industry.

Recently, Kourentas *et al.*,[76] introduced a new setup (biorelevant gastrointestinal transfer system-BioGIT) for simulating GI transfer and assessing duodenal concentrations, drug supersaturation or precipitation of highly
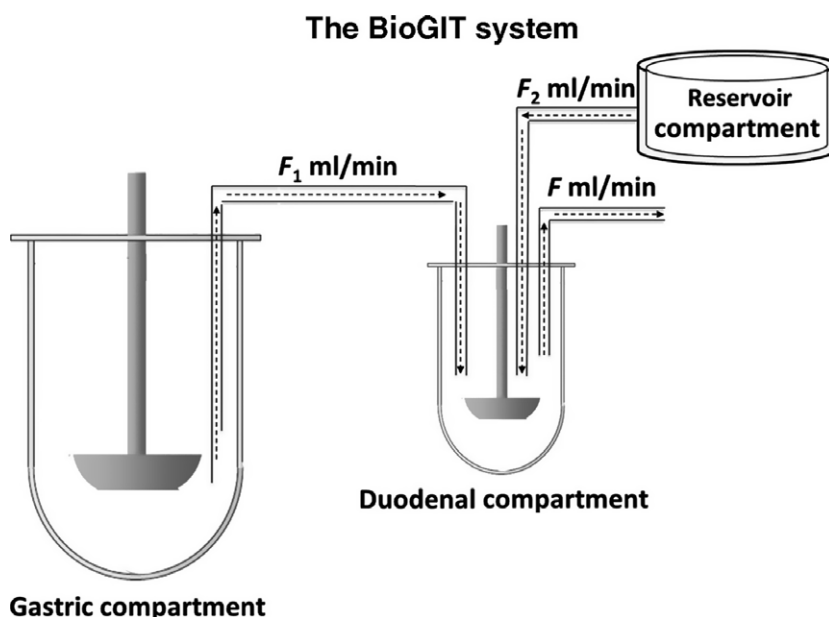

Figure 7 The BioGIT system proposed by Kourentas *et al.*[76] F_1 and F_2 are the incoming flow rates and F is the outgoing flow rate ($F = F_1 + F_2$). Reproduced with permission from Elsevier.

permeable APIs, using commercially available equipment. This setup also consists of three compartments: gastric, duodenal and reservoir compartment (Figure 7). The reservoir compartment is used for maintaining the composition of the medium in the duodenal compartment constant. Gastric emptying half-life is 15 min. The volume of the dissolution medium in the gastric compartment is 250 ml (10 ml resting volume, plus 240 ml to account for administration with a glass of water) and the volume of the duodenal compartment is set at 40 ml. Fluid from the duodenal compartment is moved away with a constant flow rate of 11.6 ml/min, so that the volume in the duodenal compartment is kept constant throughout the experiment. These flow rate and
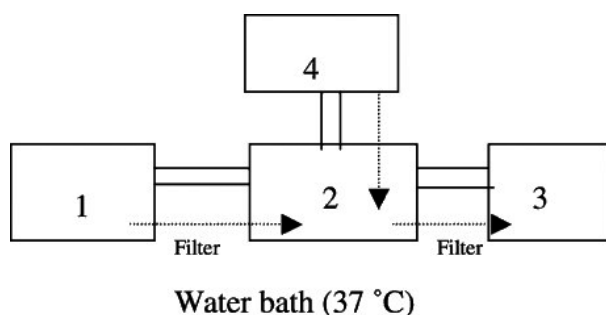

Figure 8 Multicompartment dissolution system by Gu *et al.*[82] Vessel 1 'gastric' compartment simulating the stomach conditions; Vessel 2: 'intestinal' compartment simulating the intestinal conditions; Vessel 3: 'absorption' compartment simulating absorption; Vessel 4: reservoir vessel containing the dissolution medium identical to that in Vessel 2. Reproduced with permission from Elsevier.

volumetric values were estimated from luminal data previously collected from healthy adults. In this study, the ability of the BioGIT model to predict intraluminal concentrations of dipyridamole, ketoconazole and posaconazole was evaluated. With the BioGIT setup the precipitated fraction *in vivo* was successfully predicted in every case.[77,78] The method has been shown to be useful for providing information on the impact of GI transfer on intraluminal concentrations of drugs, which are given as fast disintegrating tablets and capsules, dispersions or solutions. Recently, BioGIT data were successfully used for informing PBPK modelling software and predicting the plasma profile of a moderately precipitating salt of weak base.[79] However, one should note here, that BioGIT has been designed to simulate intraluminal concentrations of highly permeable drugs, after administration in the fasted state. Therefore, flow rates might need to be adjusted to simulate concentrations of drugs with different permeability characteristics.[80] Evaluation of intra- and inter-laboratory reproducibility of BioGIT data is currently in process.[81]

Utilising a similar approach, based on the compendial dissolution apparatus II, Gu *et al.*,[82] described a multi-compartmental model with four compartments, comprising of a gastric, intestinal, absorption and a reservoir compartment, to maintain the composition in the intestinal compartment (Figure 8). The novelty of this setup was the addition of the 'absorption compartment', to simulate the uptake of drug across the intestinal membrane. All compartments were placed in a water bath at 37 °C temperature and the pH in each vessel was maintained at a constant
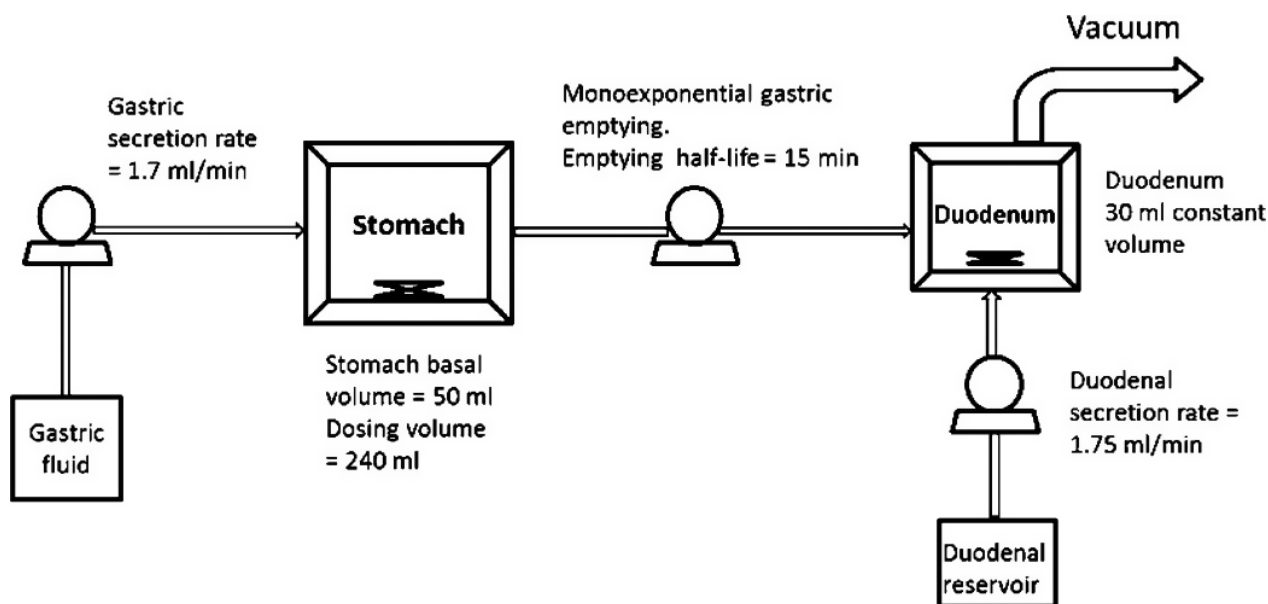

Figure 9 Schematic diagram of the simulated stomach duodenum model (SSD).[8] Reprinted (adapted) with permission from Mitra *et al.* Copyright 2014 American Chemical Society.

value. The drug was transferred with different flow rates between the compartments, the volumes of which were kept constant and controlled by a peristaltic pump. Vessel 1 contained 250 ml of dissolution medium to simulate the available volume of gastric fluids in the stomach in the fasted state. Vessel 2 contained 250 ml of dissolution medium, simulating the composition of the upper small intestine, and after the inflow from vessel 1 for 1 h the volume in vessel 2 increased to 500 ml. Vessel 3 contained 600 ml of ethanol and 100 ml of 0.1 N HCl solution to maintain drug concentrations below their solubility values throughout the experiment. In this study, the precipitation kinetics of two weak bases, cinnarizine and dipyridamole was investigated. It was concluded that this method could successfully predict drug precipitation in the lumen, and the results from this multi-compartmental system correlated better with the *in vivo* data compared with the conventional dissolution methods. Cinnarizine and dipyridamole were found to have significantly different precipitation characteristics, despite both being fully dissolved at gastric pH. Approximately 40% of the cinnarizine was found to precipitate in the intestinal vessel compared to <10% of the dipyridamole dose. The setup from Gu *et al.*, simulates the absorption process in a simple dissolution apparatus and no complex additions/methods are needed. Furthermore, the flow rates between the intestinal and absorption compartments can be adjusted to reflect different permeability values, thus facilitating its use in the investigation of precipitation kinetics for APIs with different permeability properties. One issue may be the use of filter during the transfer of contents from vessel 1 to vessel 2. Also, a challenge of this setup is that it is difficult to adjust the flow rates to the absorption compartment so that they would correlate with *in vivo* permeability values.

Mitra *et al.*,[8] proposed yet another setup to simulate the dynamic environment of the GIT; the 'simulated stomach duodenum' model (SSD) (Figure 9). The SSD model was modelled after the system described by Carino *et al.*,[66] (Section Open systems) and it is a four-compartment model, where the removal of drug from the duodenum is also taken into account. The study explored the ability of the SSD to predict the supersaturation of different dose strengths of dipyridamole under fasted conditions, as well as to investigate the impact of different surfactants, which are commonly used in oral preparations. In the SSD model, basal volumes in both gastric and duodenal compartment were used, based on mean fluid volumes previously reported in clinical studies in fasted adults. The basal gastric volume was set at 50 ml and the duodenal at 30 ml. The gastric emptying was simulated by a first-order pattern with a half-life of 15 min, until the basal gastric volume was restored. Afterwards, the gastric emptying was kept constant at 1.7 ml/min. The setup was able to predict the

supersaturation kinetics of dipyridamole when compared with *in vivo* data. Furthermore, the effect of different surfactants commonly used in oral preparations, as well as the effect of different gastric emptying patterns on dipyridamole supersaturation was investigated. The SSD model provided good correlation of the amount of drug in solution in the duodenal compartment of the SSD to the bioavailability of different dosage strengths of dipyridamole *in vivo*. However, again this setup does not take into account the application of different flow rates to adjust for low permeability values. Furthermore, the SSD model is not based on a commercially available setup, such as the USP II dissolution apparatus, and agitation is performed using magnetic stirrers at 200 rpm, which entails hydrodynamics that are less reproducible and not physiologically relevant. To investigate its usefulness in predicting drug precipitation, more studies with different compounds are needed.

Another multicompartment method incorporating a chamber simulating the systemic circulation was proposed by Selen *et al.*,[83] The FloVitro™ (Dow Chemicals, Midland, MI, USA) is a three compartment system with chambers simulating the gastric, intestinal and systemic compartments (cells) and flow rates between cells. The fluid volume in the cells varies depending on the compound tested; typically 40 ml in the gastric cell, 200 ml in the intestinal cell and 1–2 l in the systemic cell are used. The primary use of the FloVitro™ has been to predict the *in vivo* plasma profile based on the profile which is achieved in the systemic cell using a variety of drugs, including ibuprofen, furosemide, paracetamol and doxycycline hydrochloride.[83,84] The effect of fed or fasted state media has also been examined on the dissolution profiles of danazol and furosemide.[85] However, there have not been any publications to date illustrating its application to precipitation of poorly soluble weak bases and further studies will need to be undertaken.

Simulating the intestinal epithelial barrier

Motz *et al.*,[86] introduced a system which consists of the flow through dissolution apparatus (USP apparatus IV) and a flow through permeation module. The latter includes an open apical and a closed basolateral compartment with a Caco-2 monolayer between them. The flow rates of the dissolution medium which was transferred from the USP IV to the permeation module had to be carefully adjusted, to assure the viability and integrity of the Caco-2 cell membrane. Indeed, the authors suggested the use of a stream splitter, which successfully allowed the combination of compendial and commercially available USP apparatus IV with a permeation/Caco-2 compartment. Krebs buffer was chosen as the dissolution and permeation buffer for the

installation of this apparatus. While the use of biorelevant dissolution media could be more physiologically relevant and perhaps produce better results, the authors acknowledged that a first evaluation of this new setup was the initial scope of the study. Even though the Caco-2 cell monolayers is a useful *in vitro* technique to assess drug permeation and allows good predictions of *in vivo* drug permeability,[87–89] their implementation in methods for assessing precipitation in the donor compartment may not be straightforward, as also mentioned above in the presentation of small scale methods to assess precipitation. These limitations include different cultures of Caco-2 cells resulting in data variability, difficulty in predicting paracellular transport as a result of tighter junctions between the colonic cells and long period of time required for cell culture.[90] The lower surface area for the Caco-2 cell line compared with the intestinal membrane is also disadvantageous when examining the relationship between precipitation and absorption.

As mentioned previously, an alternative to the absorptive cell monolayers for simulating drug absorption is through the use of biphasic media.[91–93] In this case, the drug is dissolved in the aqueous phase and partitions in the organic phase. The drug concentration profile that is acquired from the organic phase could be an effective surrogate of the amount of drug available for absorption. Vagani *et al.*,[94] developed a system by combining biphasic media and a flow through (USP IV) technique. In particular, the USP apparatus IV is combined with a USP II apparatus. The cells from the USP IV apparatus are used to hold the formulations and the dissolution vessels from the USP II apparatus contain the biphasic dissolution media, maintained at 37 °C. This system has also been used by Shi *et al.*[95] Overall, this system established good IVIVC with the drug concentrations obtained in the organic phase and the biopharmaceutical performance of the different formulations was well discriminated. Tsume *et al.*,[96] combined the gastrointestinal simulator (GIS) introduced by Takeuchi *et al.*, with biphasic media to investigate whether the addition of the organic layer would lead to better predictions of the plasma concentrations of two poorly soluble, weakly basic compounds, raloxifene and ketoconazole. Indeed, the results of ketoconazole showed slower decline of drug concentration in the small intestinal compartments with the presence of the organic phase, than those without the addition of the biphasic system, thus providing another calculated precipitation rate constant. Incorporation of these data to physiologically based pharmacokinetic (PBPK) models and simulation with Gastroplus® suggested a slight improvement in the *in vivo* predictions of ketoconazole. The combination of GIS with an organic layer provided also information about the partitioning characteristics of these two drugs to the organic phase.
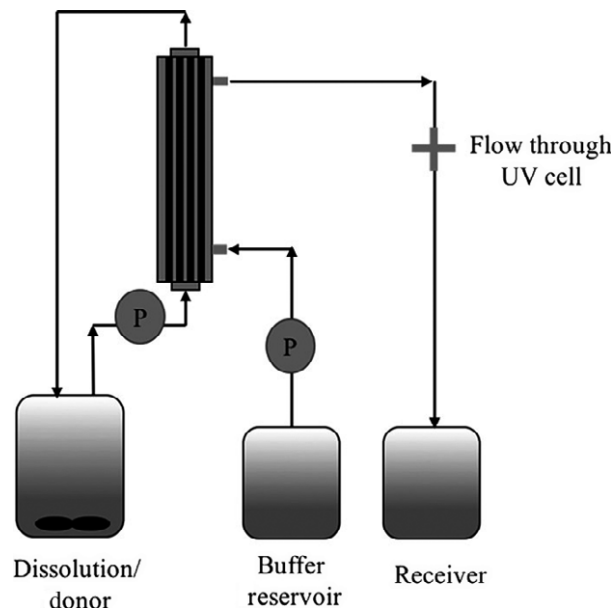

Figure 10 Schematic of the apparatus used by Hate *et al.*[97] The hollow fibre membrane is represented by the grey and black tube. Reprinted (adapted) with permission from Hate *et al.* Copyright 2017 American Chemical Society.

To account for the absorption process, Hate *et al.*,[97] developed an apparatus coupled with a high surface membrane area. The apparatus consisted of a donor compartment, where drug dissolution takes place, a buffer reservoir and a receiver chamber, to collect drug after diffusion through the membrane (Figure 10). A hollow fibre membrane was used to simulate intestinal absorption, due to its high surface area per unit volume of fluid, thus facilitating higher mass transfer. A pump is used to control the transfer of fluid. In particular, fluid from the donor compartment is transferred to the inner side of the hollow membrane, where at the same time fluid from the reservoir compartment is transferred to the outer side of the hollow membrane. The drug diffused through the membrane into the fresh buffer, which was collected into the receiver chamber. The donor fluid emerging from the membrane module was then recycled back into the donor chamber. Three different formulations of the weakly basic drug nevirapine were tested using this apparatus. Initially, the media in the donor chamber was 0.1 M HCL. After 30 min, the pH was adjusted to pH 6.5 using 0.17 M Na_2HPO_4 and the absorption system was connected. When assessing the performance of nevirapine tablets and powder, rapid precipitation of nevirapine down to its equilibrium solubility was observed in the donor compartment, upon transition to pH 6.5. When a precipitation inhibitor (HPMC-AS) was used, there was no precipitation observed in the donor chamber for up to 160 min, while an increase in drug concentration was observed in the receiver chamber. However,
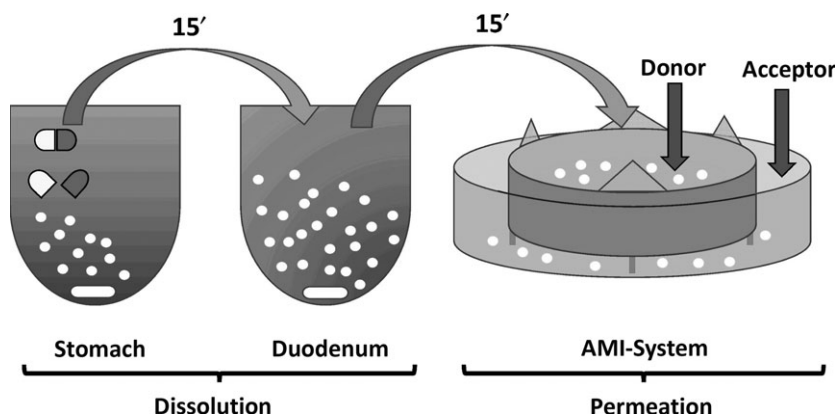
Figure 11 Schematic of the AMI-system proposed by Berben *et al.*[99] Reproduced with permission from Elsevier.

no significant differences were observed in the dissolution profiles, when the performance of nevirapine tablet, with or without the addition of the absorption membrane was assessed. Overall, the apparatus could be a useful tool for formulation screening and for assessing drug precipitation or supersaturation. However, more data is needed to support its further application.

The artificial membrane insert system (AMI system) was proposed by Berben *et al.*,[98] as a method to simulate the passive absorption of drug in the intestine without the use of cells based systems, such as Caco-2. The AMI system consists of a regenerated cellulose membrane mounted between two plastic rings, as shown in Figure 11,[98] and has shown comparable results to Caco-2 cells when assessing the permeability coefficients of poorly soluble drugs. To study the interplay between supersaturation, precipitation and absorption, Berben *et al.*,[99] carried out an experiment to examine the potential of the AMI system using loviride, posaconazole, itraconazole and fenofibrate. Initially, samples were added to Level II fasted state simulated gastric fluid (FaSSGF) with constant stirring at 300 rpm, with magnetic stirrers. After 15 min, the acidic medium was added to concentrated Level II FaSSIF. Following another 15-min period of stirring, a sample of the intestinal fluid (665 µl) was added to the donor side of the AMI system. In the case of loviride, the meta-stabilised supersaturated state resulted in higher concentrations of drug in the acceptor compartment, whereas lower concentrations of drug were found in the acceptor chamber when precipitation was induced. An enhanced permeation into the acceptor compartment was also observed for posaconazole when it was administered as an acidified suspension compared with a neutral suspension using the AMI system (concentration at 120 min: acidified suspension: 1.12 ± 0.01 nmol and neutral suspension: 0.44 ± 0.01 nmol). This trend corresponded to an *in vivo* study carried out by Hens *et al.*,[12] which found a twofold increase in AUC_{0-8h} following

administration of the acidified suspension vs the neutral suspension. When evaluating the performance of the AMI system using three different bio-enabling formulations: Sporanox® solution (itraconazole), Lipanthyl® capsules and Lipanthylnano® tablets (fenofibrate), the drug concentrations achieved in the acceptor compartment of the AMI system were qualitatively well correlated with the respective intraluminal drug concentrations. However, further validation of the setup is required with other compounds. Overall, the AMI system when coupled with the two-stage dissolution test proved to be a useful early screening tool in assessing the possible *in vivo* precipitation of APIs as well as the performance of formulated drug products.

Finally, the TNO TIM-1 is a computer controlled multi-compartmental model of the human GIT. It was developed by the TNO Nutrition and Food Research centre based on data from *in vivo* human studies[100] and simulates the dynamic digestive and physiological processes in the stomach and small intestine.[101] The TIM-1 system models the absorption of small molecules through their uptake from filtration membrane systems or dialysis in the ileal and jejunal sections of the system. In this way, the amount of drug in solution which is available for absorption (expressed as 'bioaccessibility') can be measured. However, some active processes such as active absorption, efflux and intestinal metabolism are not modelled by this system. It has been suggested that the TNO TIM-1 system can be coupled with other intestinal absorption systems to facilitate modelling of these processes, thus enabling an estimation of oral bioavailability of compounds.[102] The majority of studies carried out with the TIM-1 have focused on the absorption of nutritional compounds and there are only a limited number of published studies focusing on the uptake of pharmaceutical compounds.[103–106] The biorelevance of the TIM-1 system would indicate significant potential to model precipitation of drug in the GIT. However, the time required for set up and the

limited throughput are significant limitations when considering its potential use as a tool to predict *in vivo* precipitation.

Recently, Van Den Abeele *et al.*,[107] have used an updated version of TIM-1 (TIMagc) with the aim of investigating the intraluminal behaviour of diclofenac in the fasted and fed state. The results obtained from the *in vitro* setup were compared with intraluminal and systemic data collected from healthy volunteers after the administration of diclofenac tablets along with 240 ml of water. The data obtained with this method can suggest slow dissolution or precipitation of diclofenac in the stomach, but it was not possible to mechanistically discern between these two mechanisms. The potential of TIM-1 to assess precipitation in the upper small intestine must be further investigated using weakly basic drugs and bio-enabling formulations.

Coupling full scale *in vitro* testing with physiologically based pharmacokinetic modelling

Physiologically based pharmacokinetic modelling has been widely used and rapidly developed in the last years with many applications in academia and in the pharmaceutical industry. Furthermore PBPK modelling has gained acceptance at various regulatory agencies as part of the submission package. In 2016 the Committee for Medicinal Products for Human Use (CHMP) of EMA and FDA published a draft guidance regarding the qualification of PBPK modelling, concerning its use to support marketing authorisation.[108,109] This guidance aims to provide general information on which details should be included in a PBPK modelling report and which elements are needed in order for a PBPK platform to be qualified and evaluated for an intended purpose. Generally, PBPK modelling can be used for the prediction of human PK profiles from preclinical data and it is a useful tool for evaluating and optimising a clinical trial design. It can also be utilised for extrapolating the drug's pharmacokinetic behaviour in healthy volunteers to patient populations, where clinical studies are difficult to be conducted. In order for a successful drug model to be built using the 'bottom-up' approach, the quality of the input data is of high importance.[110] Coupling *in vitro* data with *in silico* methods can be very important in optimising and validating both *in vitro* and *in silico* models. Commercially available software, such as Simcyp® Simulator and Gastroplus®, or open source and in-house modelling platforms can incorporate *in vitro* data of supersaturation and precipitation kinetics. This can then lead to a better understanding of the importance of supersaturation or precipitation *in vivo*. In many cases, combination of the *in silico* and *in vitro* methods to assess supersaturation and precipitation

has proven to be successful.[61,111–113] Gastroplus® software handles precipitation by incorporating a mean precipitation time. This parameter is the mean time for particles to precipitate from solution, when the local concentration exceeds the drug solubility and it is a function of luminal pH. Default precipitation time is 900 s, which was determined from exponential fit to the dipyridamole transfer data, published by Kostewicz *et al.*[62] Certara® recently introduced the 'Simcyp *In Vitro* Data Analysis Toolkit-SIVA' which is designed to model *in vitro* experiments and estimate parameters for input to *in vivo* simulations with the mechanistic PBPK Simcyp® Simulator. For modelling supersaturation and precipitation, SIVA and Simcyp® Simulator use an empirical approach based on critical supersaturation concentration and precipitation rate constant obtained in *in vitro* experiments.[111] One issue with the available software is that they rely mostly on precipitation kinetics which at best have been estimated with non-validated *in vitro* setups. Validation of *in vitro* methodologies should ideally be based on intraluminal data in humans. It should also be noted that it is difficult to build a successful, validated model which can predict the behaviour of a drug *in vivo*, especially for BCS II, III and IV drugs.[114] Nonetheless, coupling *in vitro* data with *in silico* models can help also to optimise the *in vitro* techniques which are currently being used and understand which are the critical parameters for drug supersaturation and precipitation.

Conclusions

The increasing prevalence of poorly soluble drugs and use of bio-enabling formulations to achieve supersaturated states *in vivo* has triggered great interest in *in vitro* precipitation modelling. Overall, much progress has been made from the standard equipment used in QC testing and various *in vitro* models have been developed. Small-scale tests are beneficial, especially in early stage of drug development, as drug quantities are often limited. Employing a small-scale approach also facilitates the rapid parallel screening of multiple prospective formulations. Multicompartment models have proven useful to evaluate precipitation of drug upon transfer from the gastric to the intestinal environment. However, it would be reasonable to state that no single *in vitro* test is suitable for modelling precipitation in all circumstances. Further progress is still to be made to improve the predictive capabilities of such models, especially in terms of simulating the absorption of drug along the intestinal lumen. Coupling the results of *in vitro* tests with PBPK modelling has significant potential and must be investigated further. Improving the biopharmaceutics tools to predict *in vivo* precipitation will be a key step to improving the efficacy and reducing the development costs of medicines.

Declaration

Acknowledgements

References

1. Paulekuhn GS *et al.* Trends in active pharmaceutical ingredient salt selection based on analysis of the orange book database. *J Med Chem* 2007; 50: 6665–6672.

2. Bevernage J *et al.* Evaluation of gastrointestinal drug supersaturation and precipitation: strategies and issues. *Int J Pharm* 2013; 453: 25–35.

3. Augustijns P, Brewster ME. Supersaturating drug delivery systems: fast is not necessarily good enough. *J Pharm Sci* 2012; 101: 7–9.

4. Kalepu S, Nekkanti V. Insoluble drug delivery strategies: review of recent advances and business prospects. *Acta Pharm Sin B* 2015; 5: 442–453.

5. Kawakami K. Modification of physicochemical characteristics of active pharmaceutical ingredients and application of supersaturatable dosage forms for improving bioavailability of poorly absorbed drugs. *Adv Drug Deliv Rev* 2012; 64: 480–495.

6. Brewster ME *et al.* Comparative interaction of 2-hydroxypropyl-β-cyclodextrin and sulfobutylether-β-cyclodextrin with itraconazole: phase-solubility behavior and stabilization of supersaturated drug solutions. *Eur J Pharm Sci* 2008; 34: 94–103.

7. Gao P, Shi Y. Characterization of supersaturatable formulations for improved absorption of poorly soluble drugs. *AAPS J* 2012; 14: 703–713.

8. Mitra A, Fadda HM. Effect of surfactants, gastric emptying, and dosage form on supersaturation of dipyridamole in an in vitro model simulating the stomach and duodenum. *Mol Pharm* 2014; 11: 2835–2844.

9. Jakubiak P *et al.* Development of a unified dissolution and precipitation model and its use for the prediction of oral drug absorption. *Mol Pharm* 2016; 13: 586–598.

10. Psachoulias D *et al.* Precipitation in and supersaturation of contents of the upper small intestine after administration of two weak bases to fasted adults. *Pharm Res* 2011; 28: 3145–3158.

11. Rubbens J *et al.* Gastrointestinal dissolution, supersaturation and precipitation of the weak base indinavir in healthy volunteers. *Eur J Pharm Biopharm* 2016; 109: 122–129.

12. Hens B *et al.* Supersaturation and precipitation of posaconazole upon entry in the upper small intestine in humans. *J Pharm Sci* 2016; 105: 2677–2684.

13. Hens B *et al.* Gastrointestinal and systemic monitoring of posaconazole in humans after fasted and fed state administration of a solid dispersion. *J Pharm Sci* 2016; 105: 2904–2912.

14. Kourentas A *et al.* Effectiveness of supersaturation promoting excipients on albendazole concentrations in upper gastrointestinal lumen of fasted healthy adults. *Eur J Pharm Sci* 2016; 91: 11–19.

15. Bevernage J *et al.* Supersaturation in human gastric fluids. *Eur J Pharm Biopharm* 2012; 81: 184–189.

16. Griffin BT *et al.* Comparison of in vitro tests at various levels of complexity for the prediction of in vivo performance of lipid-based formulations: case studies with fenofibrate. *Eur J Pharm Biopharm* 2014; 86: 427–437.

17. Kuentz M. Analytical technologies for real-time drug dissolution and precipitation testing on a small scale. *J Pharm Pharmacol* 2015; 67: 143–159.

18. Klein S, Shah VP. A standardized mini paddle apparatus as an alternative to the standard paddle. *AAPS PharmSciTech* 2008; 9: 1179–1184.

19. Klein S. The mini paddle apparatus – a useful tool in the early developmental stage? Experiences with immediate-release dosage forms *Dissolution Technol* 2006; 13: 6–11.

20. Alsenz J *et al.* Development of a partially automated solubility screening (PASS) assay for early drug development. *J Pharm Sci* 2007; 96: 1748–1762.

21. Dai WG. In vitro methods to assess drug precipitation. *Int J Pharm* 2010; 393: 1–16.

22. Markopoulos C *et al.* In-vitro simulation of luminal conditions for evaluation of performance of oral drug products: choosing the appropriate test media. *Eur J Pharm Biopharm* 2015; 93: 173–182.

23. Chandran S *et al.* A high-throughput spectrophotometric approach for evaluation of precipitation resistance. *J Pharm Biomed Anal* 2011; 56: 698–704.

24. Yamashita T *et al.* Solvent shift method for anti-precipitant screening of poorly soluble drugs using biorelevant medium and dimethyl sulfoxide. *Int J Pharm* 2011; 419: 170–174.

25. Petruševska M *et al.* Evaluation of a high-throughput screening method for the detection of the excipient-mediated precipitation inhibition of poorly soluble drugs. *Assay Drug Dev Technol* 2013; 11: 117–129.

26. Petruševska M *et al.* Evaluation of the light scattering and the turbidity microtiter plate-based methods for the detection of the excipient-mediated drug precipitation inhibition. *Eur J Pharm Biopharm* 2013; 85 (3, Part B):1148–1156.

27. Christfort JF *et al.* Development of a video-microscopic tool to evaluate

the precipitation kinetics of poorly water soluble drugs: a case study with tadalafil and HPMC. *Mol Pharm* 2017; 14: 4154–4160.

28. Tsinman K *et al.* Powder dissolution method for estimating rotating disk intrinsic dissolution rates of low solubility drugs. *Pharm Res* 2009; 26: 2093–2100.

29. Avdeef A *et al.* Miniaturization of powder dissolution measurement and estimation of particle size. *Chem Biodivers* 2009; 6: 1796–1811.

30. Palmelund H *et al.* Studying the propensity of compounds to supersaturate: a practical and broadly applicable approach. *J Pharm Sci* 2016; 105: 3021–3029.

31. Plum J *et al.* Investigation of the intra- and interlaboratory reproducibility of a small scale standardized supersaturation and precipitation method. *Mol Pharm* 2017; 14: 4161–4169.

32. Klein S *et al.* Miniaturized transfer models to predict the precipitation of poorly soluble weak bases upon entry into the small intestine. *AAPS PharmSciTech* 2012; 13: 1230–1235.

33. Alsenz J *et al.* Miniaturized intrinsic dissolution screening (MINDISS) assay for preformulation. *Eur J Pharm Sci* 2016; 87: 3–13.

34. Box KJ *et al.* Small-scale assays for studying dissolution of pharmaceutical cocrystals for oral administration. *AAPS PharmSciTech* 2016; 17: 245–251.

35. Gravestock T *et al.* The "GI dissolution" method: a low volume, in vitro apparatus for assessing the dissolution/precipitation behaviour of an active pharmaceutical ingredient under biorelevant conditions. *Anal Methods* 2011; 3: 560–567.

36. Mathias NR *et al.* Assessing the risk of pH-dependent absorption for new molecular entities: a novel in vitro dissolution test, physicochemical analysis, and risk assessment strategy. *Mol Pharm* 2013; 10: 4063–4073.

37. Frank KJ *et al.* In vivo predictive mini-scale dissolution for weak bases: advantages of pH-shift in combination with an absorptive compartment. *Eur J Pharm Sci* 2014; 61: 32–39.

38. Locher K *et al.* Evolution of a mini-scale biphasic dissolution model: impact of model parameters on partitioning of dissolved API and modelling of in vivo-relevant kinetics. *Eur J Pharm Biopharm* 2016; 105(Supplement C): 166–175.

39. Watson H *et al.* Biphasic Dissolution Studies of Poorly Water Soluble Drugs. AAPS Annual Meeting 2016; poster No. 24W0130. Available at: http://abstracts.aaps.org/Verify/AAPS2016/PosterSubmissions/24W0130.pdf.

40. O'Dwyer PJ *et al.* Small Scale Biphasic Dissolution Testing of Itraconazole Formulations with a pH Shift. UKICRS Annual Meeting 2018.

41. Tsinman K, Tsinman O. Dissolution-permeability Apparatus with Integrated In Situ Concentration Monitoring of both Donor and Receiver Compartments. AAPS Annual Meeting 2013; poster No. W5300.

42. Zhu AZX *et al.* Utilizing in vitro dissolution-permeation chamber for the quantitative prediction of pH-dependent drug-drug interactions with acid-reducing agents: a comparison with physiologically based pharmacokinetic modeling. *AAPS J* 2016; 18: 1512–1523.

43. Sironi D *et al.* Evaluation of a dynamic dissolution/permeation model: mutual influence of dissolution and barrier-flux under non-steady state conditions. *Int J Pharm* 2017; 522: 50–57.

44. Di Cagno M *et al.* New biomimetic barrier Permeapad™ for efficient investigation of passive permeability of drugs. *Eur J Pharm Sci* 2015; 73: 29–34.

45. Bibi HA *et al.* Permeapad™ for investigation of passive drug permeability: the effect of surfactants, co-solvents and simulated intestinal fluids (FaSSIF and FeSSIF). *Int J Pharm* 2015; 493: 192–197.

46. Ginski MJ *et al.* Prediction of dissolution-absorption relationships from a continuous dissolution/Caco-2 system. *AAPS PharmSci* 1999; 1: E3.

47. Kobayashi M *et al.* Development of a new system for prediction of drug absorption that takes into account drug dissolution and pH change in the gastro-intestinal tract. *Int J Pharm* 2001; 221: 87–94.

48. Sugawara M *et al.* The use of an in vitro dissolution and absorption system to evaluate oral absorption of two weak bases in pH-independent controlled-release formulations. *Eur J Pharm Sci* 2005; 26: 1–8.

49. Kohri N *et al.* Improving the oral bioavailability of albendazole in rabbits by the solid dispersion technique. *J Pharm Pharmacol* 1999; 51: 159–164.

50. Kataoka M *et al.* In vitro system to evaluate oral absorption of poorly water-soluble drugs: simultaneous analysis on dissolution and permeation of drugs. *Pharm Res* 2003; 20: 1674–1680.

51. Kataoka M *et al.* Application of dissolution/permeation system for evaluation of formulation effect on oral absorption of poorly water-soluble drugs in drug development. *Pharm Res* 2012; 29: 1485–1494.

52. Takano R *et al.* Integrating drug permeability with dissolution profile to develop IVIVC. *Biopharm Drug Dispos* 2012; 33: 354–365.

53. Dokoumetzidis A, Macheras P. A century of dissolution research: from Noyes and Whitney to the biopharmaceutics classification system. *Int J Pharm* 2006; 321: 1–11.

54. Kostewicz ES *et al.* In vitro models for the prediction of in vivo performance of oral dosage forms. *Eur J Pharm Sci* 2014; 57: 342–366.

55. McAllister M. Dynamic dissolution: a step closer to predictive dissolution testing? *Mol Pharm* 2010; 7: 1374–1387.

56. Dressman JB, Krämer J. *Pharmaceutical Dissolution Testing*. Boca Raton, FL: Taylor & Francis, 2005.

57. Schiller C *et al.* Intestinal fluid volumes and transit of dosage forms as assessed by magnetic resonance imaging. *Aliment Pharmacol Ther* 2005; 22: 971–979.

58. Mudie DM *et al.* Quantification of gastrointestinal liquid volumes and distribution following a 240 mL dose of water in the fasted state. *Mol Pharm* 2014; 11: 3039–3047.

59. Hamlin WE *et al.* Relationship between in vitro dissolution rates and

solubilities of numerous compounds representative of various chemical species. *J Pharm Sci* 1965; 54: 1651–1653.

60. Wagner C *et al.* Predicting the oral absorption of a poorly soluble, poorly permeable weak base using biorelevant dissolution and transfer model tests coupled with a physiologically based pharmacokinetic model. *Eur J Pharm Biopharm* 2012; 82: 127–138.

61. Kambayashi A *et al.* Prediction of the precipitation profiles of weak base drugs in the small intestine using a simplified transfer ("dumping") model coupled with in silico modeling and simulation approach. *Eur J Pharm Biopharm* 2016; 103: 95–103.

62. Kostewicz ES *et al.* Predicting the precipitation of poorly soluble weak bases upon entry in the small intestine. *J Pharm Pharmacol* 2004; 56: 43–51.

63. Arnold YE *et al.* Advancing in-vitro drug precipitation testing: new process monitoring tools and a kinetic nucleation and growth model. *J Pharm Pharmacol* 2011; 63: 333–341.

64. Ruff A *et al.* Prediction of Ketoconazole absorption using an updated in vitro transfer model coupled to physiologically based pharmacokinetic modelling. *Eur J Pharm Sci* 2017; 100: 42–55.

65. Carino SR *et al.* Relative bioavailability of three different solid forms of PNU-141659 as determined with the artificial stomach-duodenum model. *J Pharm Sci* 2010; 99: 3923–3930.

66. Carino SR *et al.* Relative bioavailability estimation of carbamazepine crystal forms using an artificial stomach-duodenum model. *J Pharm Sci* 2006; 95: 116–125.

67. Ding X *et al.* Assessment of in vivo clinical product performance of a weak basic drug by integration of in vitro dissolution tests and physiologically based absorption modeling. *AAPS J* 2015; 17: 1395–1406.

68. Bhattachar SN *et al.* Effect of gastric pH on the pharmacokinetics of a BCS class II compound in dogs: utilization of an artificial stomach and duodenum dissolution model and GastroPlus,™ simulations to predict absorption. *J Pharm Sci* 2011; 100: 4756–4765.

69. Kobayashi Y *et al.* Physicochemical properties and bioavailability of carbamazepine polymorphs and dihydrate. *Int J Pharm* 2000; 193: 137–146.

70. Takeuchi S *et al.* Evaluation of a three compartment in vitro gastrointestinal simulator dissolution apparatus to predict in vivo dissolution. *J Pharm Sci* 2014; 103: 3416–3422.

71. Matsui K *et al.* In vitro dissolution of fluconazole and dipyridamole in gastrointestinal simulator (GIS), predicting in vivo dissolution and drug-drug interaction caused by acid-reducing agents. *Mol Pharm* 2015; 12: 2418–2428.

72. Tsume Y *et al.* In vitro dissolution methodology, mini-Gastrointestinal Simulator (mGIS), predicts better in vivo dissolution of a weak base drug, dasatinib. *Eur J Pharm Sci* 2015; 76: 203–212.

73. Tsume Y *et al.* The impact of supersaturation level for oral absorption of BCS class IIb drugs, dipyridamole and ketoconazole, using in vivo predictive dissolution system: Gastrointestinal Simulator (GIS). *Eur J Pharm Sci* 2017; 102: 126–139.

74. Psachoulias D *et al.* An in vitro methodology for forecasting luminal concentrations and precipitation of highly permeable lipophilic weak bases in the fasted upper small intestine. *Pharm Res* 2012; 29: 3486–3498.

75. Dimopoulou M *et al.* In-vitro evaluation of performance of solid immediate release dosage forms of weak bases in upper gastrointestinal lumen: experience with miconazole and clopidogrel salts. *J Pharm Pharmacol* 2016; 68: 579–587.

76. Kourentas A *et al.* An in vitro biorelevant gastrointestinal transfer (BioGIT) system for forecasting concentrations in the fasted upper small intestine: design, implementation, and evaluation. *Eur J Pharm Sci* 2016; 82: 106–114.

77. Kourentas A *et al.* Evaluation of the impact of excipients and an albendazole salt on albendazole concentrations in upper small intestine using an in vitro biorelevant gastrointestinal transfer (BioGIT) system. *J Pharm Sci* 2016; 105: 2896–2903.

78. Kourentas A *et al.* In vitro evaluation of the impact of gastrointestinal transfer on luminal performance of commercially available products of posaconazole and itraconazole using BioGIT. *Int J Pharm* 2016; 515: 352–358.

79. Kesisoglou F *et al.* Physiologically based absorption modeling of salts of weak bases based on data in hypochlorhydric and achlorhydric biorelevant media. *AAPS PharmSciTech* 2018. https://doi.org/10.1208/s12249-018-1059-3. [Epub ahead of print].

80. Hens B *et al.* Gastrointestinal transfer: in vivo evaluation and implementation in in vitro and in silico predictive tools. *Eur J Pharm Sci* 2014; 63: 233–242.

81. Barmpatsalou V *et al.* Biorelevant Gastrointestinal Transfer (BioGIT) System: Evaluation of Data Reproducibility and Its Usefulness in Estimating Indinavir and Fosamprenavir Concentrations in the Upper Intestinal Lumen after Oral Administration of Immediate Release Dosage Forms. Available at: http://abstracts.aaps.org/Verify/AAPS2017/PosterSubmissions/T6019.pdf.

82. Gu CH *et al.* Using a novel multicompartment dissolution system to predict the effect of gastric pH on the oral absorption of weak bases with poor intrinsic solubility. *J Pharm Sci* 2005; 94: 199–208.

83. Selen A *et al.* Exploring Suitability and Feasibility of a Novel In Vitro Dissolution System. AAPS Annual Meeting 2008; poster No. R6313.

84. Selen A *et al.* Exploring Sensitivity and Robustness of FloVitro® Technology a Novel in vitro Dissolution System. AAPS Annual Meeting 2010; poster No. T3047.

85. Selen A *et al.* Application of FloVitroTM Technology to Evaluate Dissolution of Furosemide and Danazol in Simulated Media at Fed and Fasted Conditions. AAPS Annual Meeting 2011; poster No. W5274.

86. Motz SA *et al.* Permeability assessment for solid oral drug formulations based on Caco-2 monolayer in combination with a flow through dissolution cell. *Eur J Pharm Biopharm* 2007; 66: 286–295.

87. Hidalgo IJ *et al.* Characterization of the human colon carcinoma cell line (Caco-2) as a model system for intestinal epithelial permeability. *Gastroenterology* 1989; 96: 736–749.

88. Artursson P, Karlsson J. Correlation between oral drug absorption in humans and apparent drug permeability coefficients in human intestinal epithelial (Caco-2) cells. *Biochem Biophys Res Commun* 1991; 175: 880–885.

89. Yamashita S *et al.* Analysis of drug permeation across Caco-2 monolayer: implication for predicting in vivo drug absorption. *Pharm Res* 1997; 14: 486–491.

90. Sun H *et al.* The Caco-2 cell monolayer: usefulness and limitations. *Expert Opin Drug Metab Toxicol* 2008; 4: 395–411.

91. Hoa NT, Kinget R. Design and evaluation of two-phase partition-dissolution method and its use in evaluating artemisinin tablets. *J Pharm Sci* 1996; 85: 1060–1063.

92. Grundy JS *et al.* Studies on dissolution testing of the nifedipine gastrointestinal therapeutic system. I. Description of a two-phase in vitro dissolution test. *J Control Release* 1997; 48: 1–8.

93. Gabriëls M, Plaizier-Vercammen J. Design of a dissolution system for the evaluation of the release rate characteristics of artemether and dihydroartemisinin from tablets. *Int J Pharm* 2004; 274: 245–260.

94. Vangani S *et al.* Dissolution of poorly water-soluble drugs in biphasic media using USP 4 and fiber optic system. *Clin Res Regul Aff* 2009; 26: 8–19.

95. Shi Y *et al.* Application of a biphasic test for characterization of in vitro drug release of immediate release formulations of celecoxib and its relevance to in vivo absorption. *Mol Pharm* 2010; 7: 1458–1465.

96. Tsume Y *et al.* The combination of GIS and biphasic to better predict in vivo dissolution of BCS class IIb drugs, ketoconazole and raloxifene. *J Pharm Sci* 2018; 107: 307–316.

97. Hate SS *et al.* Absorptive dissolution testing of supersaturating systems: impact of absorptive sink conditions on solution phase behavior and mass transport. *Mol Pharm* 2017; 14: 4052–4063.

98. Berben P *et al.* Assessment of passive intestinal permeability using an artificial membrane insert system. *J Pharm Sci* 2018; 107: 250–256.

99. Berben P *et al.* The artificial membrane insert system as predictive tool for formulation performance evaluation. *Int J Pharm* 2018; 537: 22–29.

100. Minekus M *et al.* Multicompartmental dynamic computer-controlled model simulating the stomach and small intestine. *Altern to Lab Anim ATLA* 1995; 23: 197–209.

101. Blanquet S *et al.* A dynamic artificial gastrointestinal system for studying the behavior of orally administered drug dosage forms under various physiological conditions. *Pharm Res* 2004; 21: 585–591.

102. Déat E *et al.* Combining the dynamic TNO-gastrointestinal tract system with a Caco-2 cell culture model: application to the assessment of lycopene and α-tocopherol bioavailability from a whole food. *J Agric Food Chem* 2009; 57: 11314–11320.

103. Larsson M *et al.* Estimation of the bioavailability of iron and phosphorus in cereals using a dynamic in vitro gastrointestinal model. *J Sci Food Agric* 1997; 74: 99–106.

104. Verwei M *et al.* Predicted serum folate concentrations based on in vitro studies and kinetic modeling are consistent with measured folate concentrations in humans. *J Nutr* 2006; 136: 3074–3078.

105. Krul C *et al.* Application of a dynamic in vitro gastrointestinal tract model to study the availability of food mutagens, using heterocyclic aromatic amines as model compounds. *Food Chem Toxicol* 2000; 38: 783–792.

106. Raskin I, Yousef GGGM. Distribution of ingested berry polyphenolics. *J Agric Food Chem* 2013; 60: 5763–5771.

107. Van Den Abeele J *et al.* Gastrointestinal and systemic disposition of diclofenac under fasted and fed state conditions supporting the evaluation of *in vitro* predictive tools. *Mol Pharm* 2017; 14: 4220–4232.

108. European Medicines Agency. *Guideline on the Qualification and Reporting of Physiologically Based Pharmacokinetic (PBPK) Modelling and Simulation Guideline on the Qualification and Reporting of Physiologically Based Pharmacokinetic (PBPK) Modelling and Simulation*, Vol. 44. London, UK: European Medicines Agency, 2016: 1–18.

109. Food and Drug Administration. *Physiologically Based Pharmacokinetic Analyses — Format and Content Guidance for Industry*. Silver Spring, MD: Food and Drug Administration, 2016.

110. Margolskee A *et al.* IMI – oral biopharmaceutics tools project – evaluation of bottom-up PBPK prediction success part 2: an introduction to the simulation exercise and overview of results. *Eur J Pharm Sci* 2017; 96: 610–625.

111. Hens B *et al.* *In silico* modeling approach for the evaluation of gastrointestinal dissolution, supersaturation, and precipitation of posaconazole. *Mol Pharm* 2017; 14: 4321–4333.

112. Ruff A *et al.* Evaluating the predictability of the in vitro transfer model and in vivo rat studies as a surrogate to investigate the supersaturation and precipitation behaviour of different Albendazole formulations for humans. *Eur J Pharm Sci* 2017; 105: 108–118.

113. Sjögren E *et al.* *In silico* modeling of gastrointestinal drug absorption: predictive performance of three physiologically based absorption models. *Mol Pharm* 2016; 13: 1763–1778.

114. Hansmann S *et al.* Forecasting oral absorption across biopharmaceutics classification system classes with physiologically based pharmacokinetic models. *J Pharm Pharmacol* 2016; 68: 1501–1515.

Combining biorelevant *in vitro* and *in silico* tools to simulate and better understand the *in vivo* performance of a nano-sized formulation of aprepitant in the fasted and fed states

Chara Litou[a], Nikunjkumar Patel[b], David B. Turner[b], Edmund Kostewicz[a], Martin Kuentz[c], Karl J. Box[d], Jennifer Dressman[a],*

[a] *Institute of Pharmaceutical Technology, Goethe University, Frankfurt am Main, Germany*
[b] *Certara UK Limited, Simcyp Division, Level 2-Acero, 1 Concourse Way, Sheffield S1 2BJ, UK*
[c] *University of Applied Sciences and Arts Northwestern Switzerland, Gründenstr. 40, 4132, Switzerland*
[d] *Pion Inc. (UK) Ltd., Forest Row, East Sussex, UK*

ARTICLE INFO

ABSTRACT

Introduction: When developing bio-enabling formulations, innovative tools are required to understand and predict *in vivo* performance and may facilitate approval by regulatory authorities. EMEND® is an example of such a formulation, in which the active pharmaceutical ingredient, aprepitant, is nano-sized. The aims of this study were 1) to characterize the 80 mg and 125 mg EMEND® capsules *in vitro* using biorelevant tools, 2) to develop and parameterize a physiologically based pharmacokinetic (PBPK) model to simulate and better understand the *in vivo* performance of EMEND® capsules and 3) to assess which parameters primarily influence the *in vivo* performance of this formulation across the therapeutic dose range.

Methods: Solubility, dissolution and transfer experiments were performed in various biorelevant media simulating the fasted and fed state environment in the gastrointestinal tract. An *in silico* PBPK model for healthy volunteers was developed in the Simcyp Simulator, informed by the *in vitro* results and data available from the literature.

Results: *In vitro* experiments indicated a large effect of native surfactants on the solubility of aprepitant. Coupling the *in vitro* results with the PBPK model led to an appropriate simulation of aprepitant plasma concentrations after administration of 80 mg and 125 mg EMEND® capsules in both the fasted and fed states. Parameter Sensitivity Analysis (PSA) was conducted to investigate the effect of several parameters on the *in vivo* performance of EMEND®. While nano-sizing aprepitant improves its *in vivo* performance, intestinal solubility remains a barrier to its bioavailability and thus aprepitant should be classified as DCS IIb.

Conclusions: The present study underlines the importance of combining *in vitro* and *in silico* biopharmaceutical tools to understand and predict the absorption of this poorly soluble compound from an enabling formulation. The approach can be applied to other poorly soluble compounds to support rational formulation design and to facilitate regulatory assessment of the bio-performance of enabling formulations.

1. Introduction

In recent years there has been increasing interest from various regulatory authorities in facilitating earlier access to innovative medicines, without compromising their safety and/or efficacy. Indeed, EMA and FDA have taken initiatives to accelerate the approval of innovative medicines which address unmet medical needs (European Medicines Agency, 2016; Press Announcements, 2018; Information for Consumers (Drugs), 2015). On the other hand, the development of new drug products has become more demanding due to the implementation of stricter safety and quality requirements (Parekh et al., 2015). Contributing further to long development times are the increasingly challenging properties of new active pharmaceutical ingredients (APIs), which make formulation development more difficult and pose a significant barrier to drug absorption and clinical efficacy. Indeed, although about 40% of APIs in marketed drug products exhibit poor

solubility and/or permeability, almost 90% of APIs in early drug development stages are saddled with these undesirable characteristics (Kalepu and Nekkanti, 2015; Lipinski, 2000). In response to these issues, the European Research Program "PEARRL" (www.pearrl.eu) aims to 1) develop creative bio-enabling formulations, 2) establish, validate and optimize innovative biopharmaceutical *in vitro* tools and 3) understand and predict the *in vivo* behavior of various drug products with physiologically-based pharmacokinetic (PBPK) modeling and simulation.

As part of the PEARRL consortium, the present research aims to link the results obtained using biorelevant *in vitro* tools with *in silico* PBPK models to simulate and better understand the *in vivo* performance of the marketed formulation of aprepitant in the fasted and fed states. Aprepitant is a selective substance P neurokinin (NK1) receptor antagonist which, in combination with other antiemetic agents, is indicated for the prevention of both acute and delayed nausea and vomiting associated with emetogenic cancer chemotherapy (EMA, 2009; FDA, 2003). It is available as oral capsules (40, 80 and 125 mg), under the brand name EMEND® (reference listed product) and as a water soluble prodrug form, fosaprepitant dimeglumine, for intravenous administration (EMEND® for injection) (EMA, 2009). For ambulant therapy, EMEND® is administered for three days with a recommended dosing regimen of 125 mg orally once on Day 1 and 80 mg orally once daily on Days 2 and 3 (EMA, 2009).

Aprepitant has both very weak acidic and very weak basic properties and possesses a logD of 4.8 at pH 7.0 (Shono et al., 2010; Kesisoglou and Mitra, 2012; Wu et al., 2004; Georgaka et al., 2017; Sjögren et al., 2016). According to Wu et al. (2004) it exhibits very low aqueous solubility (3–7 μg/mL over the pH range 2–10), although solubilities of just 0.37 μg/mL and 0.8 μg/mL in phosphate buffers at pH 6.5 were reported by Söderlind et al. (2010) and Takano et al. (2008), respectively. In line with the expected protonation behavior, Niederquell and Kuentz recently concluded that aprepitant acts like a neutral compound at small intestinal pH (Niederquell and Kuentz, 2018). Concurrently, solubility values of 13 μg/mL in Human Intestinal Fluids (HIF) (Söderlind et al., 2010) and of 21 μg/mL in media simulating the canine fasted small intestine [FaSSIF$_{dog}$, 5 mM sodium taurocholate (NaTc), 1.25 mM lecithin] (Takano et al., 2008) have been reported, suggesting a pronounced effect of native surfactants on the solubility of aprepitant.

With regard to the permeability of aprepitant, a wide range of permeability values from Caco-2 assays has been reported in the open literature, including a P_{app} of 7.8×10^{-6} cm/s (no reference substance value provided) (Kesisoglou and Mitra, 2012; Wu et al., 2004), a P_{app} of 170×10^{-6} cm/s (no reference substance value provided) (Sjögren et al., 2016), or a P_{app} of 21×10^{-6} cm/s with metoprolol as a reference compound ($P_{app} = 5 \times 10^{-6}$ cm/s) (Takano et al., 2008). Due to its permeability and solubility properties, aprepitant has been classified as a borderline BCS II/IV compound (Shono et al., 2010; Kesisoglou and Mitra, 2012).

The aprepitant tablet formulations used in the early clinical phases exhibited high variability and a large food effect on absorption. Considering the target patient group addressed by aprepitant (cancer patients suffering from nausea and vomiting), administration with food was deemed unacceptable and, therefore, the next formulation efforts were focused on attenuating the food effect and improving dissolution characteristics. This was accomplished by decreasing the particle size to the nanoscale range (approx. 200 nm) (EMA, 2009; FDA, 2003). As illustrated *e.g.* by the study of Shono et al. (2010) nano-sizing aprepitant proved to be a successful strategy for reducing the food effect over the clinical dose range (FDA, 2003). After administration of the EMEND® 80 mg and 125 mg capsules (the currently marketed formulation), the absolute bioavailability under fasting conditions is 67% (62–73%) and 59% (53–65%), respectively. In the therapeutic dose range a standard breakfast results in a mild increase in bioavailability (the geometric means AUC$_{fed}$/AUC$_{fasted}$ for the 125 mg and 80 mg dose are reported to be 1.20 and 1.09, respectively), but this is not considered clinically

relevant (EMA, 2009; FDA, 2003; Majumdar et al., 2006).

The aims of this study were threefold: 1) to investigate the advantages of using biorelevant media *vs.* simple buffers in simulating the *in vivo* performance of aprepitant, 2) to build a PBPK model following the "middle-out" approach, combining experimental data and information available in literature with the commercially available *in silico* software Simcyp Simulator V16.1 (Certara UK Ltd.) and 3) to mechanistically understand the *in vivo* behavior of aprepitant in both the fasted and fed states.

2. Materials and methods

2.1. Chemicals and reagents

Aprepitant was obtained as the European Pharmacopeia reference standard (code: Y0001825). Acetonitrile and water of HPLC-grade were from Merck KGaA (Darmstadt, Germany). Sodium dihydrogen phosphate dihydrate of analytical grade was from Merck KGaA (Darmstadt, Germany). Phosphoric acid, sodium chloride and sodium hydroxide, also of analytical grade, were purchased from VWR chemicals (Leuven, Belgium). Pepsin was from Sigma-Aldrich (Lot # SLBQ2263V). EMEND® capsules were purchased from MSD SHARP & DOHME GMBH (Lot # MO 49340 and MO 45740 for the 80 mg and 125 mg, respectively, Haar, Germany). Lipofundin® MCT/LCT 20% was purchased from B. Braun (B. Braun Melsungen AG, Melsungen, Germany). FaSSGF/FaSSIF/FeSSIF, FeSSIF V2 and FaSSIF V3 powders were kindly donated by biorelevant.com (London, England).

2.2. Experimental methods

2.2.1. Solubility experiments

The solubility of pure aprepitant powder was investigated using the method of Andreas et al. (2015) in Level I and Level II biorelevant media (Markopoulos et al., 2015), utilizing the Uniprep™ system (Whatman®, Piscataway, NJ, USA). Briefly, an excess amount of aprepitant is added to a 3 mL aliquot of the medium and the samples are shaken for 1, 2, 4, 24 or 48 h at 37 °C on an orbital mixer. After shaking, the samples are immediately filtered through pre-warmed 0.45 μm PTFE filters and analyzed by HPLC. Solubility measurements were carried out at least in triplicate (n = 3).

2.2.2. Dissolution experiments

Dissolution experiments of the EMEND® capsules were performed using the paddle (USP II) apparatus (Erweka DT 600, Heusenstamm, Germany). Each vessel contained 250 mL or 500 mL, respectively, for media simulating gastric fluids or intestinal fluids. The rotating speed of the paddle was set at 75 rpm. The temperature in the vessels was maintained at 37 ± 0.5 °C throughout the experiment. No sinkers were utilized. All dissolution experiments were performed in triplicate (n = 3).

Samples were withdrawn at 1, 2.5, 5, 7.5, 10, 20, 30, 40, 60, 90 and 120 min with glass syringes and filtered through a cylindrical polyethylene filter stick with a pore size of 4 μm attached to the end of the sampling tubes. Immediately thereafter, the samples were filtered through 0.1 μm Anotop 25 filters (Whatman GmBH, Dassel, Germany). After discarding the first 1 mL, the filtrate was diluted with mobile phase and analyzed by HPLC.

The efficiency of filtration was confirmed with Nanoparticle Tracking Analysis (NTA) on a Malvern Nanosight NS300 (Malvern Instruments, Malvern, UK) instrument that was equipped with a green laser (excitation at 468 nm, emission at 508 nm).

2.2.3. Transfer experiments

Transfer experiments were performed for both the 80 mg and 125 mg EMEND® capsules utilizing the USP II apparatus, as described previously by Berlin et al. (2014). Briefly, 250 mL of Level III FaSSGF

pH 2.0 and 350 mL of Level II FaSSIF V1 or FaSSIF V3 were used as the dissolution media in the gastric and duodenal compartment, respectively. The rotating speed of the paddles was set at 75 rpm. The temperature in the vessels was maintained at 37 ± 0.5 °C throughout the experiment. A peristaltic pump set to first order kinetics ($t_{1/2}$ = 9 min) was used to transfer the medium from the gastric to the duodenal compartment, from which samples were withdrawn at 5, 10, 15, 20, 30, 45, 60, 75, 90, 120, 180 and 240 min. Sample handling and analysis were as described for the dissolution experiments.

2.2.4. Chromatographic assays

For the quantitative analysis of samples, a HPLC-UV system was used (Hitachi Chromaster; Hitachi Ltd., Tokyo, Japan or Spectra System HPLC, ThermoQuest Inc., San Jose, USA). The analytical column was a BDS Hypersil C18, 3 μm, 150 × 3 mm (Thermo Scientific) combined with a pre-column (BDS Hypersil C-18, 3 μm, 10 × 4 mm). The mobile phase consisted of 50:50% v/v buffer (NaH_2PO_4, 10 mM, pH = 2.5):acetonitrile. The detection wavelength was set at 220 nm, the injection volume at 50 μL and the flow rate at 1 mL/min. The LOD (limit of detection) and LOQ (limit of quantification) were 0.02 μg/mL and 0.07 μg/mL, respectively.

2.3. Pharmacokinetic data and methods

2.3.1. Literature pharmacokinetic data

In order to build the PBPK model for aprepitant following the "middle-out" approach (Jamei et al., 2009a; Cristofoletti et al., 2017), plasma data for both dose strengths for fasted and fed state were derived from the study of Majumdar et al. and digitalized with WebPlotDigitizer v. 4.0, Texas, USA (Majumdar et al., 2006). The study reported by Majumdar et al. consisted of two parts. The first part was a single-period, double blind study, in which 2 mg of aprepitant were intravenously administered to nine healthy volunteers (mean age was 31 years with a range of 24–40). The second part was a randomized, four period, cross-over study with the aim of investigating the absolute bioavailability of the 80 mg and 125 mg EMEND® capsules under fasted and fed state conditions. In this part of the study, twenty-five healthy volunteers (mean age was 28 years with a range of 18–43) were administered: 1) one aprepitant 80 mg capsule orally following a standard breakfast, 2) one aprepitant 125 mg capsule orally following a standard breakfast, 3) one aprepitant 80 mg capsule orally with 8 oz. of water, along with 2 mg intravenous, isotope-labelled aprepitant, and 4) one aprepitant 125 mg capsule orally with 8 oz. of water, along with 2 mg intravenous, isotope-labelled aprepitant. The authors commented that the co-administration of the 2 mg intravenous isotope-labelled aprepitant had little effect on the disposition of the drug relative to the 80 mg and 125 mg capsules. Since there were earlier data demonstrating non-linearity of the pharmacokinetics of aprepitant with increasing dose, the bioavailability of the capsule formulations was determined by comparing the dose-standardized AUC values following the capsule dose to the dose-standardized AUC values following the capsule dose simultaneously administered with 2 mg intravenous, isotope-labelled aprepitant (FDA, 2003; Majumdar et al., 2006).

2.3.2. Modeling methods and strategies

The *in vivo* performance of aprepitant capsules was modeled with the Simcyp Simulator V16.1 (Certara UK Ltd., Sheffield, UK). The substrate parameters for building the i.v. and/or oral PBPK model are presented in Table 1.

Disposition parameters were calculated from the available i.v. data and the resulting fit of the model to the observed data is shown in Fig. 1 (Majumdar et al., 2006). The distribution of aprepitant was described using a minimal PBPK model with a Single Adjusting Compartment (SAC). SAC is a non-physiological compartment that represents a cluster of tissues (excluding the liver and portal vein). It is used to extend the use of minimal PBPK models to APIs with high volumes of distribution,

i.e. where the tissue concentration exceeds the blood concentration. The Q_{SAC} (inter-compartment clearance), V_{SAC} (apparent volume associated with the SAC) and V_{ss} (steady state volume of distribution) were estimated using the Parameter Estimation Tool and simultaneous fit of the three intravenous PK profiles available in the open literature (Majumdar et al., 2006).

To model the clearance, the "Enzyme Kinetics" option in Simcyp was chosen since aprepitant exhibits saturable metabolism and non-linear pharmacokinetics. As mentioned in the Public Assessment Report of the EMA and FDA of EMEND® capsules, as well as the research article of Sanchez et al., aprepitant is mainly metabolized by CYP3A4 (FDA, 2003; Sanchez et al., 2004; EMA, 2004), although CYP2C19 and CYP1A2 may also be involved to some extent. The V_{max} (*in vitro* maximum velocity for metabolism of the compound by the given isoform of enzyme) and K_m (*in vitro* Michaelis-Menten constant for metabolism of the compound by the given isoform of enzyme) for CYP3A4 were derived by Sanchez et al. (2004). The f_{umic} (fraction of compound unbound in an *in vitro* microsomal preparation) was predicted using the Simcyp Prediction Toolbox (Turner et al., 2006). Furthermore, as indicated in the EMA scientific discussion document for the approval of EMEND® capsules, after intravenous administration of the radio-labelled prodrug of aprepitant (which is rapidly and completely converted to aprepitant) no unchanged drug is recovered in the urine (EMA, 2004; Bubalo et al., 2012). Therefore, the renal clearance for aprepitant was set at a minimum value corresponding to the product of plasma f_u (fraction unbound) and urine flow (Rowland and Tozer, 1995). This approach is further supported by the fact that impaired renal function does not result in a clinically significant difference in the PK of aprepitant when compared to healthy control subjects and no dose adjustment is required for patients with renal insufficiency, end-stage renal disease or those undergoing hemodialysis (FDA, 2003; EMA, 2004; Bergman et al., 2005).

To model the absorption process, the Advanced Dissolution, Absorption and Metabolism (ADAM) model was utilized (Jamei et al., 2009b). The segmental (total) solubility input option was used, based on the maximum concentration measured in the dissolution experiments in each biorelevant medium (Section 3.1). Permeability was estimated by using the Parameter Estimation Tool by fitting the *in vivo* PK data following oral administration in the fasted state (simultaneous fit of PK profiles after administration of 80 mg and 125 mg) and was in line with the P_{app} values reported in the literature by Shono et al. (2010), Wu et al. (2004) and Takano et al. (2008).

All physiological parameters of the gastrointestinal (GI) tract were maintained at the default values for the healthy volunteer population in the Simcyp Simulator for both the fasted and fed state simulations.

2.4. Statistics

To assess the prediction accuracy, average fold error (AFE) and absolute average fold error (AAFE) were calculated according to the equations published by Obach et al. (1997), as also described by Andreas et al. (2017). The 95% confidence intervals were calculated with the Simcyp Simulator V16.1.

3. Results

3.1. Experimental part

3.1.1. Solubility experiments

Mean solubility values (± SD) of pure aprepitant (Form I, most thermodynamically stable polymorph) at 24 h in Level I and Level III FaSSGF, Level I and Level II FaSSIF V1 and FaSSIF V3, Level I and Level II FeSSIF V1 and FeSSIF V2 are presented in Table 2, together with the pH value at the end of the solubility experiment (pH_{final}). In every case the pH_{final} was only slightly or not at all different from the initial pH value of the medium.

Table 1

Parameter values used for the simulations of the *in vivo* performance of EMEND® in the fasted and fed states.

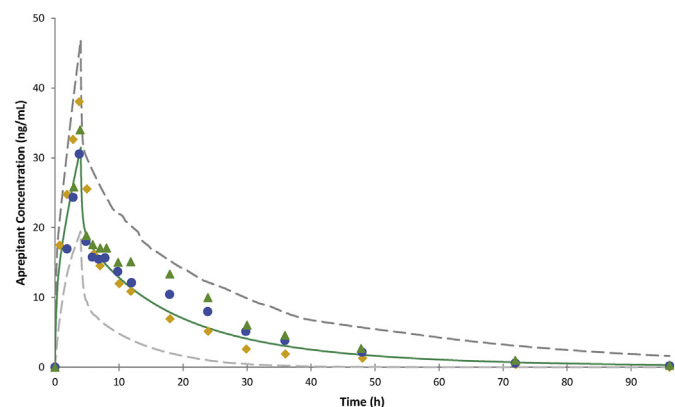| Parameters		References and comments
Dosage form	IR	
Molecular weight (g/mol)	534.44	
Log P	4.8	(Shono et al., 2010; Kesisoglou and Mitra, 2012; Wu et al., 2004; Liu et al., 2015)
B/P (blood/plasma coefficient)	1.20	Estimated using the PE Tool after fitting the available *in vivo* data (see Section 2.3.1)
f_u (unbound plasma)	0.02	(EMA, 2009; FDA, 2003; Bergman et al., 2005)
	Absorption	
Absorption model	ADAM	
Diffusion layer model		
Permeability method		
$P_{eff,man}$ ($\times 10^{-4}$ cm/s)	2.15	Estimated using the PE Tool
Solubility fasted state (µg/mL)	13, 30	Stomach, small intestine
Solubility fed state (µg/mL)	75, 120	Stomach, small intestine
	Distribution	
Distribution model	Minimal PBPK model with SAC	
SAC Q (L/h)	21.92	Estimated after fitting the available intravenous *in vivo* data (see Section 2.3.1)
Volume [V_{SAC}] (L/kg)	0.7837	
V_{ss} (L/kg)	0.875	(EMA, 2009)
	Elimination	
Elimination type	Enzyme kinetics	
CYP3A4	V_{max} = 120 pmol/mg/min	(Sanchez et al., 2004)
	K_m = 10.5 µM	(Sanchez et al., 2004)
	f_{umic} = 0.143	Simcyp Prediction Toolbox
Renal clearance (L/h)	0.0024	(EMA, 2004; Rowland and Tozer, 1995)

Fig. 1. Simulated (thick solid line, population mean; thin dashed lines, 5th and 95th percentile of population) and clinically reported plasma concentration-time profiles after i.v. administration of 2 mg radio-labelled aprepitant (diamonds), 2 mg radio-labelled aprepitant i.v. concurrently with one 80 mg EMEND® capsule (circles) and 2 mg radio-labelled aprepitant i.v. concurrently with one 125 mg EMEND® capsule (triangles) (Majumdar et al., 2006).

Table 2

Mean (± SD) solubility of aprepitant in fasted and fed state biorelevant media at 24 h.

Biorelevant medium	Solubility (µg/mL)	pH$_{initial}$	pH$_{final}$
Fasted state			
Level I FaSSGF	7.62 ± 0.64	1.6	1.6
Level III FaSSGF	5.76 ± 0.35	1.6	1.7
Level I FaSSIF V1	< LOD	6.5	6.6
Level II FaSSIF V1	9.87 ± 2.40	6.5	6.5
Level I FaSSIF V3	< LOD	6.7	6.8
Level II FaSSIF V3	3.03 ± 0.06	6.7	6.7
Fed state			
Level I FeSSIF V1	< LOD	5.0	5.0
Level II FeSSIF V1	53.89 ± 11.76	5.0	5.0
Level I FeSSIF V2	< LOD	5.8	5.8
Level II FeSSIF V2	68.58 ± 6.86	5.8	5.8

The solubility values obtained in Level II compared with Level I biorelevant media indicate a major impact of native surfactants on the solubility of aprepitant. Similar observations have been reported by Zhou et al. (2017) and Niederquell and Kuentz (2018).

3.1.2. Dissolution and transfer experiments

Dissolution and transfer experiments were performed, as described in Sections 2.2.2 and 2.2.3, for EMEND® capsules at both dose strengths in biorelevant media simulating the contents of the fasted stomach (Level III FaSSGF), fasted upper small intestine (Level II FaSSIF V1, Level II FaSSIF V3), fed stomach (Level II FeSSGF$_{middle}$) and fed upper small intestine (Level II FeSSIF V1, Level II FeSSIF V2) (Markopoulos et al., 2015). The mean values of % dissolved with time in fasted and fed state biorelevant media for the 80 mg and 125 mg dose are presented in Figs. 2 and 3, respectively.

In the case of the USP II dissolution experiments the dissolution was fast, incomplete and reached a plateau value within approximately the first 10 min. Interestingly, the concentrations of dissolved drug in the dissolution vessels exceeded the thermodynamic solubility observed for the pure API in the respective media. In particular, the mean maximum concentrations of dissolved drug in Level III FaSSGF, Level II FaSSIF V1, Level II FaSSIF V3, Level II FeSSGF$_{middle}$, Level II FeSSIF V1 and Level II FeSSIF V2 were approx. 15 µg/mL, 27 µg/mL and 26 µg/mL, 75 µg/mL, 120 µg/mL and 150 µg/mL respectively, at both doses. These results are consistent with those of Shono et al. (2010) and Takano et al. (2008).

Decreasing the particle size of aprepitant to the nanoscale results in a much higher dissolution rate, which can be attributed to the large increase in surface area and surface energy. As reported by Kesisoglou and Mitra, apart from the increase in the dissolution rate, nano-sizing can also lead to some increase in the apparent solubility of the API, according to the Freundlich-Ostwald equation (Kesisoglou and Mitra, 2012). However, the quantitative effect of nano-sizing on saturation solubility remains unclear (Shono et al., 2010; Kaptay, 2012; Letellier et al., 2007). Additionally, some authors have suggested that apparent increases in solubility that have been reported may be largely due to the use of stabilizers (*e.g.* surfactants) (Tuomela et al., 2016). As reported in the Summary of Product Characteristics, the EMEND® capsules contain sodium lauryl sulfate as one of the excipients, which could lead to an increase in aprepitant solubility (EMA, 2009). Nonetheless, the increase in surface area likely plays the predominant role in the increase in
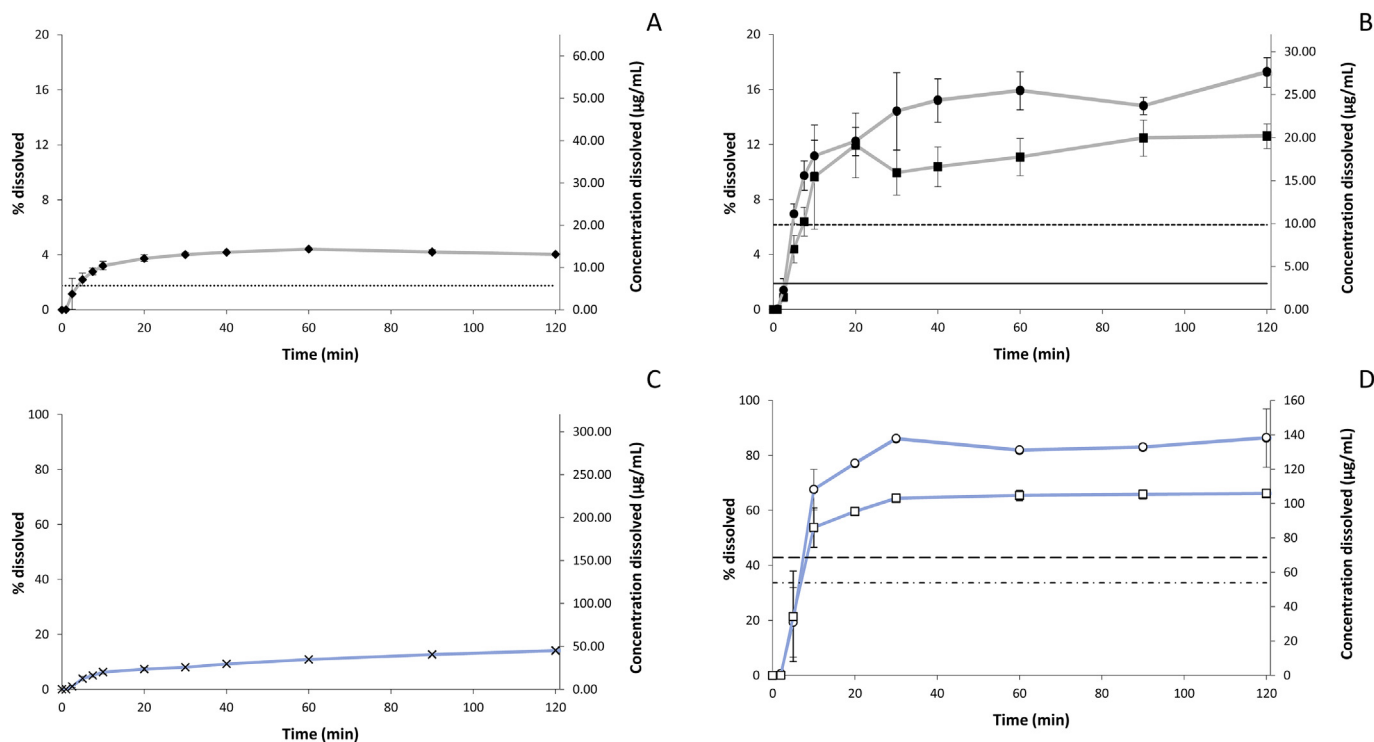
Fig. 2. Mean (± SD) % and concentrations of aprepitant dissolved from 80 mg EMEND® capsules in: A) Level III FaSSGF (◆) B), Level II FaSSIF V1 (■), Level II FaSSIF V3 (•), C) Level II FeSSGF_middle (x) and D) Level II FeSSIF V1 (□) and Level II FeSSIF V2 (○). With the round dotted line, square dotted line, solid line, dashed-dotted line and dashed line the solubility of the crystalline aprepitant in Level III FaSSGF, Level II FaSSIF V1, Level II FaSSIF V3, Level II FeSSIF V1 and Level II FeSSIF V2 is presented, respectively.
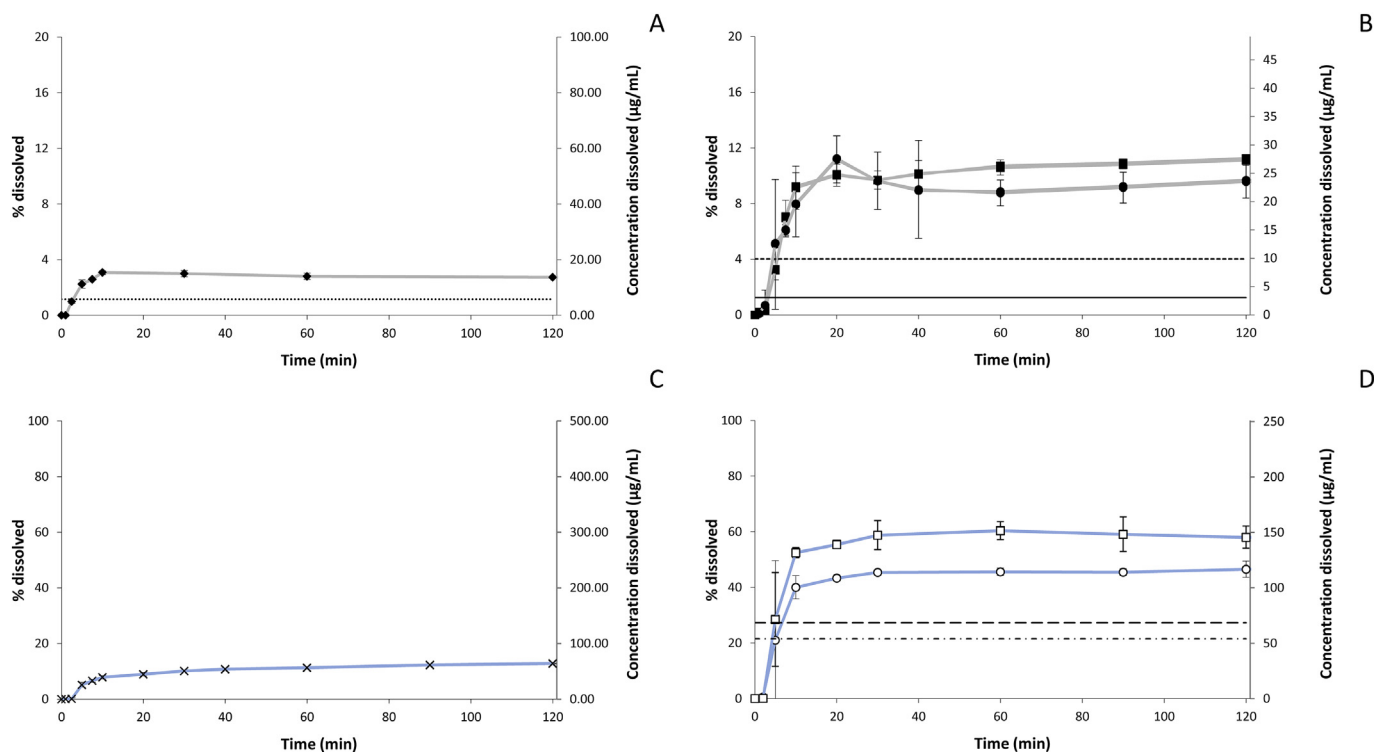

Fig. 3. Mean (± SD) % and concentrations of aprepitant dissolved from 125 mg EMEND® capsules in: A) Level III FaSSGF (◆), B) Level II FaSSIF V1 (■), Level II FaSSIF V3 (•), C) Level II FeSSGF_middle (x) and D) Level II FeSSIF V1 (□) and Level II FeSSIF V2 (○). With the round dotted line, square dotted line, solid line, dashed-dotted line and dashed line the solubility of the crystalline aprepitant in Level III FaSSGF, Level II FaSSIF V1, Level II FaSSIF V3, Level II FeSSIF V1 and Level II FeSSIF V2 is presented, respectively.
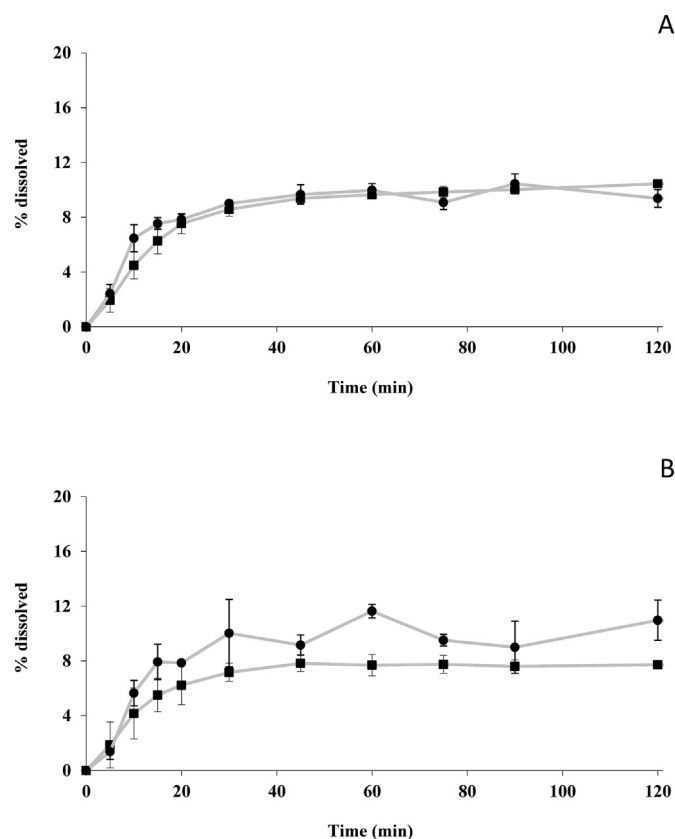
Fig. 4. Mean (± SD) % aprepitant dissolved from: A) 80 mg EMEND® capsules and B) 125 mg EMEND® capsules, sampled from the intestinal compartment during transfer experiments from Level III FaSSGF (pH = 2) to Level II FaSSIF V1 (■)and to Level II FaSSIF V3 (●).

dissolution rate for nanosized formulations.

With regard to the transfer experiments, no precipitation of aprepitant was observed over the four hour experimental duration. The maximum dissolved concentration was achieved more slowly than in the dissolution experiments, since the appearance of the drug in the intestinal compartment is limited by the rate of transfer from the compartment representing the stomach to the one representing the small intestine. Additionally, the maximum dissolved concentration and plateau values achieved in the transfer experiments were somewhat lower than those of the dissolution experiments in media simulating the fasted upper small intestine. This is attributable to the dilution of the intestinal compartment by fluid transferred from the gastric compartment. The results of the transfer experiments with the 80 mg and 125 mg doses are presented in Fig. 4.

3.2. PBPK model and simulations

Initially, modeling and simulation of the *in vivo* intravenous (i.v.) data was performed to estimate the post-absorptive parameters, as described in Section 2.3.2. The PBPK model for oral administration of aprepitant was then built using the "middle-out" approach. The middle-out approach is a way of informing the modeling process with known clinical data, rather than relying only on the structure, permeability and physicochemical properties of the drug. In particular, this entailed implementation of (i) the calculated post-absorptive parameters from the i.v. data together with (ii) results from the *in vitro* dissolution experiments to simulate the plasma profiles. These simulated plasma profiles were then compared with data obtained by Majumdar et al. after oral administration of 80 mg or 125 mg EMEND® capsules in healthy volunteers in the fasted and fed states (Majumdar et al., 2006).
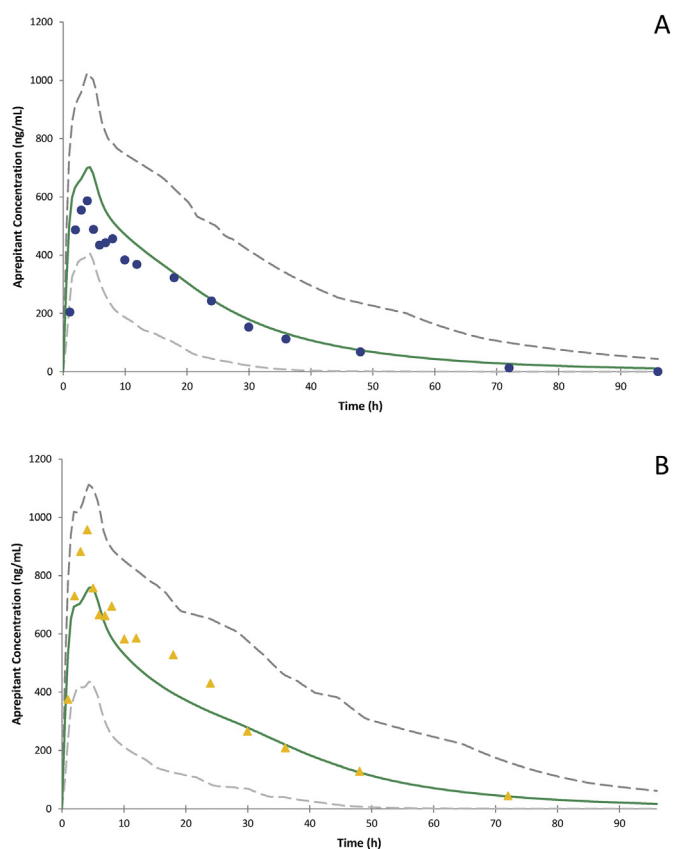

Fig. 5. Simulated (thick solid line, population mean; thin dashed lines, 5th and 95th percentile of population) and clinically reported plasma concentration-time profiles after administration of an: A) 80 mg EMEND® capsule (circles) and B) 125 mg EMEND® capsule (triangles), in the fasted state (Majumdar et al., 2006).

Since the results from the transfer experiments indicated no precipitation over a four hour period, there was no need to invoke precipitation in the PBPK simulations.

The simulated plasma profiles after i.v. administration of radio-labelled aprepitant, as well as after oral administration of capsules at both dose strengths in fasted and fed states *vs.* the observed plasma concentrations, are presented in Figs. 1, 5 and 6, respectively. The AAFE and AFE for each simulation are presented in Table 3.

4. Discussion

4.1. Fasted state

The *in vitro* solubility and dissolution experiments suggest that the solubilization of aprepitant by native surfactants is likely one of the major properties affecting the *in vivo* dissolution of aprepitant from the marketed formulation. The solubility experiments performed with the pure API powder exhibited great differences between the solubility values measured in Level I (simple buffers) and Level II (addition of bile salts and lecithin) biorelevant media. For example the solubility in Level I FaSSIF V1 was below the limit of detection (0.02 µg/mL), but in Level II FaSSIF V1 it was 9.87 ± 2.40 µg/mL. From the dissolution experiments performed with the formulated (nano-sized) drug, the importance of surfactants on the plateau value attained is also evident. Illustratively, the plateau value reached in Level II FaSSIF V1, containing 3 mM NaTc, was approximately double the plateau value reached in Level III FaSSGF, which contains only 0.08 mM NaTc. In agreement with these results, Roos et al. recently demonstrated the importance of colloidal structures in increasing the bioavailability of
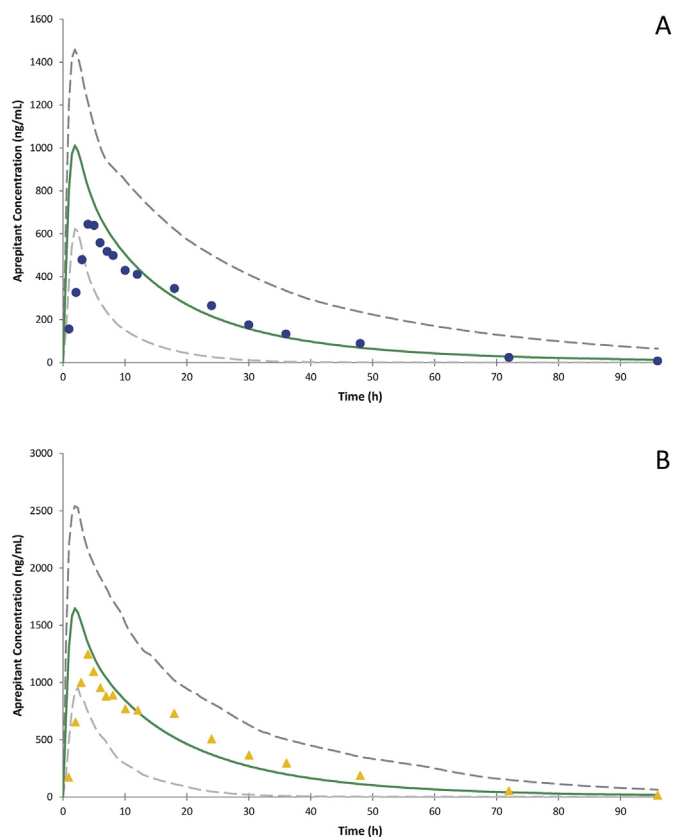
Fig. 6. Simulated (thick solid line, population mean; thin dashed lines, 5th and 95th percentile of population) and clinically reported plasma concentration-time profiles after administration of an: A) 80 mg EMEND® capsule (circles) and B) 125 mg EMEND® capsule (triangles), in the fed state (Majumdar et al., 2006).

Table 3
Calculated average fold error (AFE) and absolute average fold error (AAFE) for the simulations after oral administration of EMEND® capsules.

Dose	80 mg		125 mg	
Metrics	Fasted state	Fed state	Fasted state	Fed state
AFE	1.58	1.31	0.94	1.12
AAFE	1.58	1.44	1.14	1.45

aprepitant from various nano-suspensions in rat intestinal perfusion experiments (Roos et al., 2017).

In the present study, dissolution experiments in the Level II biorelevant media proved more useful than the equilibrium solubility experiments for identifying the relevant apparent solubility of the marketed aprepitant formulation. Thus, the experimental results demonstrated not only that the final concentration of aprepitant in the dissolution experiments was well above the equilibrium solubility, but also that application of the plateau values from the dissolution experiments led to a more accurate simulation of the plasma profiles.

The role of bile salts in the dissolution and hence bioavailability of EMEND® in the fasted state was further investigated with the Parameter Sensitivity Analysis (PSA) tool. It should be noted that, due to the way the PBPK model was developed for aprepitant, it was not able to account for inter-individual variations in bile salt concentrations, because the "segmental" (total) solubility input option was used (in this case the plateau value from the dissolution experiment). An alternative way to simulate potential effects of inter-subject solubility differences on *in vivo* performance would be to use the estimated micelle-water partition co-efficient ($K_{m:w}$) in the Simcyp Simulator. This would require a
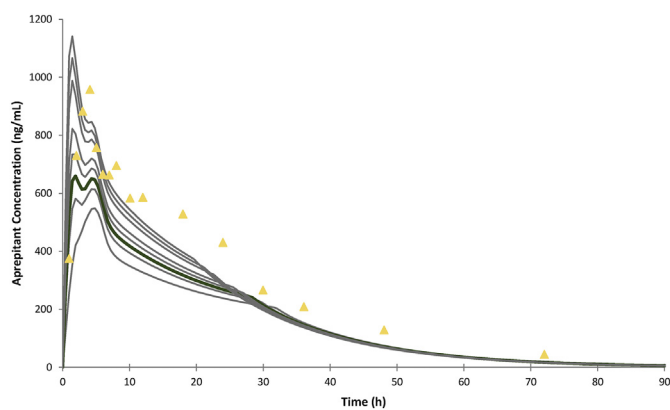

Fig. 7. The sensitivity of the simulated profiles after administration of an EMEND® 125 mg capsule in the fasted state to variations in the duodenal solubility (*i.e.* from 10 to 90 μg/mL). The thick line represents the profile using approximately the same solubility value as the one implemented in the currently developed PBPK model.

precise value of the intrinsic solubility of aprepitant as an input parameter. However, the solubility of aprepitant is a) very small, b) is associated with a relatively large coefficient of variation and c) is not representative of the concentrations achieved in dissolution experiments.

Using PSA, the duodenal total solubility value was allowed to range from 10 μg/mL to 90 μg/mL, *i.e.* three times lower and higher than the value experimentally derived from the dissolution experiments and used in the PBPK model for aprepitant in the fasted state (30 μg/mL). This range of values for the total solubility reflects the range of bile salt concentrations that has been observed *in vivo* (approx. 2–6 mM in fasted state duodenum and jejunum) (Fuchs and Dressman, 2014; Bergström et al., 2014). The PSA is presented in Fig. 7. The results suggest that variations in intestinal bile concentration among individuals would mainly affect C_{max} rather than AUC values. Furthermore, according to the PSA for both the 80 mg dose and 125 mg dose, variations in the observed C_{max} can be explained by differences in bile component concentrations among subjects.

The PSA is largely in agreement with conclusions drawn by Shono et al., who identified intestinal solubility as the most important parameter driving the predicted C_{max} in the fasted state (Shono et al., 2010). The results are also in general agreement with the observations of Takano et al., who investigated the rate-limiting step for absorption of various poorly soluble drugs, including aprepitant, in dogs (Takano et al., 2008). In that study it was shown that reducing the particle size of aprepitant below 2 μm produces no further increase in the bioavailability of aprepitant in dogs, even though the dissolution rate continued to increase with particle size reduction. Takano et al.'s study underlined the fact that, for poorly soluble drugs, the rate limiting step to absorption can shift from dissolution to solubility, depending on the formulation strategy adopted (Takano et al., 2008). Taking all of these points into consideration, it seems that aprepitant should be classified as a DCS IIb compound (Butler and Dressman, 2010) and that, for fast-dissolving formulations, the *in vivo* solubility is likely to remain a limitation to its *in vivo* performance.

4.2. Fed state

The *in vitro* experiments conducted in biorelevant media simulating the fed state also highlight the importance of surfactants on the apparent solubility of nano-sized aprepitant. For example, the maximum concentration achieved in FeSSIF V1 was more than four times greater than that achieved in FaSSIF V1 (similar to the ratio of NaTc in FeSSIF V1 to FaSSIF V1, which is 15:3). Comparing the plateau values reached in the dissolution experiments in FeSSIF V1 and FeSSIF V2, a slightly

higher value (approximately 120 μg/mL *vs.* 150 μg/mL, respectively) was observed in FeSSIF V2. This increase might be due to the additional presence of glyceryl monooleate in FeSSIF V2, which has been found to have a positive solubilization effect on aprepitant powder (Zhou et al., 2017).

When the PBPK model was adapted to simulate the plasma profile of aprepitant in the fed state, the fits to the observed data were generally very good (AFE and AAFE both < 1.5). However, the predicted profiles exhibited an earlier t_{max} of about 2 h compared to the clinically observed mean value, *i.e.* 4 h. We note that the default value for mean gastric residence time in Simcyp is set at 1 h, which seems rather short for the fed state. It is believed that in the fed state, liquids and smaller particles (< 3–4 mm) such as disintegrated tablets and capsules often empty with food over a time-span which depends largely on the caloric value of the meal (O'Shea et al., 2018). Thus, the gastric emptying time in the fed state can vary and high caloric meals can result in long gastric emptying times (O'Shea et al., 2018; Hunt and Stubbs, 1975; Cassilly et al., 2008; Koziolek et al., 2015; Koziolek et al., 2018). In the study of Majumdar et al., the EMEND® capsules were administered to the volunteers 15 min following a "standard light breakfast", although no specific information, *e.g.* the caloric value of the meal, was provided with regard to the nature of the breakfast. According to the information provided in the FDA Public Assessment Report, the effect of food on the performance of EMEND® capsules was investigated after the administration of a meal that "is similar to FDA recommended high-fat, high-calorie breakfast" (FDA, 2003). We therefore used the PSA Tool to explore the sensitivity of the simulated pharmacokinetic profiles of the EMEND® capsules in the fed state to the mean gastric residence time (MGRT). Sensitivity analysis was performed by floating the MGRT values over the range of 1 h (default value in Simcyp Simulator) to 4 h (maximum value allowed in Simcyp Simulator). The results of this
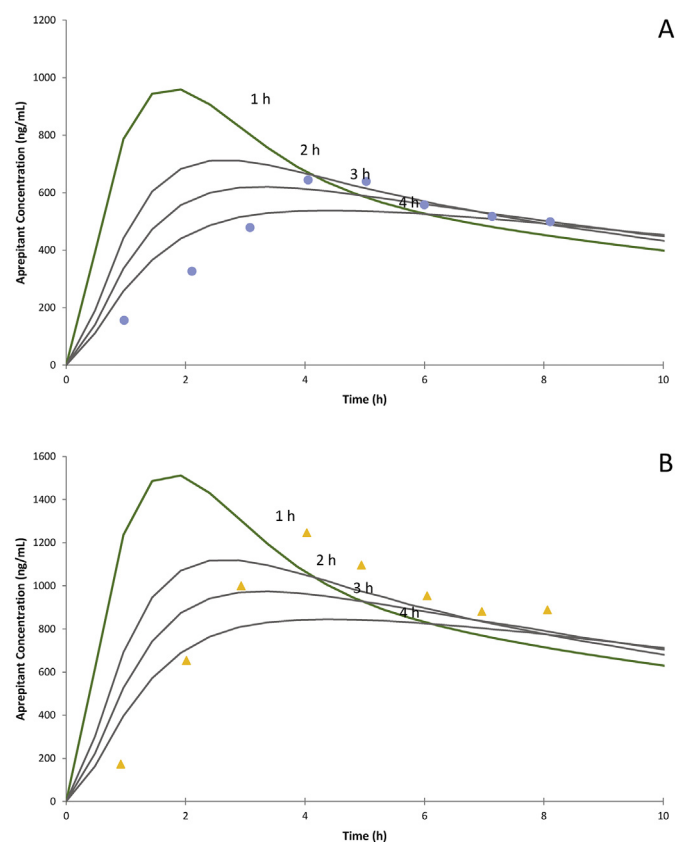
Fig. 9. The sensitivity of the simulated t_{max} after administration of an: A) 80 mg EMEND® capsule and B) 125 mg EMEND® capsule, in the fed state to vari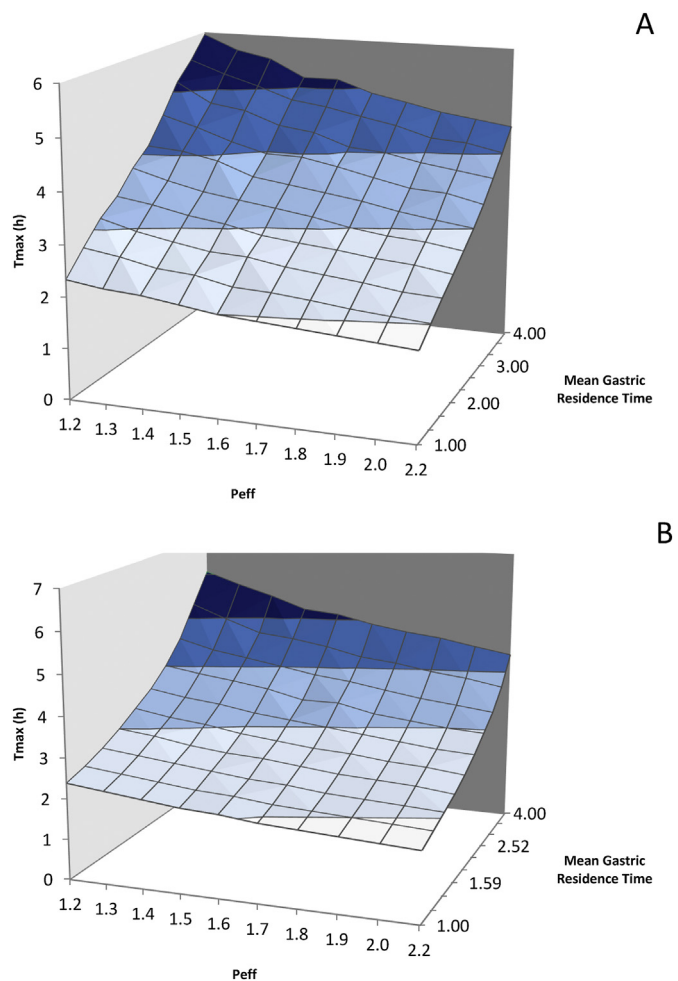ations in mean gastric residence time (*i.e.* from 1 to 4 h) and permeability values (*i.e.* P_{eff} from 1.16 to 2.15 × 10^{-6} cm/s).

analysis are presented in Fig. 8. Fig. 8 indicates that a MGRT greater or equal to 2.5 h would improve the goodness of fit of the simulated profiles. For example, for a MGRT equal to 3 h, the AFE and AAFE for the 80 mg and 125 mg doses would be 1.26 and 1.32, and 1.09 and 1.34, respectively.

Since aprepitant is characterized as borderline BCS Class II/IV and various permeability values have been reported in the literature, a further PSA was conducted in which the MGRT values were allowed to float over the range 1 h to 4 h and the P_{eff} values were simultaneously allowed to float over the range of 1.16–2.15 × 10^{-4} cm/s (based on the lowest value reported in literature and the value used in the PBPK model developed, respectively). The results from this additional sensitivity analysis (shown in Fig. 9) indicate that, for a mean gastric residence time equal to or greater than 2 h, a relatively small decrease in the permeability would result in a significant prolongation of the predicted t_{max}, without a profound effect on the AUC or C_{max}. For example, if a MGRT of 2.5 h and a P_{eff} of 1.4 × 10^{-6} cm/s (*i.e.* 35% smaller value than the one used in the currently developed model) are implemented, the predicted t_{max} increases by 30%, whereas the C_{max} and AUC decrease only by 8.7% and 2.2%, respectively, compared to simulation with a MGRT of 2.5 h and no change in permeability. For this particular example, the AFE and AAFE for the 80 mg and 125 mg dose are 1.22 and 1.29, and 1.04 and 1.29, respectively. Therefore, it seems that inter-individual differences in permeability may also affect the absorption of EMEND® in the fed state.

Fig. 8. The sensitivity of the simulated profiles after administration of an: A) 80 mg EMEND® capsule and B) 125 mg EMEND® capsule, in the fed state to variations in mean gastric residence time (*i.e.* from 1 to 4 h).

4.3. Verification of the model and clinical implications

Ideally, an appropriate validation of a compound-specific PBPK model would require access to individual *in vivo* data from all clinical trials conducted for the compound. However, in practice, academic scientists usually have to rely on mean plasma profiles, along with their respective variability (if available), or even on single values of summary pharmacokinetic parameters (C_{max}, AUC) reported in the open literature. In order to validate the model presented in this study, simulated plasma profiles or single pharmacokinetic data (C_{max}, t_{max} and AUC values) were compared to information available in the literature. To this end, virtual trials (10 trials, each with 10 volunteers) were performed in the Simcyp Simulator by implementing the PBPK model described in Sections 2.3.2 and 3.2. For the fed state model, based on the results of the PSA, a MGRT of 2.5 h was used (instead of 1 h, which is the default value in Simcyp for IR formulations administered in the fed state).

Plasma concentration profiles for aprepitant after administration of one 125 mg EMEND® capsule in the fed state in healthy volunteers were reported in the study of Gore et al. (2009). In the same study, the AUC_{0-24h} and C_{max} values were presented as geometric means together with their respective ranges; AUC_{0-24h} 19,456 (15,251, 24,817) ng·h/mL and C_{max} = 1539 (1229, 1927) ng/mL. Majumdar et al. conducted a second study with the aim of investigating the pharmacokinetic profile during a three-day 125 mg/ 80 mg aprepitant regimen (Majumdar et al., 2006). In that study, the volunteers were administered a single oral dose of one 125 mg EMEND® capsule on Day 1 and one 80 mg EMEND® capsule on Days 2 and 3. The doses were administered 15 min following administration of a light standard breakfast. The mean plasma profile of aprepitant up to the 24th hour (end of Day 1) was used for model evaluation purposes. The data from these studies were digitalized, as described earlier, and compared with the predicted plasma profiles for the 125 mg capsule in the fed state. The results are presented in Fig. 10. For both cases the fit was acceptable, with AFE and AAFE < 1.5.

It should be mentioned that a third study, published by Ridhurkar et al., was also identified. This was a bioequivalence study of 125 mg EMEND® capsules after administration of a high-caloric breakfast (Ridhurkar et al., 2013). Since the reported pharmacokinetic parameters (mean C_{max} 2304 ng/mL, mean AUC 82997 ng·h/mL, mean t_{max} 7.7 h, $t_{1/2}$ of 25.4 h) were much higher than those of the FDA and EMA Public Assessment Report of EMEND® capsules, or any other comparable clinical study, this study was not considered further for modeling.
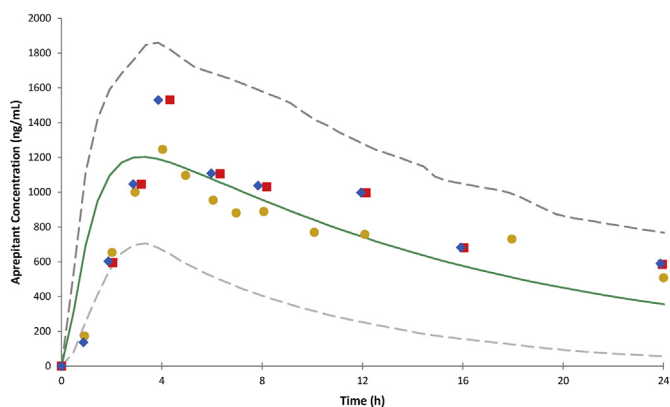

Fig. 10. Simulated (thick solid line, population mean; thin dashed lines, 5th and 95th percentile of population) and clinically reported plasma concentration-time profiles after administration of 125 mg EMEND® capsules in fed state. Circles represent the data from Majumdar et al., upon which the PBPK model was based, squares represent the second clinical study conducted by Majumdar et al. to evaluate the pharmacokinetics of the 3-days aprepitant regimen and diamonds represent the study reported by Gore et al. (Majumdar et al., 2006; Gore et al., 2009).

With regard to cancer patients, who are the patients most often prescribed aprepitant, the EMA Public Assessment Report stated that, based on limited data, the pharmacokinetics of EMEND® capsules in healthy volunteers and patient populations seem to be similar (EMA, 2004). That said, the pharmacokinetic studies in cancer populations that have been published to date are not completely consistent with this appraisal. Takahashi et al. investigated the pharmacokinetics of EMEND® as a 125 mg/ 80 mg three-day dose regimen in twenty Japanese cancer patients who were concomitantly receiving intravenous granisetron (40 μg/kg on Day 1) and dexamethasone (on Days 1–3) (Takahashi et al., 2011). In this study the reported C_{max} and AUC for the Day 1 of the 125 mg/80 mg dose regimen are 2210 ± 870 ng/mL and 30,000 ± 8700 ng·h/mL, respectively, which are slightly higher than those reported for healthy volunteers in the fasted state (C_{max} = 1003 ng/mL, AUC = 21,633 ng·h/mL) (Majumdar et al., 2006; Takahashi et al., 2011). In a later study, Bubalo et al. investigated the pharmacokinetics of aprepitant in cancer patients undergoing hematopoietic stem cell transplantation. In this study, fourteen Caucasian patients were administered one 125 mg EMEND® capsule 1 h before the first chemotherapy or radiation dose. Ondansetron and dexamethasone (12 mg on Day 1 and 8 mg on the subsequent days) were co-administered prophylactically to all subjects. In this study greater overall variability, as well as the changes in the post-absorptive parameters of the pharmacokinetics of aprepitant were observed. The observed geometric means (range) of key pharmacokinetic parameters were: t_{max} = 7 h, C_{max} = 977 (741–1289) ng/mL, AUC 27190 (12878–53,269) ng·h/mL, CL 0.93 (0.47–1.85) mL/min/kg and V_{ss} 1.54 (1.30–1.84) L/kg. The authors commented that in all subjects the observed V_{ss} was larger than that reported for healthy volunteers and that an altered fraction of unbound drug either in plasma or in tissues could have led to a greater V_{ss} (Bubalo et al., 2012). The observed discrepancies between the pharmacokinetic parameters reported for healthy volunteers and those reported for cancer patients in the studies of Bubalo et al. and Takahashi et al. may be partly attributable to the co-administration of dexamethasone, which is reported to result in a 30% increase in the AUC of aprepitant on Day 1, when administered at higher doses (EMA, 2009; FDA, 2003), or to the combined effect of all concomitantly administered compounds. Nonetheless, there may be yet other factors, which could also affect the pharmacokinetics of aprepitant in diseased populations. Further data in cancer populations would be needed to reach solid conclusions about the *in vivo* performance of EMEND® in these patients.

Last but not least, the relationship between aprepitant pharmacokinetics and its clinical effect should be considered. It has been reported that 80–90% brain NK-1 receptor occupancy results in significant antiemetic effect, while maximum antiemetic effect is achieved with a > 95% NK-1 receptor blockade (FDA, 2003). Furthermore, it has been shown that plasma concentrations of approx. 100 ng/mL produce brain NK-1 receptor occupancy of approximately 90% (EMA, 2009). As previously discussed, the maximum plasma concentrations at the indicated doses (125 mg/80 mg dose regimen) can be as high as 1500 ng/mL and the trough levels on the third day of treatment are 600 ng/mL (EMA, 2009; FDA, 2003), indicating high receptor occupancy throughout the whole treatment period. Provided there is no lag-phase for achieving the appropriate receptor concentrations, a three-day regimen of 80 mg/ 80 mg, or administration of another formulation that achieves the requisite plasma concentrations is expected to be clinically equivalent to the 125 mg/ 80 mg dose-regimen. The high dosing compared to the concentrations required to produce efficacy is likely the reason why the regulatory authorities do not consider the differences in the pharmacokinetic data of aprepitant between the fasted and fed state or between healthy volunteers and cancer patients to be clinically significant.

5. Conclusions

The *in vivo* performance of the aprepitant "enhanced" formulation

(EMEND® capsules) in healthy volunteers, in both the fasted and fed state, was successfully predicted by coupling *in vitro* data acquired with biorelevant *in vitro* tools with a commercial PBPK modeling platform (the Simcyp Simulator). This study demonstrated the importance of evaluating the effect of gastric residence time as well as the permeability-solubility interplay when predicting the absorption of a poorly soluble API under various dosing and prandial conditions. Using these *in vitro* and *in silico* biopharmaceutical tools, the performance of poorly soluble compounds can be characterized according to a mechanistically-based framework. This approach can support new and generic drug development by promoting rational formulation design and fewer and smaller, but equally robust clinical trials.

Acknowledgments

References

Andreas, C.J., et al., 2015. In vitro biorelevant models for evaluating modified release mesalamine products to forecast the effect of formulation and meal intake on drug release. Eur. J. Pharm. Biopharm. 97, 39–50. https://doi.org/10.1016/j.ejpb.2015.09.002.

Andreas, C.J., et al., 2017. Mechanistic investigation of the negative food effect of modified release zolpidem. Eur. J. Pharm. Sci. 102, 284–298. https://doi.org/10.1016/j.ejps.2017.03.011.

Bergman, E., et al., 2005. Effect of impaired renal function and haemodialysis on the pharmacokinetics of aprepitant. Clin. Pharmacokinet. 44 (6), 637–647. https://doi.org/10.2165/00003088-200544060-00005.

Bergström, C.A.S., et al., 2014. Early pharmaceutical profiling to predict oral drug absorption: current status and unmet needs. Eur. J. Pharm. Sci. 57 (1), 173–199. https://doi.org/10.1016/j.ejps.2013.10.015.

Berlin, M., et al., 2014. Prediction of oral absorption of cinnarizine – a highly supersaturating poorly soluble weak base with borderline permeability. Eur. J. Pharm. Biopharm. 88 (3), 795–806. https://doi.org/10.1016/j.ejpb.2014.08.011.

Bubalo, J.S., et al., 2012. Aprepitant pharmacokinetics and assessing the impact of aprepitant on cyclophosphamide metabolism in cancer patients undergoing hematopoietic stem cell transplantation. J. Clin. Pharmacol. 52 (4), 586–594. https://doi.org/10.1177/0091270011398243.

Butler, J.M., Dressman, J.B., 2010. The developability classification system: application of biopharmaceutics concepts to formulation development. J. Pharm. Sci. 99 (12), 4940–4954. https://doi.org/10.1002/JPS.22217.

Cassilly, D., et al., 2008. Gastric emptying of a non-digestible solid: assessment with simultaneous SmartPill pH and pressure capsule, antroduodenal manometry, gastric emptying scintigraphy. Neurogastroenterol. Motil. 20 (4), 311–319. https://doi.org/10.1111/j.1365-2982.2007.01061.x.

Cristofoletti, R., et al., 2017. Assessment of bioequivalence of weak base formulations under various dosing conditions using physiologically based pharmacokinetic simulations in virtual populations. Case examples: ketoconazole and posaconazole. J. Pharm. Sci. 106 (2), 560–569. https://doi.org/10.1016/j.xphs.2016.10.008.

EMA. EMEND® - scientific discussion. 2004; (June): 1–30. Available at: http://www.ema.europa.eu/docs/en_GB/document_library/EPAR_-_Scientific_Discussion/human/000527/WC500026534.pdf.

EMA, 2009. EMEND: summary of product characteristics. Available at: http://www.ema.europa.eu/docs/en_GB/document_library/EPAR_-_Product_Information/human/000527/WC500026537.pdf, Accessed date: 25 October 2017.

FDA, 2003. Clinical pharmacology and biopharmaceutics review. Available at: https://www.accessdata.fda.gov/drugsatfda_docs/nda/2003/21-549_Emend_biopharmr.pdf, Accessed date: 31 August 2017.

European Medicines Agency, 2016. Research and development - PRIME: priority medicines. Available at. http://www.ema.europa.eu/ema/index.jsp?curl=pages/regulation/general/general_content_000660.jsp, Accessed date: 2 February 2018.

FDA, 2003. EMEND®, Clinical pharmacology and biopharmaceutics review. Available at. https://www.accessdata.fda.gov/drugsatfda_docs/nda/2003/21-549_Emend_biopharmr.pdf, Accessed date: 31 August 2017.

Fuchs, A., Dressman, J.B., 2014. Composition and physicochemical properties of fasted-state human duodenal and jejunal fluid: a critical evaluation of the available data. J. Pharm. Sci. 103 (11), 3398–3411. https://doi.org/10.1002/jps.24183.

Georgaka, D., et al., 2017. Evaluation of dissolution in the lower intestine and its impact on the absorption process of high dose low solubility drugs. Mol. Pharm. 14 (12), 4181–4191. https://doi.org/10.1021/acs.molpharmaceut.6b01129.

Gore, L., et al., 2009. Aprepitant in adolescent patients for prevention of chemotherapy-induced nausea and vomiting: a randomized, double-blind, placebo-controlled study of efficacy and tolerability. Pediatr. Blood Cancer 52 (2), 242–247. https://doi.org/10.1002/pbc.21811.

Hunt, J.N., Stubbs, D.F., 1975. The volume and energy content of meals as determinants of gastric emptying. J. Physiol. 245 (1), 209–225. Available at. http://www.ncbi.nlm.nih.gov/pubmed/1127608, Accessed date: 9 August 2018.

Information for Consumers (Drugs), 2015. FDA's drug review process: continued. Available at. https://www.fda.gov/Drugs/ResourcesForYou/Consumers/ucm289601.htm#review, Accessed date: 2 February 2018.

Jamei, M., et al., 2009a. A framework for assessing inter-individual variability in pharmacokinetics using virtual human populations and integrating general knowledge of physical chemistry, biology, anatomy, physiology and genetics: a tale of "bottom-up" vs "top-down" recognition of covariates. Drug Metab. Pharmacokinet. 24 (1), 53–75. Available at: http://www.ncbi.nlm.nih.gov/pubmed/19252336, Accessed date: 17 April 2019.

Jamei, M., et al., 2009b. Population-based mechanistic prediction of oral drug absorption. AAPS J. 11 (2), 225–237. https://doi.org/10.1208/s12248-009-9099-y.

Kalepu, S., Nekkanti, V., 2015. Insoluble drug delivery strategies: review of recent advances and business prospects. Acta Pharm. Sin. B 5 (5), 442–453. https://doi.org/10.1016/j.apsb.2015.07.003.

Kaptay, G., 2012. On the size and shape dependence of the solubility of nano-particles in solutions. Int. J. Pharm. 430 (1–2), 253–257. https://doi.org/10.1016/j.ijpharm.2012.03.038.

Kesisoglou, F., Mitra, A., 2012. Crystalline nanosuspensions as potential toxicology and clinical oral formulations for BCS II/IV compounds. AAPS J. 14 (4), 677–687. https://doi.org/10.1208/s12248-012-9383-0.

Koziolek, M., et al., 2015. Intragastric pH and pressure profiles after intake of the high-caloric, high-fat meal as used for food effect studies. J. Control. Release 220, 71–78. https://doi.org/10.1016/j.jconrel.2015.10.022.

Koziolek, M., et al., 2018. Physiological considerations and in vitro strategies for evaluating the influence of food on drug release from extended-release formulations. AAPS PharmSciTech 19 (7), 2885–2897. https://doi.org/10.1208/s12249-018-1159-0.

Letellier, P., et al., 2007. Solubility of nanoparticles: nonextensive thermodynamics approach. J. Phys. Condens. Matter 19 (43), 436229. https://doi.org/10.1088/0953-8984/19/43/436229.

Lipinski, C.A., 2000. Drug-like properties and the causes of poor solubility and poor permeability. J. Pharmacol. Toxicol. Methods 44 (1), 235–249. Available at: http://www.ncbi.nlm.nih.gov/pubmed/11274893, Accessed date: 2 February 2018.

Liu, J., et al., 2015. Characterization and pharmacokinetic study of aprepitant solid dispersions with soluplus®. Molecules 20 (6), 11345–11356. https://doi.org/10.3390/molecules200611345.

Majumdar, A.K., et al., 2006. Pharmacokinetics of aprepitant after single and multiple oral doses in healthy volunteers. J. Clin. Pharmacol. 46 (3), 291–300. https://doi.org/10.1177/0091270005283467.

Markopoulos, C., et al., 2015. In-vitro simulation of luminal conditions for evaluation of performance of oral drug products: choosing the appropriate test media. Eur. J. Pharm. Biopharm. 93, 173–182. https://doi.org/10.1016/j.ejpb.2015.03.009.

Niederquell, A., Kuentz, M., 2018. Biorelevant drug solubility enhancement modeled by a linear solvation energy relationship. J. Pharm. Sci. 107 (1), 503–506. https://doi.org/10.1016/j.xphs.2017.08.017.

Obach, R.S., et al., 1997. The prediction of human pharmacokinetic parameters from preclinical and in vitro metabolism data. J. Pharmacol. Exp. Ther. 283 (1), 46–58. Available at. http://www.ncbi.nlm.nih.gov/pubmed/9336307, Accessed date: 9 February 2018.

O'Shea, J.P., et al., 2018. Food for thought: formulating away the food effect - a PEARRL review. J. Pharm. Pharmacol. https://doi.org/10.1111/jphp.12957.

Parekh, A., et al., 2015. Catalyzing the critical path initiative: FDA's progress in drug development activities. Clin. Pharmacol. Ther. 97 (3), 221–233. https://doi.org/10.1002/cpt.42.

Press Announcements, 2018. Statement from FDA Commissioner Scott Gottlieb, M.D. on new steps to facilitate efficient generic drug review to enhance competition, promote access and lower drug prices. Available at. https://www.fda.gov/newsevents/newsroom/pressannouncements/ucm591184.htm, Accessed date: 2 February 2018.

Ridhurkar, D.N., et al., 2013. Inclusion complex of aprepitant with cyclodextrin: evaluation of physico-chemical and pharmacokinetic properties. Drug Dev. Ind. Pharm. 39 (11), 1783–1792. https://doi.org/10.3109/03639045.2012.737331.

Roos, C., et al., 2017. In vivo mechanisms of intestinal drug absorption from aprepitant nanoformulations. Mol. Pharm. 14 (12), 4233–4242. https://doi.org/10.1021/acs.molpharmaceut.7b00294.

Rowland, M., Tozer, T.N., 1995. Clinical pharmacokinetics: concepts and applications. Available at: Williams & Wilkinshttps://openlibrary.org/books/OL1101417M/Clinical_pharmacokinetics, Accessed date: 7 August 2018.

Sanchez, R.I., et al., 2004. Cytochrome P450 3A4 Is the Major Enzyme Involved in the Metabolism of the Substance P Receptor Antagonist Aprepitant Abstract. 32(11). pp. 1287–1292. https://doi.org/10.1124/dmd.104.000216.

Shono, Y., et al., 2010. Forecasting in vivo oral absorption and food effect of micronized and nanosized aprepitant formulations in humans. Eur. J. Pharm. Biopharm. 76 (1), 95–104. https://doi.org/10.1016/j.ejpb.2010.05.009.

Sjögren, E., et al., 2016. In silico modeling of gastrointestinal drug absorption: predictive performance of three physiologically based absorption models. Mol. Pharm. 13 (6), 1763–1778. https://doi.org/10.1021/acs.molpharmaceut.5b00861.

Söderlind, E., et al., 2010. Simulating fasted human intestinal fluids: understanding the roles of lecithin and bile acids. Mol. Pharm. 7 (5), 1498–1507. https://doi.org/10.1021/mp100144v.

Takahashi, T., et al., 2011. Pharmacokinetics of aprepitant and dexamethasone after administration of chemotherapeutic agents and effects of plasma substance P

concentration on chemotherapy-induced nausea and vomiting in Japanese cancer patients. Cancer Chemother. Pharmacol. 68 (3), 653–659. https://doi.org/10.1007/s00280-010-1519-2.

Takano, R., et al., 2008. Rate-limiting steps of oral absorption for poorly water-soluble drugs in dogs; prediction from a miniscale dissolution test and a physiologically-based computer simulation. Pharm. Res. 25 (10), 2334–2344. https://doi.org/10.1007/s11095-008-9637-9.

Tuomela, A., et al., 2016. Stabilizing agents for drug nanocrystals: effect on bioavailability. Pharmaceutics 8 (2). https://doi.org/10.3390/pharmaceutics8020016.

Turner DB et al. Prediction of non-specific hepatic microsomal binding from readily available physicochemical properties. In: 9th European ISSX Meeting. Manchester, UK. Available at: https://www.certara.com/wp-content/uploads/Resources/Posters/DavidISSX2006.pdf.

Wu, Y., et al., 2004. The role of biopharmaceutics in the development of a clinical nanoparticle formulation of MK-0869: a Beagle dog model predicts improved bioavailability and diminished food effect on absorption in human. Int. J. Pharm. 285 (1–2), 135–146. https://doi.org/10.1016/j.ijpharm.2004.08.001.

Zhou, Z., et al., 2017. Statistical investigation of simulated fed intestinal media composition on the equilibrium solubility of oral drugs. Eur. J. Pharm. Sci. 99, 95–104. https://doi.org/10.1016/j.ejps.2016.12.008.

Combining biorelevant *in vitro* and *in silico* tools to investigate the *in vivo* performance of the amorphous solid dispersion formulation of etravirine in the fed state

Chara Litou[a], David B. Turner[b], Nico Holmstock[c], Jens Ceulemans[c], Karl J. Box[e], Edmund Kostewicz[a], Martin Kuentz[d], Rene Holm[c], Jennifer Dressman[a,f,∗]

[a] *Institute of Pharmaceutical Technology, Goethe University, Frankfurt am Main, Germany*
[b] *Certara UK Limited, Simcyp Division, Level 2-Acero, 1 Concourse Way, Sheffield, S1 2BJ, United Kingdom*
[c] *Drug Product Development, Janssen R&D, Johnson & Johnson, Turnhoutseweg 30, 2340 Beerse, Belgium*
[d] *University of Applied Sciences and Arts Northwestern Switzerland, Hofackerstr. 30, 4132, Switzerland*
[e] *Pion Inc. (UK) Ltd., Forest Row, East Sussex, United Kingdom*
[f] *Fraunhofer Institute of Translational Pharmacology and Medicine, Frankfurt, Germany*

A B S T R A C T

Introduction: In the development of bio-enabling formulations, innovative *in vivo* predictive tools to understand and predict the *in vivo* performance of such formulations are needed. Etravirine, a non-nucleoside reverse transcriptase inhibitor, is currently marketed as an amorphous solid dispersion (Intelence® tablets). The aims of this study were 1) to investigate and discuss the advantages of using biorelevant *in vitro* setups to simulate the *in vivo* performance of Intelence® 100 mg and 200 mg tablets in the fed state, 2) to build a Physiologically Based Pharmacokinetic (PBPK) model by combining experimental data and literature information with the commercially available *in silico* software Simcyp® Simulator V17.1 (Certara UK Ltd.), and 3) to discuss the challenges of predicting the *in vivo* performance of an amorphous solid dispersion and identify the parameters which influence the pharmacokinetics of etravirine most.

Methods: Solubility, dissolution and transfer experiments were performed in various biorelevant media simulating the fasted and fed state environment in the gastrointestinal tract. An *in silico* PBPK model for etravirine in healthy volunteers was developed in the Simcyp® Simulator, using *in vitro* results and data available from the literature as input. The impact of pre- and post-absorptive parameters on the pharmacokinetics of etravirine was investigated by simulating various scenarios.

Results: In vitro experiments indicated a large effect of naturally occurring solubilizing agents on the solubility of etravirine. Interestingly, supersaturated concentrations of etravirine were observed over the entire duration of dissolution experiments on Intelence® tablets. Coupling the *in vitro* results with the PBPK model provided the opportunity to investigate two possible absorption scenarios, i.e. with or without implementation of precipitation. The results from the simulations suggested that a scenario in which etravirine does not precipitate is more representative of the *in vivo* data. On the post-absorptive side, it appears that the concentration dependency of the unbound fraction of etravirine in plasma has a significant effect on etravirine pharmacokinetics.

Conclusions: The present study underlines the importance of combining *in vitro* and *in silico* biopharmaceutical tools to advance our knowledge in the field of bio-enabling formulations. Future studies on other bio-enabling formulations can be used to further explore this approach to support rational formulation design as well as robust prediction of clinical outcomes.

1. Introduction

Various innovative formulation approaches have emerged in recent years to address the increasingly challenging physicochemical properties of new Active Pharmaceutical Ingredients (APIs). Inadequate solubility and/or dissolution rate often limit the rate and extent of absorption of such APIs after oral administration. Bio-enabling formulation strategies, such as nano-formulations, complexation with

cyclodextrins, amorphous dispersions and self-emulsifying drug delivery systems, are nowadays utilized in drug development pipelines with the goal of increasing bioavailability. (Buckley et al., 2013; Wilson et al., 2018) However, the *in vitro* characterization of the *in vivo* behavior of these formulations could still benefit from an approach providing more fundamental mechanistic insight. (Wilson et al., 2018; Elkhabaz et al., 2018)

One of the goals of the European Research Program "PEARRL" (www.pearrl.eu) is to design and deliver tools which will enable a better understanding of the *in vivo* performance of bio-enabling formulations. Within the framework of the PEARRL consortium (and as a follow-up to a recently published case example) (Litou et al., 2019), the present study aims to combine results obtained with biorelevant *in vitro* tools with *in silico* modeling techniques to simulate and better understand the *in vivo* behavior of the amorphous solid dispersion of etravirine. This formulation of etravirine is commercially available under the brand name Intelence® and its labeling specifies administration in the fed state.

Etravirine is a second generation non-nucleoside reverse transcriptase inhibitor used for the treatment of HIV-1 infection in treatment-experienced adult patients and pediatric patients two years of age and older, usually in combination with other anti-retroviral agents. (Deeks and Keating, 2008; EMA, 2019; FDA 2019) It has been classified as a BCS Class IV compound as it has very low aqueous solubility, irrespective of the pH (solubility in water is reported to be lower than 1 µg/mL) (Weuts et al., 2011), and low to intermediate permeability. (Intelence, 2008) It is a weakly basic compound (reported pKa values are 4.5, 3.75 and <3) (Bevernage et al., 2012; Moltó, 2015; Schöller-Gyüre et al., 2008b) with a high log*P* value (reported values are 5.2 and 5.54) (Bevernage et al., 2012; Rajoli et al., 2015). In the literature there have only been a few attempts thus far to characterize etravirine *in vitro*. Bevernage et al. measured the solubility of crystalline etravirine in various versions of biorelevant media, as well as in pooled human gastric and intestinal aspirates. The measured solubility values at 24 h were 0.061, 1.48 and 4.05 µg/mL in pooled fasted human gastric fluids ("FaHGF"), pooled fasted human intestinal fluids ("FaHIF") and pooled fed human intestinal fluids (obtained after the administration of 400 mL of Ensure Plus®, "FeHIF"), respectively. (Bevernage et al., 2012; Bevernage et al., 2010)

To overcome the poor physicochemical properties of crystalline etravirine and to improve its bioavailability, the manufacturer attempted a variety of different enabling technologies. However, most of them did not result in advantageous outcomes (for example, an orally dosed nano-suspension resulted in negligible plasma concentrations in dogs) (Weuts et al., 2011). Among the various formulations developed and administered in different phases of the clinical trials, the amorphous solid dispersion of etravirine was the most promising formulation, and is nowadays the commercial formulation (Intelence®). (Weuts et al., 2011; Intelence, 2008) In particular, according to the EMA Public Assessment Report, the formulations used in the clinical studies were as follows: 1) TF002: PEG-4000-based capsule, early Phase I and IIa studies, 2) TF035: HPMC tablet using granulo-layering technology, late Phase I and II studies, 3) F060: HPMC tablet using spray-drying technology, pivotal Phase III studies (commercial formulation). (Intelence, 2008)

Despite the extensive clinical study program conducted and the various bridging bioequivalence studies between the different formulations, the pharmacokinetics and *in vivo* behavior of etravirine have not yet been fully explained. (FDA 2019; Intelence, 2008) For example, in Study C141 a single dose of 100 mg of the commercial formulation (F060) was found to be bioequivalent to a single dose of 800 mg of the exploratory formulation TF035, but in Study C228 bioequivalence could not be confirmed between the 100 mg of F060 and 800 mg of TF035 after multiple dosing for 7 days b.i.d. Additionally, multiple-dose administration of F060 at a dose of 200 mg resulted in an etravirine exposure that was approximately 70% higher than that obtained with

the 800 mg multiple-dose administration of the TF035. (Intelence, 2008)

The recommended dose of Intelence® for adults is 100 mg or 200 mg, taken orally twice daily following a meal. (EMA, 2019; FDA 2019) The bioavailability of Intelence® in the fed state is increased by up to 50% in comparison to the bioavailability in the fasted state. (FDA 2019; Intelence, 2008; Schöller-Gyüre et al., 2008b) Moreover, the pharmacokinetics of Intelence® seem to be more than dose proportional. However, the absolute bioavailability has not been determined since no intravenous formulation is available.

The aims of this study were threefold: 1) to investigate the advantages of using biorelevant *in vitro* setups in simulating the *in vivo* performance of Intelence® in the fed state, 2) to build a physiologically based pharmacokinetic (PBPK) model for etravirine in the fed state by combining experimental data and literature information with the commercially available *in silico* software Simcyp® Simulator V17.1 (Certara UK Ltd.), and 3) to assess the importance of pre- and post-absorptive aspects in determining the pharmacokinetic response to administration of the amorphous solid dispersion (ASD) of etravirine.

2. Materials and methods

2.1. Chemicals and reagents

Etravirine powder was kindly donated by Janssen, Belgium. Acetonitrile and water of HPLC grade were obtained from Merck KGaA (Darmstadt, Germany). Sodium dihydrogen phosphate dehydrate of analytical grade was from Merck KGaA (Darmstadt, Germany). Phosphoric acid, sodium chloride and sodium hydroxide were of analytical grade and purchased from VWR chemicals (Leuven, Belgium). Intelence® tablets were commercially purchased from a German pharmacy (Lot # and PZN were HKL1Q00, 06733695 for the 100 mg and IEL3Y00, 08894758 for the 200 mg strength, respectively). Pepsin was purchased from Sigma-Aldrich (Lot # SLBQ2263V). Lipofundin® MCT/LCT 20% was purchased from BRAUN (B. Braun Melsungen AG, Melsungen, Germany). Fasted state simulated gastric fluid (FaSSGF)/fasted state simulated intestinal fluid (FaSSIF V1)/fed state simulated intestinal fluid (FeSSIF V1) powder (lot 01–1512–05NP), FeSSIF V2 powder (lot 03–1610–02) and FaSSIF V3 powder (lot PHA S 1306023) were kindly donated by Biorelevant.com Ltd., (Surrey, UK).

2.2. Experimental methods

2.2.1. Solubility experiments

The solubility of crystalline etravirine was investigated in various Level I and Level II biorelevant media, (Markopoulos et al., 2015; Fuchs et al., 2015) using the Uniprep™ system (Whatman®, Piscataway, NJ, USA), as previously described by Andreas et al. (Andreas et al., 2015) Briefly, an excess amount of etravirine was added to a 3 mL aliquot of the medium and the samples were shaken for 2, 4, 8 and 24 h at 37 °C on an orbital mixer. In agreement with literature data for etravirine, equilibrium was reached by 24 h. (Bevernage et al., 2010) After shaking, the samples were immediately filtered through pre-warmed 0.45 µm PTFE filters and analyzed by HPLC. Solubility measurements were carried out at least in triplicate ($n \geq 3$) and the final pH of the medium (pH_{final}) was recorded in all cases. In every case the pH_{final} was only slightly or not at all different from the initial pH value of the medium.

2.2.2. Dissolution experiments

Dissolution experiments of the Intelence® tablets were performed using the paddle (USP II) apparatus (Erweka DT 600, Heusenstamm, Germany). Each vessel contained 250 mL for media simulating gastric fluids and 500 mL when simulating intestinal fluids. The rotation speed of the paddle was set at 75 rpm. The temperature in the vessels was maintained at 37.0 ± 0.5 °C throughout the experiment. Samples were

withdrawn at 5, 7.5, 10, 15, 20, 30, 40, 60, 90, 120, 150, 180, 210, 240 and 1440 min with glass syringes, through a cylindrical polyethylene filter stick with a pore size of 4 μm attached to the end of the sampling tubes. Immediately thereafter, the samples were filtered through 0.45 μm PTFE filters (Whatman®, Piscataway, NJ, USA). After discarding the first 1 mL, the filtrate was diluted with mobile phase and analyzed by HPLC. All dissolution experiments were performed in triplicate ($n = 3$) and the final pH in the vessels was recorded in all cases. At the end of the 24 h dissolution experiment, any solid remaining in the dissolution vessel was collected, separated from the liquid medium, dried in a vacuum drying oven (Heraeus VTR 5022, Heraeus Holding GmbH, Hanau, Germany) and analysed by Differential Scanning Calorimetry (DSC 6000 with Autosampler, Perkin Elmer, Waltham, USA).

2.2.3. Transfer experiments

Transfer experiments were performed for both the 100 mg and 200 mg Intelence® capsules utilizing the USP II apparatus, as described previously by Berlin et al. (Berlin et al., 2014) Briefly, 250 mL of Level III FaSSGF pH 2.0 and 350 mL of Level II FaSSIF V1, FaSSIF V3, or FaSSIF V1$_{concentrated}$ (5.14 mM NaTC, in order to account for the dilution occurring after transfer) were used as the dissolution media in the gastric and duodenal compartments, respectively. The rotation speed of the paddles was set at 75 rpm. The temperature in the vessels was maintained at 37.0 ± 0.5 °C throughout the experiment. A peristaltic pump set to first order kinetics ($t_{1/2} = 9$ min) was used to transfer the medium from the gastric to the duodenal compartment, from which samples were withdrawn at 5, 10, 15, 20, 30, 45, 60, 75, 90, 120, 180 and 240 min. Sample handling and analysis were as described for the dissolution experiments.

2.2.4. Chromatographic assays

For the quantitative analysis of the samples, a HPLC-UV system was used (Hitachi Chromaster; Hitachi Ltd., Tokyo, Japan or Spectra System HPLC, ThermoQuest Inc., San Jose, USA). The analytical column was a BDS Hypersil C18, 3 μm, 150 × 3 mm (Thermo Scientific) combined with a pre-column (BDS Hypersil C-18, 3 μm, 10 × 4 mm). The mobile phase consisted of 60:40% v/v AcN: H$_2$O. The detection wavelength was set at 310 nm, the injection volume at 20 μL and the flow rate at 0.8 mL/min. The limit of detection (LOD) and of quantification (LOQ) were 0.01 μg/mL and 0.05 μg/mL, respectively.

2.3. Pharmacokinetic data and methods

2.3.1. In vivo studies

Data from five clinical studies with the commercial formulation (F060) were used to support the development and verification of the PBPK model of etravirine. In all cases, etravirine was administered orally, since no intravenous formulation is available. (Intelence, 2008)

The first study was an open-label, randomized, crossover study conducted in 37 healthy volunteers (29% females). The subjects were administered one 100 mg Intelence® (non-coated) tablet, four 25 mg non-coated etravirine tablets, or one 100 mg etravirine tablet dispersed in 100 mL water, along with approximately 200 mL of water and a standardized breakfast. (Kakuda et al., 2013)

The second study was an open-label, randomized, crossover study, conducted in 24 healthy volunteers (25% females), with the aim of comparing the bioavailability of etravirine administered as one 200 mg Intelence® tablet, or as two 100 mg Intelence® tablets. In this study, the subjects were administered a) two 100 mg Intelence® tablets, or b) one 200 mg Intelence® tablet, after the administration of a standard breakfast, c) two 100 mg coated etravirine tablets, or d) one 200 mg coated etravirine tablet. (Kakuda et al., 2013)

The third study was an open-label, randomized, crossover study, conducted in 24 healthy male volunteers with the aim of investigating the effect of various meals on the bioavailability of etravirine. The subjects were administered one 100 mg Intelence® tablet along with approximately 200 mL of water and one of the following meals: a) standard, b) light, c) enhanced fiber or d) high-fat breakfast. A standard lunch was served 4.5 h after dosing. (Schöller-Gyüre et al., 2008b)

The fourth study was an open-label, randomized, crossover study, conducted in 18 healthy volunteers (58% females). The subjects were administered a 100 mg Intelence® tablet alone, along with 200 mL of water and a standardized breakfast, or with a) 150 mg ranitidine b.i.d. for eleven days, or b) 40 mg of omeprazole q.d. for eleven days. (Schöller-Gyüre et al., 2008a)

The fifth study aimed to investigate the pharmacokinetics of etravirine in HIV-patients with mild and moderate hepatic impairment (% female not reported), in comparison to their matched healthy control volunteers ($n = 8$). The subjects were administered a 200 mg Intelence® tablet twice daily along with 200 mL of water and a standardized breakfast/lunch, on study days 1 to 7. (Schöller-Gyüre et al., 2010) Only the pharmacokinetic profiles of Day 1 of the healthy matched controls were used for the purposes of the current study.

For the first two clinical studies, individual pharmacokinetic data were available (kindly provided by Janssen, Belgium - data on file) (Kakuda et al., 2013), whereas for the later three clinical studies, only mean (without standard deviations) pharmacokinetic profiles were available, which were derived and digitalized from the respective studies (Schöller-Gyüre et al., 2008b; Schöller-Gyüre et al., 2008a; Schöller-Gyüre et al., 2010) using the WebPlotDigitizer (version 4.1; PLOTCON; Oakland, USA). All available demographic data from the aforementioned clinical studies were used in the simulations of the clinical trials.

2.3.2. Etravirine pharmacokinetic parameters obtained from the literature

Etravirine is extensively bound to plasma proteins (approximately 99%, albumin and α1-acid glycoprotein) and the reported average blood to plasma concentration ratio in humans is 0.7, although intersubject variation is high. (Intelence, 2008) A detailed study in which the metabolism of etravirine was evaluated using human liver microsomes, cDNA expressed cytochromes P450s and UDP-glucuronosyltransferases has been published by Yanakakis and Bumpus. (Yanakakis and Bumpus, 2012) Etravirine is mainly metabolized by CYP3A4 and CYP2C19, although CYP2C9 and UGT 1A3 and 1A8 are also involved. Seven metabolites were identified in total by Yanakakis and Bumpus, however, K_m and V_{max} values were provided only for four out of the seven. (Yanakakis and Bumpus, 2012) By contrast, the renal clearance of etravirine is minimal. The mean plasma half-life is reported to be approximately 41 h and ranges from 21 h to 61 h. (Brayfield, 2011) Etravirine also exhibits large inter- (approximately 80%) and intra-individual (approximately 40%) variability in other pharmacokinetic parameters. Even taking this variability into account, the pharmacokinetics of this compound appear to be more than dose proportional. (Intelence, 2008) It has additionally been noted that etravirine exposure appears to be lower in HIV-1 infected patients than in healthy subjects. (Intelence, 2008)

In the literature there have only been a few attempts to explain the *in vivo* behavior of this compound using *in silico* approaches. Of these, most have focused on the metabolism of the drug and potential Drug-Drug Interactions (DDIs) in population pharmacokinetic studies conducted in HIV-1 infected patients. (Moltó et al., 2016; Green et al., 2017; Lubomirov et al., 2013; Kakuda et al., 2010) Despite efforts to explain the observed variability in the elimination of etravirine, no robust conclusions could be reached and only a small percentage of the variability could be explained. In all the aforementioned studies, body weight was identified as an important parameter affecting the PK of etravirine, however, no specific data were made available regarding body composition of the enrolled subjects.

Green et al. (Green et al., 2017) and Lubomirov et al. (Lubomirov et al., 2013) attempted to identify the impact of CYP2C9/CYP2C19 phenotype on the pharmacokinetics of etravirine. Despite the

Table 1
Parameter values used for the simulations of the *in vivo* performance of Intelence® in the fed state.

Parameter	Value	Reference/ comments
Physicochemical & blood binding		
MW (g/mol)	453.28	
$\log P_{o:w}$	5.2	Janssen data on file
pKa	3.5	Janssen data on file
Blood/ plasma ratio	0.7	(FDA, 2019; Intelence, 2008)
Fraction unbound in plasma	0.01	(Intelence, 2008; Moltó, 2015; Moltó et al., 2016)
Absorption		
Model	ADAM	
$P_{app,\ Caco2}$ (x10^{-6} cm/s)	6.5	Janssen data on file
Formulation type	Immediate release	Commercial labeling
Solubility-diffusion layer model		
		No precipitation approach
Total solubility in segment		
For 100 mg dose (μg/mL)	140, 143	Stomach, small intestine
For 200 mg dose (μg/mL)	310, 170	Stomach, small intestine
		Implementation of precipitation approach
Total solubility in segment		
For both 100 mg and 200 mg (μg/mL)	29.4, 23.9	Stomach, small intestine
Kinetic solubility (model 1)		
Critical supersaturation ratio	6, 8	100 mg, 200 mg
Precipitation rate constant (1/h)	0.31, 0.41	100 mg, 200 mg
Distribution		
Model	Full PBPK	
V_{ss} (L/kg)	5.36	PE Tool, method 2
Elimination		
Elimination type	Enzyme kinetics	
V_{max} (pmol/mg/min)	0.072, 0.067, 5.57, 0.166	For CYP3A4-M1, CYP3A4-M2, CYP2C19 and CYP3A4-M3, respectively (Yanakakis and Bumpus, 2012)
K_m (μM)	5.83, 72.85, 7.33, 27.8	
f_{umic}	0.0935	Simcyp prediction toolbox
Additional clearance-HLM (μL/min/mg protein)	900, 400	PE Tool for 100 mg, 200 mg
Renal clearance (L/h)	0.0006	

fact that variations in the CYP2C9/CYP2C19 phenotype (*i.e.* extensive, intermediate, poor metabolizer) had an effect on the metabolism of etravirine, only 5–16% of the overall variability in the apparent clearance of etravirine could be explained by the genetic differences, indicating that other factors must be involved in the elimination of etravirine.

Last, but not least, it is interesting to note the wide range of apparent volume of distribution for etravirine reported in the respective population-pharmacokinetic studies *i.e.* 420–1370 L, (Rajoli et al., 2015; Green et al., 2017; Lubomirov et al., 2013; Kakuda et al., 2010; Siccardi et al., 2013) again suggesting that etravirine is a compound with challenging post-absorptive behavior.

2.3.3. Modeling methods and strategies

PBPK modeling and simulations were performed using the Simcyp® Simulator (V17.1; Certara, Sheffield, UK). All relevant input parameters for the development of the PBPK models and simulations are summarized in Table 1.

Based on the properties of the compound as well as the apparent volumes of distribution (420–1370 L) (Rajoli et al., 2015; Green et al., 2017; Lubomirov et al., 2013; Kakuda et al., 2010; Siccardi et al., 2013) reported in the literature, a full PBPK model was set up for etravirine. The apparent volume of distribution and clearance were estimated using the Parameter Estimation (PE) Tool, by simultaneously fitting these parameters to all individual PK profiles available for the 100 mg and 200 mg dose strength. In particular, the apparent volume of distribution was estimated based on the Rodgers-Rowland equation and was kept constant at both doses (*i.e.* same apparent volume of distribution for 100 mg and 200 mg dose strength). For the enzyme kinetics the values reported in the study of Yanakakis and Bumpus (Yanakakis and Bumpus, 2012) were used, as previously described in population PK studies in the literature (Moltó et al., 2016; Green et al., 2017), whereas the clearance due to other pathways was estimated

from the available individual *in vivo* profiles for the 100 mg and 200 mg doses under the assumption of a constant apparent volume of distribution at both doses. Since etravirine pharmacokinetics are not dose-proportional, the clearance estimated for the additional pathways was different for each dose, such that for the 200 mg dose the value was approximately half of the value estimated for the 100 mg dose. It should be noted that despite all efforts, only approximately 20% of the clearance can be accounted for in a mechanistic way in the current adult PBPK model and further efforts are required to elucidate the mechanisms involved.

To model the absorption process, the Advanced Dissolution, Absorption and Metabolism (ADAM) model was utilized. This model divides the gastrointestinal tract to 9 anatomically distinct segments starting from stomach through small intestine to the colon, and has been described in detail by Jamei et al. and Darwich et al. (Jamei et al., 2009; S. Darwich et al., 2010) The apparent permeability of etravirine was set at 6.5×10^{-6} cm/s, as reported in a Caco2 assay (but, with no accompanying permeability values for reference compounds, Janssen data on file).

One of the challenges that is often faced when attempting to build a detailed solubility/dissolution model for bio-enabling formulations based on *in vitro* data is that the properties of the drug may have been deliberately altered in the formulation vis à vis those of the unformulated drug. In this case etravirine is presented in the amorphous form in the commercial formulation, whereas the pure drug is crystalline. Based on the *in vitro* results obtained in the current study (see Results section) and with a view to investigating the *in vivo* behavior of etravirine, two approaches were followed. In the first approach, the maximum concentration of dissolved etravirine observed in the medium was used as the "solubility" of the amorphous/formulated drug. This approach assumes that etravirine does not precipitate *in vivo*, due to rapid absorption of the API and/or its dilution in the intestinal fluids, and will subsequently be referred to as the "no-precipitation

approach". In the second approach, the concentration achieved in the dissolution vessel after 24 h was used to represent the "solubility" of the amorphous/formulated drug. Additionally, the observed supersaturation ratio and calculated precipitation rate constant parameter were implemented. The critical supersaturation ratio was calculated from the maximum observed concentration dissolved in the individual dissolution vessel divided by the 24 h concentration in the same vessel. The precipitation rate constant was calculated according to the timeframe over which the concentration reverted from the maximum concentration to the 24 h concentration. This approach will subsequently be referred to as the "implementation of precipitation" approach.

2.4. Data analysis and statistics

The data derived from solubility, dissolution and transfer experiments are presented as the arithmetic means with standard deviations. All PK profiles obtained from the literature were digitalized with the WebPlotDigitizer (version 4.1; PLOTCON; Oakland, USA). The estimation of the post-absorptive parameters within the Parameter Estimation module of the Simcyp® Simulator was performed with the Maximum Likelihood method. (Tsamandouras et al., 2015) The prediction accuracy of the simulated plasma profiles was evaluated with the average fold error (AFE) and absolute average fold error (AAFE) (Eqs. (1) and (2),

$$AFE = 10^{\frac{1}{n} \sum \log\left(\frac{pred_t}{obs_t}\right)} \tag{1}$$

$$AAFE = 10^{\frac{1}{n} \sum \left| \log\left(\frac{pred_t}{obs_t}\right) \right|} \tag{2}$$

where n is the number of time points at which the concentration was determined and $pred_t$, obs_t are the predicted and observed concentrations at a given time point t, respectively. An *AFE* greater or smaller than one indicates an overestimation or underestimation of the observed data, respectively, whereas *AAFE* is a measure of the absolute error from the true value. An *AAFE* $\leq$ 2 can be considered as a successful prediction. (Obach et al., 1997; Poulin and Theil, 2009)

Statistical analysis (including calculation of 95% CIs) was performed with Simcyp® (V17.1; Certara, Sheffield, UK).

3. Results

3.1. In vitro studies

3.1.1. Solubility experiments
Mean solubility values ($\pm$ SD) of crystalline etravirine at 24 h in Level I and Level III FaSSGF, Level I and Level II FaSSIF V1, FaSSIF V2, FaSSIF V3, FeSSIF V1, FeSSIF V2 and FeSSGF are presented in Table 2, together with the pH values recorded at the end of the solubility experiment (pH$_{final}$), as well as solubility values in pooled human aspirates that have been reported in literature.

The solubility of crystalline etravirine was below LOQ, *i.e.* 0.05 µg/mL, in all Level I biorelevant media measured. It is interesting to note that the solubility of crystalline etravirine in Level III FaSSGF was also below the LOQ, despite the fact that etravirine is a weak base and thus higher solubility values are expected in media with acidic pH. These data are in line with those of Bevernage et al., who reported extremely low solubility values in Level II FaSSGF (approximately 0.009 µg/mL). (Bevernage et al., 2012)

By contrast, the solubility values of crystalline etravirine in Level II biorelevant media simulating the intestinal fluids in the fasted and the gastric and intestinal fluids in the fed state were measurable and were dependent on the amount and type of surfactants used in the respective medium. In particular, comparison of solubility between Level I and II media reveals the role of naturally occurring surfactants in the solubility of etravirine. These data are in line with those of Bevernage et al., who reported similar values in Level II FaSSIF V1 and Level II FeSSIF V1

Table 2
Mean solubility ($\pm$ SD) at 24 h of crystalline etravirine in various biorelevant media used in the present study, pH recorded at the end of the solubility experiment (pH$_{final}$) and solubility of crystalline etravirine in human aspirates reported in literature.

Medium	Solubility $\pm$ SD (µg/mL)	pH$_{final}$
Biorelevant media		
Level I FaSSGF	<LOQ	1.6
Level III FaSSGF	<LOQ	1.6
Level I FaSSIF V1	<LOQ	6.5
Level II FaSSIF V1	0.70 $\pm$ 0.02	6.5
Level I FaSSIF V2	<LOQ	6.5
Level II FaSSIF V2	0.24 $\pm$ 0.02	6.5
Level I FaSSIF V3	<LOQ	6.5
Level II FaSSIF V3	0.11 $\pm$ 0.03	6.7
Level II FeSSGF	3.66 $\pm$ 0.09	5.0
Level I FeSSIF V1	<LOQ	5.0
Level II FeSSIF V1	3.25 $\pm$ 0.13	5.0
Level I FeSSIF V2	<LOQ	5.9
Level II FeSSIF V2	3.47 $\pm$ 0.13	5.9
Human aspirates (Bevernage et al., 2012; Bevernage et al., 2010)		
FaHGF	0.06	1.6
FaHIF	1.5	6.7
FeHIF	4.05	6.2
Fat enriched-FeHIF	8.3	6.0

(approximately 1 µg/mL and 6.2 µg/mL, respectively). (Bevernage et al., 2012; Bevernage et al., 2010)

Bevernage et al. also performed solubility measurements of crystalline etravirine in pooled human aspirates. These researchers aspirated gastric and intestinal fluids from healthy volunteers in the fasted state (FaHGF, $n = 4$ and FaHIF, $n = 5$, respectively), as well as in the fed state after administration of Ensure Plus® (29% fat content, FeHIF), or Scandishake Mix® (46% fat content, "Fat enriched"-FeHIF). (Bevernage et al., 2012; Bevernage et al., 2010) The solubility of etravirine observed in FaHIF (with a total bile salt concentration of 5.4 $\pm$ 0.058 mM) was approximately 1.5 µg/mL, whereas in FeHIF (with a total bile salt concentration of 10.4 $\pm$ 1.2 mM) it was around 4 µg/mL and in "Fat enriched"-FeHIF (with a total bile salt concentration of 12.7 $\pm$ 0.2 mM) it was 8.3 µg/mL. These results underline the large effect of native surfactants on the solubilization of etravirine.

3.1.2. Dissolution experiments
Dissolution experiments were performed on Intelence® tablets at both dose strengths in biorelevant media simulating the contents of the fasted stomach (Level III FaSSGF), fasted upper small intestine (Level II FaSSIF V1, FaSSIF V2 and FaSSIF V3), fed stomach (Level II FeSSGF) and fed upper small intestine (Level II FeSSIF V1 and FeSSIF V2). (Markopoulos et al., 2015) The mean concentration ($\pm$ SD) of dissolved etravirine with time during the first 4 h of dissolution in these experiments are presented in Figs. 1–3.

As observed in these figures, dissolution at both doses is fast, incomplete and reaches a maximum value of dissolved etravirine concentration within 15–30 min. The dissolution results in biorelevant media simulating the fed *vs*. fasted state are clearly in agreement with the large food effect (approximately 50%) observed *in vivo* for Intelence® tablets.

After the maximum value is reached, the concentration of dissolved drug decreases to the 24 h value, which is similar for the 100 mg and 200 mg tablets. The time to reach this 24 h value is dependent on the type of biorelevant medium used for the dissolution experiment and the dose / maximum dissolved concentration of etravirine achieved. The 24 h concentrations in the dissolution experiments with the formulated
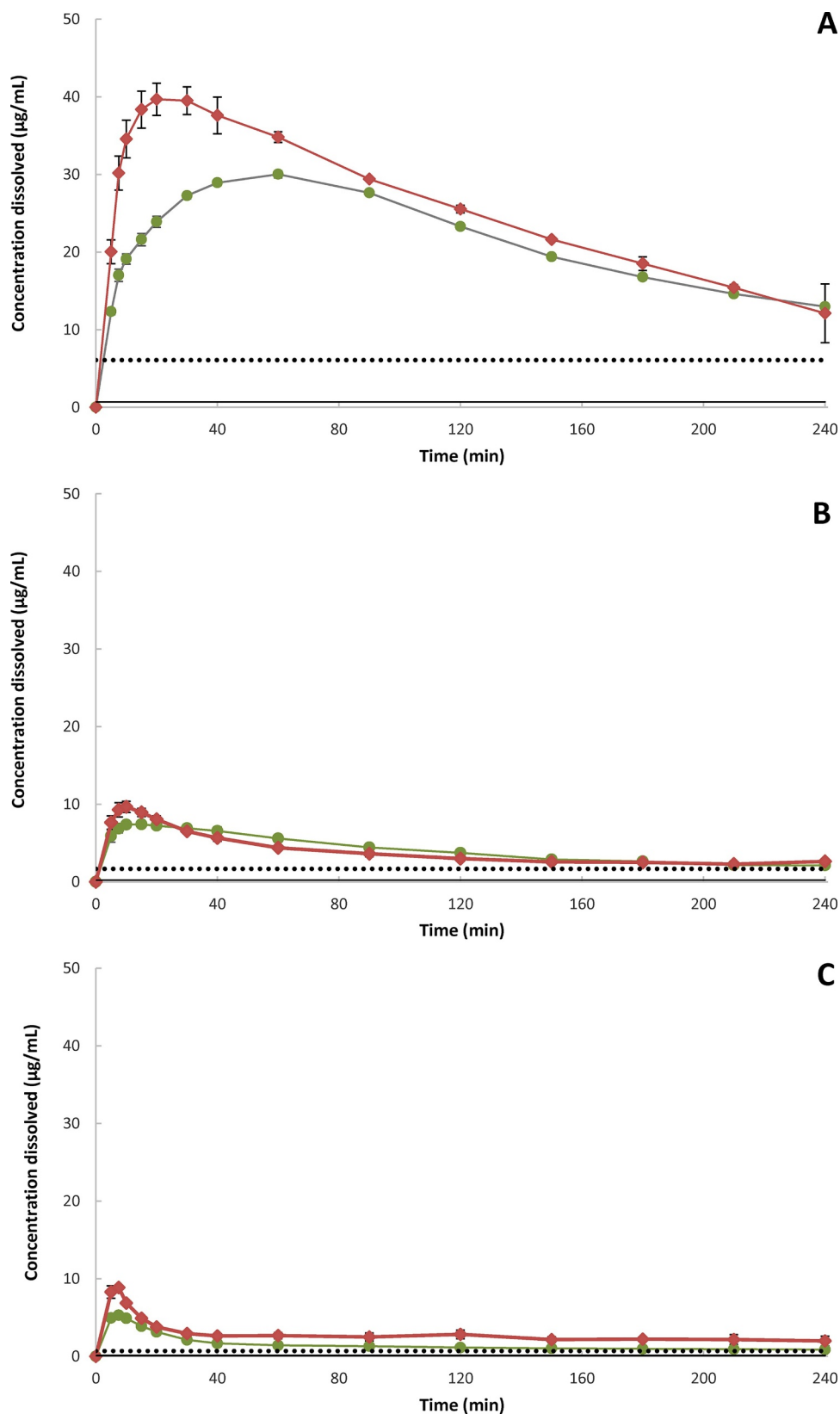
Fig. 1. Mean (± SD) concentration of dissolved etravirine from 100 mg (●) and 200 mg (◆) Intelence® tablets in various media simulating the fasted upper small intestine: A) Level II FaSSIF V1, B) Level II FaSSIF V2 and C) Level II FaSSIF V3. The solid and dotted lines represent the 24 h solubility value of crystalline etravirine and the 24 h value resulting from the dissolution experiments of the formulated drug, respectively.

drug, as well as their ratios to the 24 h solubility value of crystalline etravirine in the respective media, are presented in Table 3. When the 24 h value from the dissolution experiment with the formulated drug is compared with the 24 h solubility value for the crystalline API, it is observed that the concentration of etravirine in the tablet dissolution

experiment remains supersaturated over the entire duration of the experiment. DSC experiments conducted with the solid collected at the end of the dissolution experiments revealed the absence of any crystalline drug. Taken together with the concentrations achieved in dissolution of the Intelence® tablets, this result suggests that the solubility
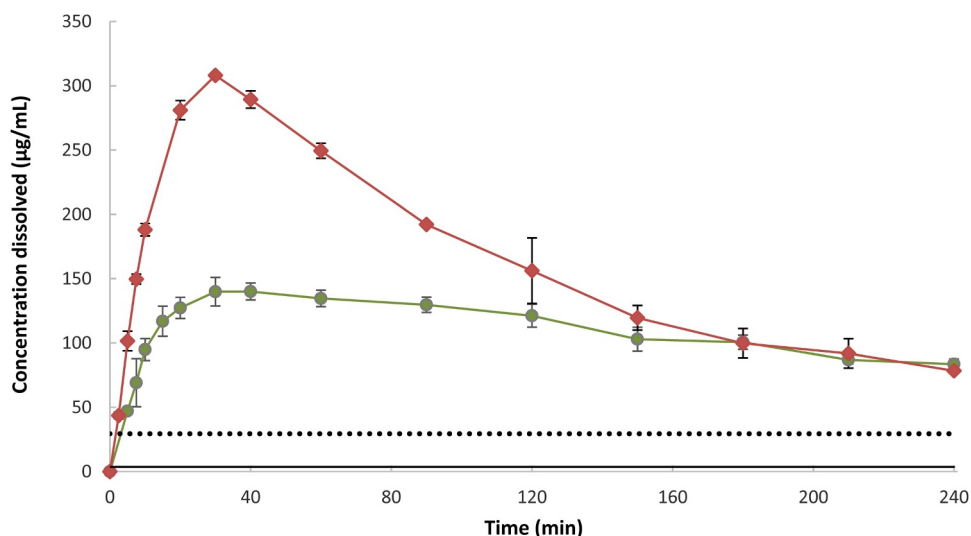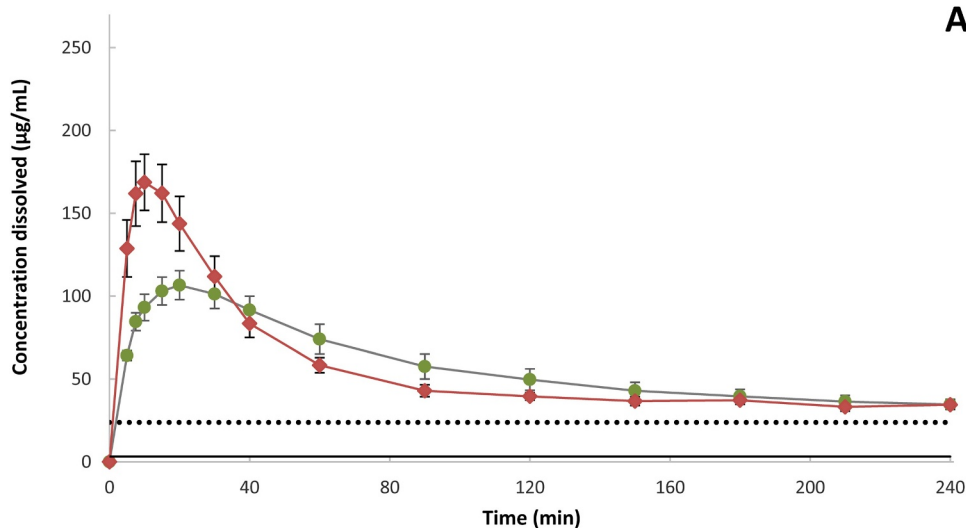
Fig. 2. Mean (± SD) concentration of dissolved etravirine from 100 mg (●) and 200 mg (◆) Intelence® tablets in Level II FeSSGF. The solid and dotted lines represent the 24 h solubility value of crystalline etravirine and the 24 h value resulting from the dissolution experiments of the formulated drug, respectively.

of the amorphous form is substantially higher than that of the crystalline form.

When comparing the ratios of the maximum concentrations reached after dissolution of the 200 mg and 100 mg Intelence® tablets in the various versions of biorelevant media, it is interesting to note that the higher ratios (greater than 2) are observed in the media which also contain other components (*e.g.* glyceryl monooleate in Level II FeSSIF V2) rather than just sodium taurocholate (NaTC) and lecithin (*e.g.* Level

Fig. 3. Mean (± SD) concentration of dissolved etravirine from 100 mg (●) and 200 mg (◆) Intelence® tablets in various media simulating the fed upper small intestine: a) Level II FeSSIF V1 and b) Level II FeSSIF V2. The solid and dotted lines represent the 24 h solubility value of crystalline etravirine and the 24 h value resulting from the dissolution experiments of the formulated drug, respectively.
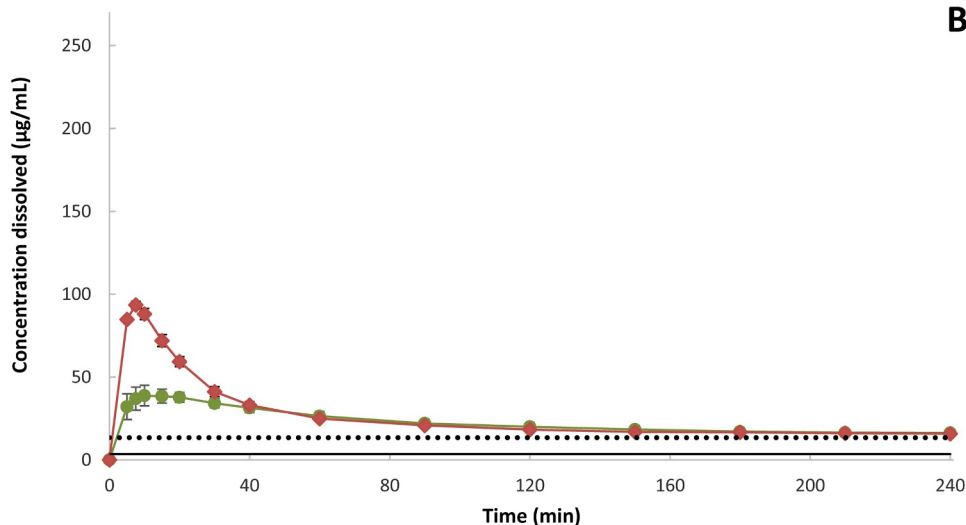
Table 3

Etravirine mean (± SD) dissolved concentrations resulting after 24 h dissolution experiments of 100 mg and 200 mg Intelence® tablets (formulated drug) in various biorelevant media and ratios to the 24 h solubility value of the crystalline API.

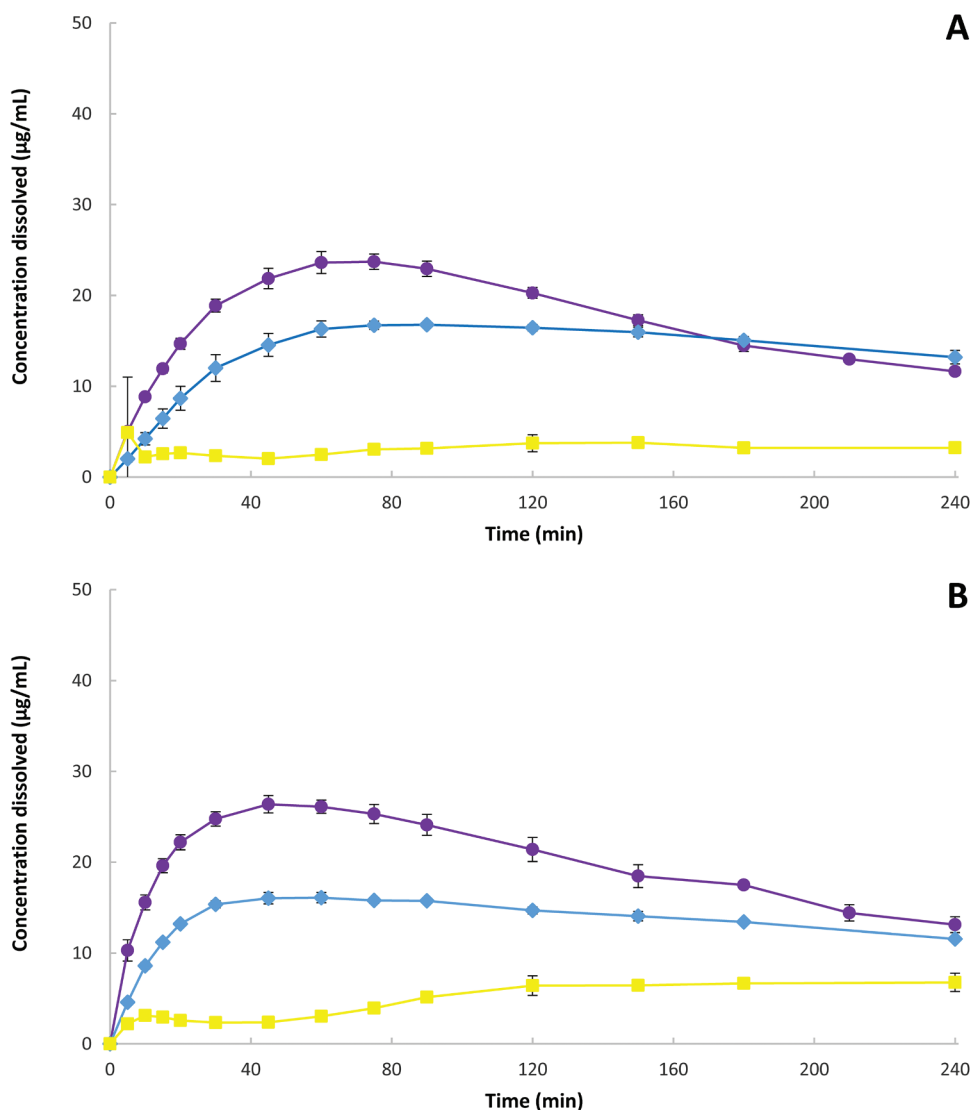| Medium	Mean concentration of drug dissolved (± SD) after 24 h of dissolution (μg/mL)	Ratio (formulated drug dissolved concentration at 24 h/ crystalline drug solubility at 24 h)
Level II FaSSIF V1	6.08 ± 0.22	8.7
Level II FaSSIF V2	1.67 ± 0.10	7.0
Level II FaSSIF V3	0.68 ± 0.08	6.2
Level II FeSSGF	29.42 ± 3.19	8.0
Level II FeSSIF V1	23.87 ± 0.26	7.3
Level II FeSSIF V2	13.40 ± 0.84	3.7

II FaSSIF V1 and FeSSIF V1). This observation suggests that etravirine interacts differently with the various biorelevant components, such that addition of additional lipid components like glycerylmonooleate not only increases the amount of etravirine dissolved, but also leads to a longer duration of drug in solution. This observation is also in agreement with the study of Elkhabaz et al., who observed different interactions between the biorelevant components and the amorphous form of ezetimibe. (Elkhabaz et al., 2018)

3.1.3. Transfer experiments

Transfer experiments were performed to further investigate the potential for supersaturation and precipitation of etravirine. The mean concentration (± SD) of dissolved etravirine with time during the 4 h transfer experiments from Level III FaSSGF to Level II FaSSIF V1, Level II FaSSIF V3 or Level II FaSSIF V1$_{concentrated}$ for the 100 mg and 200 mg Intelence® tablets are presented in Fig. 4.

In accordance with the monophasic dissolution and solubility experiments, there is a pronounced effect of the amount and type of surfactants of the biorelevant medium on the concentration of etravirine generated in the transfer studies. In particular, the maximum concentration dissolved during the transfer experiments are the highest when the drug is transferred to a medium with an initially higher

Fig. 4. Mean (± SD) concentration of dissolved etravirine from A) 100 mg and B) 200 mg Intelence® tablets in Level II FaSSIF V1 (◆), Level II FaSSIF V3 (■) and Level II FaSSIF V1$_{concentrated}$ (●) after transfer from Level III FaSSGF.
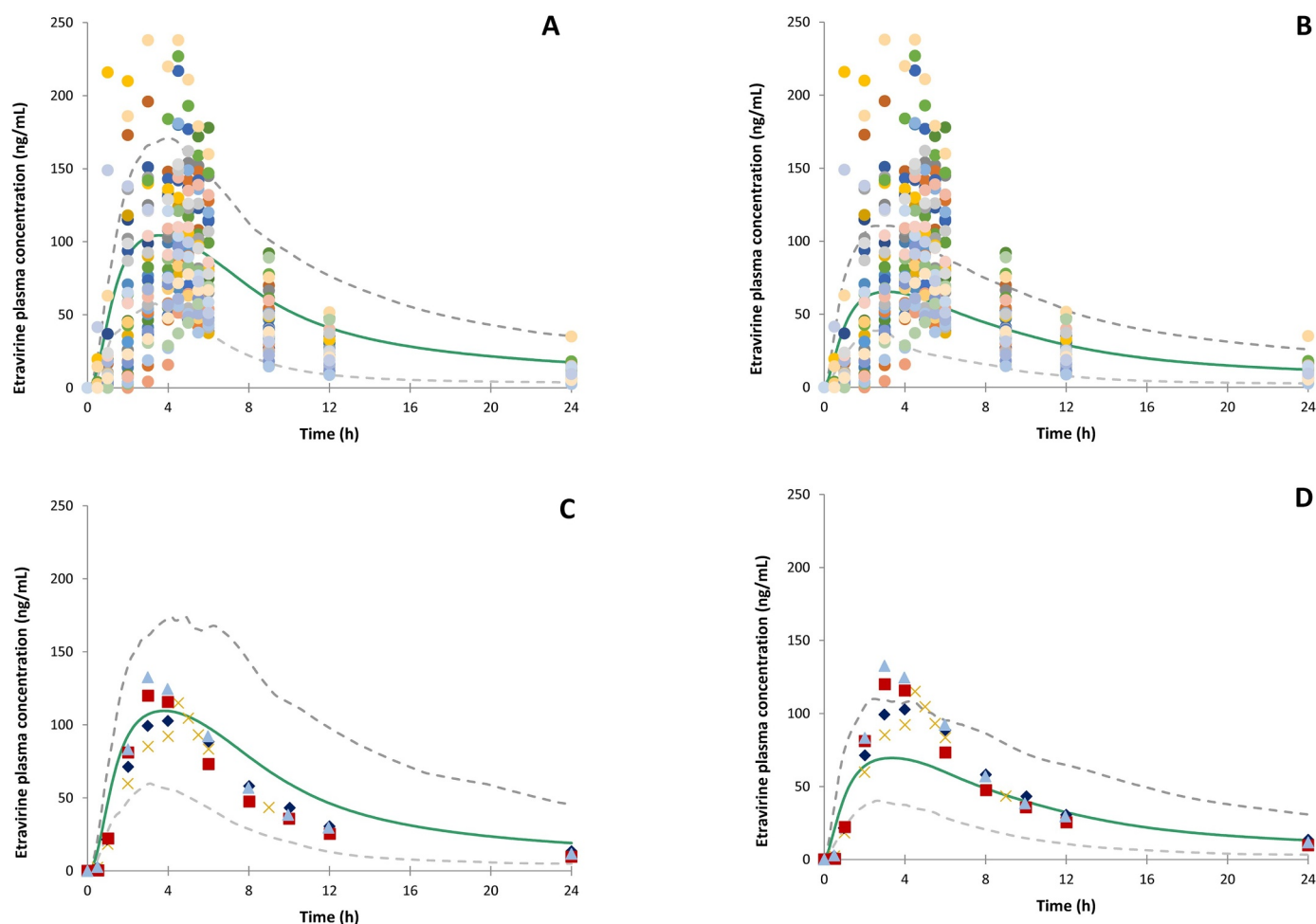
Fig. 5. Simulated (thick solid line, population mean; thin dashed lines, 5th and 95th percentile of population) and clinically reported plasma concentrations after administration of a 100 mg Intelence® tablet following: A)/C) the first ("no-precipitation") and B)/D) the second ("implementation of precipitation") approach, in the fed state. With circles (●) the individual pharmacokinetic data (Janssen data on file), whereas with x's (×) and diamonds (◆), squares (■) and triangles (▲) the mean pharmacokinetic profiles reported by Kakuda et al. (Kakuda et al., 2013) and Schöller-Gyüre et al. (Schöller-Gyüre et al., 2008b; Schöller-Gyüre et al., 2008a) are presented.

surfactant concentration, *i.e.* Level II FaSSIF V1$_{concentrated}$ (5.14 mM NaTC) *vs.* Level II FaSSIF V1 (3 mM NaTC). Furthermore, as previously mentioned, the type of the surfactant seems to play a role in the dissolution of the amorphous etravirine. When etravirine is transferred from the amorphous solid dispersion into Level II FaSSIF V3, which also contains glycocholate and cholesterol, there is a greater ratio between the maximum concentration dissolved from 200 mg tablets *vs.* 100 mg tablets in comparison to the ratios achieved when the same formulation is transferred to media containing only sodium taurocholate and lecithin *i.e.* Level II FaSSIF V1 and Level II FaSSIF V1$_{concentrated}$.

Comparing the transfer with the dissolution experiments in media simulating the fasted state, the etravirine concentration starts to decrease later in the transfer experiments (after approximately 90–120 min) than in the dissolution experiments (after 30 min), and at a slower rate than observed in the single medium dissolution experiments. Although it would be interesting to know whether similar differences are observed under fed state conditions, there is currently no validated transfer setup for simulating drug transfer from the fed stomach to the fed small intestine (noting that some early attempts have been made). (Pentafragka et al., 2019) Nonetheless, the similar maximum concentrations of dissolved etravirine achieved in Level II FeSSGF and Level II FeSSIF V1, together with the moderate permeability of etravirine, suggest that precipitation is unlikely to happen in the fed state *in vivo*.

3.2. PBPK model and simulations

3.2.1. Input of in vitro derived parameters and effect of possible precipitation on the simulated profiles

When evaluating the results from the *in vitro* experiments of etravirine and implementing them into the PBPK model, the questions that arise are, for example, which "solubility" is appropriate for the formulated drug? Would etravirine really precipitate *in vivo*? If the answer to the latter question is yes, does it precipitate to a crystalline form or does it form amorphous aggregates? Furthermore, if it does precipitate *in vivo* in the fed state, are the precipitation rate constants observed in the monophasic fed state dissolution experiments representative of the *in vivo* precipitation?

In order to account for all possible scenarios and gain a better understanding of the *in vivo* behavior of etravirine, two approaches were followed when implementing the *in vitro* data in the PBPK model: "no precipitation" and "implementation of precipitation". The simulated plasma profiles after oral administration of a 100 mg or 200 mg Intelence® tablet in the fed state *vs.* the individual observed plasma concentrations (Janssen data on file), as well as the observed mean pharmacokinetic profiles reported in the literature (Schöller-Gyüre et al., 2008b; Kakuda et al., 2013; Schöller-Gyüre et al., 2008a), following both approaches are presented in Fig. 5 and 6. The AFE and AAFE for each simulation approach compared to the observed mean pharmacokinetic profiles are presented in Table 4.
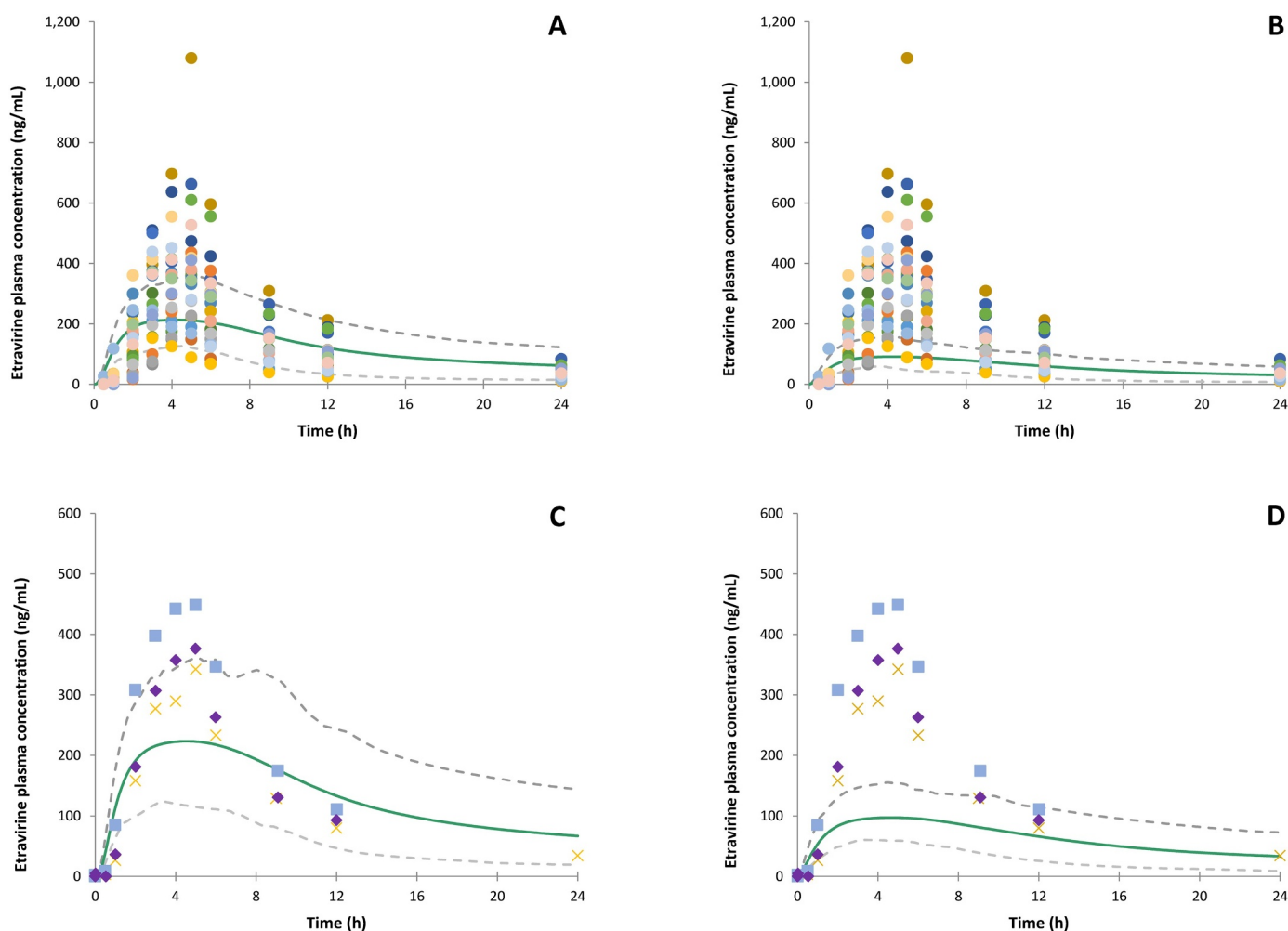
Fig. 6. Simulated (thick solid line, population mean; thin dashed lines, 5th and 95th percentile of population) and clinically reported plasma concentrations after administration of a 200 mg Intelence® tablet following: A)/C) the first ("no-precipitation") and B)/D) the second ("implementation of precipitation") approach, in the fed state. With circles (●) the individual pharmacokinetic data (Janssen data on file), whereas with x's (×) and diamonds (◆), squares (■) and triangles (▲) the mean pharmacokinetic profiles reported by Kakuda et al. (Kakuda et al., 2013) and Schöller-Gyüre et al. (Schöller-Gyüre et al., 2010) are presented.

As can be observed in Figs. 5 and 6 and Table 4, the first approach, *i.e.* "no precipitation", appears to be more representative of the behavior of etravirine *in vivo*. In particular, the "no precipitation" approach resulted in a good representation of the individual pharmacokinetic data (Janssen data on file, Fig. 5A) after the administration of a 100 mg Intelence® tablet in fed state as well as leading to overall good predictions of the mean observed pharmacokinetic profiles reported in the literature (Schöller-Gyüre et al., 2008b; Kakuda et al., 2013; Schöller-Gyüre et al., 2008a) (Fig. 5C), with AAFE mostly ≤ 2. By contrast, the second approach ("implementation of precipitation") led to substantial underprediction of the pharmacokinetics of etravirine (Figs. 5B and 5D). For the 200 mg Intelence® tablets an overall trend to underprediction of the pharmacokinetics of etravirine is observed, however, this trend is far greater when the "implementation of precipitation"

Table 4
Calculated average fold error (AFE) and absolute average fold error (AAFE) for the simulations of observed plasma profiles after oral administration of Intelence® tablets in the fed state.

Dose	100 mg		200 mg		Published clinical data
Metrics	No precipitation	With precipitation	No precipitation	With precipitation	
AFE	1.55	1.11	1.57	0.74	(Kakuda et al., 2013)
AAFE	1.56	1.60	1.93	2.31	
AFE	1.53	1.38	–	–	(Schöller-Gyüre et al., 2008b)
AAFE	1.53	1.82	–	–	
AFE	1.97	1.78	–	–	(Schöller-Gyüre et al., 2008b)
AAFE	2.04	2.34	–	–	
AFE	1.40	1.25	–	–	(Schöller-Gyüre et al., 2008a)
AAFE	1.51	1.94	–	–	
AFE	–	–	0.89	0.42	(Schöller-Gyüre et al., 2010)
AAFE	–	–	1.70	3.00	
AFE	–	–	1.99	0.93	(Schöller-Gyüre et al., 2010)
AAFE	–	–	2.80	3.92	

approach is used (Fig. 6). To further address the goodness of fit, the simulations were also evaluated by using the method proposed by Abduljalil et al., (Abduljalil et al., 2014) in which the sample size and the variance around the pharmacokinetic parameter of interest are also considered. In this method, the 99.998% confidence intervals (CI) for the pharmacokinetic parameter of interest are calculated from the available clinical data. According to the authors, if the simulated value falls within this CI range, the simulation can be considered successful. It should be noted that Abdulljalil et al. only assessed this method using compounds with linear kinetics. The results of these calculations for etravirine can be found in Table 5 of the Supplementary Material. Comparing the simulations, it appears that etravirine does not precipitate to a significant extent when administered in the fed state *in vivo*. This observation, along with the high permeability of etravirine (a P_{app} value of 6.5×10^{-6} cm/sec which is translated to a P_{eff} of approx. 1.1×10^{-4} cm/sec with Simcyp® Simulator internal calculation), suggests that it is more informative to consider etravirine as a DCS IIb compound (Butler and Dressman, 2010) rather than as a BCS Class IV compound.

3.2.2. Post-absorptive parameters that could affect etravirine pharmacokinetics

The model developed for etravirine was able to successfully predict the mean pharmacokinetic profiles of etravirine after administration of a 100 mg Intelence® tablet. However, the model generally under-predicted the mean pharmacokinetic profiles after administration of a 200 mg Intelence® tablet. Furthermore, the 95% CIs were not able to cover all of the individual PK profiles at either dose strength. These observations, in combination with the information provided in the Public Assessment Report of Intelence® regarding the non-linear pharmacokinetics of etravirine (Intelence, 2008), the large range of apparent volume of distribution applied in pharmacokinetic models that have been reported so far in the literature (*i.e.* 420–1370 L) (Rajoli et al., 2015; Green et al., 2017; Lubomirov et al., 2013; Kakuda et al., 2010; Siccardi et al., 2013), as well as the failure to mechanistically account for more than 20% of etravirine elimination by the enzyme kinetics and the fact that only 5–16% of the overall variability in the apparent clearance of etravirine can be explained by the different phenotypes of CYP2C19 (Sections 2.3.2 and 2.3.3), suggest that various post-absorptive parameters can have an important effect on the pharmacokinetics of etravirine and that these should be taken into consideration when simulating the *in vivo* behavior of this compound.

With particular regard to plasma protein binding, Nguyen et al. (Nguyen et al., 2013) measured the unbound fraction (f_u) of etravirine as well as the total etravirine plasma concentrations of nine HIV-1 infected patients, who had been taking Intelence® 200 mg twice daily for at least 2 weeks (median duration of etravirine use: eight months). It was shown that the unbound fraction of etravirine varied with the total etravirine plasma concentration, with the fraction unbound increasing with increasing etravirine plasma concentration. The non-linearity of protein binding may therefore contribute to the *in vivo* variability of etravirine. Similar non-linearity of plasma protein binding has been associated with a high *in vivo* variability in f_u among subjects for other anti-retrovirals such as indinavir, saquinavir, atazanavir, darunavir and lopinavir. (Sudhakaran et al., 2007; Anderson et al., 2000; Bohnert and Gan, 2013; Delille et al., 2014; Back, 2004)

Assuming a concentration dependency of both f_u and V_d, it is an oversimplification to represent the fraction unbound with a single f_u value and the apparent volume of distribution of etravirine with a single V_d value at all time points and all volunteers, at both dose levels. Furthermore, if f_u and V_d are changing with concentration, clearance will also be changing with time. These concentration-dependent effects are challenging to model, especially since residual clearance is typically set at a fixed value. In simulations performed in the current study, the f_u was set at 0.01, as published in the Public Assessment Report (Intelence, 2008) and as used in previously published pop-PK studies

e.g. by Molto et al. (Moltó et al., 2016)

To dig a little deeper into potential causes of the high variability of etravirine pharmacokinetics as well as the differences in ability to simulate the plasma profiles after administration of the 100 mg and 200 mg dose, a minimal PBPK (mPBPK) model was built. This was performed since in an mPBPK model, in Simcyp® Simulator V17, the user can directly input the relationship between the drug plasma concentration and the fraction unbound in plasma and then simulate a continuously changing f_u with or without a simultaneous, concentration dependent change in the apparent volume of distribution. Following a "middle-out" strategy, the post-absorptive parameters associated with the Single Adjusting Compartment (SAC) *i.e.* Q_{SAC} (inter-compartment clearance) (5.70 L/h) and V_{SAC} (apparent volume associated with the SAC) (2.56 L/kg), and additional clearance through other pathways (other than the "Enzyme Kinetic" parameters described in Section 2.3.3 and Table 1) (450 and 100 μL/min/mg protein for the 100 mg and 200 mg dose, respectively) were estimated using the Parameter Estimation (PE) Tool by simultaneously fitting of the available pharmacokinetic profiles. A linear relationship between plasma concentration and etravirine plasma f_u was derived from the study of Nuygen et al. (Nguyen et al., 2013) since no analogous studies are available for healthy volunteers. It should be noted that the Nuygen study was performed in HIV-positive volunteers who were concomitantly receiving other medications, including emtricitabine (89%), tenofovir (78%), darunavir/ritonavir (78%), raltegravir (56%), enfuvirtide (33%), maraviroc (22%), didanosine (11%) and lamivudine (11%). According to the literature, there are no clinically significant interactions with emtricitabine, tenofovir and raltegravir, (Brayfield, 2011) and, while boosted darunavir decreases the concentrations of etravirine, no dose adjustment is required. (Brayfield, 2011) For the absorption part of the model, the "no precipitation" approach was followed.

The simulated plasma profiles after oral administration of a 100 mg or 200 mg Intelence® tablet in the fed state *vs.* the individual observed plasma concentrations (Janssen data on file) following the minimal PBPK concentration dependent f_u and concentration dependent f_u and V_d strategy are presented in Figs. 7 and 8. As can be observed in Fig. 7 and Fig. 8, this approach was able to capture the overall *in vivo* variability of the pharmacokinetics of etravirine within the 95% CIs, as well as the plasma concentrations after administration of a 200 mg Intelence® tablet in the fed state, more closely than simulations applying fixed values for f_u and V_d. The results suggest that f_u likely plays a key role in the pharmacokinetics of etravirine, especially when considering that etravirine binds to α1-acid glycoprotein, for which high inter-subject variability in expression is observed. However, there are still many questions around the role of f_u in etravirine's pharmacokinetic behavior and more *in vitro* data would assist in improving the quality of the model and confirming/refuting the assumption of a concentration dependent f_u.

4. Discussion

Bio-enabling formulations have been proven to be a viable solution to overcome difficult challenges, *e.g.* poor aqueous solubility, associated with many APIs in current development pipelines and thus facilitate access to innovative medicines. However, there is still considerable lack of understanding regarding the *in vitro* characterization and *in vivo* behavior of these formulations, as well as the mechanisms and extent to which they can improve bioavailability. For example, the *in vitro* characterization of ASDs can be quite complex because of their supersaturation and precipitation behavior, which may be dependent on interactions between the amorphous API and various components of the biorelevant media used to characterize them. (Wilson et al., 2018; Elkhabaz et al., 2018; Park, 2018) To date, there has been limited application of PBPK / absorption models in predicting the *in vivo* performance of ASDs due to the complex *in vitro* and *in vivo* dissolution process. (Mitra et al., 2016; Purohit et al., 2018; Emami Riedmaier et al.,
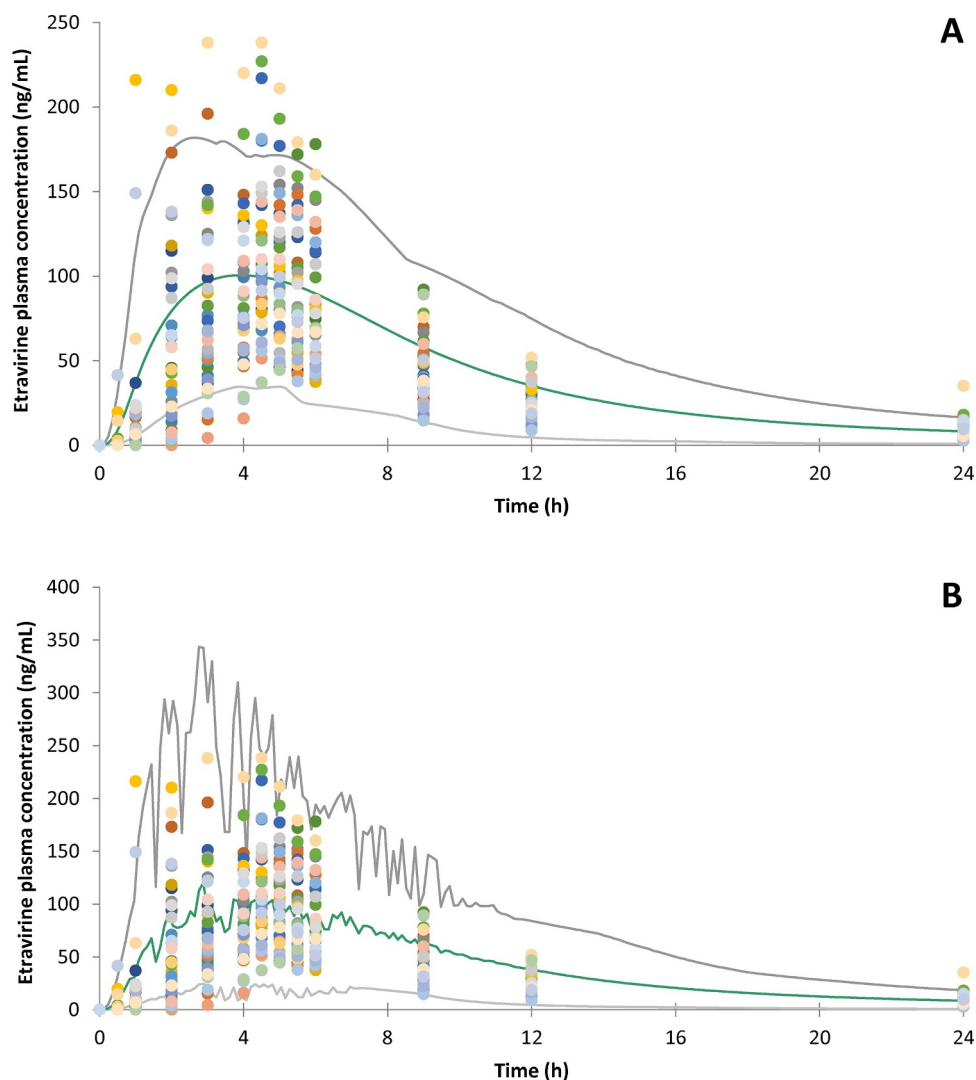
Fig. 7. Simulated (thick solid line, population mean; thin solid lines, 5th and 95th percentile of population) and clinically reported plasma concentrations after administration of a 100 mg Intelence® tablet following the minimal PBPK strategy with A) concentration dependent f_u and B) concentration dependent f_u and V_d, in fed state. Circles (•) represent the individual pharmacokinetic data (Janssen data on file).

2018) However, some early attempts have already been published and more studies of this nature are needed to advance our understanding in this field. (Mitra et al., 2016; Purohit et al., 2018; Emami Riedmaier et al., 2018) As demonstrated in the current study, the use of biorelevant *in vitro* tools in combination with modeling and simulation techniques provides a promising way forward to better understand the *in vivo* performance of such formulations.

Since dissolution rate is proportional to C_s-C_t, where C_s is the solubility at particle surface in the respective medium and C_t the concentration of drug in the bulk solution at time t, for bio-enabling formulations it is of great importance to use an appropriate "solubility" value for the formulated drug in order to achieve successful simulations. For etravirine, solubility and dissolution experiments conducted in biorelevant media demonstrated a large effect of naturally occurring surfactants on solubility and consequently the large food effect which is observed *in vivo* for etravirine. Further, comparison of the 24 h solubility of crystalline etravirine with the 24 h concentration achieved in the dissolution vessel during the dissolution experiments of Intelence® tablets in biorelevant media revealed that etravirine remains supersaturated over the entire course of dissolution when presented as an amorphous solid dispersion. Likewise, comparison of results using alternate simulation approaches, *i.e.* "no precipitation" and "implementation of precipitation", led to the conclusion that etravirine

does not precipitate *in vivo* when administered in the fed state. For etravirine, it was reasoned that if no precipitation was observed in a transfer experiment conducted under fasted state conditions, it would be even less likely to precipitate in the fed state, where the solubility differential for a weak base is lower than in the fasted state (assuming the fasted state gastric pH is low). This is further supported by the similar maximum concentration of dissolved etravirine achieved in the media simulating the fed stomach and fed upper small intestine. Nevertheless, a standardized model setup which can simulate the transfer of the drug from the fed stomach to the fed upper small intestine would be beneficial to understanding the *in vivo* performance of complex bio-enabling formulations in the fed state.

Lack of precipitation *in vivo* has also been hypothesized in the literature for several other basic compounds. Mitra et al. attempted to predict the *in vivo* performance of the ASDs of three basic compounds (two BCS Class II and one BCS Class IV) by combining *in vitro* data with PBPK modeling. (Mitra et al., 2016) In all cases, there was no need to invoke precipitation in the PBPK absorption models to achieve successful simulations of the *in vivo* plasma profiles. The same conclusion was reached by Emami-Riedmaier et al. who combined biorelevant *in vitro* data with PBPK modeling to predict the *in vivo* performance of the ASD of the BCS Class IV drug venetoclax. (Emami Riedmaier et al., 2018) Similar results have also been observed by Wilson et al. for the
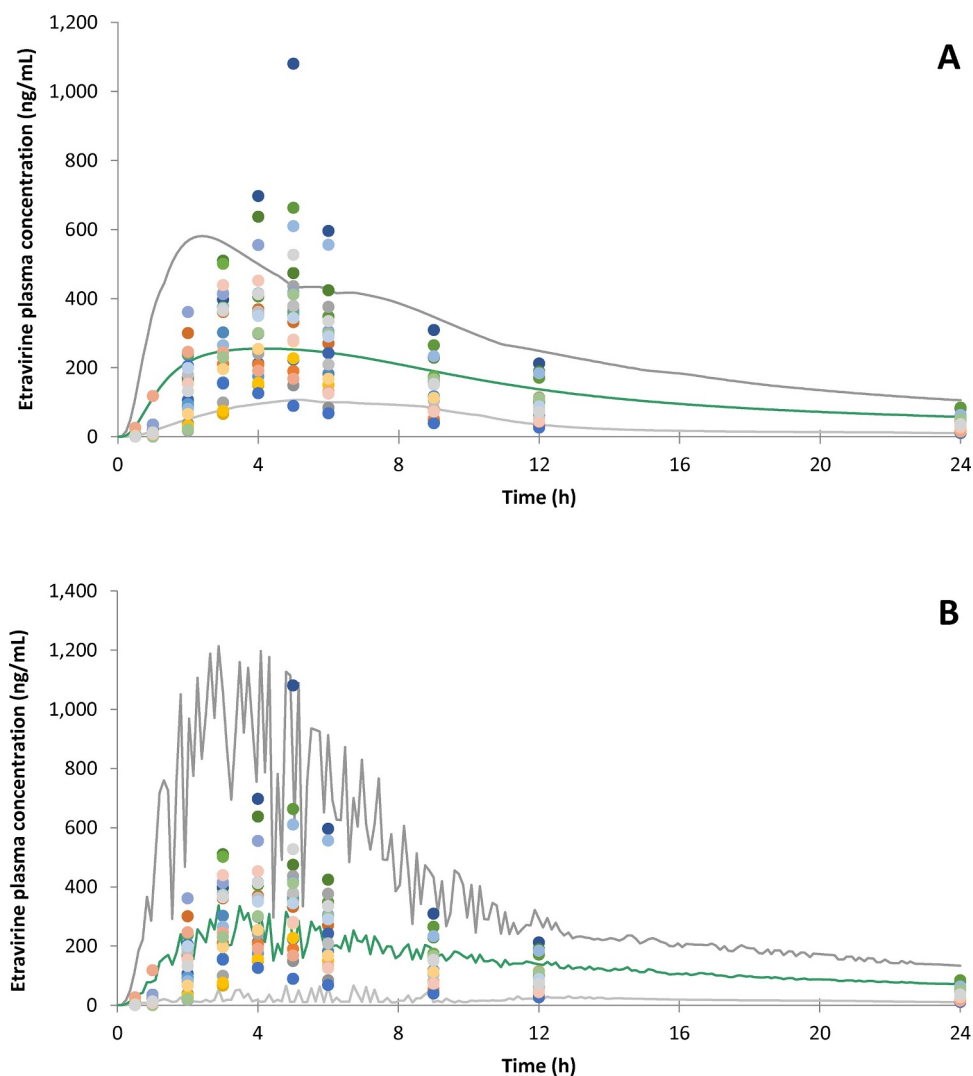
Fig. 8. Simulated (thick solid line, population mean; thin solid lines, 5th and 95th percentile of population) and clinically reported plasma concentrations after administration of a 200 mg Intelence® tablet following the minimal PBPK strategy with A) concentration dependent f_u and B) concentration dependent f_u and V_d, in fed state. Circles (•) represent the individual pharmacokinetic data (Janssen data on file).

ASD of enzalutamide in rats. (Wilson et al., 2018) The authors opined that the absence of crystallization of enzalutamide along with the interplay of *in vivo* permeation, diffusion and dissolution creates a continuous sink for an amorphous compound and thus facilitates its *in vivo* absorption. (Wilson et al., 2018) From the aforementioned studies published in literature, as well as from the present study, it is interesting to note that the maximum dissolved concentration achieved in the dissolution vessel in the respective biorelevant media was used in every case to represent the *in vivo* solubility of the API administered as the respective ASD.

By contrast, the use of the *in vitro* solubility of the crystalline API to represent *in vivo* solubility can result in a large underprediction of absorption (Emami Riedmaier et al., 2018), as shown previously, for example, by Litou et al. for the bio-enabling formulation of aprepitant (Litou et al., 2019).

Last but not least, as observed for etravirine pharmacokinetics, post-absorptive processes can also have a significant effect on the plasma profiles of many APIs and these should not be ignored. Rather, these parameters should also be investigated in order to be able to understand the overall *in vivo* behavior of these APIs and draw robust conclusions about the extent to which formulation options can be used to influence the API's pharmacokinetics. Using a minimal PBPK approach, it was

feasible to investigate the scenario of a concentration dependent f_u and V_d for etravirine. By invoking a concentration dependent relationship instead of single values for these parameters, it was possible to better represent the variability of etravirine pharmacokinetics observed *in vivo*. As no data in healthy volunteers is available for the concentration dependency of f_u and V_d, it was necessary to apply data from HIV-positive volunteers to the healthy population. Although the results may not be fully representative, they do suggest that these two post-absorptive parameters contribute to the variability in the pharmacokinetics of etravirine more than metabolic variations, and should thus be taken into account in future simulations of etravirine and other APIs with suspected/ proven concentration-dependent plasma binding and volume of distribution.

Comparing the influence of pre- and post-absorptive parameters on the pharmacokinetic profile of etravirine after oral administration of the commercial ASD formulation, it appears that the key factor on the pre-absorption side is the maximum achievable supersaturation concentration attainable with the ASD, which is the driving force for increasing the extent of absorption. On the post-absorptive side, the concentration dependency of plasma binding and volume of distribution appear to be the key contributors to the extensive variability in plasma profiles.

5. Conclusions

Despite intensive recent research around bio-enabling formulations, there is still lack of fundamental understanding with regard to their *in vivo* performance, the changes that may occur in the physicochemical properties of the API (for example, formation of amorphous or nano-crystalline drug, interactions with polymers which act as precipitation inhibitors, etc.) and how this information can be implemented into *in silico* PBPK models. In this study, the *in vivo* performance of the etra-virine "enhanced" formulation (Intelence® tablets) in healthy volunteers in the fed state was successfully predicted by coupling *in vitro* data, acquired with biorelevant *in vitro* tools, with a commercial PBPK modeling platform (the Simcyp Simulator). This case example demonstrates the potential application and importance of absorption modeling in rational formulation design and in strengthening biopharmaceutics knowledge around amorphous solid dispersions. Furthermore, this study also demonstrated the importance of evaluating the effect of both pre- and post-absorptive parameters. By applying this approach, the main parameters which affect the pharmacokinetic behavior of poorly soluble APIs formulated as bio-enabling formulations can be identified and in turn enable a more robust prediction of clinical outcomes.

Acknowledgements

Supplementary materials

Supplementary material associated with this article can be found, in the online version, at doi:10.1016/j.ejps.2020.105297.

References

Abduljalil, K., et al., 2014. Deciding on success criteria for predictability of pharmacokinetic parameters from *in vitro* studies: an analysis based on *in vivo* observations. Drug. Metab. Dispos. 42 (9), 1478–1484. https://doi.org/10.1124/dmd.114.058099.

Anderson, P.L., et al., 2000. Indinavir plasma protein binding in HIV-1-infected adults. AIDS 14 (15), 2293–2297. https://doi.org/10.1097/00002030-200010200-00010.

Andreas, C.J., et al., 2015. *In vitro* biorelevant models for evaluating modified release mesalamine products to forecast the effect of formulation and meal intake on drug release. Eur. J. Pharm. Biopharm. 97, 39–50. https://doi.org/10.1016/j.ejpb.2015.09.002.

Back, MBHLBSKDP, 2004. Lopinavir protein binding in vivo through the 12-hour dosing interval. Ther. Drug. Monit. 26 (1), 35–39.

Berlin, M., et al., 2014. Prediction of oral absorption of cinnarizine – A highly supersaturating poorly soluble weak base with borderline permeability. Eur. J. Pharm. Biopharm. 88 (3), 795–806. https://doi.org/10.1016/j.ejpb.2014.08.011.

Bevernage, J., et al., 2010. Drug supersaturation in simulated human intestinal fluids representing different nutritional states. J. Pharm. Sci. 99 (11), 4525–4534. https://doi.org/10.1002/jps.22154.

Bevernage, J., et al., 2012. Supersaturation in human gastric fluids. Eur. J. Pharm. Biopharm. 81 (1), 184–189. https://doi.org/10.1016/j.ejpb.2012.01.017.

Bohnert, T., Gan, L.S, 2013. Plasma protein binding: from discovery to development. J. Pharm. Sci. 102 (9), 2953–2994. https://doi.org/10.1002/jps.23614.

Brayfield, A., 2011. In: Sweetman, SC (Ed.), 37th ed. Pharmaceutical Press, London, UK.

Buckley, S.T., et al., 2013. Biopharmaceutical classification of poorly soluble drugs with respect to "enabling formulations". Eur. J. Pharm. Sci. 50 (1), 8–16. https://doi.org/10.1016/j.ejps.2013.04.002.

Butler, J.M., Dressman, J.B., 2010. The developability classification system: application of biopharmaceutics concepts to formulation development. J. Pharm. Sci. 99 (12), 4940–4954. https://doi.org/10.1002/jps.22217.

Deeks, E.D., Keating, G.M., 2008. Etravirine. Drugs 68 (16), 2357–2372.

Delille, C.A., et al., 2014. Effect of protein binding on unbound Atazanavir and Darunavir cerebrospinal fluid concentrations. J. Clin. Pharmacol. 54 (9), 1063–1071. https://doi.org/10.1002/jcph.298.

Elkhabaz, A., et al., 2018. Variation in supersaturation and phase behavior of ezetimibe amorphous solid dispersions upon dissolution in different biorelevant media. Mol. Pharm. 15 (1), 193–206. https://doi.org/10.1021/acs.molpharmaceut.7b00814.

Emami Riedmaier, A., et al., 2018. Mechanistic physiologically based pharmacokinetic modeling of the dissolution and food effect of a biopharmaceutics classification

system iv compound—the venetoclax story. J Pharm Sci. https://doi.org/10.1016/j.xphs.2017.09.027.

EMA 2019. Intelence summary of product characteristics. Available at https://www.ema.europa.eu/en/documents/product-information/intelence-epar-product-information_en.pdf.

FDA. Intelence drug approval package. Available at:https://www.accessdata.fda.gov/drugsatfda_docs/nda/2008/022187TOC.cfm. Accessed July 24, 2019.

Fuchs, A., et al., 2015. Advances in the design of fasted state simulating intestinal fluids: faSSIF-V3. Eur. J Pharm. Biopharm. 94, 229–240. https://doi.org/10.1016/j.ejpb.2015.05.015.

Green, B., et al., 2017. Evaluation of concomitant antiretrovirals and CYP2C9/CYP2C19 polymorphisms on the pharmacokinetics of etravirine. Clin. Pharmacokinet. 56 (5), 525–536. https://doi.org/10.1007/s40262-016-0454-8.

Intelence. 2008 Etravirine CHMP assessment report. 439522008: 1–52. Available at http://www.ema.europa.eu/docs/en_GB/document_library/EPAR_-_Public_assessment_report/human/000900/WC500034183.pdf.

Jamei, M., et al., 2009. Population-based mechanistic prediction of oral drug absorption. AAPS J 11 (2), 225–237. https://doi.org/10.1208/s12248-009-9099-y.

Kakuda, T.N., et al., 2010. Pharmacokinetics and pharmacodynamics of the non-nucleoside reverse-transcriptase inhibitor etravirine in treatment-experienced HIV-1-Infected patients. Clin. Pharmacol. Ther. 88 (5), 695–703. https://doi.org/10.1038/clpt.2010.181.

Kakuda, T.N., et al., 2013. Single-dose pharmacokinetics of pediatric and adult formulations of etravirine and swallowability of the 200-mg tablet: results from three phase 1 studies. Int. J. Clin. Pharmacol. Ther. 51 (9), 725–737. https://doi.org/10.5414/CP201770.

Litou, C., et al., 2019. Combining biorelevant *in vitro* and in silico tools to simulate and better understand the *in vivo* performance of a nano-sized formulation of aprepitant in the fasted and fed states. Eur. J. Pharm. Sci. 138, 105031. https://doi.org/10.1016/j.ejps.2019.105031.

Lubomirov, R., et al., 2013. Pharmacogenetics-based population pharmacokinetic analysis of etravirine in HIV-1 infected individuals. Pharmacogenet. Genom. 23 (1), 9–18. https://doi.org/10.1097/FPC.0b013e32835ade82.

Markopoulos, C., et al., 2015. In-vitro simulation of luminal conditions for evaluation of performance of oral drug products: choosing the appropriate test media. Eur. J. Pharm. Biopharm. 93, 173–182. https://doi.org/10.1016/j.ejpb.2015.03.009.

Mitra, A., et al., 2016. Physiologically based absorption modeling for amorphous solid dispersion formulations. Mol. Pharm. 13 (9), 3206–3215. https://doi.org/10.1021/acs.molpharmaceut.6b00424.

Moltó, J., et al., 2016. Use of a physiologically based pharmacokinetic model to simulate drug–drug interactions between antineoplastic and antiretroviral drugs. J. Antimicrob. Chemother.(December 2016). https://doi.org/10.1093/jac/dkw485. dkw485.

Moltó, J., 2015. Physiologically based pharmacokinetic model to predict drug-drug interaction in patients receiving antiretroviral and antineoplastic therapies. In: 16th HIVHEPPK. Alexandria, VA.

Nguyen, A., et al., 2013. Etravirine in CSF is highly protein bound. J. Antimicrob. Chemother. 68 (5), 1161–1168. https://doi.org/10.1093/jac/dks517.

Obach, R.S., et al., 1997. The prediction of human pharmacokinetic parameters from preclinical and *in vitro* metabolism data. J. Pharmacol. Exp. Ther. 283 (1), 46–58. Available at: http://www.ncbi.nlm.nih.gov/pubmed/9336307 Accessed February 9, 2018.

Park, K., 2018. Different phase behaviors of enzalutamide amorphous solid dispersions. J. Control Release 292, 277–278. https://doi.org/10.1016/j.jconrel.2018.11.021.

Pentafragka, C., et al., 2019. The impact of food intake on the luminal environment and performance of oral drug products with a view to *in vitro* and *in silico* simulations: a pearrl review. J. Pharm. Pharmacol. 71 (4), 557–580. https://doi.org/10.1111/jphp.12999.

Poulin, P., Theil, F.-.P., 2009. Development of a novel method for predicting human volume of distribution at steady-state of basic drugs and comparative assessment with existing methods. J. Pharm. Sci. 98 (12), 4941–4961. https://doi.org/10.1002/JPS.21759.

Purohit, H.S., et al., 2018. Investigating the impact of drug crystallinity in amorphous tacrolimus capsules on pharmacokinetics and bioequivalence using discriminatory in vitro dissolution testing and physiologically based pharmacokinetic modeling and simulation. J. Pharm. Sci. 107 (5), 1330–1341. https://doi.org/10.1016/j.xphs.2017.12.024.

Rajoli, R.K.R., et al., 2015. Physiologically based pharmacokinetic modelling to inform development of intramuscular long-acting nanoformulations for HIV. Clin. Pharmacokinet. 54 (6), 639–650. https://doi.org/10.1007/s40262-014-0227-1.

S. Darwich, A., et al., 2010. Interplay of metabolism and transport in determining oral drug absorption and gut wall metabolism: a simulation assessment using the "Advanced dissolution, absorption, metabolism (ADAM)" model. Curr. Drug. Metab. 11 (9), 716–729. https://doi.org/10.2174/138920010794328913.

Schöller-Gyüre, M., et al., 2008a. A pharmacokinetic study of etravirine (TMC125) co-administered with ranitidine and omeprazole in HIV-negative volunteers. Br. J. Clin. Pharmacol. 66 (4), 508–516. https://doi.org/10.1111/j.1365-2125.2008.03214.x.

Schöller-Gyüre, M., et al., 2008b. Effects of different meal compositions and fasted state on the oral bioavailability of etravirine. Pharmacotherapy 28 (10), 1215–1222. https://doi.org/10.1592/phco.28.10.1215.

Schöller-Gyüre, M., et al., 2010. Effects of hepatic impairment on the steady-state pharmacokinetics of etravirine 200mg BID: an open-label, multiple-dose, controlled phase I study in adults. Clin. Ther. 32 (2), 328–337. https://doi.org/10.1016/j.clinthera.2010.02.013.

Siccardi, M., et al., 2013. Prediction of etravirine pharmacogenetics using a physiologically based pharmacokinetic approach. In: 20th Conf Retroviruses Opportunistic

Infect. Atlanta, USA.

Sudhakaran, S., et al., 2007. Differential protein binding of indinavir and saquinavir in matched maternal and umbilical cord plasma. Br. J. Clin. Pharmacol. 63 (3), 315–321. https://doi.org/10.1111/j.1365-2125.2006.02766.x.

Tsamandouras, N., et al., 2015. Combining the "bottom up" and "top down" approaches in pharmacokinetic modelling: fitting PBPK models to observed clinical data. Br. J. Clin. Pharmacol. 79 (1), 48–55. https://doi.org/10.1111/bcp.12234.

Weuts, I., et al., 2011. Physicochemical properties of the amorphous drug, cast films, and spray dried powders to predict formulation probability of success for solid dispersions: etravirine. J. Pharm. Sci. 100 (1), 260–274. https://doi.org/10.1002/jps.

22242.

Wilson, V., et al., 2018. Relationship between amorphous solid dispersion *in vivo* absorption and *in vitro* dissolution: phase behavior during dissolution, speciation, and membrane mass transport. J. Control Release 292, 172–182. https://doi.org/10.1016/j.jconrel.2018.11.003.

Yanakakis, L.J., Bumpus, N.N., 2012. Biotransformation of the antiretroviral drug etravirine: metabolite identification, reaction phenotyping, and characterization of autoinduction of cytochrome P450-dependent metabolism. Drug. Metab. Dispos. 40 (4), 803–814. https://doi.org/10.1124/dmd.111.044404.

A.4 Curriculum Vitae

PERSONAL INFORMATION

Name	Charalampia Litou
Date of Birth	24.03.1991
Place of Birth	Athens, Greece
E-mail	litouchara@gmail.com

ACADEMIC CAREER

October 2016-ongoing	**PhD Candidate, Marie-Curie Research Fellow**
	Laboratory of Biopharmaceutics-Pharmacokinetics,
	Department of Pharmaceutical Technology, Goethe University, Frankfurt, Germany
	• Project: "Predicting the *in vivo* performance of bio-enabling formulations by coupling *in vitro* data, attained with biorelevant in *vitro* tools, with physiologically-based population pharmacokinetic modeling (pop-PBPK)."
	PEARRL Website: http://www.pearrl.eu/esr6.html
	Advisor: Prof. Dr. Jennifer Dressman
October 2014-September 2016	**Master of Science (MSc) in Industrial Pharmacy**
	Laboratory of Biopharmaceutics-Pharmacokinetics,
	School of Pharmacy, National and Kapodistrian University of Athens, Greece
	• GPA: 9.34/10 (ranked 1st in class)

• Thesis: "Characteristics of the Human Upper Gastrointestinal Contents in the Fasted State under Conditions of Reduced Acid Secretion in Stomach"

Advisor: Prof. Dr. Christos Reppas

September 2009-September 2014	**Diploma Pharmacy**

School of Pharmacy, National and Kapodistrian University of Athens, Greece

• GPA: 9.05/10 (ranked 1st in class)

• Thesis: "Simulation of the intragastric environment to assess solubility in fed gastric contents"

PROFESSIONAL CAREER

February 2019-May 2019	**Visiting Scientist at Janssen Pharmaceutica NV**

Research and Development, Biopharmaceutics Department, Beerse, Belgium

• Project: "PBPK modelling to predict the in vivo performance of bio-enabling formulations

Advisor: Dr. Rene Holm, Dr. Nico Holmstock, Dr. Jens Ceulemans

May 2017-August 2017	**Visiting Scientist at BfArM**

Federal Institute for Drugs and Medical Devices, Department of European Affairs

(Biopharmaceutics-Pharmacokinetics & Quality Working Party), Bonn, Germany

• Project: "Finished Product Monographs in Ph.Eur."
(presented at EDQM Meeting, September 2018, Strasbourg)

Advisor: Dr. Jobst Limberg

December 2015-May 2016	**Pharmacist in chief**

Private pharmacy "Artemisia Pothitaki", Athens, Greece

July 2015-August 2015	**Trainee at Genepharm S.A**
	Formulation Department, Athens, Greece
July 2013-December 2013	**Trainee Clinical Pharmacist at General Hospital of Chest Diseases "Sotiria"**
	Athens, Greece

DISTICTIONS AND AWARDS

2020	**Abschluss-Stipendien für Internationale Promovierende (DAAD)**
2020	**Franz Adickes Stiftungsfonds**
2016-2019	**Marie-Curie scholarship (MSCA), EU Horizon 2020 No 67490**
2015-2017	**A.G. Leventis Foundation scholarship for exceptional performance**
2014	**Onassis Foundation scholarship (Onassis Science Lecture Series)**
2014	**Greek State scholarship for ranking 1st in Pharmacy School**

PUBLICATIONS

- Litou C, Turner DB, Holmstock N, Ceulemans J, Box KJ, Kostewicz ES, Kuentz M, Holm R, Dressman JB. (2020), *"Combining biorelevant in vitro and in silico tools to investigate the in vivo performance of the amorphous solid dispersion formulation of etravirine in the fed state."* in European Journal of Pharmaceutical Sciences*.*

- Litou C, Psachoulias D, Vertzoni M, Dressman JB, Reppas C. (2020), "*Measuring pH and buffer capacity in fluids aspirated from the fasted upper gastrointestinal tract of healthy adults*", In Journal of Pharmaceutical Research.

- Litou C, Patel N, Turner DB, Kostewicz ES, Kuentz M, Box KJ, Dressman JB. (2019), *"Combining biorelevant in vitro and in silico tools to simulate and better understand the in vivo performance of a nano-sized formulation of aprepitant in the fasted and fed states."* in European Journal of Pharmaceutical Sciences.

- Litou C, Effinger A, Kostewicz ES, Box KJ, Fotaki N, Dressman JB. (2018), "*Effects of medicines used to treat gastrointestinal diseases on the pharmacokinetics of coadministered drugs: a PEARRL Review*", in Journal of Pharmacy Pharmacology.

- O'Dwyer PJ, Litou C, Box KJ, Dressman JB, Kostewicz ES, Kuentz M, Reppas C. (2018), "*In vitro methods to assess drug precipitation in the fasted small intestine - a PEARRL Review*", in Journal of Pharmacy Pharmacology.

- Litou C, Vertzoni M, Xu W, Kesisoglou F, Reppas C. (2017), "*The impact of reduced gastric acid secretion on dissolution of salts of weak bases in the fasted upper gastrointestinal lumen: Data in biorelevant media and in human aspirates*", in European Journal of Pharmaceutics & Biopharmaceutics.

- Litou C, Vertzoni M, Xu W, Kesisoglou F, Reppas C. (2016), "*The impact of reduced gastric acid secretion on drug dissolution in upper gastrointestinal lumen in the fasted state: Case example pioglitazone hydrochloride*", In AAPS, Colorado, USA, November 13-17, 2016.

- Litou C, Vertzoni M, Goumas C, Vasdekis V, Xu W, Kesisoglou F, Reppas C. (2016), "*Characteristics of the Human Upper Gastrointestinal Contents in the Fasted State under Conditions of Reduced Acid Secretion in Stomach*", In Journal of Pharmaceutical Research.

- Litou C, Vertzoni M, Goumas C, Vasdekis V, Xu W, Kesisoglou F, Reppas C. (2015), "*Characteristics of the Human Upper Gastrointestinal Contents in the Fasted State under Conditions of Reduced Acid Secretion in Stomach*", in AAPS, Orlando, FL, USA, October 26-29, 2015.